7. POINT-SOURCE MODEL VALIDATION

Model validation is the process used to establish confidence that a mathematical model and its underlying conceptual model adequately represent with sufficient accuracy the system, process, or phenomenon in question (LP-SIII.10Q-BSC, Section 3.15). LP-SIII.10Q, *Models*, identifies a number of methods for validating models that range from simple documentation to peer review. Model validation includes activities during model development to build confidence in the model and post-development model validation. In this section, the validation of the stochastic point-source ground motion model is described.

The guidelines for minimum levels of model validation (LP-2.29Q-BSC, *Planning for Science Activities*, Attachment 3) do not address seismic ground motion models. As stated in the TWP, because the model is being used to determine site-specific V/H ratios, its validation is assess as needing a high confidence (Level III). Validation will consist of comparing model results to data not used to develop or calibrate the model (LP-SIII.10Q-BSC, Section 5.3.2(a)(1)) and a technical review by a reviewer independent of the development, checking, and review of the model documentation (LP-SIII.10Q-BSC, Section 5.3.2(a)(5)). The criterion for validation is that the model produces ground motion response spectra that are in reasonable agreement with observed data as judged by the modeler. Reasonable agreement will be based on calculations of modeling variability and model bias. Model variability is defined as the standard error of the residuals of the logarithm of the response spectra (5% damped). The residual is defined as the difference of the logarithms of the observed and predicted response spectra. At each structural frequency of the response spectra, the residuals are squared and summed over the total number of sites for which data are being modeled for one or more earthquakes. Dividing the sum by the number of site provides an estimate of the model variance. Model bias (average offset) is also determined and will form part of the model validation assessment. Additional confidence will be provided by concurrence of the checker and reviewer of the model report in which the model and its validation will be documented.

For the technical review, the validation criterion is that technical review comments, if any, are acceptably resolved or a reason is provided for why the comment is not accepted. Review comments will be documented on comment sheets or in some other written format. Responses to comment and their acceptance will also be documented. Concurrence by the independent technical reviewer on the revised model documentation will also be obtained. Definition of subject matter expertise, qualifications for reviewer(s), criteria for selecting reviewers, and specific responsibilities for each reviewer are addressed in the TWP.

Technical review through publication in a referred professional journal or review by an external agency, documented by the external agency, may be used to demonstrate additional confidence in the model, if publication or review is used in conjunction with one or more of the model validation activities described in Sept 5.3.2a of LP-SIII.10Q (see 1 and 2).

This section describes the results of previous studies that provide the needed level of confidence in the validity of the stochastic point-source model. The stochastic point-source model was validated for DOE in a study supported by the Engineering Research and Applications Division, Department of Nuclear Energy, and Brookhaven National Laboratory. The report "Description and Validation of the Stochastic Point Source Ground Motion Model" by Silva et al. (1996

[DIRS 110474]) provides the basis for the following discussion. The validation and comparison exercises presented are entirely in terms of 5%-damped pseudo-absolute response spectra. This representation of strong ground motions is the most appropriate, currently acceptable, and least ambiguous approach to defining design ground motions.

The validation study consisted of two elements; both are quantitative but one is more inferential and will be called ‘qualitative’. The quantitative analyses modeled 16 earthquakes at over 500 sites. Fourier amplitude spectra were inverted for stress drop, crustal damping (Q[f]), and site kappa followed by forward modeling of response spectra from these parameters. Modeling uncertainty was estimated as a chi-square on the average horizontal component response spectra for each earthquake as well as over all earthquakes.

The qualitative validation more closely tied to recorded motions is a comparison of response spectral shapes (SA/PGA). In this comparison exercise, point-source model shapes were compared to statistical shapes computed from recordings in magnitude bins over the range of about **M** 5.0 to 7.4. This analysis provides a comparison of the magnitude scaling of the model in terms of the change in relative frequency content with magnitude with that displayed by recorded motions. It also provides an evaluation of the model’s ability to accommodate site effects.

The combinations of the quantitative validation exercises, using 16 well-recorded earthquakes, with the qualitative comparison exercises comprising a total of 503 sites represents a comprehensive evaluation intended to clearly illustrate both the model’s strengths and weaknesses.

The stochastic point-source model has been used extensively in the seismological community for the past two decades (Hanks and McGuire 1981 [DIRS 163510]; Boore 1983 [DIRS 103317]; Boore and Atkinson 1987 [DIRS 182044]; Toro and McGuire 1987 [DIRS 183435]; Ou and Herrmann 1990 [DIRS 170648]; Boore and Atkinson 1992 [DIRS 184133]; EPRI 1993 [DIRS 103319]; Atkinson and Boore 1995 [DIRS 184123]; Silva and Darragh 1995 [DIRS 105398]). Publications in peer-reviewed scientific journals attest to its acceptance and validity by seismologists and earthquake engineers. The stochastic point source model is primarily used to provide response spectral estimates for design purposes but has also been used to develop time histories (Boore 1983 [DIRS 103317], Silva and Lee 1987 [DIRS 103325]). Boore (2000 [DIRS 184354]) provides a program SMSIM_TD to calculate synthetic seismograms using a point-source model to fill the gaps in empirical strong motion database useful for engineering purposes.

The stochastic point source has also been used to develop ground motion attenuation relationships for stable continental regions, such as the central and eastern United States (CEUS) where there are few earthquakes large enough to provide enough data for a statistically robust empirical ground motion attenuation relationship. Toro et al. (1997 [DIRS 183438]) computed separate attenuation relationships for two subregions, eastern North America, and Mid-continent and Gulf Coast, based on stochastic point source simulations. Atkinson and Boore (1995 [DIRS 184123], 1997 [DIRS 183437]) also use a stochastic point source model to develop their attenuation relations for eastern North America but also use empirical recordings of small to moderate sized earthquakes and historical earthquake isoseismals to help constrain some of the parameters. Atkinson and Boore (1997 [DIRS 184801]) also developed an attenuation relation for the Cascadia subduction zone earthquakes using the point-source model due to the paucity of strong motion recordings from subduction zone earthquakes in the United States. Most attenuation relationships for subduction zones are based on recordings from Japan and South America and are recorded at large distances because of the depth or distance from shore (Abrahamson and Shedlock 1997 [DIRS 164486]). The Atkinson and Boore (1997 [DIRS 183437]) point-source model appears to provide conservative estimates of ground motions for earthquakes of **M** < 7 at distances less than 100 km, but appears to over predict near-source ground motions and under predict large distance (>100 km) ground motions.

A natural progression of the point-source model was the development of the finite-fault source model which computes ground motions from a series of point sources distributed over a fault plane. The simple point-source model motions are then just summed. This method appears to produce motions of comparable accuracy to more seismologically rigorous semi-empirical methods (Schneider et al. 1993 [DIRS 110467], EPRI 1993 [DIRS 103319], Schneider et al. 1996 [DIRS 103270]).

7.1 VALIDATION STUDIES

The point-source model is applied in two ways which are reflected in the validation exercises. It may be used to simulate motions for a single deterministic scenario – a specific set of magnitude, distance, and site condition parameters – or for a grid of scenarios to develop or extend attenuation relations. Assessments of model and parametric variability are achievable in both applications.

7.1.1 Models

The parameters used in the point-source model validation are:

- Crustal and site velocity profiles
- Randomization methodology
- Damping models
- Inversions of recorded data for stress drop, crustal damping (Q[f]), and site kappa (for earthquakes used in quantitative validation, only)

The qualitative comparisons additionally require the suite of model parameters that represent the data on which the attenuation relation and statistical spectra are based. The development of all models is discussed thoroughly in Silva et al. (1996 [DIRS 110474]).

7.1.1.1 Site and Crustal Models

Generic site response categories and crustal models are required input to the point-source modeling. Generic models are used because reliable velocity profiles have not been determined for most strong motion recording sites.

Use of broad site classifications is a compromise between the goals of accurately modeling site response and of constraining model variability and bias. Accurately modeling recorded motions requires detailed shear-wave velocity measurements at each site. Most strong ground motion recording sites do not have reliable velocity profiles and thus the number of sites – and recordings – is greatly reduced. Fewer records result in less well-resolved regression parameters.

For comparisons against individual earthquakes, the generic site categories are used with local (or regional) crustal models. For comparisons against statistical response spectral shapes or the empirical attenuation relation, the site models are used with a generic crustal model. When comparing against an attenuation relation, the generic site categories and generic crustal models must be consistent with the strong motion data used in the empirical regression.

Two site categories were selected: soft rock and deep soil conditions. Soft rock is a combination of Geomatrix categories (Table 7-1) for rock and shallow stiff soil. Shear-wave velocity profiles for sites classified as Geomatrix A or B were averaged and smoothed to form the soft rock profile (Figure 7-1a); the result is similar to USGS B conditions (Table 7-1). This velocity profile was used as the base case for soft rock in the validation analyses.

Deep soil was defined as encompassing conditions in wide or deep, narrow valleys (Geomatrix D and C) and the profile was developed in the same manner as soft rock (Figure 7-1b). The class comprises only cohesionless soils or low plasticity index clays; there is no parallel USGS category.

Table 7-1. Strong Motion Recording Site Classifications

Geomatrix Site Classification	
Category	Geotechnical Subsurface Characteristics
A	Rock. Instrument on rock (V_S > 600 m/sec) or less than 5m of soil over rock
B	Shallow (stiff) soil. Instrument on/in soil profile up to 20 m thick overlying rock.
C	Deep narrow soil. Instrument on/in soil profile at least 20 m thick overlying rock, in a narrow canyon or valley no more than several km wide.
D	Deep broad soil. Instrument on/in a soil profile at least 20 m thick overlying rock, in a broad valley.

USGS Site Classification	
B	Average shear-wave velocity of 360 to 750 m/sec, to a depth of 30 m.

Source: Silva et al. (1996 [DIRS 110474])

Validations against individual earthquakes use local (or regional) crustal models developed in studies of the event slip process. These are presented in the context of each earthquake, below. The purpose of the generic crustal model is simply to represent amplification for vertically propagating shear-waves from the source region to the base of the generic site profile. The amplification must be appropriate for the majority of data in the strong motion data base and thus should reflect California rock conditions. This regional profile (Figure 7-2) was developed by averaging the profiles from studies of seven California earthquakes (Table 7-2).

Table 7-2. Regional Models used for the Generic Crustal Model

Earthquake	Model Source
Loma Prieta	Wald (1991 et al. [DIRS 164086])
Coyote Lake	Liu and Helmberger (1983 [DIRS 163922])
Morgan Hill	Hartzell and Heaton (1986 [DIRS 163916])
Landers	Wald and Heaton (1994 [DIRS 164085])
North Palm Springs	Hartzell (1989 [DIRS 164078])
Cape Mendocino	Graves (1994 [DIRS 164251])
Coalinga	Eaton (1990 [DIRS 164249])

Source: Silva et al. (1996 [DIRS 110474])

7.1.1.2 Profile Randomization

In order to accommodate epistemic and aleatory uncertainties in a realistic manner, a profile randomization scheme was implemented in the comparisons to empirical attenuation and statistical response spectral shapes. Both V_S and layer thicknesses were varied using category-specific correlation models based on an analysis of variance of over 500 measured V_S profiles. The algorithm started with the base case generic site profile and generated a suite of random profiles about the base case with correlation statistics appropriate to the category. At the base of the profile, V_S was varied according to a lognormal distribution with a standard error (natural log) of 0.3 (EPRI 1993 [DIRS 103319]). Depth to competent material was also varied for the deep soil category to accommodate different profile depths for the strong motion recording sites.

7.1.1.3 Regional Damping Models

To investigate regional differences in path (Q[f]) and site (kappa) damping within California, earthquakes located within its geographic provinces were combined in inversions for these parameters (Table 7-3). Events with recordings spanning a range of distances sufficient to constrain Q and kappa were used. For the remaining earthquakes, the region-specific Q [$Q=Q_o f^{\eta}$] was fixed (Table 7-3) and inversions were performed only for the stress parameter and kappa.

In the inversion scheme, five source, path, and site parameters may be obtained by inverting Fourier amplitude spectra (log values). The parameter covariance matrix determines whether that parameter may be resolved for each event's data set. The five parameters include kappa, Q_o and η, **M** and corner frequency.

Table 7-3. Initial Regional Damping Models – Crustal Q and Kappa

Region	Number of Stations	Q_o	η	κ (sec) (Rock)	κ (sec) (Soil)
Peninsular Ranges (Northridge, San Fernando, Whittier Narrows earthquakes)	221	174	0.77	0.053	0.058
		264	0.60*	0.051	0.056
		1286	0.00*	0.047	0.052

Region	Number of Stations	Q_o	η	κ (sec) (Rock)	κ (sec) (Soil)
North Coast (Loma Prieta, Coyote Lake, Morgan Hill earthquakes)	92	348	0.32	0.056	0.069
		176	0.60*	0.059	0.072
		814	0.00*	0.053	0.066
Mojave (Landers, North Palm Springs earthquakes)	86	186	0.64	0.030	0.052
		371	0.60*	0.030	0.056
		1678	0.00*	0.023	0.049
Combined	399	346	0.53	0.050	0.059
		291	0.60*	0.051	0.060
		1518	0.00*	0.047	0.056

* Values held fixed.

Source: Silva et al. (1996 [DIRS 110474]) Table 4.1

7.1.1.4 Validation Earthquake Models (Quantitative Exercise)

The total number of recording sites is 502 covering fault distances of about 1 km to nearly 200 km for western North American (WNA) data and from about 5 to 450 km for eastern North America (ENA) data(Table 7-4). The Tabas (Iran) event was included to extend the ENA data base because its crustal model and surface velocity are generally similar to ENA sites (Silva et al. 1996 [DIRS 110474]).

Table 7-4. Earthquakes Modeled in Quantitative Exercise

Earthquake	Date	Magnitude (M)	Recording Stations
Cape Mendocino, CA	1992	6.8	5
Coyote Lake, CA	1979	5.7	10
Imperial Valley, CA	1979	6.4	35
Imperial Valley, CA (AS)	1979	5.3	16
Landers, CA	1992	7.2	57
Little Skull Mountain, NV	1992	5.7	8
Loma Prieta, CA	1989	6.9	53
Morgan Hill, CA	1984	6.2	29
Nahanni, Canada	1985	6.8	3
North Palm Springs, CA	1986	6.0	29
Northridge, CA	1994	6.7	94
Saguenay, Canada	1988	5.8	22
San Fernando, CA	1971	6.6	39
Superstition Hills, CA (B)	1987	6.4	12
Tabas, Iran	1978	7.4	4

Earthquake	Date	Magnitude (M)	Recording Stations
Whittier Narrows, CA	1987	6.0	88

Note: AS = Aftershock

Source: Silva et al. (1996 [DIRS 110474]) Table 5.2

Additional event-specific parameters (stress drop, κ) were required for the quantitative exercises. Site-specific kappa values were assessed in the regional inversions (Section 7.1.1.3). Source stress drop for each event was separately determined by inverting Fourier amplitude spectra using the point-source methodology. Event-specific crustal models were used when available and generic models were used otherwise. Generic site models were applied according to station site conditions. Inversion results are listed in Table 7-5.

Table 7-5. Source, Path, and Site Parameters for Forward Modeling

Earthquake	Stress Drop* (bars)	Q_o**	η**	κ** Rock (sec)	κ** Soil (sec)	Crustal Model
Cape Mendocino	27.2	176	0.06	0.04	0.04	Event-specific
Coyote Lake	70.1	176	0.60	0.04	0.04	Event-specific
Imperial Valley	23.2	264	0.60	0.03	0.03	Event-specific
Imperial Valley (AS)	28.7	264	0.60	0.03	0.03	Event-specific
Landers	40.7	371	0.60	0.03	0.03	Event-specific
Little Skull Mtn.	63.7	256	0.47	0.023*	(No soil sites)	Event-specific
Loma Prieta	73.7	176	0.60	0.04	0.04	Event-specific
Morgan Hill	49.0	176	0.60	0.04	0.04	Event-specific
Nahanni	13.4	317	0.86	0.016*	(No soil sites)	Event-specific
North Palm Springs	62.8	371	0.60	0.03	0.03	Event-specific
Northridge	62.9	264	0.60	0.04	0.04	Event-specific
Saguenay	572.2	317	0.86	0.023*	(No soil sites)	Event-specific
San Fernando	36.1	264	0.60	0.04	0.04	Event-specific
Superstition Hills (B)	43.4	264	0.06	0.03	0.03	Generic
Tabas	21.5	291	0.60	0.04	0.04	Event-specific
Whittier Narrows	95.7	264	0.60	0.04	0.04	Generic

* Event-specific modeling results.

** Regional modeling results. Kappas are **average** small strain values whereas site-specific values were used in forward modeling.

Source: Silva et al. (1996 [DIRS 110474])

7.1.2 Partition and Assessment of Ground Motion Variability

An essential requirement of the modeling approach is a quantitative assessment of prediction accuracy – i.e., the model and parametric variability. Modeling variability is a measure of how accurately the model predicts ground motions when specific parameter values are known and is measured by differences between model predictions and recorded motions. Parametric variability is the sensitivity of a model to a reasonable range of values for model parameters.

Both the modeling and parametric variabilities may have components of randomness and uncertainty. Uncertainty is that portion of both modeling and parametric variability which in principle can be reduced as additional information becomes available. Randomness is that component of variability which is intrinsic or irreducible.

Modeling variability (uncertainty plus randomness) is usually evaluated by comparing response spectra computed from recordings to predicted spectra and is a direct assessment of model accuracy. The modeling variability is defined as the standard error of the residuals of the log of the average horizontal component (or vertical component) response spectra. The residual is defined as the difference between the logarithms of the observed average 5%-damped acceleration response spectra and the predicted response spectra. The mean residual is termed 'bias'. In the context of these comparisons, positive bias indicates under prediction and negative bias indicates over prediction. Any model bias that exists may be estimated in the process (Abrahamson et al. 1990 [DIRS 183483], EPRI 1993 [DIRS 103319]) and used to bias-correct the variance. In this approach, the modeling variability can be separated into randomness and uncertainty where the bias-corrected variability represents randomness and the total variability represents randomness plus uncertainty.

Parametric variability is site-, path-, and source-dependent; it must be evaluated for each application (Silva 1993 [DIRS 170696]); and it is more difficult to assess. Formally, a Monte Carlo approach may be used with each parameter randomly sampled about its mean (median) value using an appropriate distribution either individually for sensitivity analyses or in combination to estimate the total parametric variability (Silva 1992 [DIRS 183482], EPRI 1993 [DIRS 103319], Silva 1993 [DIRS 170696]). There are two complicating factors. The first is knowledge of the appropriate distributions for the parameters. In general median parameter values and uncertainties are based, to the extent possible, on evaluating the parameters from previous earthquakes assuming lognormal or normal distributions (Silva 1992 [DIRS 183482], EPRI 1993 [DIRS 103319]). The second factor involves the specific parameters kept constant with all earthquakes, paths, and sites when computing the modeling variability. These parameters are thus implicitly included in model variability. The parameters which are varied during the assessment of model variation should have a degree of uncertainty and randomness associated with them for predictions of the ground motions from the next earthquake. Any ground motion prediction should then have a variation reflecting variability in the free parameters.

7.2 ACCEPTANCE CRITERIA

The criteria for acceptance in SP-SIII.10Q is that the model produces ground motion response spectra that are in reasonable agreement with observed data as judged by ground motion experts. Reasonable agreement will be based on calculations of modeling variability and model bias. We adopt a qualitative criterion of "reasonable agreement" as being similar to the fits of empirical models to observed strong motion data, e.g., ground motion attenuation models. A total standard error (sigma) (ln) of 0.5, which is typical of empirical models (e.g., Abrahamson and Silva 1997

[DIRS 104205]), is the standard adopted here for "reasonable agreement." Future cases in this report of phrases such as "poor" agreement are referenced to this standard.

Model variability is defined as the standard error of the residuals of the logarithm of the response spectra (5% damping). The residual is defined as the difference of the logarithms of the observed and predicted response spectra. At structural frequencies for which the response spectra are computed, the residuals are squared and summed over the total number of sites for which data are being modeled for one or more earthquakes. Dividing the sum by the number of sites provides an estimate of the model variance. Model bias (average offset) is also determined and will form part of the model validation assessment. Approval of this model report by the technical checker and independent technical reviewers will signify that these criteria have been met in the view of the report originators, the technical checker and the independent reviewer who have evaluated the adequacy of model validation.

7.3 VALIDATION RESULTS

The following subsections describe the results of the validation studies against recorded motions and spectral shapes.

7.3.1 Validation against Recorded Motions

To validate the point-source model, comparisons were made between each of the sixteen well-recorded earthquakes and predicted ground motions from the point-source model using regionally determined kappa and stress drop values as derived from inversions as described in sections 7.1.1.3 and 7.1.1.4. Results and a summary from each of the sixteen earthquakes are provided. For a more detailed discussion of results for each earthquake refer to Silva et al. (1996 [DIRS 110474]).

7.3.1.1 Validation Results for the 1994 Northridge Earthquake

The 1994 **M** 6.7 Northridge earthquake is one of three earthquakes used in the validation study for the Peninsula Ranges Province. A total of 94 sites were modeled using the point source model, of which 71 were rock and 23 were soil. Source-to-site distances ranged from 7 to 150km. The crustal model of Wald and Heaton (1994 [DIRS 164085]) was used for the point-source modeling with the generic soil and rock profiles appended on top. A stress drop of 62.9 bars was used from the inversion modeling results described earlier (Table 7-5) and the point-source depth is taken as 11 km, the location of the largest asperity as determined from the Wald and Heaton (1994 [DIRS 164085]) slip model. Regional rock and soil site kappa were determined from regional inversion (Table 7-3). Both soil and rock sites are allowed to exhibit material non-linearity to depths of 500 ft. For rock, generic soft rock G/G_{max} and hysteretic damping curves (e.g., EPRI 1993 [DIRS 100320]) were used and are based on laboratory test results for materials at the recording sites (Appendix D; Silva et al. 1996 [DIRS 110474]). EPRI (1993 [DIRS 100320]) cohesionless and generic deep soil curves were adopted for the Peninsular Ranges area cohesionless soils by Silva et al. (1996 [DIRS 110474]).

Figure 7-3 shows the model bias and variability over all the 94 sites for the Northridge earthquake (Silva et al. 1996 [DIRS 110474]). It is essentially zero between 1 and 20 Hz with a slight under prediction at higher frequencies (equivalent to PGA). The strong negative bias at low frequencies reflects the tendency of the point-source model to over predict the low frequency range for magnitude greater than 6.5. The model variability (uncertainty plus randomness) shown below the bias plot is about 0.5 at 1 Hz and rises significantly below 1 Hz reflecting the point-source over prediction at these frequencies (Figure 7-3). The bias-corrected variability (randomness) is significantly lower over this frequency range due to the large negative bias estimates.

Figures 7-4 and 7-5 show the model bias and variability separated by site condition (soil or rock). The 71 soil site results are very similar to the overall results, not surprisingly since these make up the largest proportion of total sites. The 23 rock sites show a broad peak of 0.4 (under prediction by a factor of 1.5) at intermediate frequencies (2-3 Hz) and an under prediction of 0.25 at high frequencies. A quarter of this bias is a result of two recordings, PUL (Pacoima Dam) and ORR (Castaic – Old Ridge Road), which recorded very high motions. Figure 7-6 compares the 5%-damped pseudo-absolute response spectra (log average of two horizontal components) for the predicted motions with the actual data. In some cases, the actual ground motions are a factor of 3 above the model predictions at particular periods (less than 2 seconds; see results for PUL and ORR in Figures 7-6a and 7-6c respectively). A similar effect is seen for the San Fernando earthquake at stations in the same general areas of PUL and ORR indicating a strong site effect (Silva et al. 1996 [DIRS 110474]).

Examining the plots in detail (Figure 7-6) shows the cause of the broad peak near 3 Hz (0.3 sec) and trough near 10 Hz (0.1 sec) on the rock bias plot (Figure 7-5). For example, station KAG (Kagel Canyon) shows the model has a peak near 0.2 sec while the actual motions have a spectral peak around 0.5 sec (middle plot in top row of Figure 7-6b). This is related to the differences between a median spectrum computed for a range of random profiles and a spectrum computed from a single smoothed profile (or recorded motion). Figure 7-7 shows this shift of the peak from short period to intermediate period motions when comparing results from a smoothed base-case soft rock profile (Figure 7-1a) and the median spectrum computed from 30 randomized profiles using the correlation model of Silva et al. (1996 [DIRS 110474] Appendix C). Figure 7-8 shows the same results for a deep soil site (see Figure 3.4 in Silva et al., 1996 [DIRS 110474]), which shows similar results but not as pronounced. The difference appears to be significant for rock sites and suggests that an appropriate approach in estimating model bias and variability for use in future predictions is to either use a median prediction at each site or select the best fitting spectrum out of the random selection of site profiles. As a result the bias and randomness estimates (particularly for rock sites) should be viewed in the context that they probably represent bounding values and use of median estimates would smooth and improve the bias estimates.

7.3.1.2 Validation Results for the 1971 San Fernando Earthquake

For the 1971 **M** 6.6 San Fernando earthquake, 39 sites are modeled of which 21 were rock and 18 soil and which encompass epicentral distances between 3 and 200 km. The crustal model of Wald and Heaton (1994 [DIRS 164085]) was adopted. For the Peninsular Ranges the average rock kappa value is 0.048 sec and the soil kappa is 0.056 sec from the inversion of the 1971, 1987 Whittier Narrows and the 1994 Northridge earthquakes (Silva et al. 1996 [DIRS 110474] Table 4.3). Bias and variability estimates were computed for all 39 sites using the point source and a stress drop of 36.1 bars (Figure 7-9). The overall bias shows the typical low frequency over prediction at frequencies greater than about 0.3 Hz. At higher frequencies the bias is positive indicating a slight under prediction. The variability plot shows larger variability than for the Northridge earthquake of about 0.6 between 0.4 and 100 Hz.

Figures 7-10 and 7-11 show the bias and variability plots for the 18 soil and 21 rock sites respectively. For soil sites, the high frequency bias (> 1 Hz) is about zero and increase to 0.25 for rock sites. The overall slight under prediction shown for all sites appears to be driven by the rock sites. The randomness plots are similar and the small bias and level of randomness is encouraging for this complex source.

Comparisons of ground motions computed at individual stations with that which was recorded (Figures 7-12a through 7-12d) indicates that a significant contribution to the rock site under prediction may be due to sites PCD (Pacoima) and ORR (Castaic) (Figure 7-12a) as was also observed with the Northridge earthquake at PUL and ORR indicating a probable strong site effects at these sites.

7.3.1.3 Validation Results for the 1987 Whittier Narrows Earthquake

The **M** 6.0 Whittier Narrows earthquake is the last of the three earthquakes in the Peninuslar Ranges Province used in the validation. This earthquake had the second largest number of sites recorded and modeled. Of the 88 sites modeled only 18 are rock and the other 70 are soil. Distances from source to site are 10 to 80 km. The Wald and Heaton (1994 [DIRS 164085]) crustal model was also used for the modeling along with a stress drop of 95.7 bars. Kappa values used are shown in Table 7-5.

Figure 7-13 shows the combined model bias and variability plots for all 88 sites. The bias is essentially zero above 1 Hz. The point source over prediction at low frequencies is quite strong, about 0.6 from 0.3 to 1.0 Hz. The bias-corrected variability (randomness) averages 0.6 but the uncorrected values rise sharply below 1 Hz. Overall the point source appears to match the ground motions well for frequencies above 1 Hz. Figures 7-14 and 7-15 show the same plots but separated into soil and rock sites groupings. The soil sites show a slight high frequency over prediction but the opposite is true for the rock sites. The variability for the soil sites is less than that for the rock sites, similar to what was observed for the San Fernando earthquake but not the Northridge earthquake.

Figures 7-16a through 7-16h compare the 5% damped response spectra with the modeled ground motions using the point source. The simple point source appears to perform well in matching the recorded ground motions. However, the 4 most distance sites (all rock) do show large short period under predictions (Figure 7-16h). The results for site CSR also showed a similar under prediction for the Northridge and San Fernando earthquakes.

7.3.1.4 Validation Results for the 1989 Loma Prieta Earthquake

The **M** 6.9 Loma Prieta earthquake is one of three earthquakes modeled in the North Coast Province group. The site kappas and stress drops determined in the point-source inversion are shown in Table 7-5. The regional models and average kappa values are shown in Table 7-3. The Loma Prieta earthquake has 53 sites of which 33 are rock and 20 soil covering a source to site distance range of 5 to 90 km. Most of the soil sites are within 30 km of the source and most of the rock sites are beyond 30 km. The crustal model of Wald et al. (1991 [DIRS 164086]) was used in the modeling. The point-source stress drop was 73.7 bars determined from the inversion and the source depth is 12 km, the depth of the largest asperity in the Wald et al. (1991 [DIRS 164086]) slip model. Based on the regional inversions (Silva et al. 1996 [DIRS 110474] Table 4.3), for the North Coast sites and average rock kappa value of 0.053 sec was used and a kappa value of 0.083 sec was used for soil sites.

The point-source model bias and variability estimates were computed over all 53 sites (Figure 7-17). The bias is essentially zero between 1 and 20 Hz and shows a slight under prediction at higher frequencies. The typical low frequency over prediction observed at frequencies greater than about 0.3 Hz exists with this earthquake to a lesser extent than several of the other events in the quantitative analysis. The model variability is about 0.6 above 2 Hz and rises noticeably below 2 Hz, reflecting unmodeled low frequency site variation as the bias is near zero (Silva et al., 1996 [DIRS 110474] Section 5.3.1.2).

Figures 7-18 and 7-19 show the analogous plots for soil and rock sites respectively. Near constant bias can be observed for frequencies above 1 Hz for the 20 soil sites. For the rock sites there is a broad peak of about 0.3 at intermediate frequencies and an under prediction of about 0.2 at very high frequencies. It appears that much of this positive bias might result from just 5 sites with very high motions (PRS, CFH, BRK, CGB and PTB), all rock sites at distances greater than 70 km (Figure 7-20e). The higher ground motions at these sites may be due to a localized crustal effect (Silva et al. 1996 [DIRS 110474]). Figures 7-20a through 7-20e show the 5% damped pseudo-absolute response spectra showing the data and the model predictions. For the above 5 sites the recorded motions are as much as 3 times that predicted at certain periods. Other nearby sites appear to have closer to expected shaking levels indicating that there is probably a strong site influence occurring at these 5 sites. In general, though, the point source appears to perform well as reflected in the low bias and small randomness shown over the wide distance range.

7.3.1.5 Validation Results for the 1979 Coyote Lake Earthquake

Only 10 sites were modeled for the **M**5.7 Coyote Lake earthquake. This earthquake also occurred in the North Coast Province. Of the 10 sites, 7 are soil and 3 rock and the site distances range from 3 to 30 km. The crustal model of Liu and Helmberger (1983 DIRS [163922]) was used for the point source model along with a stress drop of 70.1 bars and source depth of 8 km. Source, site and path parameters used are summarized in Table 7-5.

For the 10 sites the model bias and variability plots are shown in Figure 7-21. The bias is low, near zero, for frequencies above 0.4 Hz and the variability is also very low above 20 Hz and rises to 0.4 below this. Separate plots for soil and rock are not shown because of the small number of each and the results are not reliable. In general the soil sites mimic the plots for all sites and the rock sites show the typical negative bias and higher general randomness.

The plots of the individual station comparisons of the response spectra (Figure 7-22) show a reasonable match between recorded and modeled motions. The soil sites appear to match more closely than the rock sites

7.3.1.6 Validation Results for the 1984 Morgan Hill Earthquake

A total of 29 sites are modeled for the **M** 6.2 Morgan Hill earthquake, of which 21 are soil and 8 are rock. Source to site distances range from 1 to 70 km. The crustal model used is from Hartzell and Heaton (1986 [DIRS 163916]) and was used for the slip inversion. The point-source depth is taken as 8 km and the stress drop from the inversions is 49 bars. Other source, site and path parameters used are summarized in Table 7-5.

The model bias and variability estimates are shown in Figure 7-23. The bias is low and slightly negative near 1 Hz and shows the typical over prediction down to 0.5 Hz. The variability is higher at high frequency than for the Coyote Lake earthquake and about the same for frequencies below 10 Hz. The same plots for the soil and rock sites separately are shown in Figures 7-24 and 7-25 respectively. The soil sites reflect the same results as observed for all sites and as usually observed, the rock site bias are more negative at high frequency (10 Hz) and the variability is higher than for soil.

The response spectra comparisons are shown in Figures 7-24a through 7-24c and reflect a good match. The soil sites appear to be modeled more closely than the rock sites, which show over prediction over a broad range of frequencies. Using a median spectrum instead of a single run with the base case profile may reduce the rock site over prediction.

7.3.1.7 Validation Results for the 1992 Landers Earthquake

The 1992 **M** 7.2 Landers earthquake is one of two earthquakes modeled in the Mojave Province, the other earthquake being the 1978 North Palm Springs earthquake which will be discussed next. The Landers earthquake was modeled for 57 sites, 52 of which were soil and only 5 being rock. The source to site distance range is from 1 km out to 180 km. The crustal model used is from Wald and Heaton (1994 [DIRS 164085]). Generic rock and soil profiles placed above the crustal model were used to model the rock and soil sites. The point source depth is taken at 8 km, the depth of the largest asperity (Wald and Heaton 1994 [DIRS 164085]) and the stress drop from the inversions was 40.7 bars. The average rock kappa for the Mojave sites is 0.025 sec and for soil is 0.050 sec (Table 7-5).

The bias and variability plots are shown in Figure 7-27 for all sites. Over most of the frequency range the bias reflects an under prediction particularly at around 1 Hz. The variability is generally low, below 0.5, above 1 Hz and shows the typical low frequency increase due to unmodeled site variations (Silva et al., 1996 [DIRS 110474] Sectn. 5.4.1.2). In general, it shows that the point source is remarkably good at predicting ground motions for the **M** 7.2 event, despite its extended rupture, out to distances near to 200 km. Because there are only 5 rock sites, separate plots are not shown for soil and rock bias and variability. In general the rock sites show a broadband negative bias that is controlled by 2 sites, 29P and SIL.

Figure 7-28a through 7-28e compare the modeled and data spectra for each site. The point source simulations do very well out to about 100 km but appear to under predict beyond this. Site LUC at 1 km from the 80 km-long rupture is modeled remarkably well by the point source for periods up to 10 sec.

7.3.1.8 Validation Results for the 1986 North Palm Springs Earthquake

The **M** 6.0 North Palm Springs earthquake modeling includes 29 sites of which 20 are soil and 9 are rock. Distances vary between 1 and 90 km. The crustal model is taken from Hartzell (1989 [DIRS 164078]) and the point-source stress drop is 62.8 bars. The average kappa values noted above for the Landers earthquake were also used for this Mojave Province earthquake. Source, site and path parameters used are summarized in Table 7-5.

Bias and variability plots for all sites are shown in Figure 7-29. The bias shows the typical negative low frequency over prediction. At higher frequencies the bias is positive indicating a slight under prediction. The variability plot shows higher values than for the Landers earthquake, of about 0.5 between 2 and 100 Hz. The corresponding plots for soil and rock sites separately are shown in Figures 7-30 and 7-31. As expected due to the large number of soil sites, the soil site plots are very similar to the overall plots for all sites. The rock sites however show a high frequency under prediction or negative bias of nearly 0.4 (factor of 1.4) above 6 Hz. The rock site variability is higher than for soil and is large below 4 Hz.

The response spectra plots (Figures 7-32a through 7-32c) show generally poor results for the rock sites while most soil sites are modeled reasonably well. Hartzell (1989 [DIRS 164078]) obtained similar results and attributed the difficulty in modeling the ground motions was due to the complex and varied geology.

7.3.1.9 Validation Results for the 1978 Tabas Earthquake

There are only 4 sites available for the **M** 7.4 Tabas earthquake of which 3 were rock and 1 was soil. The fault distance range is from 3 to 90 km. The crustal model of Hartzell et al. (1991 [DIRS 184462]) was used for the point source modeling. The point source stress drop was 21.5 bars and an average kappa values of 0.046 sec was determined. Source, site and path parameters used are summarized in Table 7-5.

Figure 7-33 shows the bias and randomness plots for the 4 sites. The bias is essentially zero but again shows the low frequency point source over prediction (< 1 Hz). The model variability is high at 0.8. The response spectra (Figure 7-34) indicate that the modeling appears to capture the spectral shapes quite well.

7.3.1.10 Validation Results for the 1979 Imperial Valley Earthquakes

Analyses for both the 1979 **M** 6.4 Imperial Valley mainshock and M 5.3 aftershock are discussed in this section. For the mainshock 33 soil and 2 rock sites were modeled covering a distance range of 1 to 50 km. For the aftershock there were 16 soil sites only over a range of distances between 12 and 52 km. The crustal model of Liu and Helmberger (1983 [DIRS 163922]) was used with the top 98 m replaced with a smoothed version of the El Centro velocity profile of Bycroft (1980 [DIRS 163497]). The point source stress drop is 23.2 bars and point source depth was taken as 8 km for the mainshock and 9.5 km for the aftershock. Kappa values and other source, site and path parameters used are shown in Table 7-5.

First the bias and variability are shown for the **M** 5.3 aftershock (Figure 7-35) for all 16 soil sites. The bias is near zero above 1 Hz to 10 Hz and positive above. The variability is near constant at about 0.5 from 1 to 100 Hz. This is not high as smaller earthquakes tend to show more site-to-site variability than do larger earthquakes (**M** ≥ 6.5) (Silva et al. 1996 [DIRS 110474] Appendix A). The corresponding response spectral plots are shown in Figures 7-36a and 7-36b and generally reflect a good fit out to 1 sec. The high frequency under prediction is driven by site DLT which shows an under prediction by a factor of greater than 3.

For the main shock, bias and variability are shown in Figure 7-37 for all 35 sites. The bias is small from about 0.2 Hz to 100 Hz. The variability is also low and is around 0.5 over most of the frequency range. Figure 7-38 shows the same plots but just for the 33 soil sites. The bias is less positive and the variability has dropped slightly showing a general improvement. Because there are only 2 rock sites then separate plots for these are not shown. Spectral plots (Figures 7-39a through 7-39c) show reasonable agreement between recorded and modeled ground motions, particularly for the soil sites, with the exception of site DTA, which shows a large broadband under prediction. Sites EMO and E07 show mismatches in their spectral peaks between the simulation and recorded motions, indicating too little non-linear response in the equivalent-linear analyses. These two sites appear to have undergone the most non-linearity and the G/G_{max} and hysteretic damping curves are probably too linear for these sites. For the other sites close-in the spectral peaks around 0.2 sec appear to be modeled well.

7.3.1.11 Validation Results for the 1985 Nahanni Earthquake

The 1985 **M** 6.8 Nahanni earthquake occurred in western Canada but is considered to have features in common with ENA earthquakes: thrust mechanism with regional compressive stresses, area of low seismicity and high velocity crust. It is considered an ENA analogue and represents typical ENA source, path and site characteristics. Low kappa values are expected and the Q(f) model is fixed at $317f^{0.6}$ as determined in the Saguenay inversion (Silva et al. 1996 [DIRS 110474]). Only 3 sites, all hard rock, were recorded for this earthquake. The rupture surface dips 25º to the southwest with the top edge at a depth of 4 km. The crustal model of Hartzell et al. (1994 [DIRS 184135]) was used. The point source stress drop from the inversion was low at 13.4 bars and average kappa values of 0.016 sec. Source, site and path parameters used are summarized in Table 7-5.

The spectral plots (Figure 7-40) show point source modeling for sites 2 and 3 in fair agreement to the recorded motions but are high at long period and under predict at short periods. Site 1 shows the largest under prediction present. The bias and variability are unconstrained (Figure 7-41) but reflect the general fair fit at all three sites.

7.3.1.12 Validation Results for the 1987 Superstition Hills Earthquake

The 1987 **M** 6.7 Superstition Hills earthquake modeled here is the larger of the two events that occurred on the same day, November 24. A total of 12 sites were modeled, only one of which is a rock site. Because of its close proximity to the Imperial Valley, the same velocity profiles are used here for modeling this event. The point source stress drop is 43.4 bars and the point source depth is 9 km, the depth of the largest asperity in the Wald et al. (1990 [DIRS 184356]) slip model. The average kappa value for soil is 0.051 sec, very similar to that of the Imperial Valley mainshock inversion. The single rock site gave a kappa of 0.028 sec, slightly lower than that obtained from the Imperial Valley inversions. Source, site and path parameters used are summarized in Table 7-5.

Figure 7-42 shows the model bias and variability for all 11 sites. The bias is slightly negative (over prediction) and uniform from about 0.3 Hz to 100Hz. The variability is low over the same range, averaging around 0.4. The model appears to predict quite well as can also been seen in the response spectral plots (Figure 7-43) which show the over prediction, which appears largest at BRW. Except for the rock site, SSM, the model overall captures the levels and shapes well. Site PTS is over the fault and shows a small short period over prediction.

7.3.1.13 Validation Results for the 1988 Saguenay Earthquake

The **M** 5.8 Saguenay earthquake occurred in Quebec, within the geographic ENA province. This is the largest and most widely recorded earthquake in ENA tectonic environment. To match the high-frequency spectral levels for this earthquake a large point-source stress drop is required. A 2-corner source spectral model appears to best fit this earthquake's spectral shape. There are 22 rock sites modeled for this earthquake. Source to site distances go up to over 400 km. The crustal model of Hartzell et al. (1994 [DIRS 184135]) is used. The point source stress drop is very high at 572 bars and the depth is at 26 km, the center of the high slip region in the single asperity. An average kappa of 0.023 sec was determined from the inversion and the Q model is $317f^{0.86}$. Source, site and path parameters used are summarized in Table 7-5.

Figure 7-44 shows the model bias and variability plots for the Saguenay earthquake. Silva et al. (1996 [DIRS 110474] list the "frequencies at 1 Hz and above [as] the range of reliable analyses" for this earthquake, although frequencies below this limit are included in Figures 7-44 and 7-45. The bias changes from a strong over prediction at about 1 Hz to under prediction at 10 Hz. The variability is high ranging from 0.5 at high frequency (≥ 10 Hz) and increases. These high values are expected at distances out to 500 km. Also 9 of the 22 sites are vertical component stations that have been converted to horizontals using a H/V ratio of 1.4. Use of a more accurate empirical frequency-dependent H/V relationship is complicated by the choice of appropriate crustal amplification factors to apply to the converted horizontal components (Silva et al. 1996 [DIRS 110474])Taking these into account the results are generally good. The response spectral plots (Figures 7-45a and 7-45b) reflect a fair fit at high frequency and low frequency over prediction, especially close in. At more distant sites (> 100 km), there is a low-frequency under prediction. Overall, the results of modeling the Saguenay earthquake indicate that this event is significantly different in its spectral composition than the other earthquakes modeled in this validation (Silva et al. 1996 [DIRS 110474]).

7.3.1.14 Validation Results for the 1992 Little Skull Mountain Earthquake

The **M** 5.7 Little Skull Mountain earthquake occurred close to Yucca Mountain. In addition to the mainshock, two large aftershocks were used in the inversion. A total of 8 recordings were obtained, all of which are at rock sites. The crustal model used is based on a regional earthquake location model refined at the near-surface using geophysical data. The point source stress drop is 63.7 bars and the point source depth is taken as 12 km. The inversion gave a kappa value of 0.023 sec and Q(f) model of $256f^{0.47}$. Source, site and path parameters used are summarized in Table 7-5.

Figure 7-46 shows the model bias and variability plots computed over the 8 sites. The bias shows the usual point source over prediction ranging from about -1 at 0.5 Hz and increasing to zero around 5 Hz. The variability is low above 10 Hz and about 0.5 from 2 to 10 Hz. Below 2 Hz it is very high but the randomness (bias corrected variability) remains uniform. Most sites appear to have a large misfit as can been seen on the response spectral plots (Figure 7-47). Here it can be seen that the point source is doing well at short period (≤ 0.5 sec), over predicting at intermediate periods and converging to the recorded motions at long periods (> 1 sec).

7.3.1.15 Validation Results for the 1992 Cape Mendocino Earthquake

The **M** 6.8 Cape Mendocino earthquake is the largest instrumentally recorded event associated with the Cascadia subduction zone. A total of 5 sites were used for the modeling and inversion for this earthquake, all but one of which were soil sites. Source-to-site distance range is 8 to 45 km. The crustal model of Graves (1994 [DIRS 164251]) was used with generic rock and soil profiles for the near surface. The point source stress drop is 27.2 bars and the average soil kappa was 0.068 sec as determined from the regional inversion (Silva et al. 1996 [DIRS 110474] Table 5.37).

With only 5 sites, the model bias and variability estimates are poorly constrained (Figure 7-48) as can be seen in the large ±90% confidence limits. The bias indicates a large under prediction at high frequencies beginning at 1 Hz. The variability is 0.75, above 1 Hz indicating a poor fit. This can also be observed in the response spectral plots (Figure 7-49).

7.3.1.16 Summary of Comparisons with Each Earthquake

In all the sixteen earthquakes discussed in Silva et al. (1996 [DIRS 110474]), the point-source model appears to predict ground motions reasonably well, except for those of the 1992 **M** 6.8 Cape Mendocino earthquake, where none of the models fit the actual data well. The proposed explanation for this is perhaps that the point-source distance definition is poor where sites are over or near the edges of shallow-dipping rupture surfaces as is the case for the Cape Mendocino earthquake. In the 1992 **M** 7.2 Landers earthquake, the point-source model appears to predict well out to 100 km but seriously under predicts the ground motions at low frequency beyond this source-to-site distance. This under prediction is thought to be magnitude-dependent and suggests a magnitude-dependent far-field fall-off should be incorporated into the point-source model.

7.3.1.17 Comparisons for Whole Data Set

The bias and variability estimates were computed for the whole data set of the 16 earthquakes recorded at 503 sites (Table 7.4), which reflect magnitudes between **M** 5.3 (Imperial Valley aftershock) to **M** 7.4 and a site distance range of 1 to 218 km (460 km for CEUS). This is a comprehensive data set that can provide a statistically robust assessment of the point source model.

Figures 7- 50 through 7-52 show model bias and variability for all sites, and for soil or rock sites. Over all sites there is zero bias between about 1 to 10 Hz, a slightly positive bias (under prediction) for frequencies greater than 10 Hz and a negative bias below 1 Hz, which results in over prediction at these frequencies. Model variability is reasonable (about 0.5 above 3 to 4 Hz) and increases with decreasing frequency to near 1 at 0.3 Hz. Above 1 Hz there is little difference between total variability (uncertainty and randomness) and randomness (bias corrected variability) reflecting the near zero bias. Below 1 Hz there is significant uncertainty contributing to the total variability suggesting that the model can be improved upon as its predictions tend to be consistently high at low frequencies (≤1 Hz). This consistent misfit may be interpreted as a second corner frequency for WNA earthquakes.

Soil sites show a slight improvement at 1 Hz in both bias and variability (Figure 7-51) and the converse is seen for rock sites, which show a larger bias and variability estimate than for all sites (Figure 7-52). This indicates that soil sites are modeled more accurately than rock sites. Strong ground motions at rock sites thus are more variable than at soil sites and the point-source model is not predicting the increased site-to-site variation.

7.3.1.18 Summary of Validation with Recorded Motions

Overall, the point-source model gives bias estimates near zero for frequencies above 1 Hz and variabilities range from sigma (ln) 0.5 to 0.6. These are low considering that for the majority of sites, generic site conditions were used. In several cases, strong site effects were observed, which cannot be captured by the point-source model without greater knowledge of the site conditions.

7.3.2 Validation against Spectral Shapes

Further validation of the point-source model compared results of point-source simulations with statistical spectral shapes.

7.3.2.1 Variation in Spectral Shapes

It can be observed that spectral shapes depend strongly on site classifications and vary significantly (Figure 7-53) (from Seed et al. 1976 [DIRS 183433]). They result from site-dependent ground motion characteristics and from vertical variations in soil material properties. It also appears that with an increasing strong motion database, that spectral shape is also magnitude dependent as well (Joyner and Boore 1988 [DIRS 106268], Idriss 1985 [DIRS 183577], Silva and Green 1989 [DIRS 182433], Boore et al. 1994 [DIRS 124240], Silva and Darragh 1995 [DIRS 105398]) and that site effects extend to rock sites as well (Boatwright and Astrue 1983 [DIRS 184397], Campbell 1981 [DIRS 102191], Cranswick et al. 1985 [DIRS 183434], Silva and Darragh 1995 [DIRS 105398]). Figures 7-54 and 7-55 show average spectral shapes recorded on rock at close distances to small and large earthquakes. For both magnitudes, **M** 6.4 and 4.0, recorded in ENA show a dramatic shift in maximum spectral amplifications towards shorter periods compared to those in WNA. The differences are pronounced and represent a difference in shear-wave velocity and damping under the site (Boore and Atkinson 1987 [DIRS 182044], Toro and McGuire 1987 [DIRS 183435], Silva and Green 1989 [DIRS 182433], Silva and Darragh 1995 [DIRS 105398]). Also strong magnitude dependence can be seen with smaller earthquakes having a narrower bandwidth, which results from a lower corner frequency (Boore 1983 [DIRS 103317], Silva and Green 1989 [DIRS 182433], Silva 1991 [DIRS 163656], Silva and Darragh 1995 [DIRS 105398]).

7.3.2.2 Spectral Shapes

To compute statistical spectral shapes, earthquake spectra were sorted into magnitude bins of ½ magnitude units from **M** 5.5 to 7.5, so as to retain enough information in each bin and to constrain the shape. There was a 0.1 magnitude unit overlap so that some spectra are included in two bins. The distance range was selected to be 0 to 50 km to minimize distance effects on shapes as spectral shape is weakly dependent on distance in this range in WNA (Silva and Green, 1989 [DIRS 182433]; Silva et al. 1996 [DIRS 110474] Appendix A).

The soft rock statistical shapes were computed from recordings listed in Silva et al. (1996 [DIRS 110474], Appendix B) using data for Geomatrix site classes A or B. Figure 7-56 shows the clear spectral peak shift with magnitude and also spectrum broadening with increasing magnitude.

The deep soil statistical shapes were computed from recordings listed in Silva et al. (1996 [DIRS 110474]) Appendix B using data for Geomatrix site classes C or D. Figure 7-57 shows the median statistical spectra for each magnitude bin. The long-period broadening increases as magnitude increases as with soft rock spectra. The **M** 7.5 maximum spectral amplification shifts to longer period, unlike the rock case. These results indicate the strong magnitude dependence on the shape. The variability in shape has contributions from magnitude, distance and mechanism as well as class site variations. Consequently, it should be much larger than the variability introduced by site variation in the computed point-source or empirical shapes.

The point-source model shapes were computed using generic soil and rock profiles for the mean distance and magnitude bins (Silva et al. 1996 [DIRS 110474] Table 7.1). The rock and soil profiles were randomized (30 realizations) so that the variability observed is just for the site contribution alone. For soil the depth to bedrock was varied between 100 ft and 1000 ft. Stress drop was a constant 59 bars, which was taken from the inversion in the previous validation section.

Empirical spectral shapes were computed using a vertical strike-slip earthquake using an early version of the Abrahamson and Silva (1997 [DIRS 104205]) relationship in Appendix A (Silva et al. 1996 [DIRS 110474]) for the same magnitude and distance bins as used for the model shapes.

7.3.2.3 Comparison Between Statistical, Point-Source Model, and Empirical Spectral Shapes

Figure 7-58 shows the comparison for rock sites for all three spectral shape sets (statistical, point-source model and empirical attenuation relation from in Appendix A of Silva et al. (1996 [DIRS 110474]). Magnitudes and distances are listed in Table 7-6.. Each comparison of spectral shapes represents a single magnitude bin with the $\pm$ 1σ bounds for the statistical shape and the median model spectra. In general there is close agreement between all three sets of spectra over the entire bandwidth and all magnitude bins. The point-source over prediction at long periods is observed at **M** 6.5 to 7.5.

Table 7-6. Magnitude and Distance Data for Statistical Response Spectral Shapes

Magnitude (Range, Mean, Bin)	Number of Spectra	Number of Earthquakes	Distance (Range, Mean; in km)	Expected Rock PGA (Strike Slip)
Soft Rock				
4.7-5.3, 5.0, 5.0	90	15	0-50, 13.5	0.062
5.2-5.8, 5.5, 5.5	108	18	0-50, 16.9	0.077
5.7-6.3, 6.0, 6.0	146	21	0-50, 22.1	0.095
6.2-6.8, 6.5, 6.5	148	12	0-50, 27.1	0.120
6.7-7.3, 6.8, 7.0	104	7	0-50, 26.0	0.154
7.2+, 7.4, 7.5	8	8	0-50, 15.8	0.295
Deep Soil				
4.7-5.3, 5.1, 5.0	145	22	0-50, 15.8	0.060
5.2-5.8, 5.4, 5.5	159	35	0-50, 18.3	0.079
5.7-6.3, 6.0, 6.0	337	25	0-50, 23.2	0.096
6.2-6.8, 6.5, 6.5	342	17	0-50, 27.3	0.122
6.7-7.3, 6.9, 7.0	219	8	0-50, 28.3	0.140
7.2+, 7.3, 7.5	50	4	0-50, 34.0	0.145

Note: Rock PGA from empirical attenuation relationship.

Source: Silva et al. (1996 [DIRS 110474]) Table 7.1

Figure 7-59 shows the same comparison but for deep soil sites for the same magnitude bins. Note that the statistical spectra are smoother as there are a larger number of sites in the data set. The comparison shows that the agreement is generally good and even a bit better than for rock sites.

In summary, the point-source model spectra provide a good fit to the statistical shapes and the empirical shapes computed from the attenuation model in Silva et al. (1996 [DIRS 110474]) Appendix A. The main exception is the large magnitude over prediction of the point-source model, which results in an additional degree of conservatism in engineering design using this model.

7.4 APPLICABILITY OF MODEL VALIDATION APPROACHES TO YUCCA MOUNTAIN

One of the point-source validations against recorded motions was for the 1992 **M** 5.7 Little Skull Mountain earthquake that occurred at the Nevada Test Site (NTS) near Yucca Mountain. This validation exercise provides some idea of the applicability of the point-source model for this region. However, this only provides site-specific validation for earthquakes in the smaller magnitude range and does not provide for the desired full range in ground motion levels and site conditions as it was only recorded at 8 sites (Figure 7-47). The lack of strong ground motion data recorded at Yucca Mountain necessitates an appeal to validation of the modeling approach carried out at other locations. Successful validation of the modeling approach for a number of different earthquakes and sites, as discussed in Section 7.3, provides the needed confidence that the approach is appropriate for Yucca Mountain and, with the development of appropriate inputs, the Yucca Mountain site response model is also valid.

For validation of the point-source model with the recorded motions of the 1992 **M** 5.7 Little Skull Mountain mainshock, two large aftershocks were also used in the inversions to constrain the site kappa for the point-source model. In the comparison of the point-source modeling with the recorded data for the mainshock, the bias and variability estimates computed for the 8 sites have wide confidence limits due to the small number of sites (Figure 7-46). The bias shows the typical low frequency point-source over prediction with a maximum at about 0.5 Hz and a decrease to none at about 5 Hz. The variability is low above 10 Hz, somewhat greater from 2 Hz to 10 Hz, and below 2 Hz it is very high although the randomness (bias corrected variability) remains uniform. In the Little Skull Mountain comparison, the point source model appears to do well at short periods (≤ 0.5 sec), over predicts between 0.5 sec and 2.0 sec , and then converges on the recorded motions for several sites at long period (> 1 sec).

In summary, the point-source modeling of the 1992 Little Skull Mountain is similar to the validation against all 16 earthquakes (Section 7.3.1; Silva et al. 1996 [DIRS 110474]). Thus the model predicts ground motions in the Yucca Mountain region reasonably well over the range of magnitudes and distances considered in this study.

7.5 INDEPENDENT TECHNICAL REVIEW

An additional activity to build confidence in the stochastic point-source model was an independent technical review. The review was carried out on a draft of Section 7 (Point-Source Model Validation) of this report. A reviewer was selected who was independent of the checking and interdisciplinary review of the report. The reviewer has expertise in one or more of the following technical areas: probabilistic seismic hazard analyses, ground motion site response, characterization of rock/soil for site response analyses, and use of analysis results. The review was performed by Dr. Richard Lee of the Los Alamos National Laboratory. His complete review is contained in Appendix E.

In Dr. Lee's review, he concluded that "With the exception of items identified below, the point-source stochastic ground motion model validation meets the key elements (listed below) of the Model Validation Checklist (BSC Form 1098 in LP-SIII.10Q-BSC)."

Dr. Lee states in his review: "The primary element of the validation of the point-source stochastic ground motion model is the comparison of the model predictions to recorded earthquake spectra. The validation does this for fifteen earthquakes that produce a wealth of strong motion data used in engineering design. The modeling includes a large range in magnitude (**M** 5.3 to **M** 7.4) and distance from 1 to 400 km in a variety of crustal models and several site conditions. This comparison goes well beyond typical validation studies of comparing ground motions for a single well-recorded earthquake and incorporates comparisons for a large number of earthquakes identifying strengths and weaknesses including inherent conservatisms with use of the methodology."

He states also that: "The validation using spectral shapes (Section 7.3.3) is also an appropriate and important comparison that compensates somewhat for the lack of well recorded strong motion earthquakes in other tectonic environments such as the eastern United States."

In summary, the independent technical review of the stochastic point-source model concluded that the model was appropriately validated and appropriate for its intended use. Dr. Lee had a number of comments on the presentation in Section 7 and these have been addressed in this final version.

7.6 MODEL VALIDATION SUMMARY

The stochastic point-source model used to predict earthquake ground motions has been in use in the seismologic community for nearly 30 years. A number of seismologists have applied the model to numerous seismotectonic settings and published their results in peer-reviewed scientific journals as previously discussed. The point-source model was used in the Yucca Mountain Scenario ground Motion Modeling Project (Schneider et al. 1996 [DIRS 103270]) and in the Yucca Mountain PSHA (CRWMS M&O 1998 [DIRS 103731]). In the latter, seven of the leading ground motion experts in the U.S. included point-source modeling of ground motions in their interpretations (CRWMS M&O 1998 [DIRS 103731]; Stepp et al. 2001 [DIRS 158656]).

In a DOE-sponsored validation project, to provide a quantative assessment of the predictive ability of the stochastic point-source and finite-fault models in terms of estimating model bias and variability, a total of five earthquakes were modeled at 503 sites over the fault distance range of about 1 to 177 km (Silva et al. 1996 [DIRS 110474]). Point-source inversions of the earthquakes were performed to provide stress drop and regional Q(f) models to be used in forward simulations. These results showed regional differences in Q(f) models as well as rock and soil site kappa values.

Model bias and variabilities were estimated for the 16 study earthquakes over all 503 sites for both the point- and finite-source models. In general, the bias estimates were low and the variabilities small, with the best results for the most well recorded earthquakes (Silva et al. 1996 [DIRS 110474]). There were exceptions, and in these cases both the point-and finite-source model provided poor results (e.g., North Palm Springs earthquake).

The final bias and variability estimates computed for all the earthquakes and over all the sites showed near zero bias for frequencies of about 1 Hz and above the for both the point- and finite-source models (Silva et al. 1996 [DIRS 110474]). The point-source model shows a stable and significant negative bias (over prediction) from about 1 Hz to 0.3 Hz (the approximate low frequency limit for the model) (Silva et al. 1996 [DIRS 110474]).

To validate the magnitude and site dependency for response spectral shapes, the stochastic point-source model was compared to statistical shapes computed form the strong motion database as well as shapes form the empirical attenuation relation for magnitude bins centered on **M** 5.5, 6.0, 6.5, 7.0, and 7.5 (Silva et al. 1996 [DIRS 110474]). Both soft rock and deep soil comparisons were made. The results showed that the point-source model, using vertically propagating shear-waves and equivalent-linear site response provided about as good a match to the statistical shapes as did the empirical model. The main exception being a large magnitude, long-period over prediction present in both the point-source and empirical shape estimates. The point-source model generally captures the appropriate magnitude dependency shown in the statistical and empirical shapes and vertically propagating shear-waves using equivalent-linear site response captures the site dependency. These results indicate that the point-source model can be used to develop response spectral shapes for source, path, and site conditions, which are not well represented with ground motion recordings.

In general, this project has demonstrated that the stochastic point- and finite-source models produce accurate predictions for strong ground motions over the distance range of 0 to 100 km and for magnitudes **M** 5.0 to **M** 7.5. There are limitations. The point-source seriously under predicts at intermediate periods for the joint occurrence of **M** $\geq$ 6.5 and distances greater than about 100 km. A higher stress drop can be used but will result in over predictions at short distances for large magnitude. Additionally, the point-source model over predicts for frequencies below about 1 Hz, particularly for **M** $\geq$ 6.5. Finite-fault simulations reduced the under prediction by 50%, supporting the magnitude dependent attenuation rate being due to source finiteness and suggesting that the remaining 50% may be due to wave propagation effects in crossing crustal structure boundaries (Silva et al. 1996 [DIRS 110474]).

The stochastic point-source ground motion model has been validated by applying acceptance criteria based on an evaluation of the model's relative importance to the potential performance of the repository system. Validation requirements defined in LP-SIII.10Q-BSC have been fulfilled. The validation activities described establish the scientific bases for the point-source model. Based on this, the point-source model is considered to be sufficiently accurate and adequate for the intended purpose with the stated limitations and to the level of confidence required by the model's relative importance to the potential performance of the repository system.

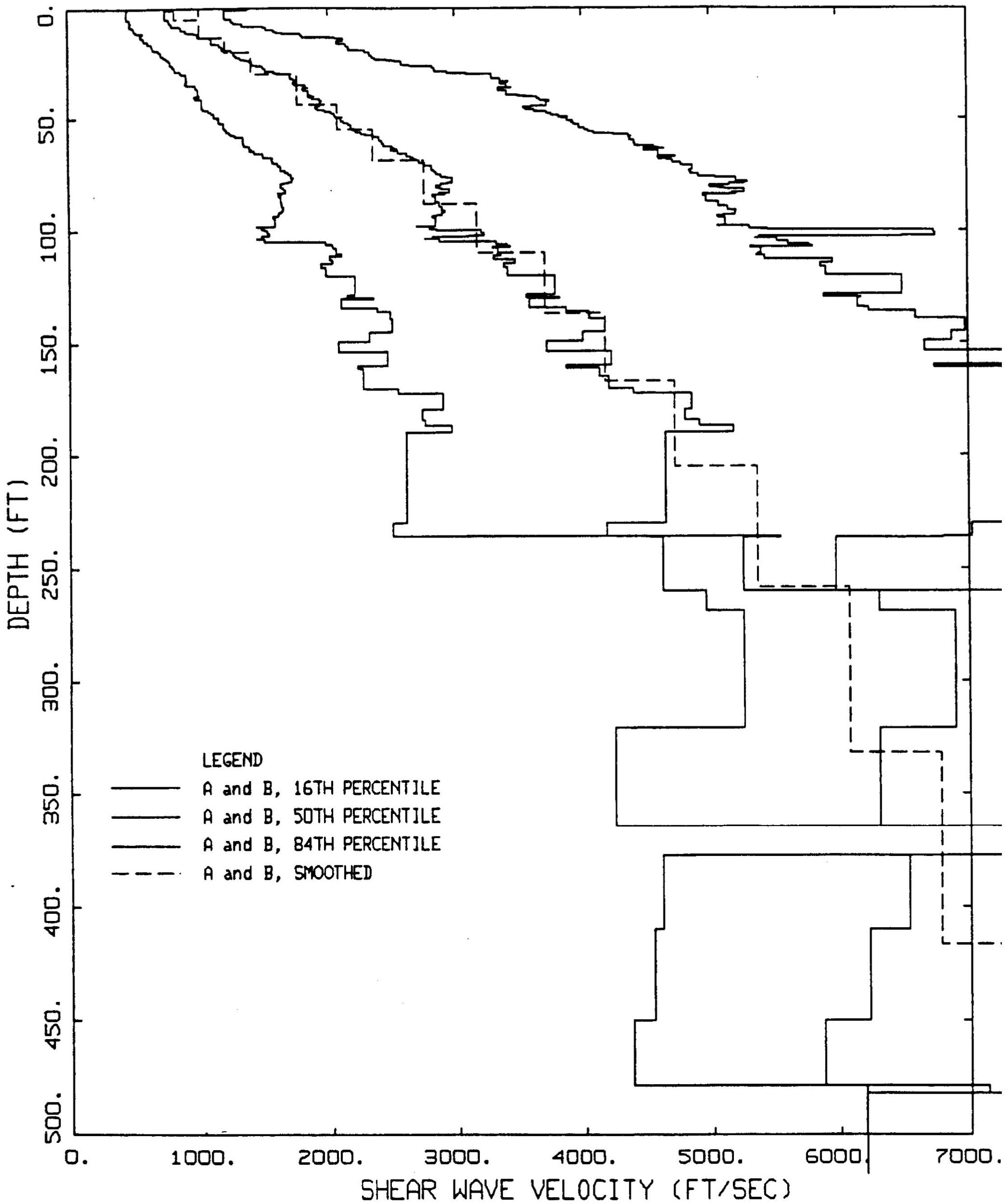

Source: Silva et al. 1996 [DIRS 110474] Figure 3.2

Figure 7-1a. Median and ± 1σ Shear-Wave Velocity Profiles for Soft Rock (Geomatrix A and B) (solid lines) and Smooth Base Case Soft Rock Profile (dashed line)

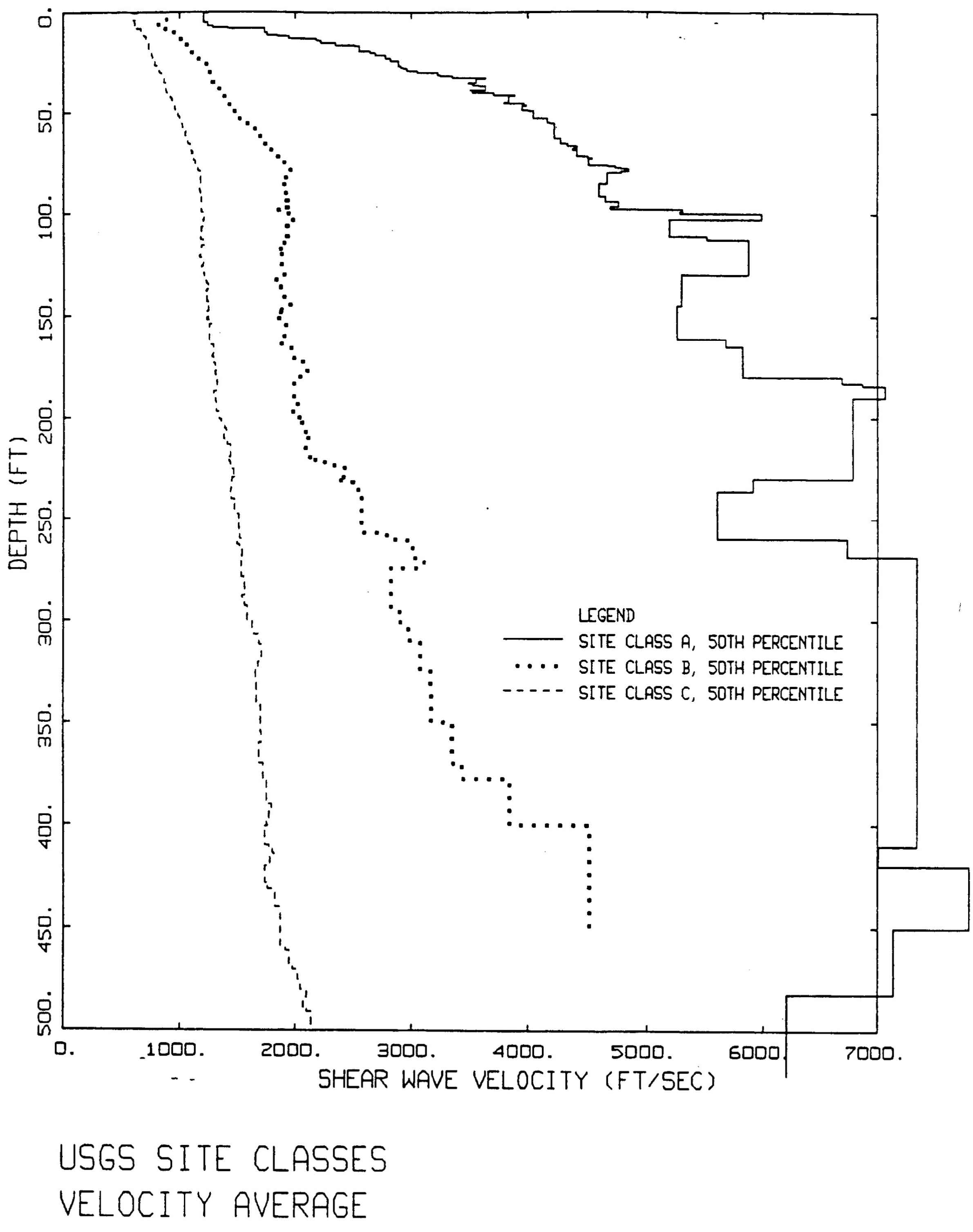

Source: Silva et al. 1996 [DIRS 110474] Figure 3.3

Figure 7-1b. Median Shear Wave Velocity Profiles for USGS Site Classes A, B and C

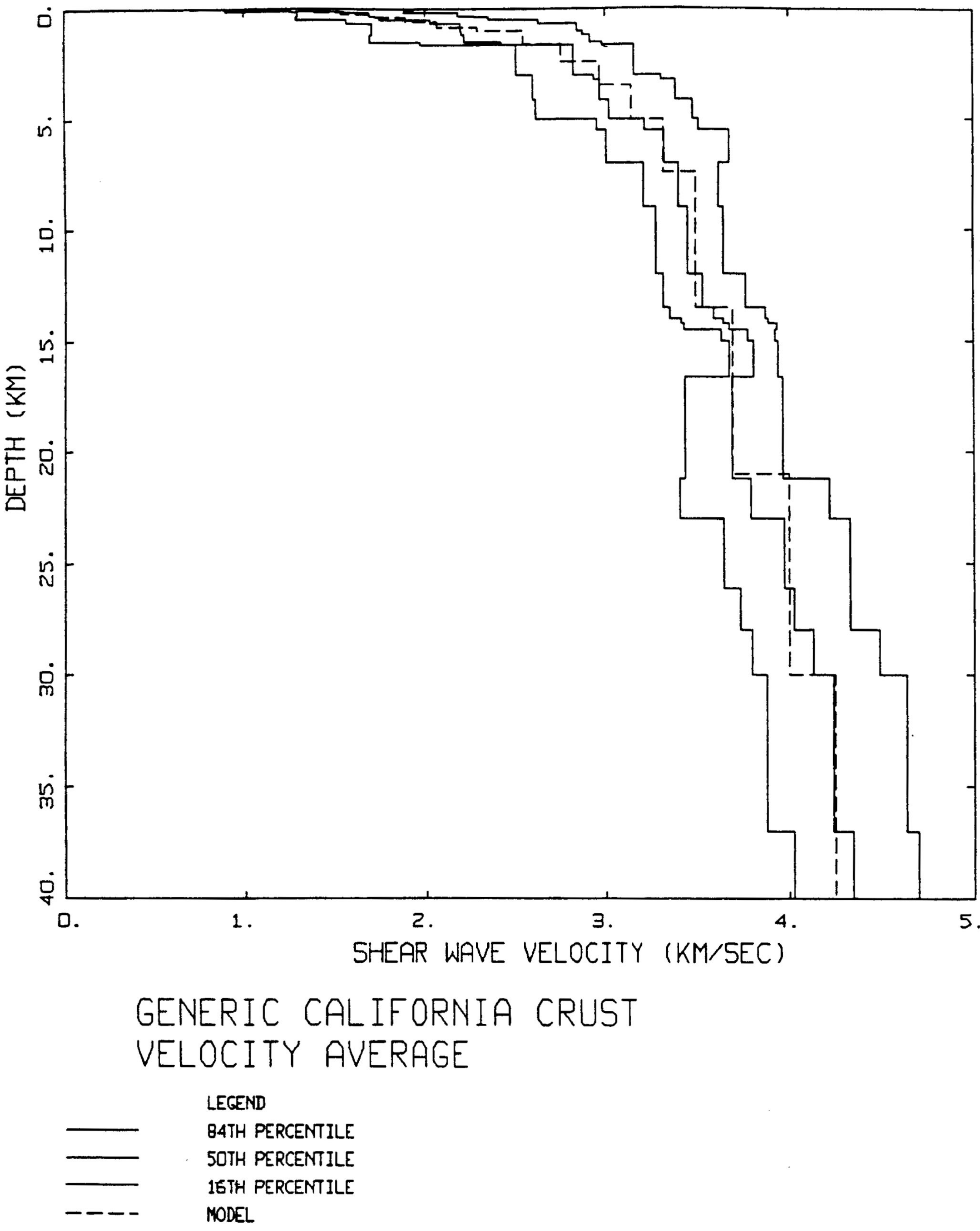

Source: Silva et al. 1996 [DIRS 110474] Figure 3.11

NOTE: Smooth base case model (dashed lines)

Figure 7-2. Median and ± 1σ Shear-Wave Velocity Profiles Computed From the Crustal Models Listed in Table 7-2 (solid lines)

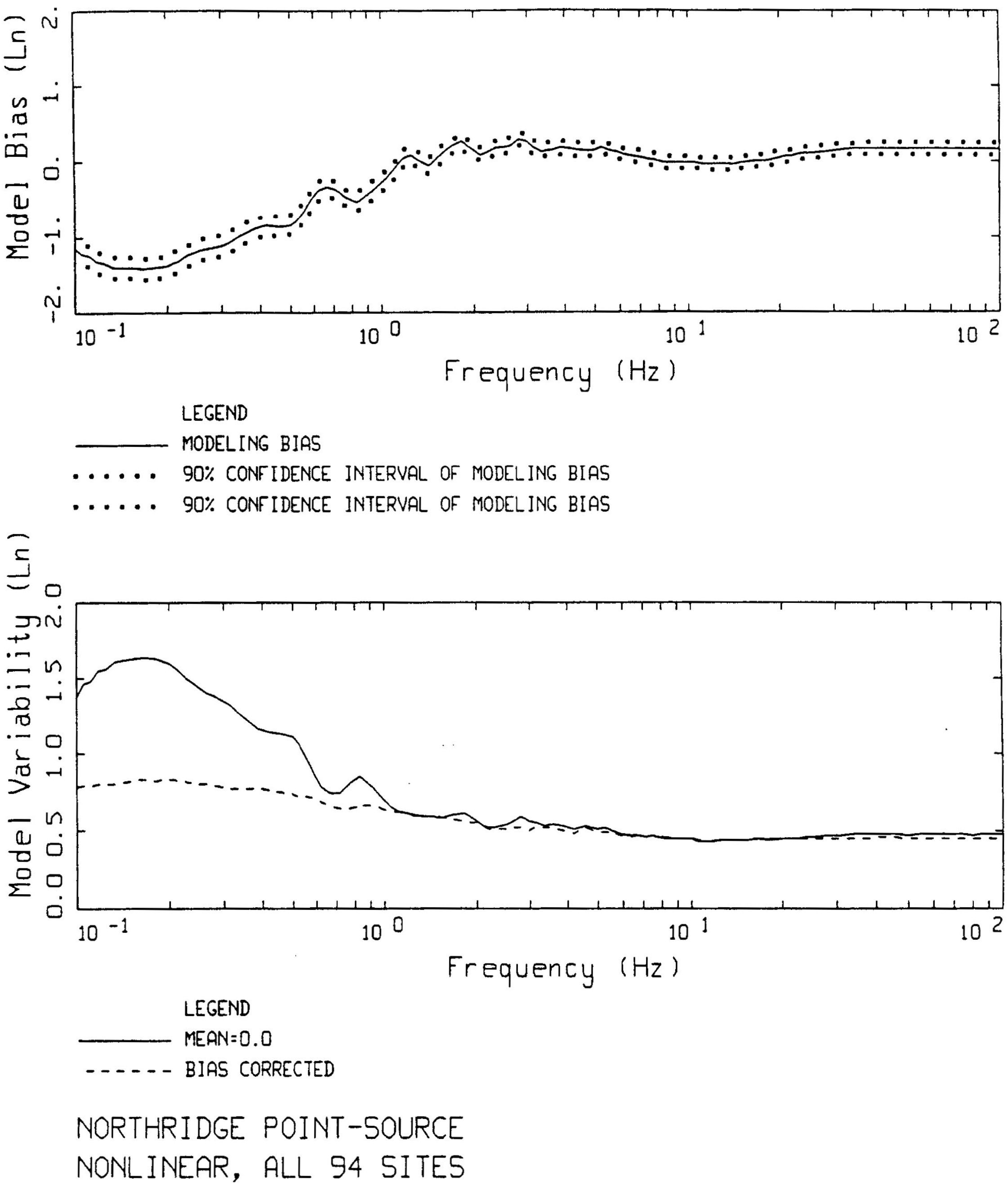

Source: Silva et al. 1996 [DIRS 110474] Figure 5.3

Figure 7-3. Model Bias and Variability Estimates fo r the Northridge Earthquake Computed Over All 94 Sites for the Point-Source Model

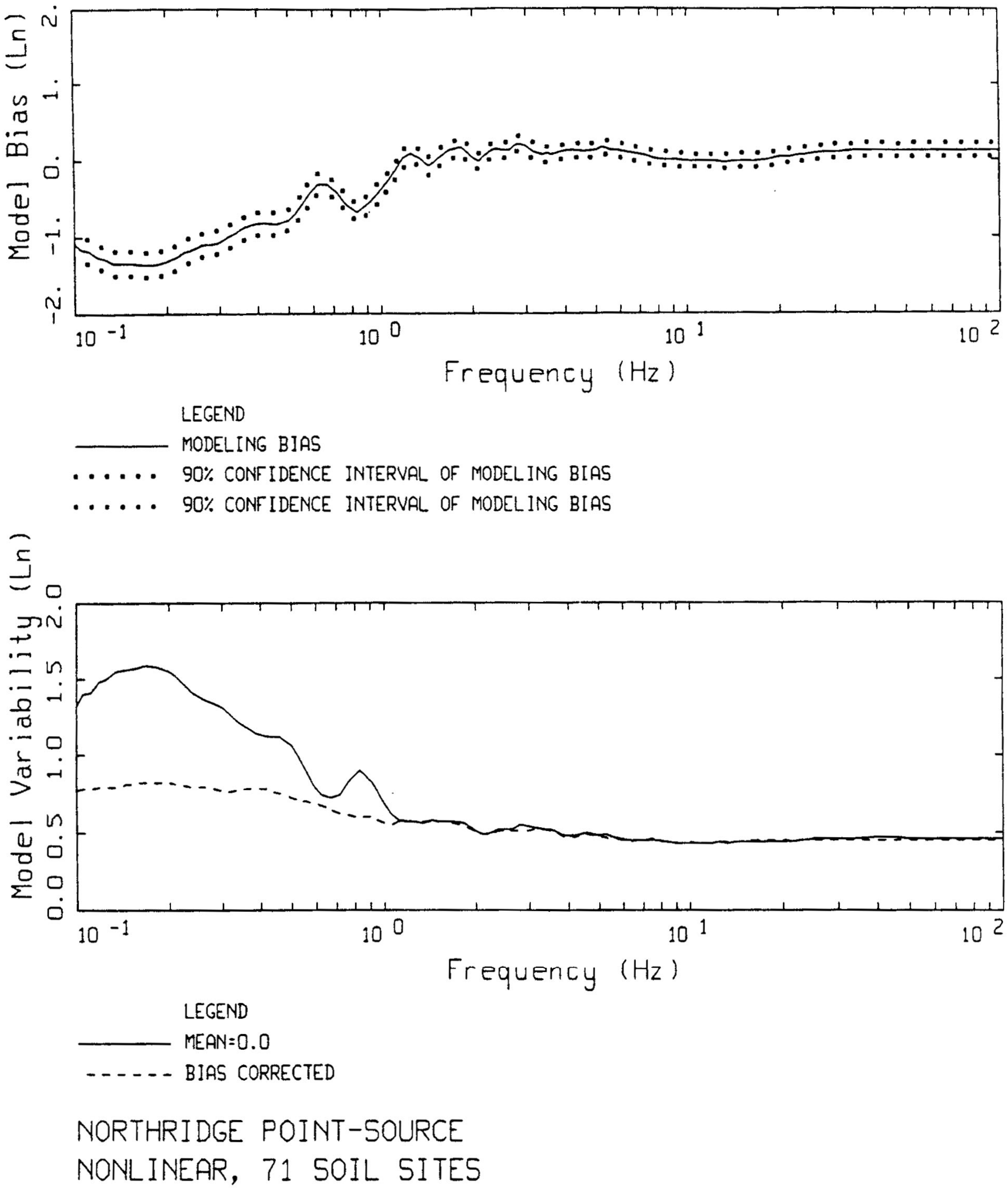

Source: Silva et al. 1996 [DIRS 110474] Figure 5.4

Figure 7-4. Model Bias and Variability Estimates fo r the Northridge Earthquake Computed Over All 71 Soil Sites for the Point-Source Model

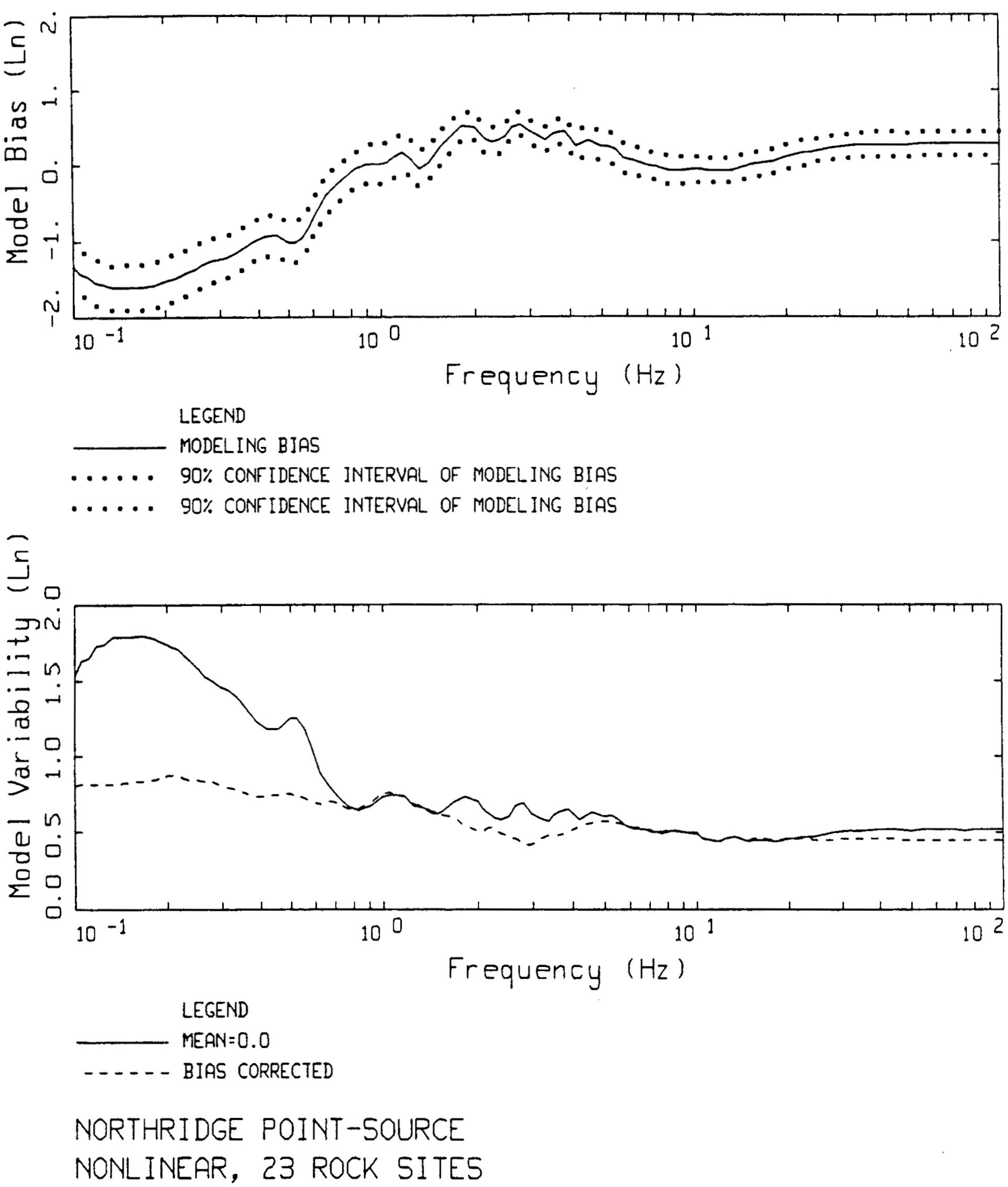

Source: Silva et al. 1996 [DIRS 110474] Figure 5.5

Figure 7-5. Model Bias and Variability Estimates fo r the Northridge Earthquake Computed Over All 23 Rock Sites for the Point-Source Model

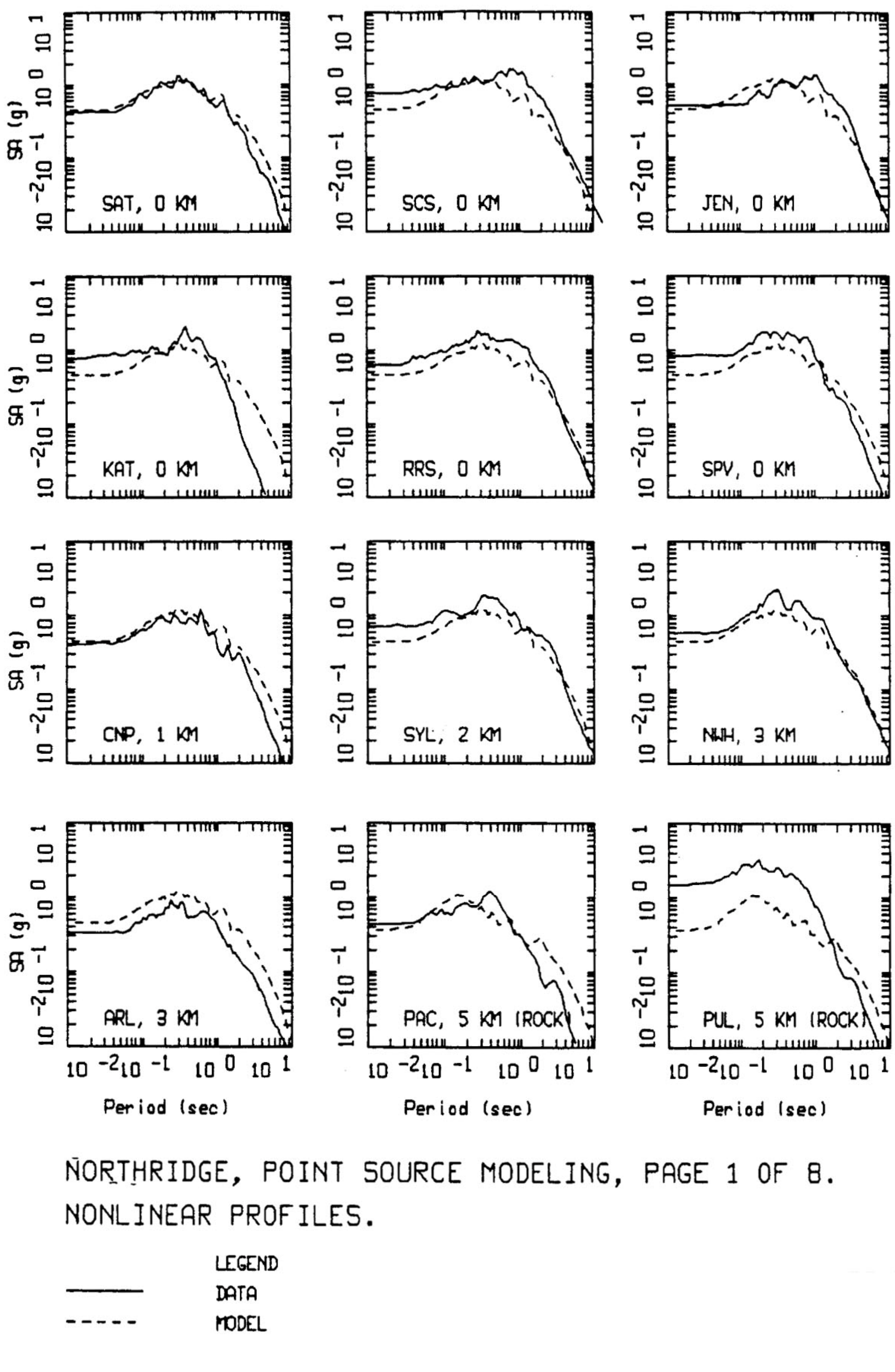

Source: Silva et al. 1996 [DIRS 110474] Figure 5.6

NOTE: Recorded Motions (solid lines), Point-Source Simulations (dashed lines)

Figure 7-6a. Comparison of Average Horizontal Component 5%-Damped Pseudo Relative Absolute Response Spectra: Northridge Earthquake

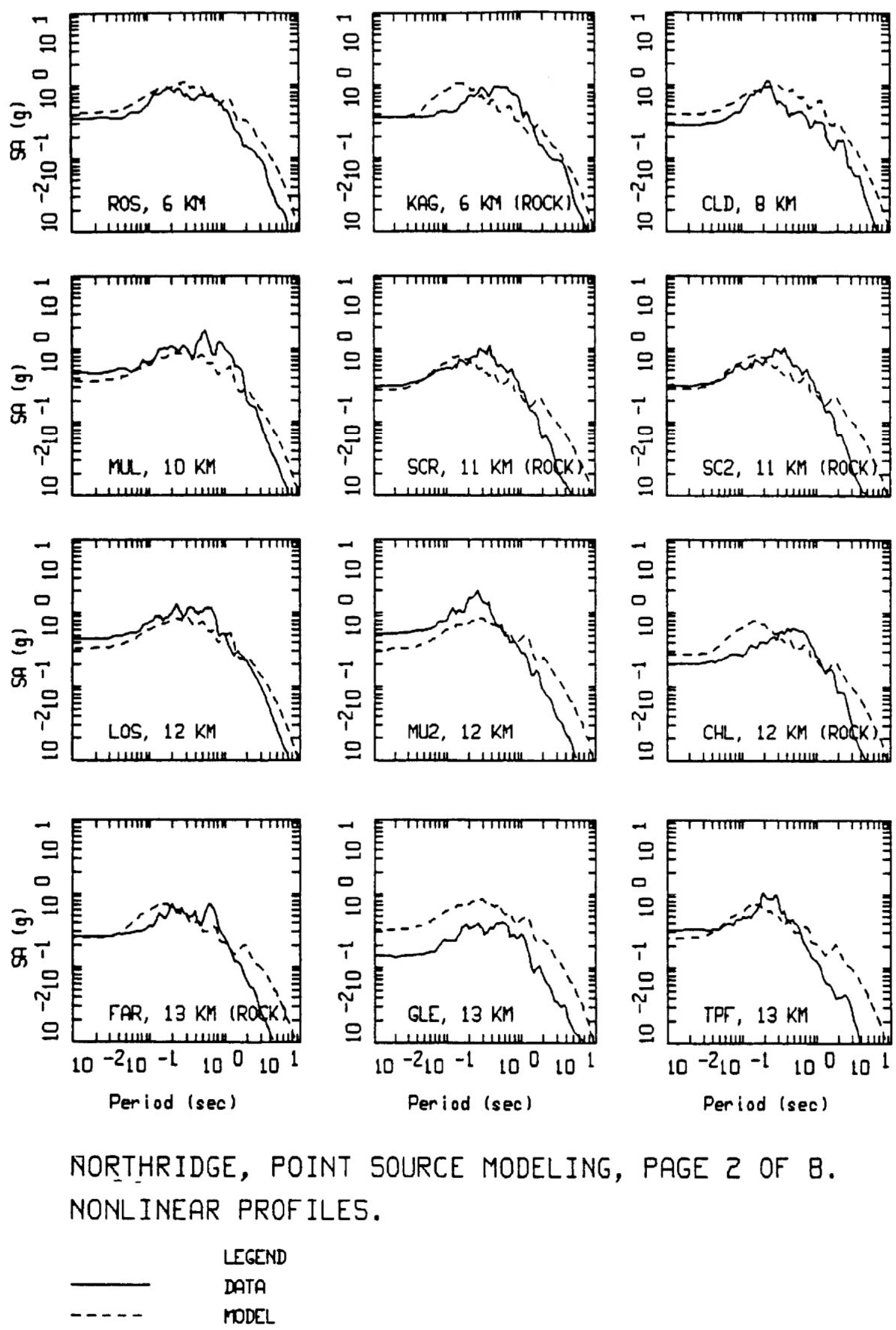

Source: Silva et al. 1996 [DIRS 110474] Figure 5.6

NOTE: Recorded Motions (solid lines), Point-Source Simulations (dashed lines)

Figure 7-6b. Comparison of Average Horizontal Component 5%-Damped Pseudo Relative Absolute Response Spectra: Northridge Earthquake

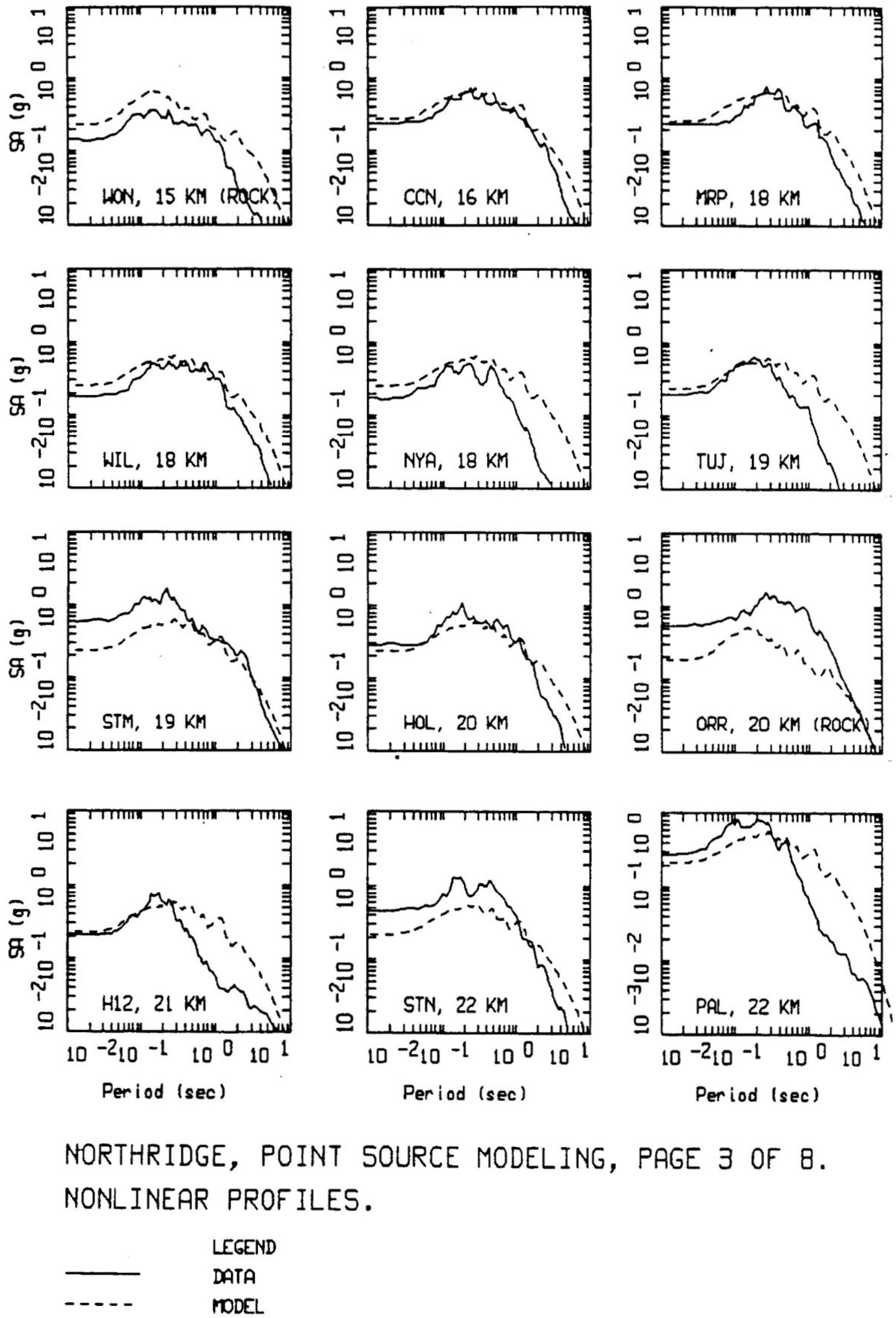

Source: Silva et al. 1996 [DIRS 110474] Figure 5.6

NOTE: Recorded Motions (solid lines), Point-Source Simulations (dashed lines)

Figure 7-6c. Comparison of Average Horizontal Component 5%-Damped Pseudo Relative Absolute Response Spectra: Northridge Earthquake

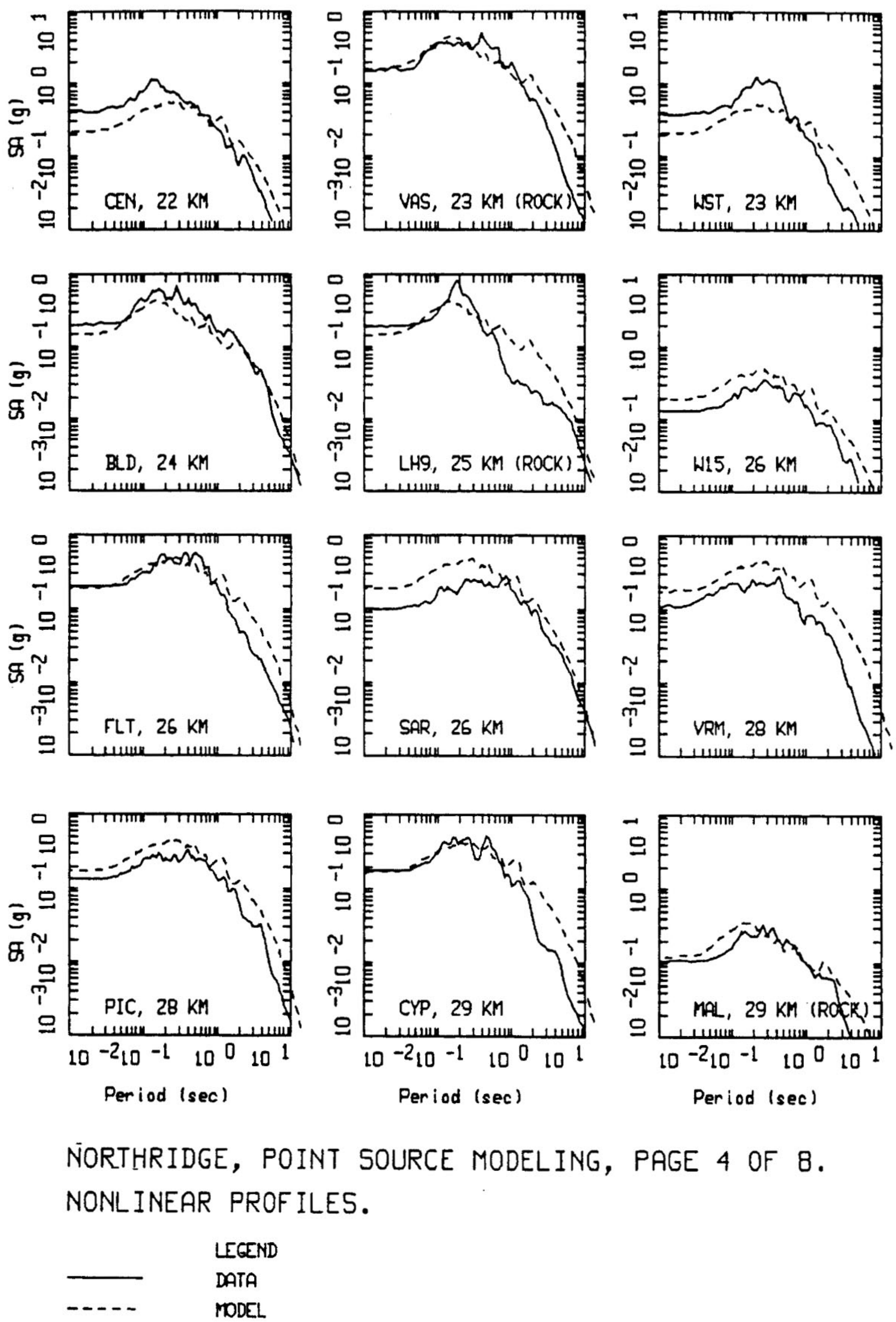

Source: Silva et al. 1996 [DIRS 110474] Figure 5.6

NOTE: Recorded Motions (solid lines), Point-Source Simulations (dashed lines)

Figure 7-6d. Comparison of Average Horizontal Component 5%-Damped Pseudo Relative Absolute Response Spectra: Northridge Earthquake

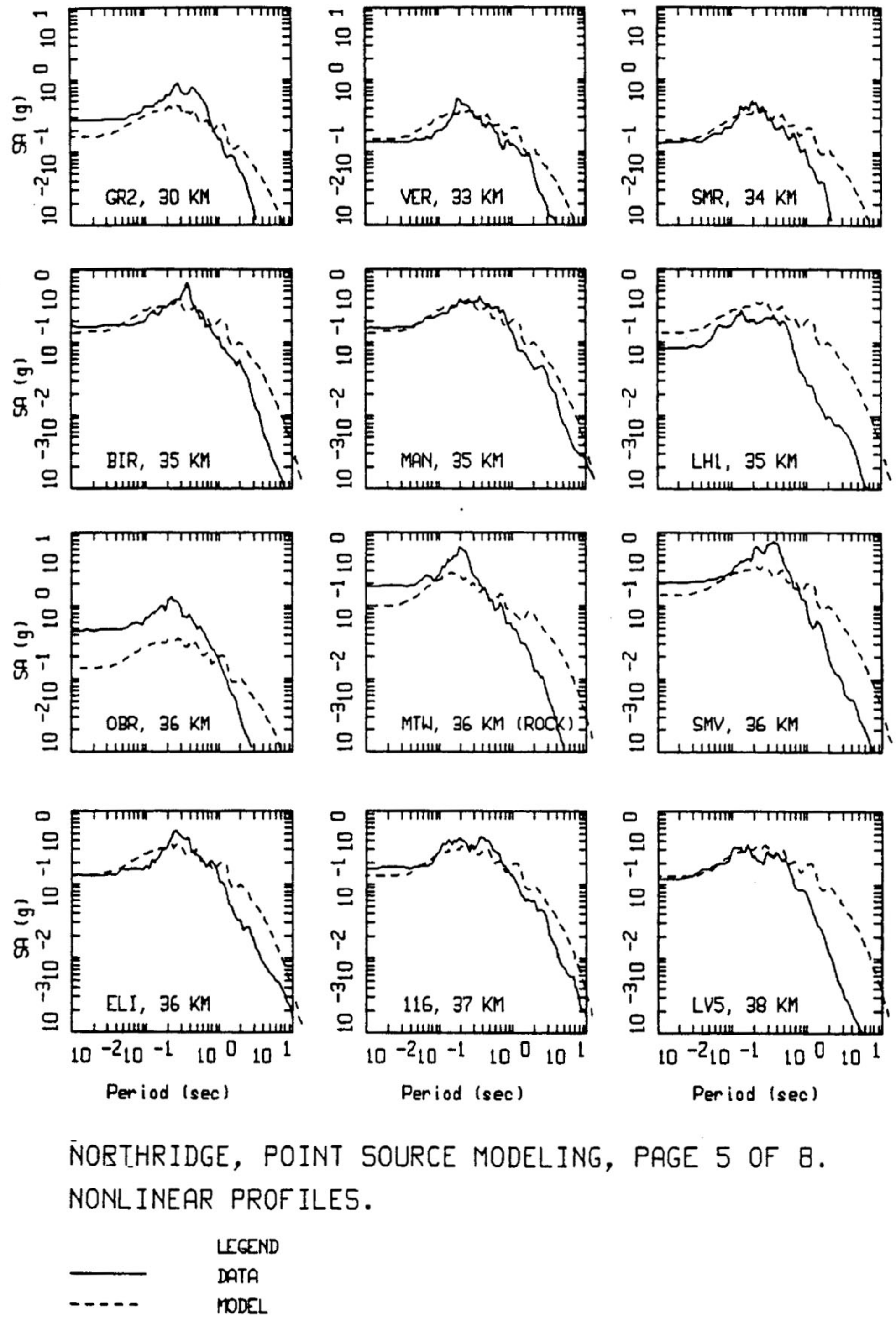

Source: Silva et al. 1996 [DIRS 110474] Figure 5.6

NOTE: Recorded Motions (solid lines), Point-Source Simulations (dashed lines)

Figure 7-6e. Comparison of Average Horizontal Component 5%-Damped Pseudo Relative Absolute Response Spectra: Northridge Earthquake

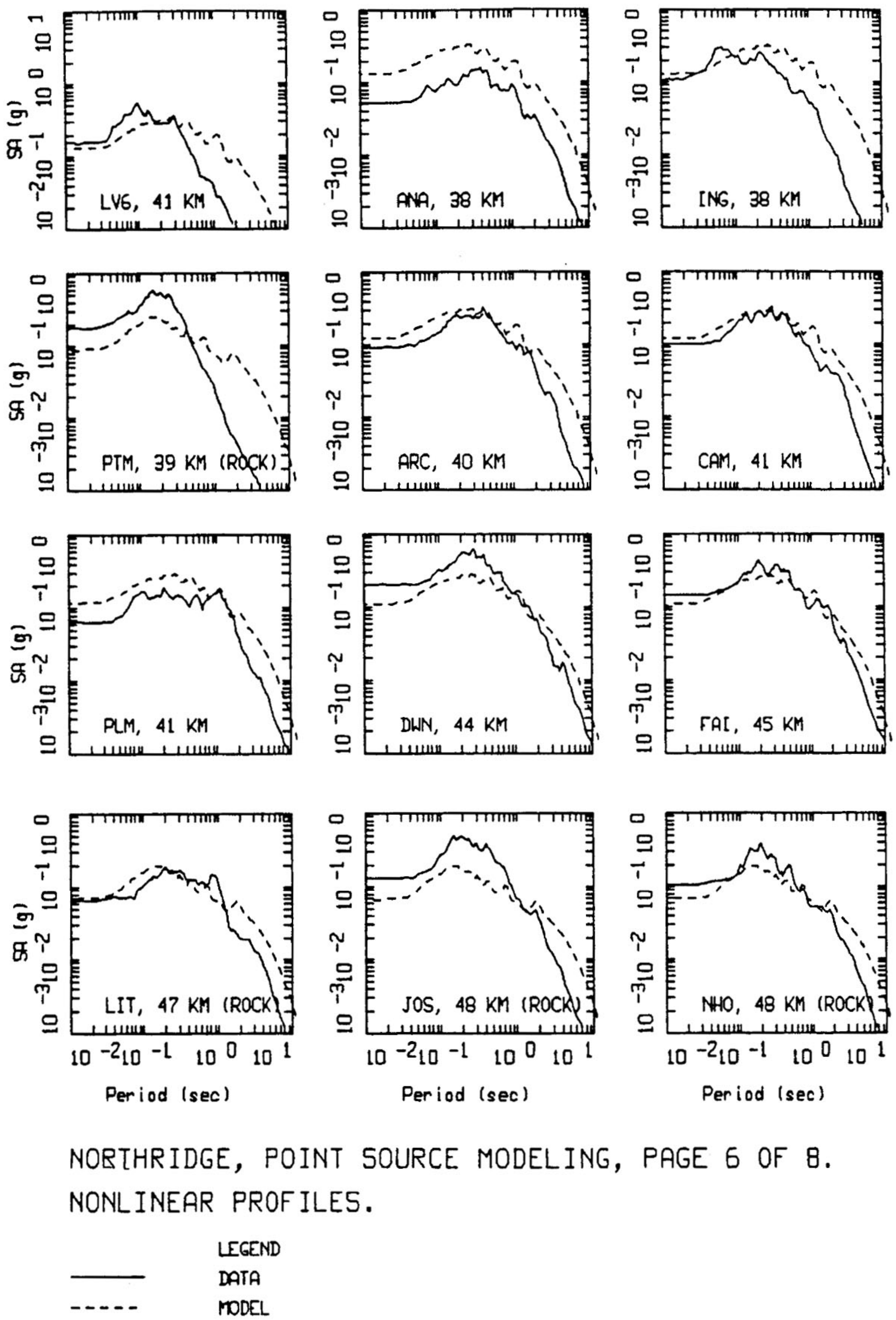

Source: Silva et al. 1996 [DIRS 110474] Figure 5.6

NOTE: Recorded Motions (solid lines), Point-Source Simulations (dashed lines)

Figure 7-6f. Comparison of Average Horizontal Component 5%-Damped Pseudo Relative Absolute Response Spectra: Northridge Earthquake

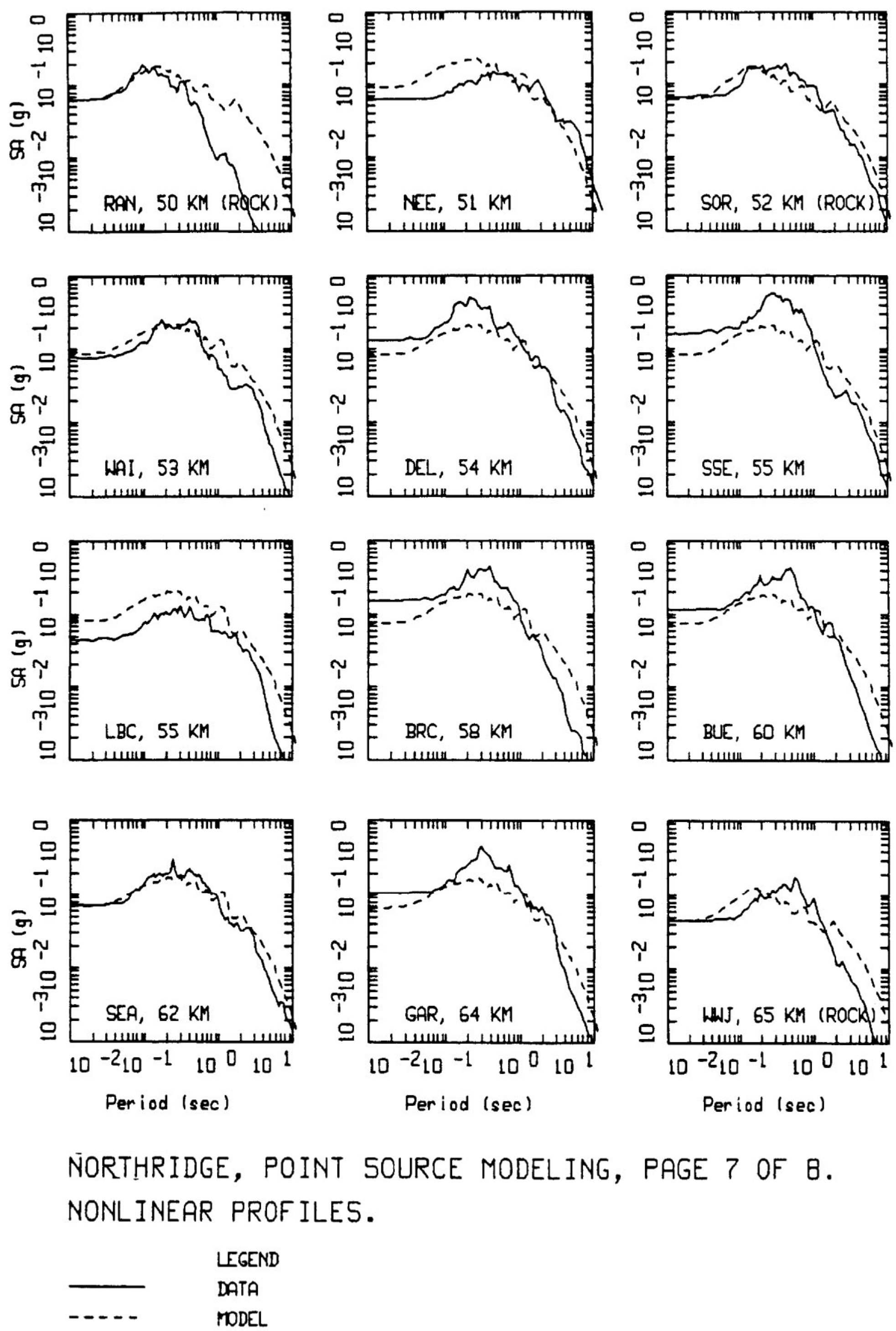

Source: Silva et al. 1996 [DIRS 110474] Figure 5.6

NOTE: Recorded Motions (solid lines), Point-Source Simulations (dashed lines)

Figure 7-6g. Comparison of Average Horizontal Component 5%-Damped Pseudo Relative Absolute Response Spectra: Northridge Earthquake

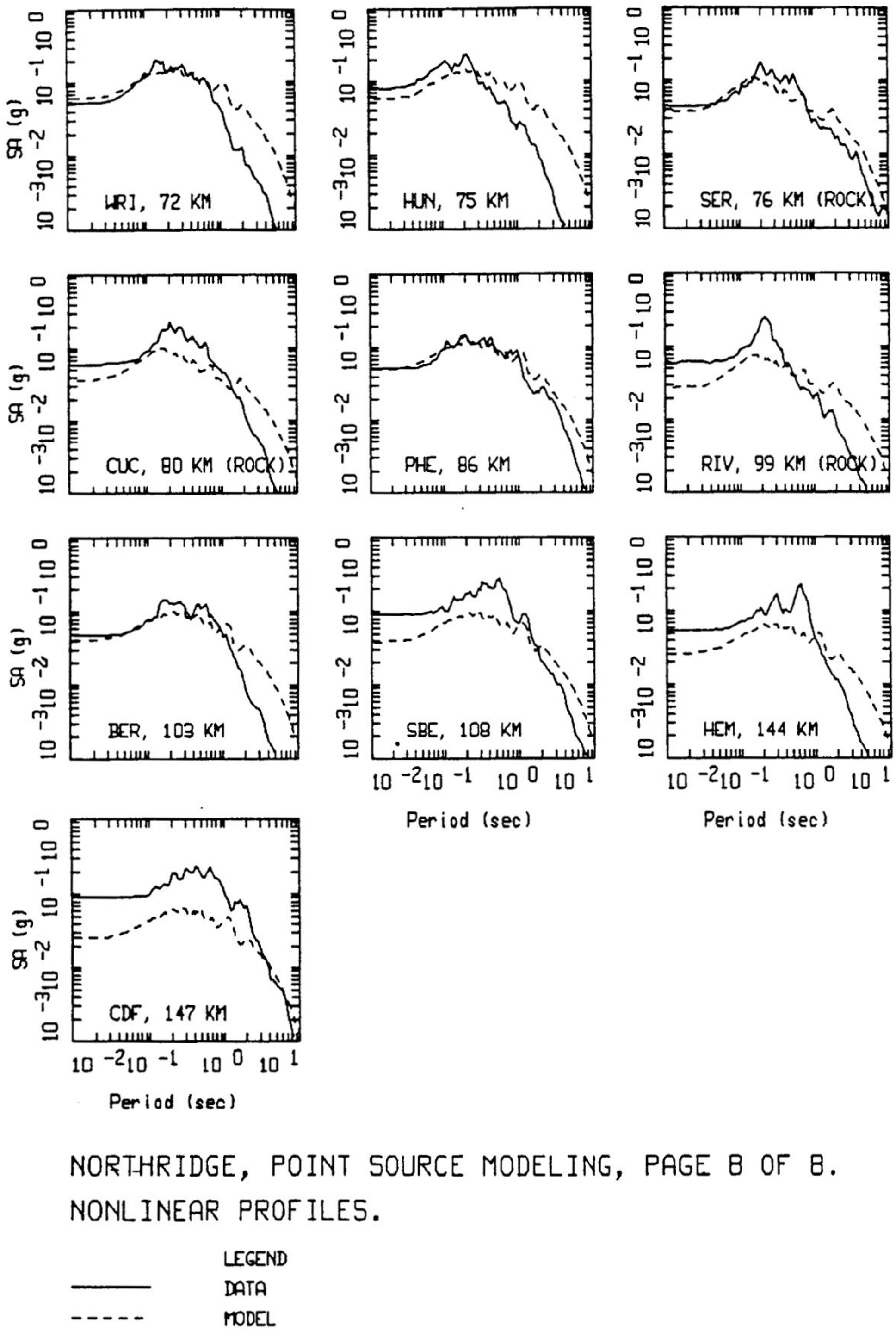

Source: Silva et al. 1996 [DIRS 110474] Figure 5.6

NOTE: Recorded Motions (solid lines), Point-Source Simulations (dashed lines)

Figure 7-6h. Comparison of Average Horizontal Component 5%-Damped Pseudo Relative Absolute Response Spectra: Northridge Earthquake

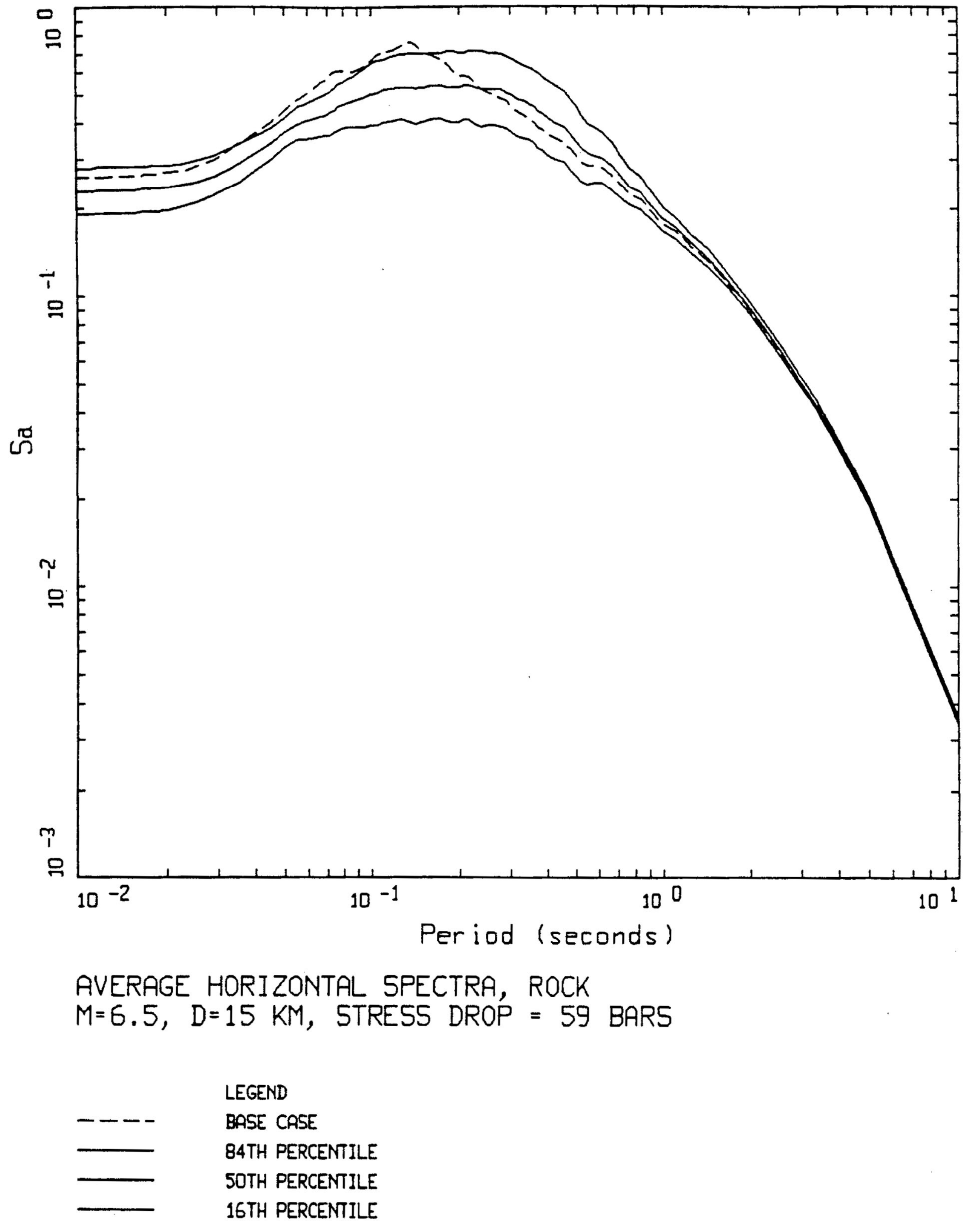

Source: Silva et al. 1996 [DIRS 110474] Figure 5.7 and 3.7

NOTE: The dashed line is the response spectrum computed using the base case soft rock profile

Figure 7-7. Median and ± 1 σ 5%-Damped Pseudo Absolute Response Spectra Computed From 30 Randomly Generated Soft Rock Profiles to a Depth of 100 ft

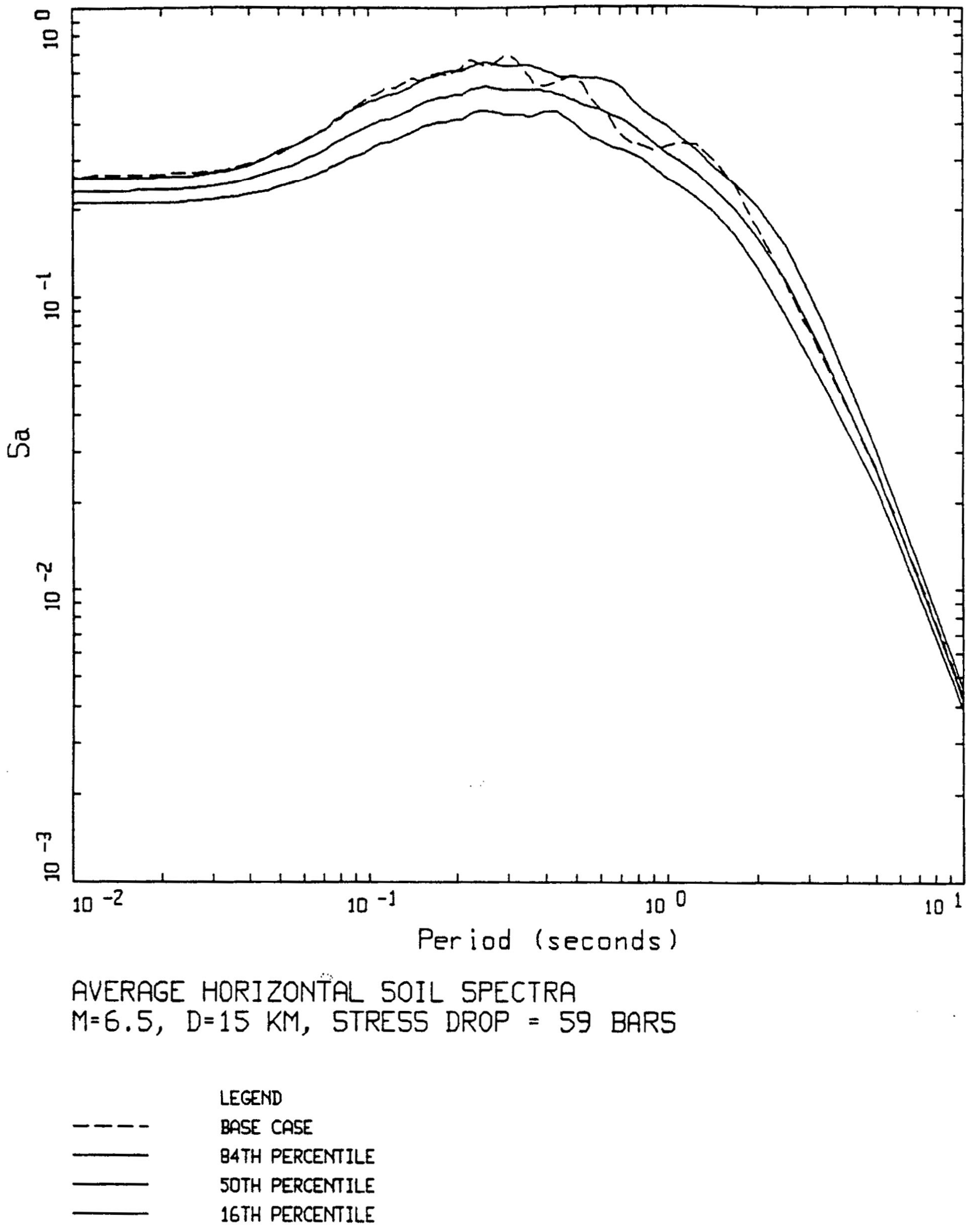

Source: Silva et al. 1996 [DIRS 110474] Figure 5.8 and 3.5

NOTE: The dashed line is the response spectrum computed using the base case deep soil profile

Figure 7-8. Median and ± 1 σ 5%-Damped Pseudo Absolute Response Spectra Computed From 30 Randomly Generated Deep Soil Profiles With Depth Varying From 100 to 1000 ft (solid line)

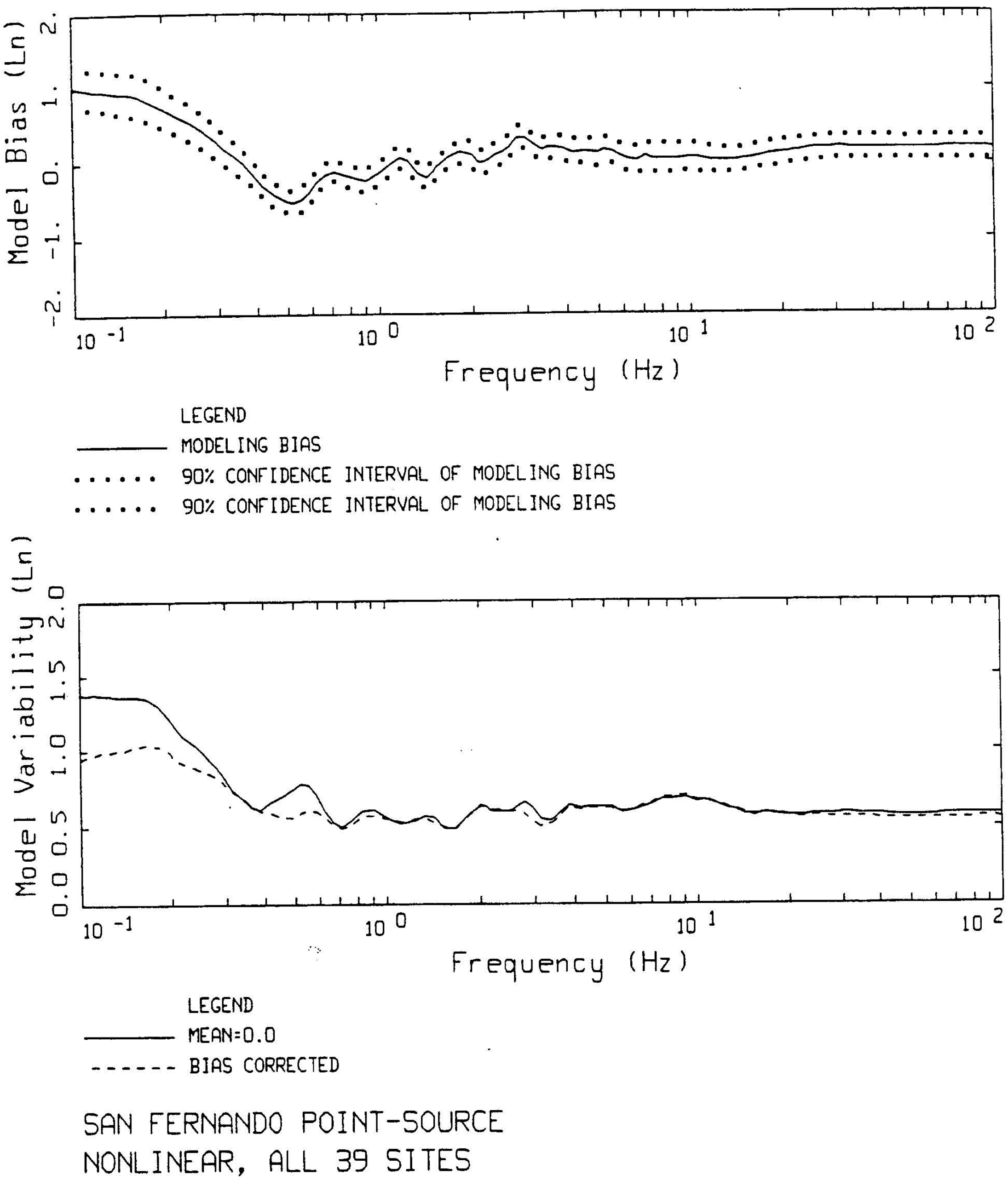

Source: Silva et al. 1996 [DIRS 110474] Figure 5.22

Figure 7-9. Model Bias and Variability Estimates for the San Fernando Earthquake Computed Over All 39 Sites for the Point-Source Model

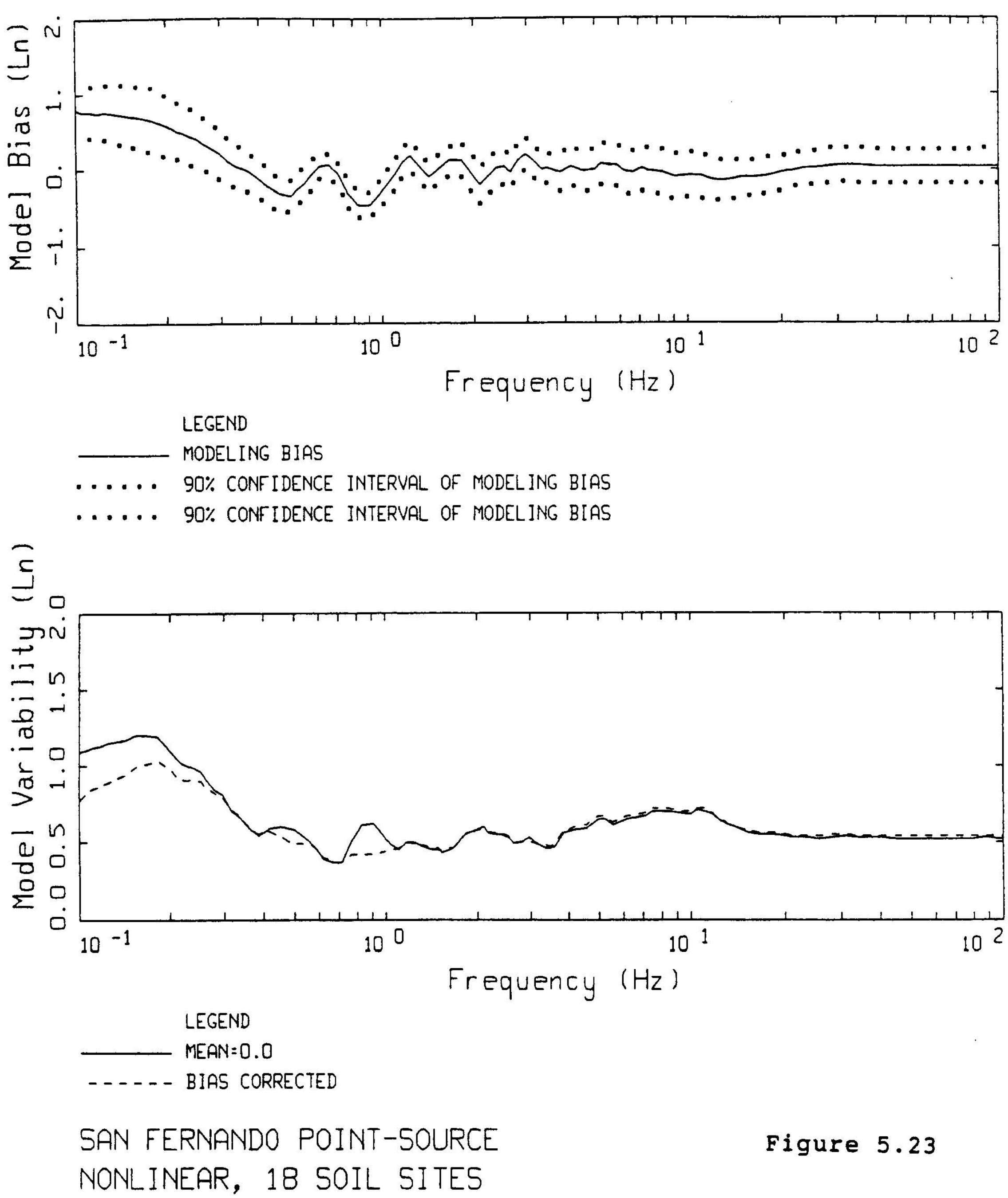

Source: Silva et al. 1996 [DIRS 110474] Figure 5.23

Figure 7-10. Model Bias and Variability Estimates for the San Fernando Earthquake Computed Over All 18 Soils Sites for the Point-Source Model

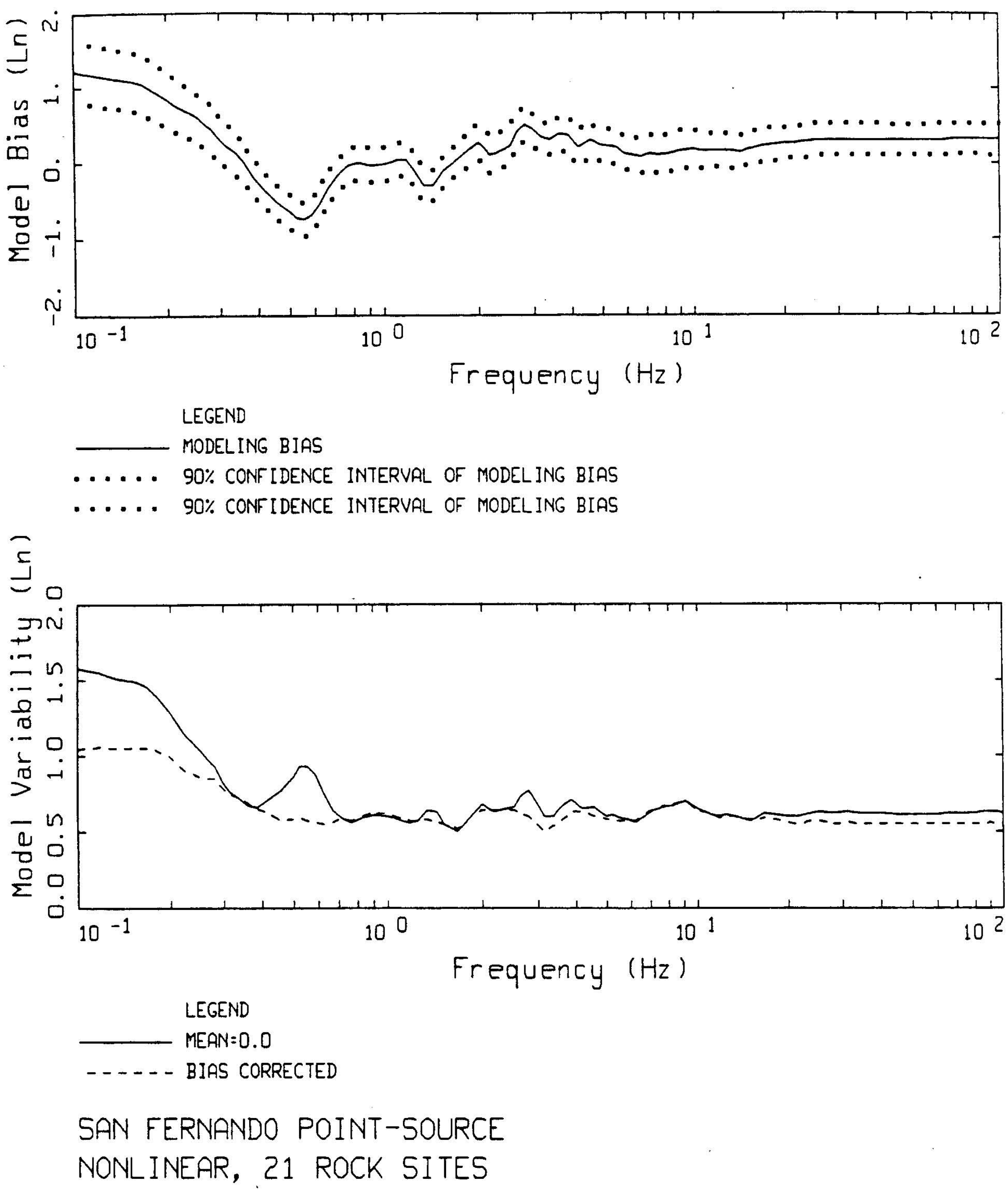

Source: Silva et al. 1996 [DIRS 110474] Figure 5.24

Figure 7-11. Model Bias and Variability Estimates for the San Fernando Earthquake Computed Over All 21 Rock Sites for the Point-Source Model

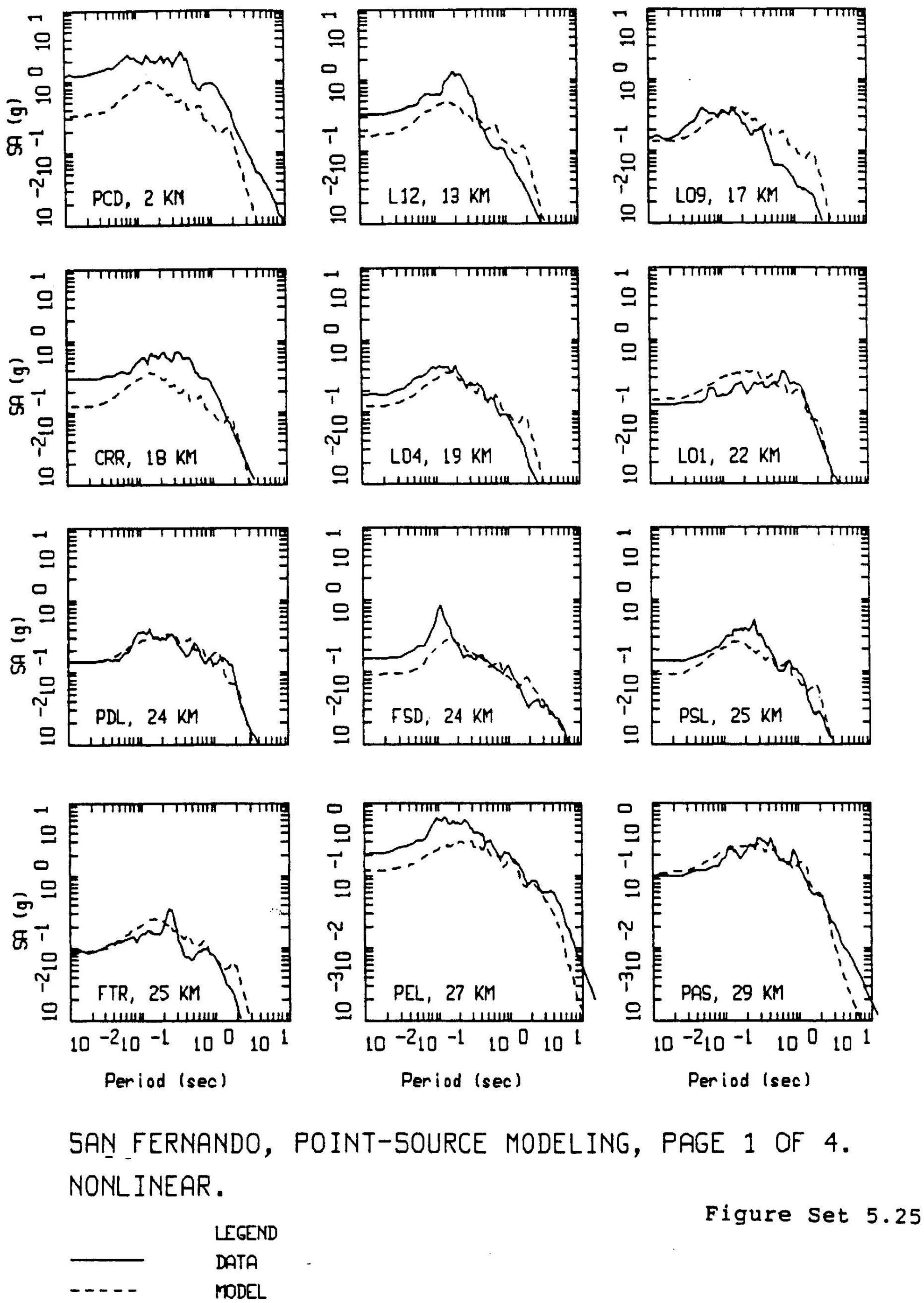

Source: Silva et al. 1996 [DIRS 110474] Figure 5.25

NOTE: Recorded Motions (solid lines), Point-Source Simulations (dashed lines)

Figure 7-12a. Comparison of Average Horizontal Component 5%-Damped Pseudo Relative Absolute Response Spectra: San Fernando Earthquake

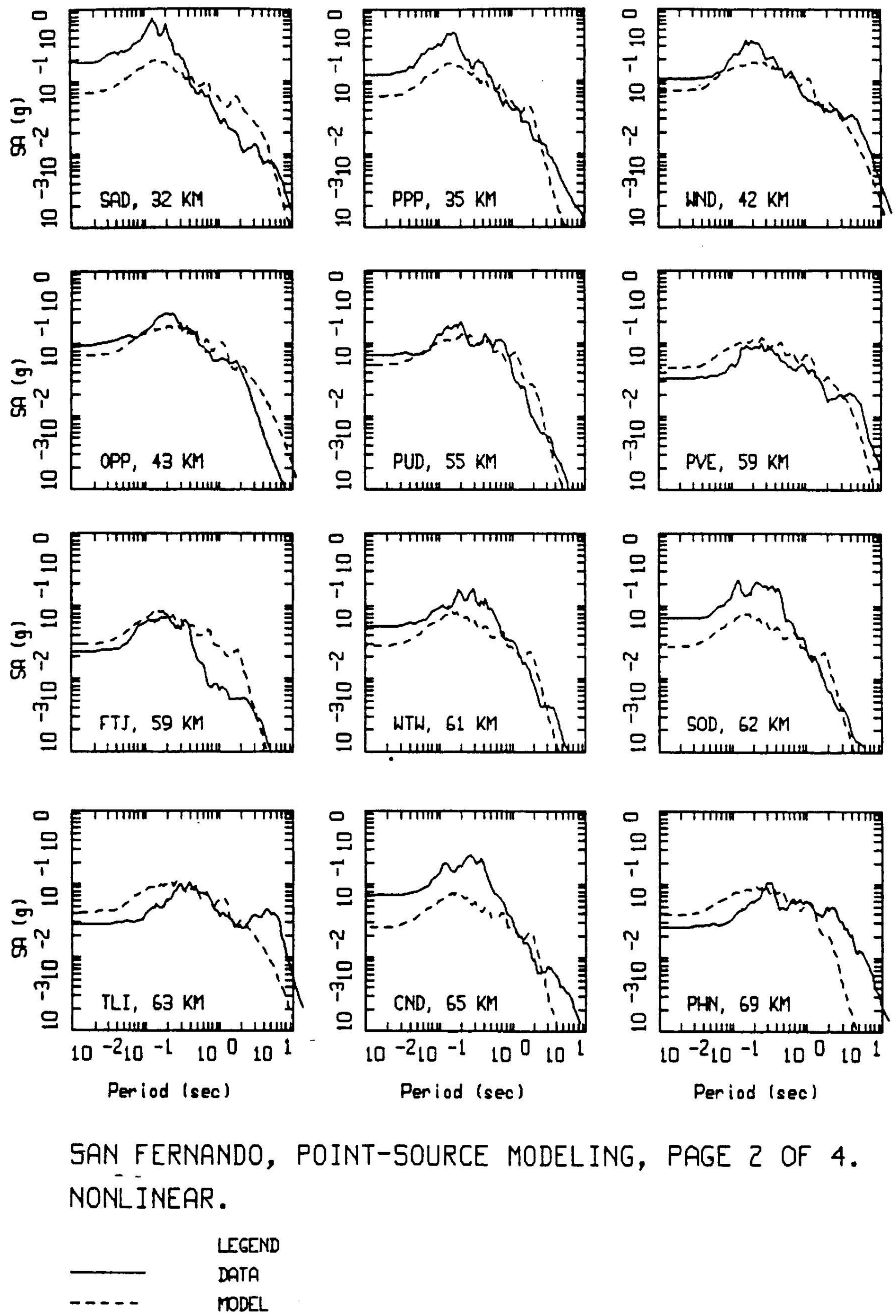

Source: Silva et al. 1996 [DIRS 110474] Figure 5.25

NOTE: Recorded Motions (solid lines), Point-Source Simulations (dashed lines)

Figure 7-12b. Comparison of Average Horizontal Component 5%-Damped Pseudo Relative Absolute Response Spectra: San Fernando Earthquake

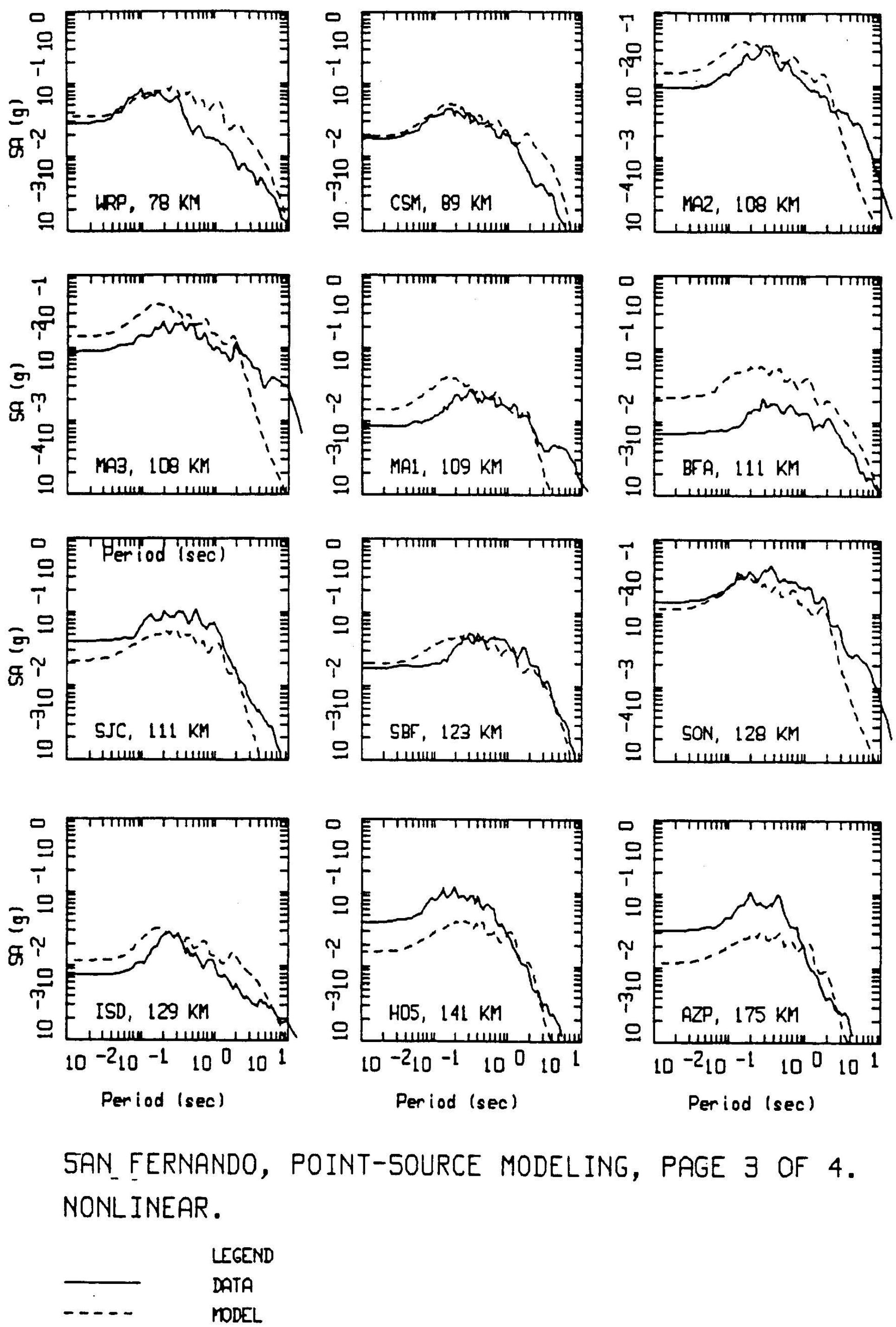

Source: Silva et al. 1996 [DIRS 110474] Figure 5.25

NOTE: Recorded Motions (solid lines), Point-Source Simulations (dashed lines)

Figure 7-12c. Comparison of Average Horizontal Component 5%-Damped Pseudo Relative Absolute Response Spectra: San Fernando Earthquake

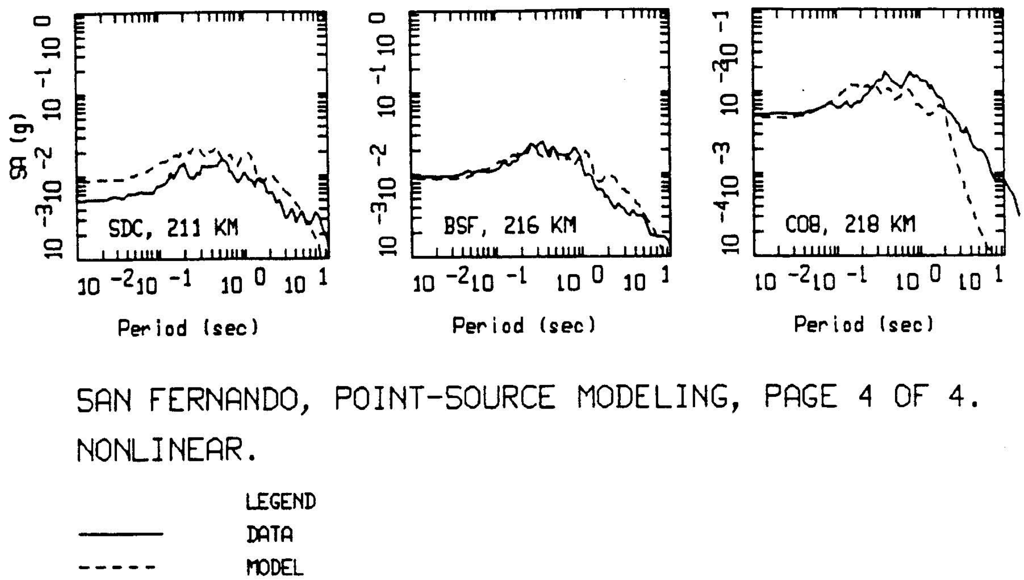

Source: Silva et al. 1996 [DIRS 110474] Figure 5.25

NOTE: Recorded Motions (solid lines), Point-Source Simulations (dashed lines)

Figure 7-12d. Comparison of Average Horizontal Component 5%-Damped Pseudo Relative Absolute Response Spectra: San Fernando Earthquake

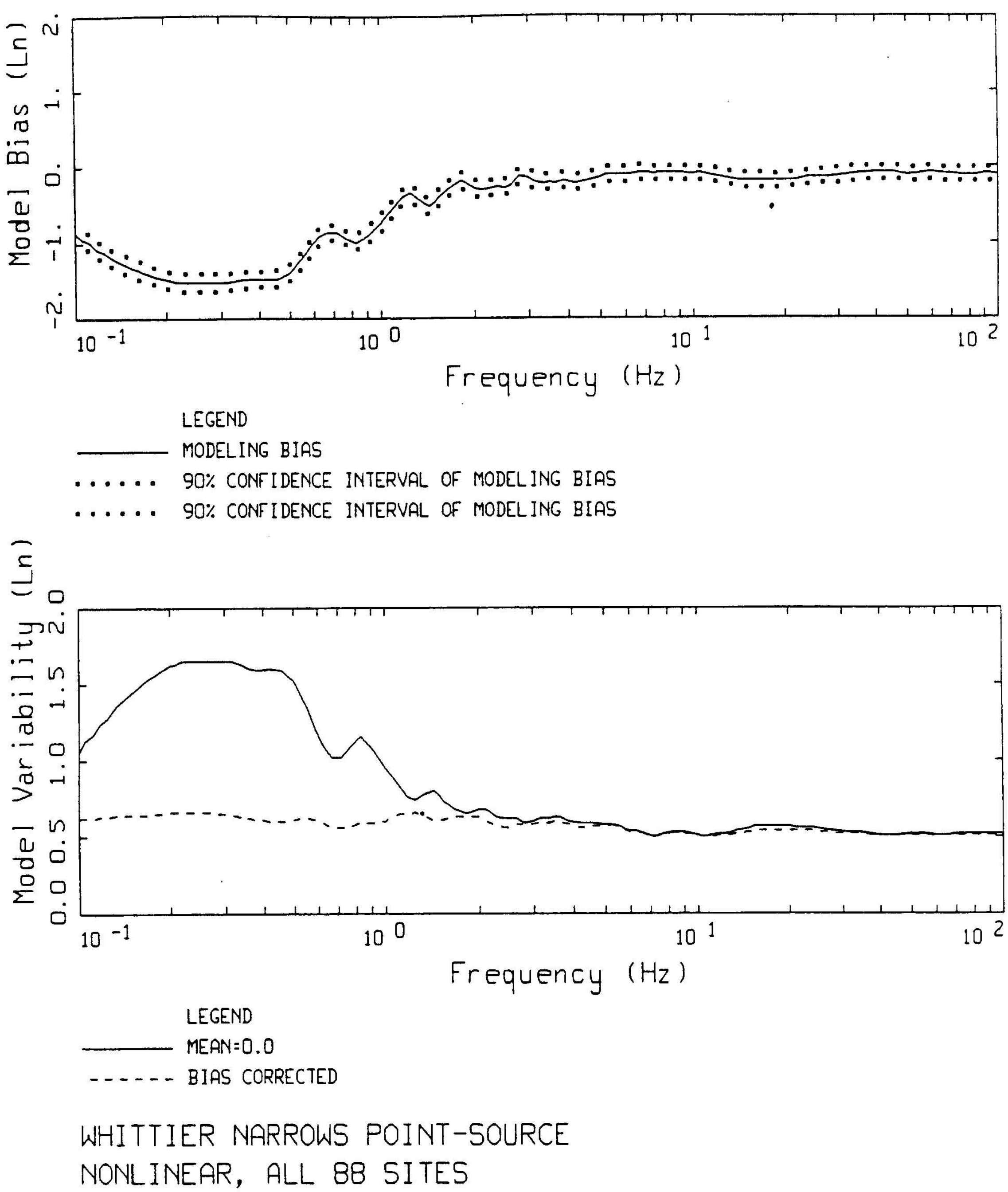

Source: Silva et al. 1996 [DIRS 110474] Figure 5.32

Figure 7-13. Model Bias and Variability Estimates for the Whittier Narrows Earthquake Computed Over All 88 Sites for the Point-Source Model

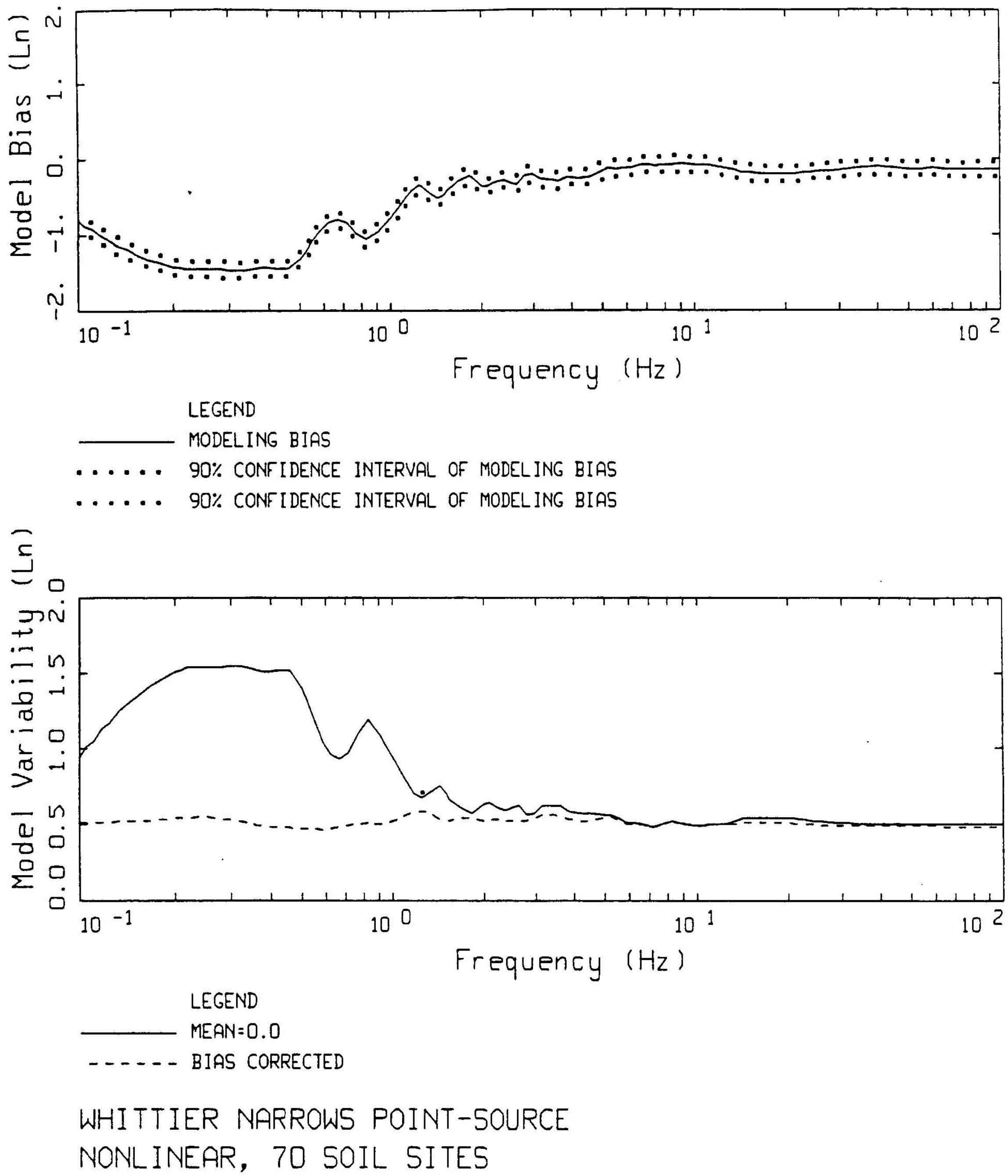

Source: Silva et al. 1996 [DIRS 110474] Figure 5.33

Figure 7-14. Model Bias and Variability Estimates for the Whittier Narrows Earthquake Computed Over All 70 Soil Sites for the Point-Source Model

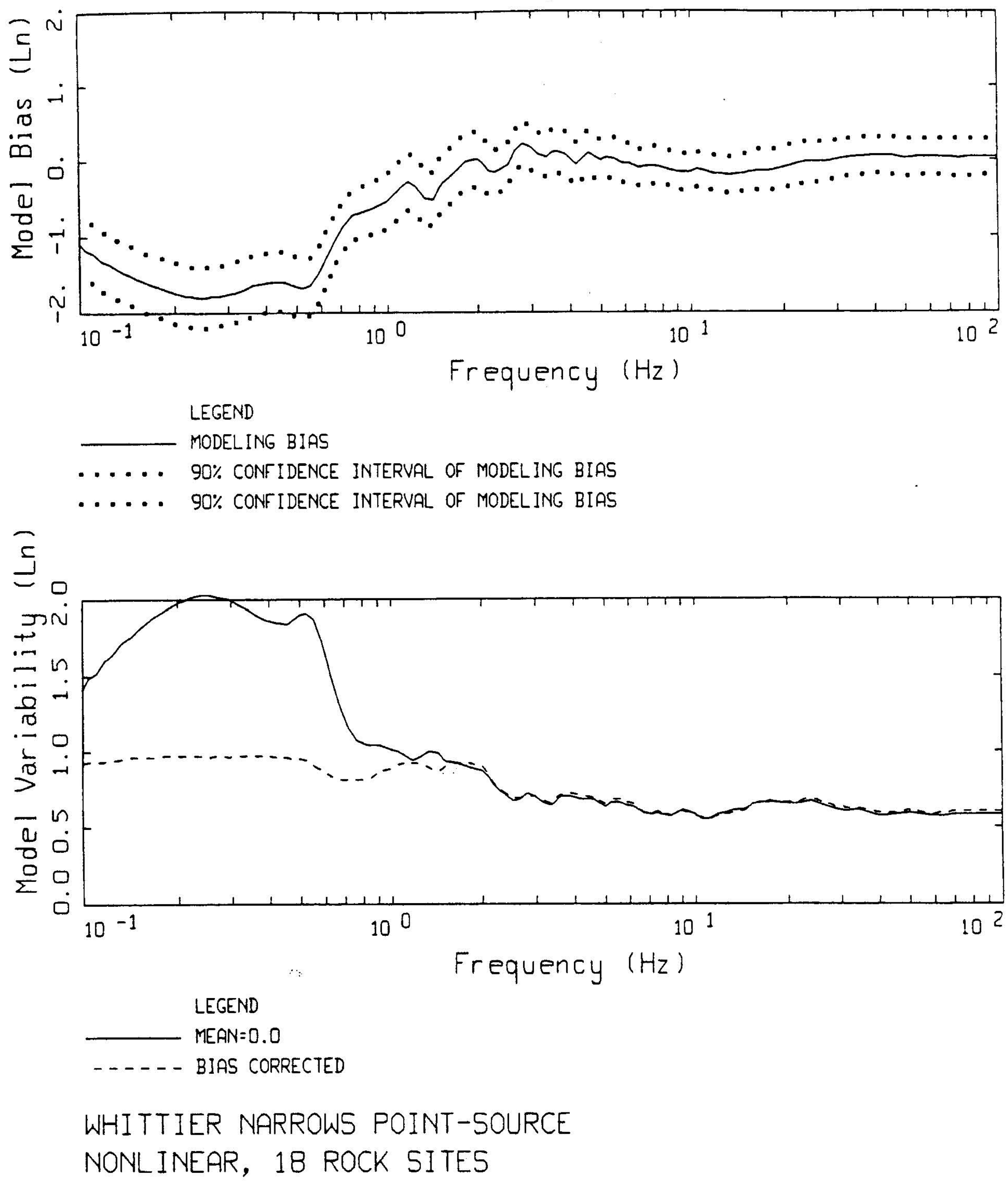

Source: Silva et al. 1996 [DIRS 110474] Figure 5.34

Figure 7-15. Model Bias and Variability Estimates for the Whittier Narrows Earthquake Computed Over All 18 Rock Sites for the Point-Source Model

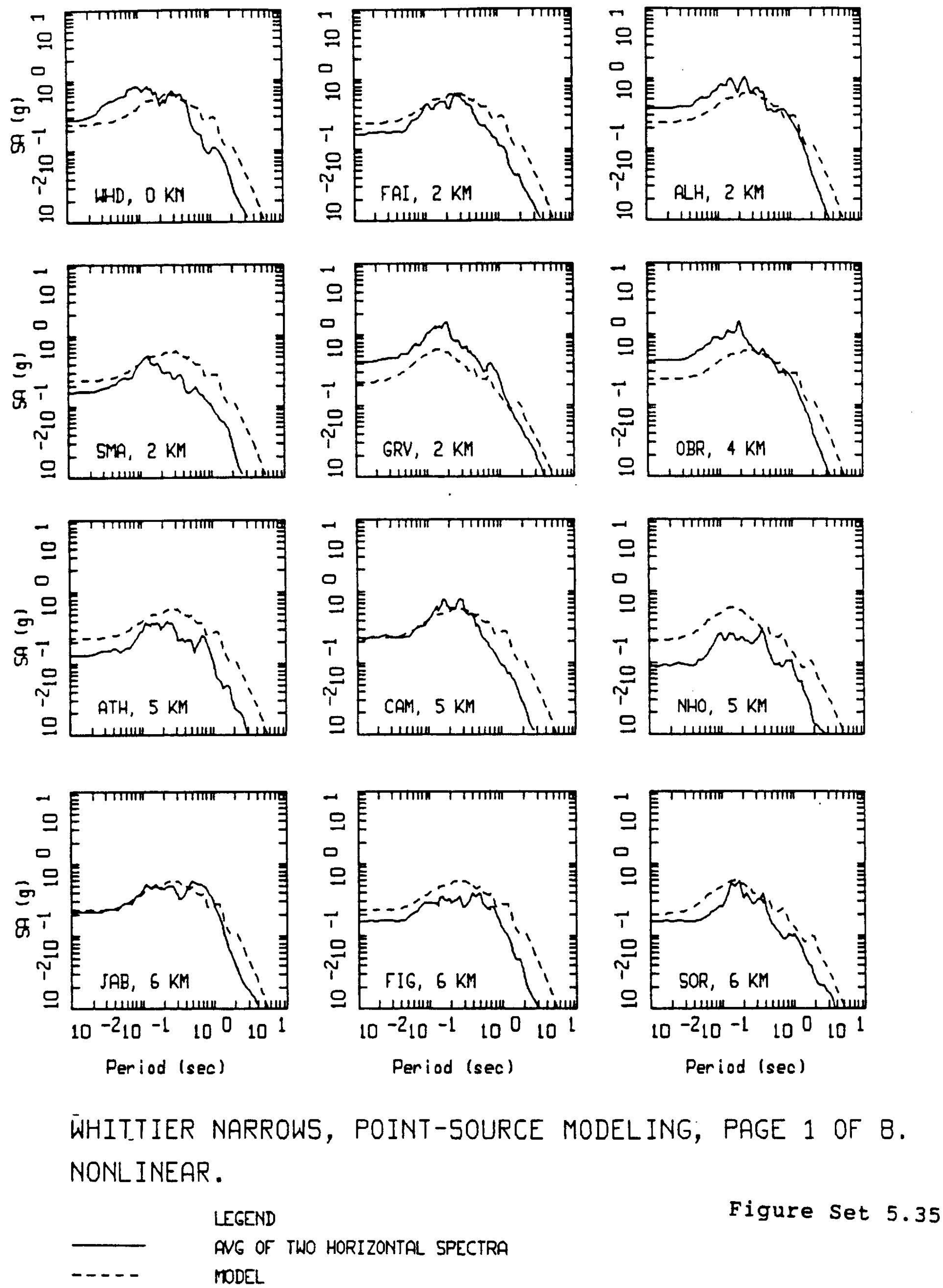

Source: Silva et al. 1996 [DIRS 110474] Figure 5.35

NOTE: Recorded Motions (solid lines), Point-Source Simulations (dashed lines)

Figure 7-16a. Comparison of Average Horizontal Component 5%-Damped Pseudo Relative Absolute Response Spectra: Whittier Narrows Earthquake

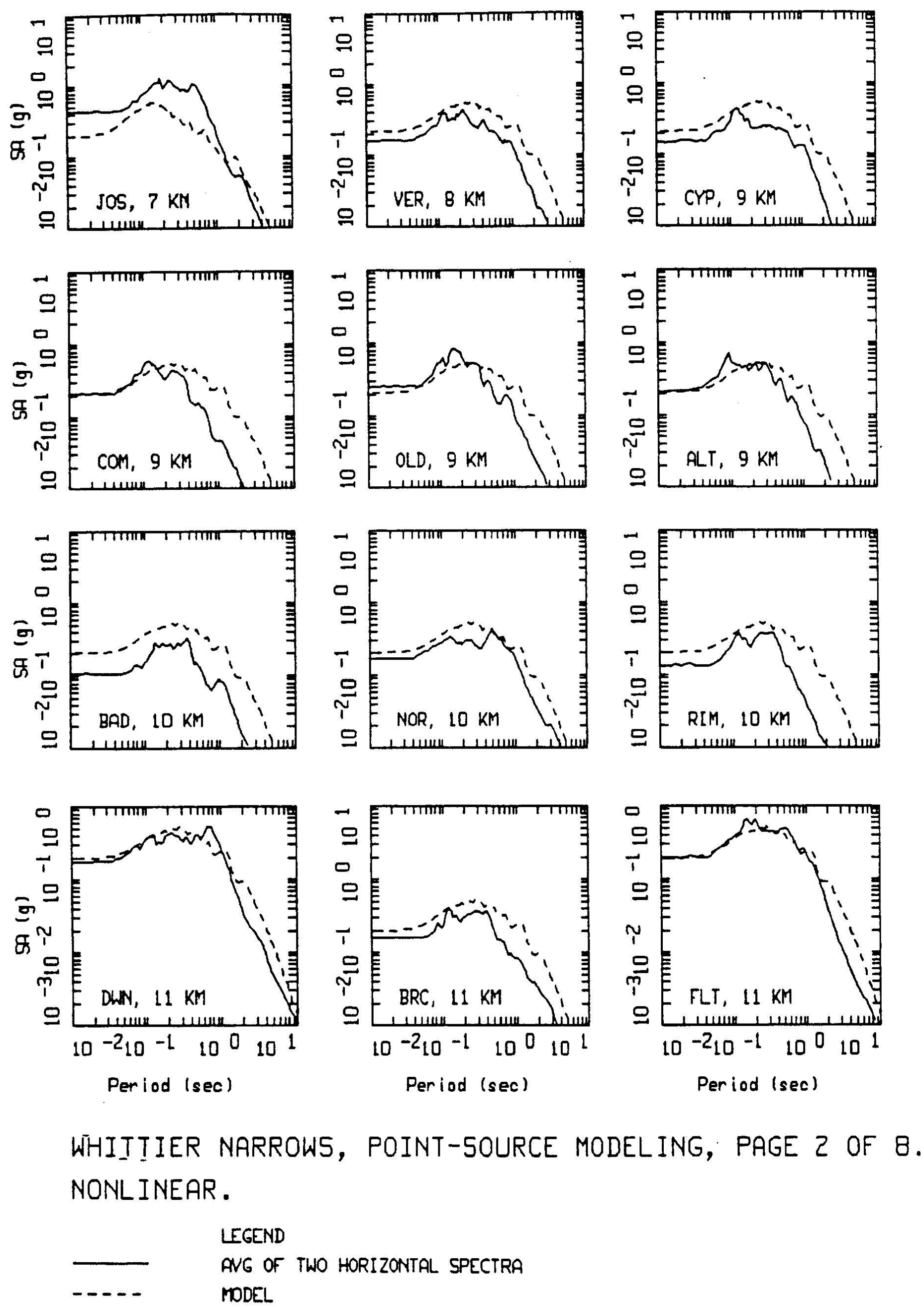

Source: Silva et al. 1996 [DIRS 110474] Figure 5.35

NOTE: Recorded Motions (solid lines), Point-Source Simulations (dashed lines)

Figure 7-16b. Comparison of Average Horizontal Component 5%-Damped Pseudo Relative Absolute Response Spectra: Whittier Narrows Earthquake

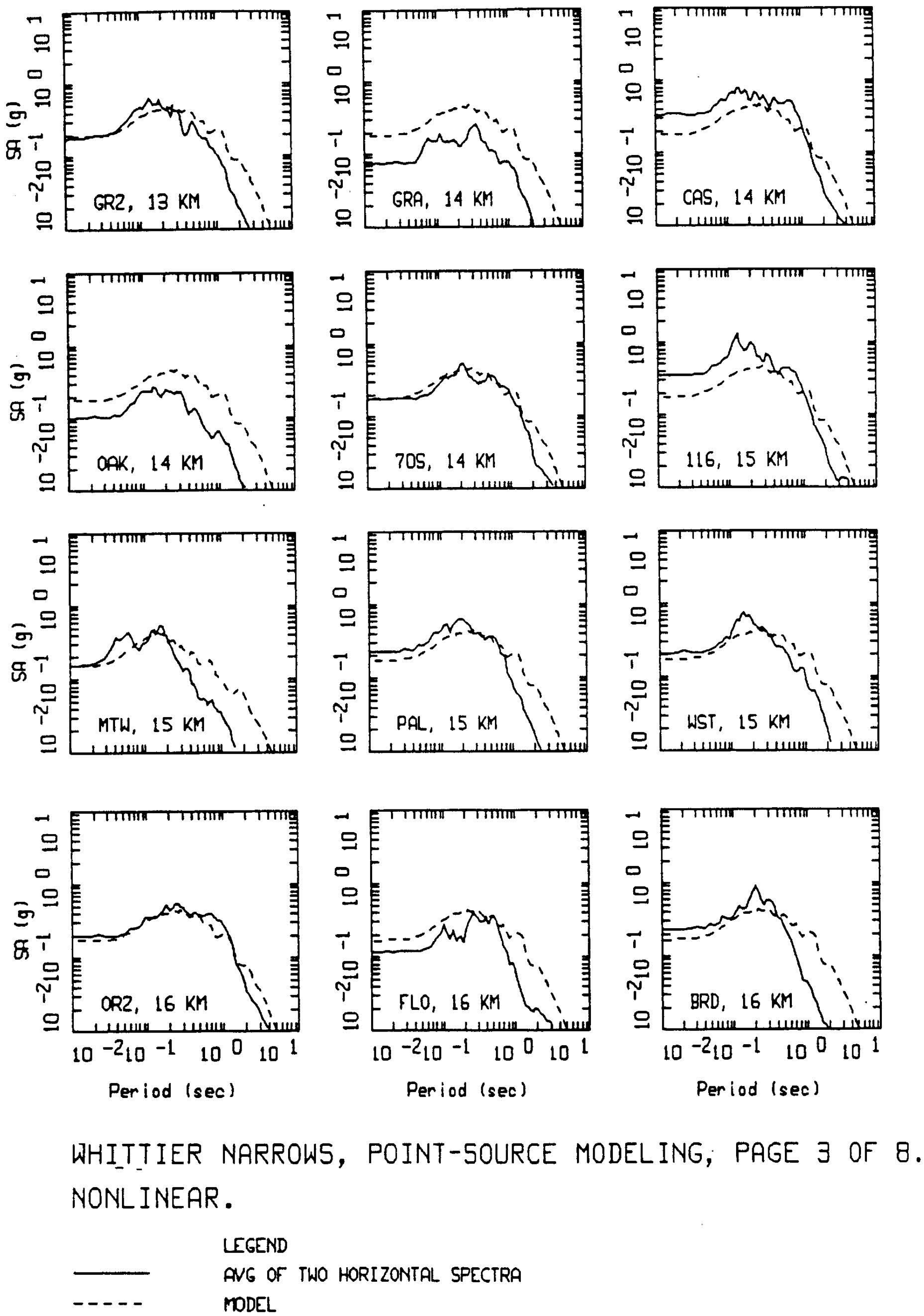

Source: Silva et al. 1996 [DIRS 110474] Figure 5.35

NOTE: Recorded Motions (solid lines), Point-Source Simulations (dashed lines)

Figure 7-16c Comparison of Average Horizontal Component 5%-Damped Pseudo Relative Absolute Response Spectra: Whittier Narrows Earthquake

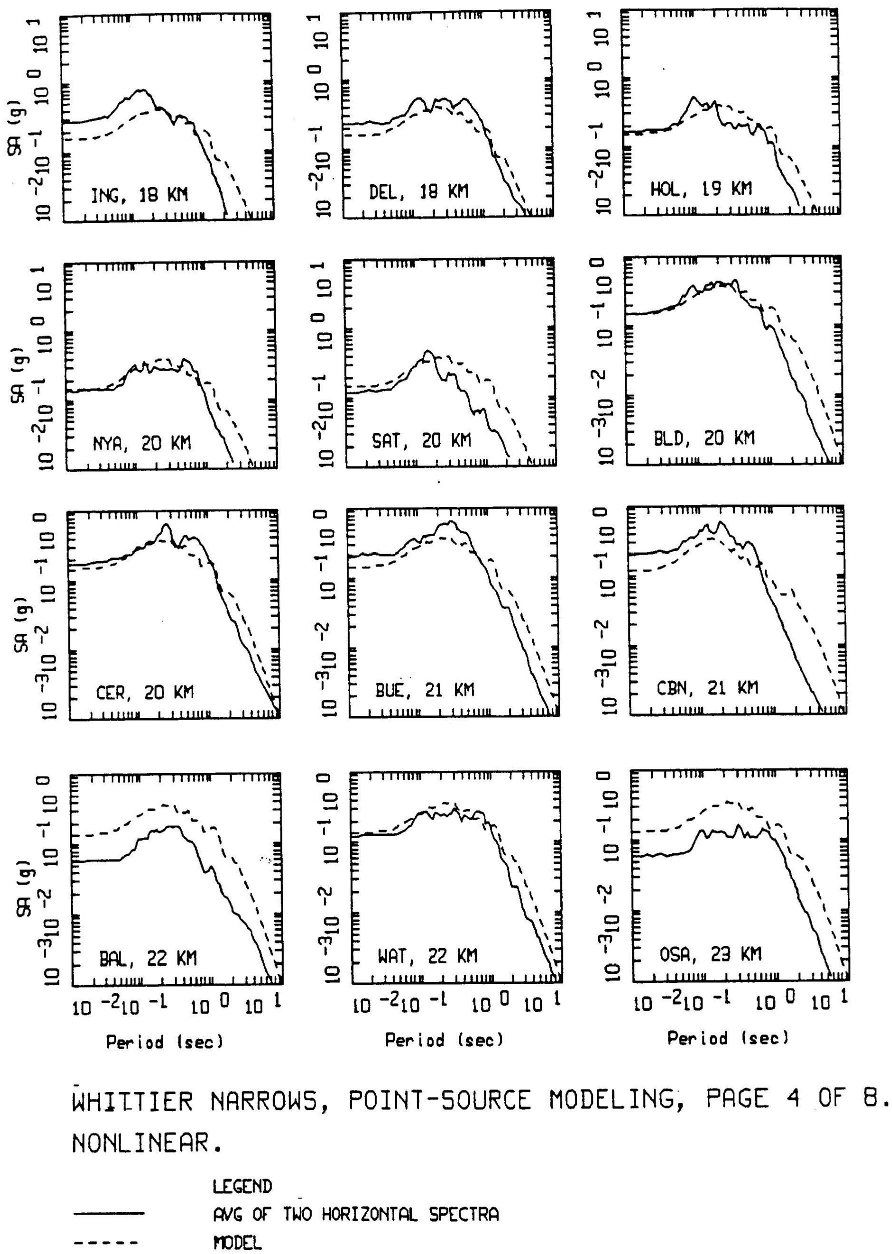

Source: Silva et al. 1996 [DIRS 110474] Figure 5.35

NOTE: Recorded Motions (solid lines), Point-Source Simulations (dashed lines)

Figure 7-16d. Comparison of Average Horizontal Component 5%-Damped Pseudo Relative Absolute Response Spectra: Whittier Narrows Earthquake

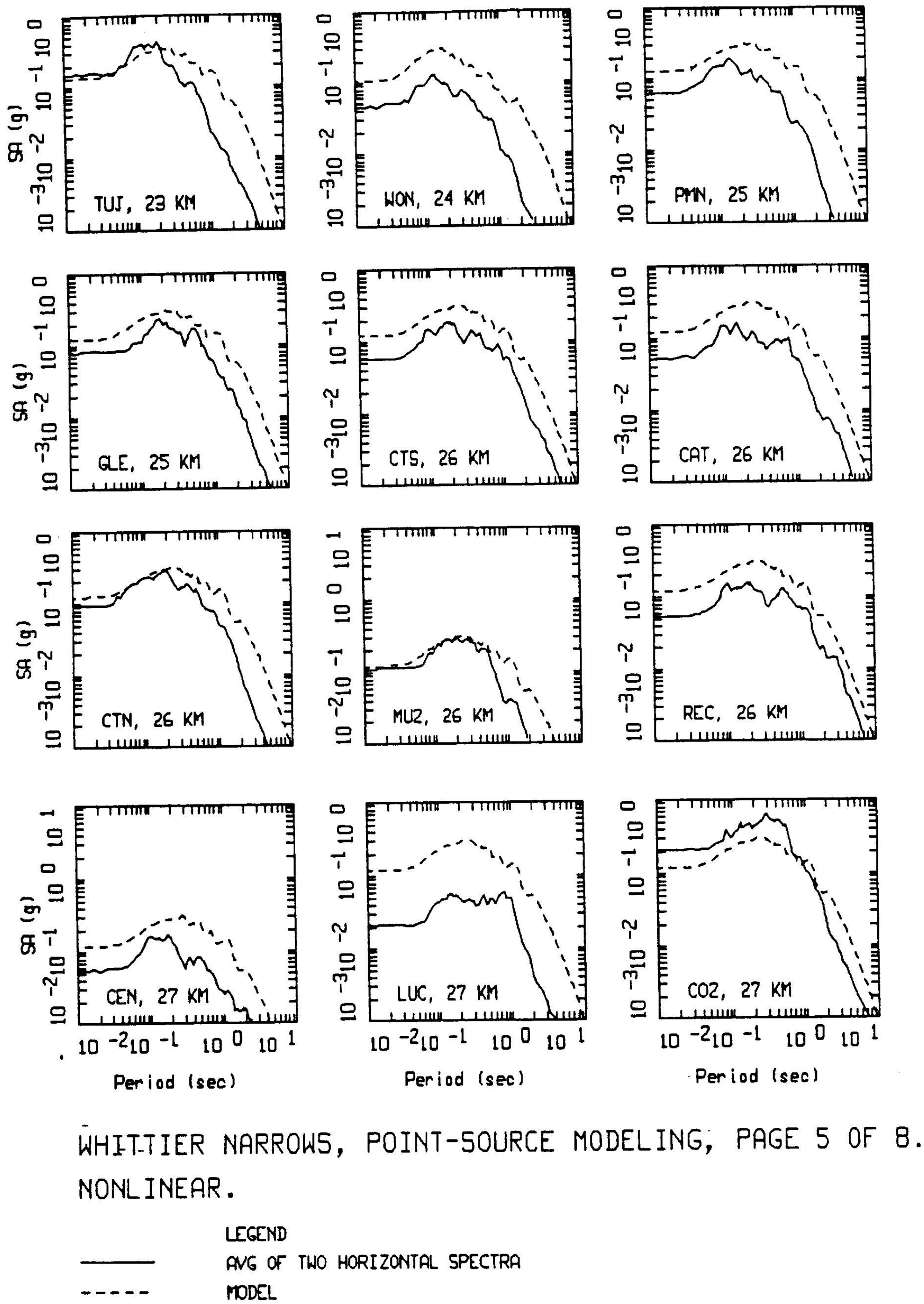

Source: Silva et al. 1996 [DIRS 110474] Figure 5.35

NOTE: Recorded Motions (solid lines), Point-Source Simulations (dashed lines)

Figure 7-16e. Comparison of Average Horizontal Component 5%-Damped Pseudo Relative Absolute Response Spectra: Whittier Narrows Earthquake

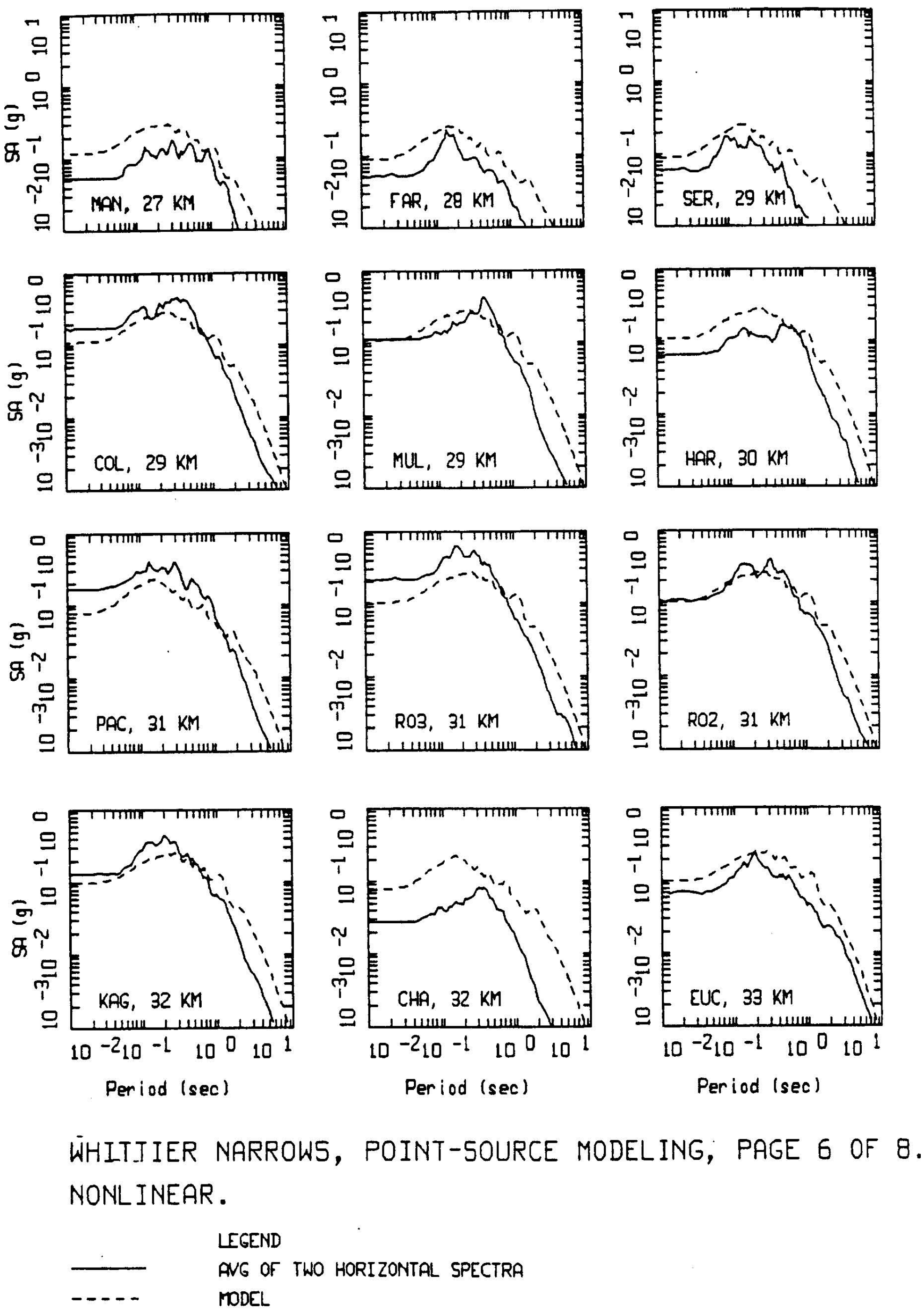

Source: Silva et al. 1996 [DIRS 110474] Figure 5.35

NOTE: Recorded Motions (solid lines), Point-Source Simulations (dashed lines)

Figure 7-16f. Comparison of Average Horizontal Component 5%-Damped Pseudo Relative Absolute Response Spectra: Whittier Narrows Earthquake

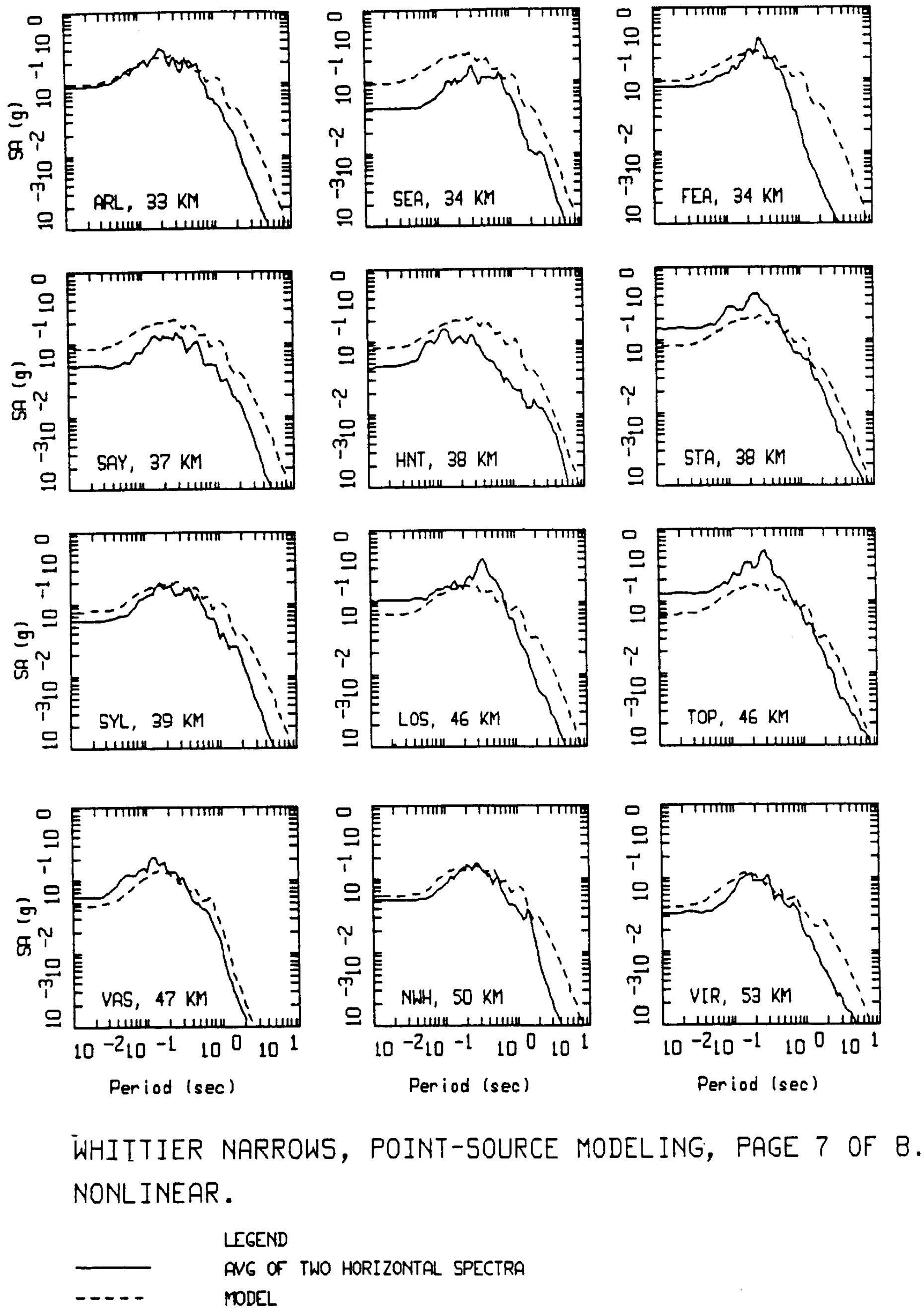

Source: Silva et al. 1996 [DIRS 110474] Figure 5.35

NOTE: Recorded Motions (solid lines), Point-Source Simulations (dashed lines)

Figure 7-16g. Comparison of Average Horizontal Component 5%-Damped Pseudo Relative Absolute Response Spectra: Whittier Narrows Earthquake

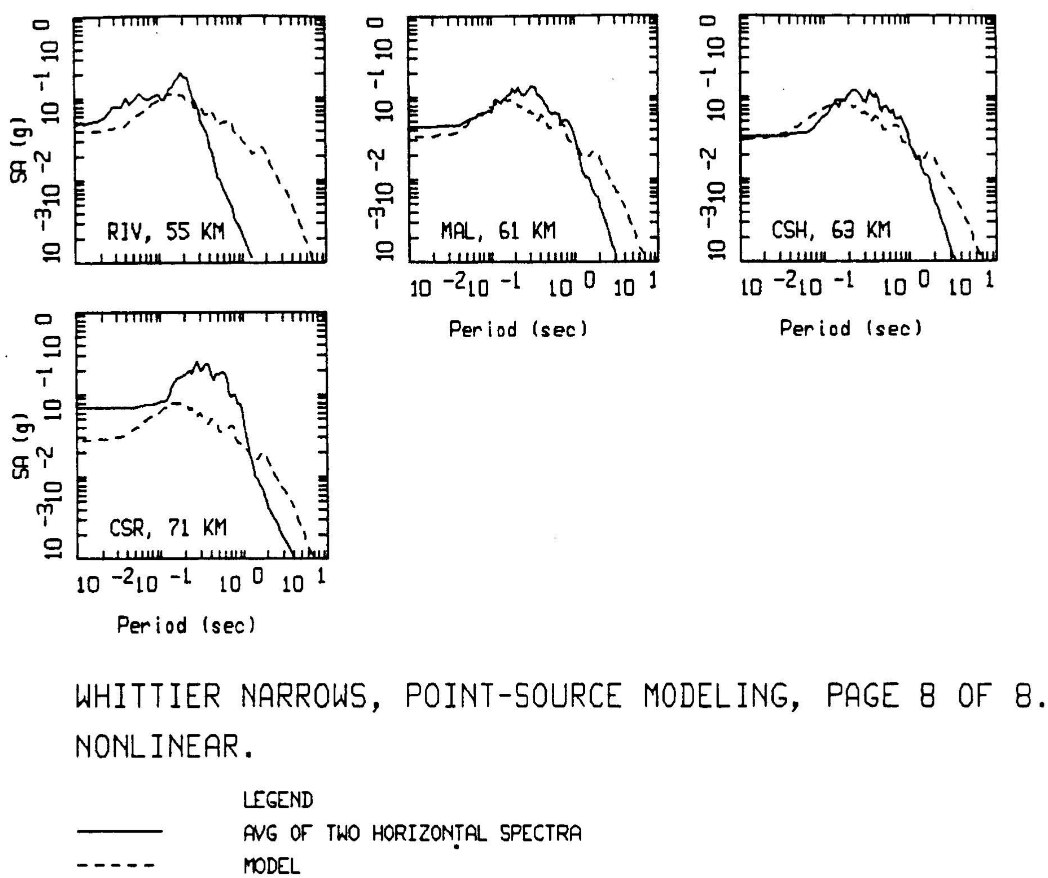

Source: Silva et al. 1996 [DIRS 110474] Figure 5.35

NOTE: Recorded Motions (solid lines), Point-Source Simulations (dashed lines)

Figure 7-16h. Comparison of Average Horizontal Component 5%-Damped Pseudo Relative Absolute Response Spectra: Whittier Narrows Earthquake

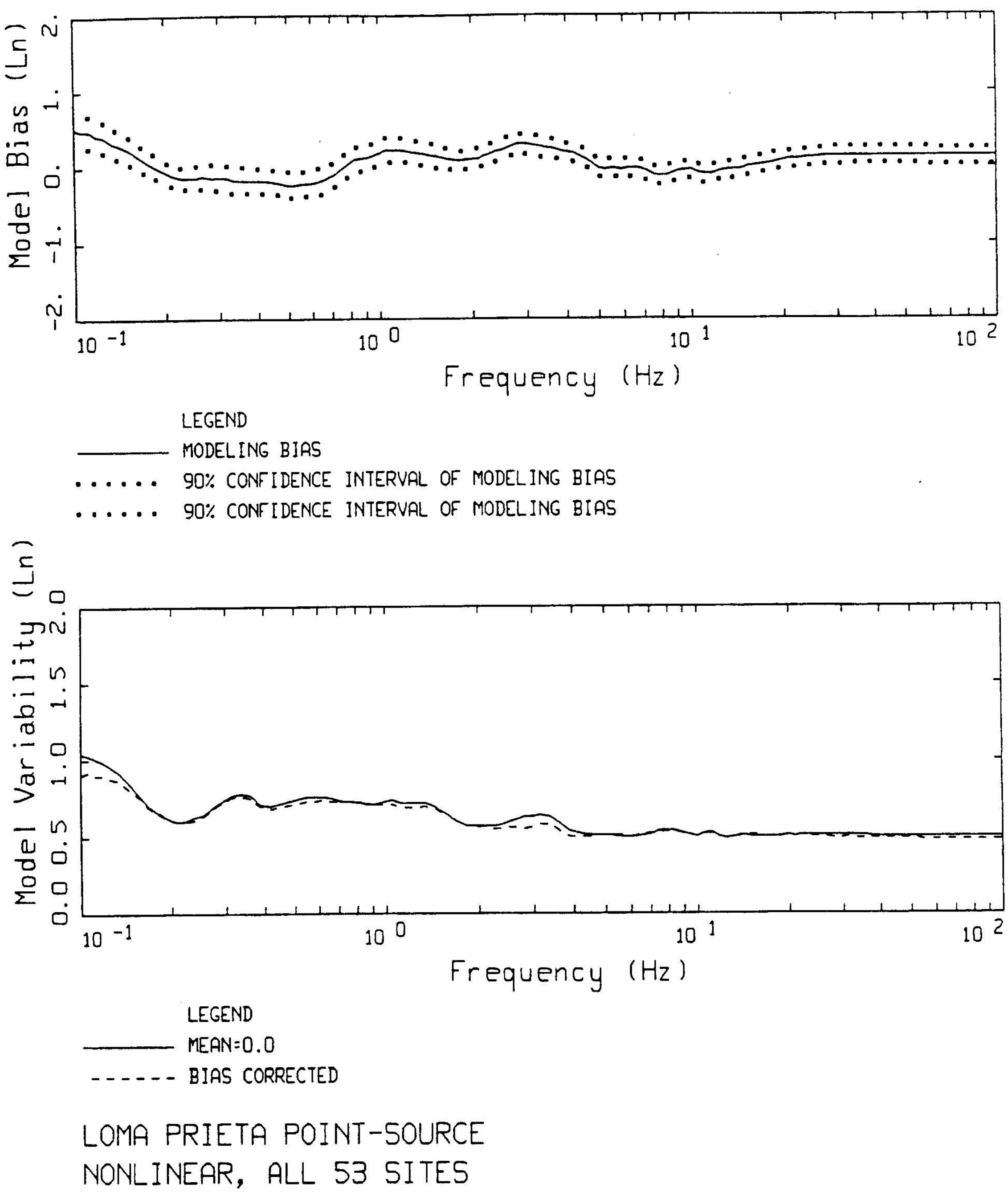

Source: Silva et al. 1996 [DIRS 110474] Figure 5.44

Figure 7-17 Model Bias and Variability Estimates for the Loma Prieta Earthquake Computed Over All 53 Sites for the Point-Source Model

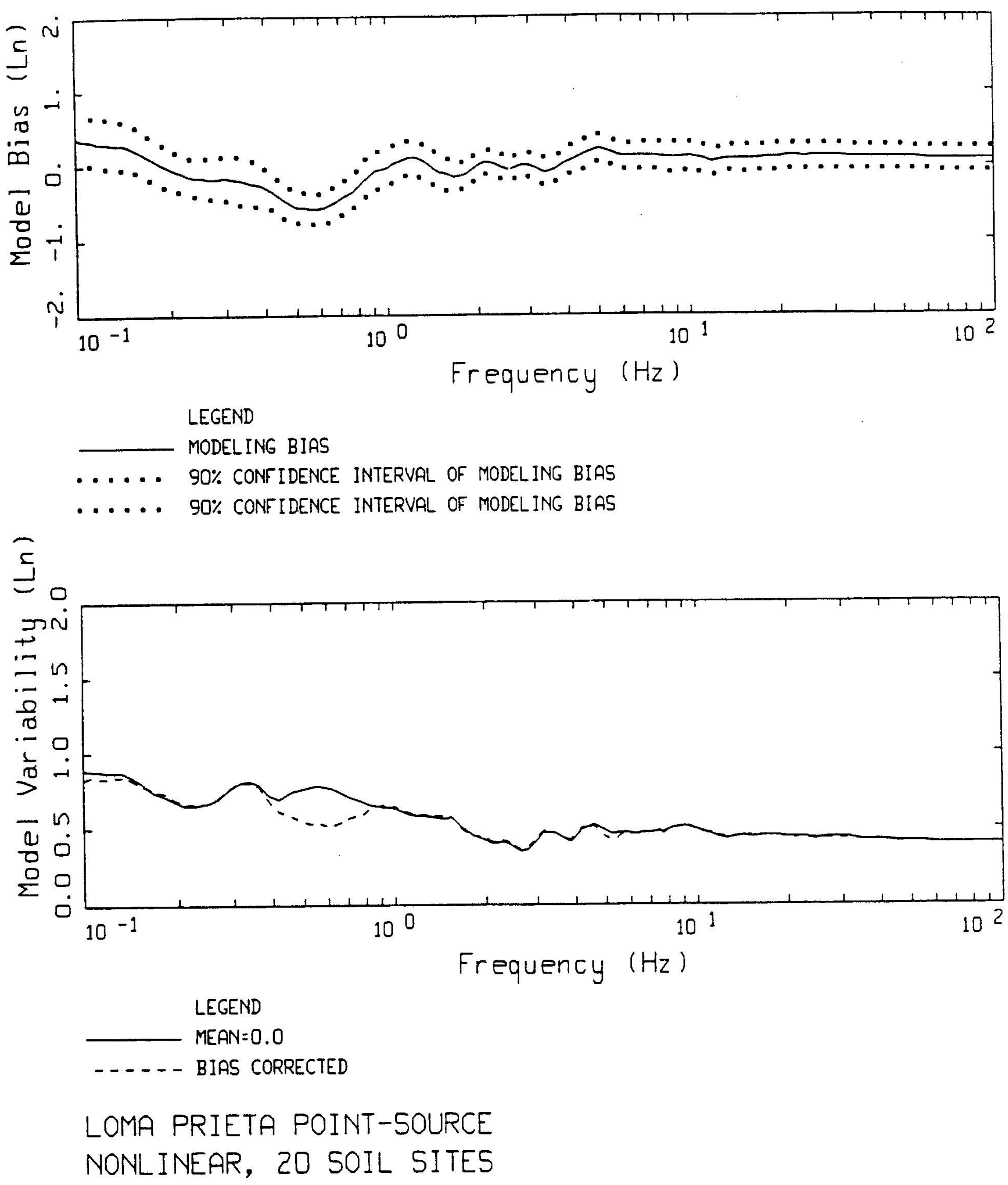

Source: Silva et al. 1996 [DIRS 110474] Figure 5.45

Figure 7-18. Model Bias and Variability Estimates for the Loma Prieta Earthquake Computed Over All 20 Soil Sites for the Point-Source Model

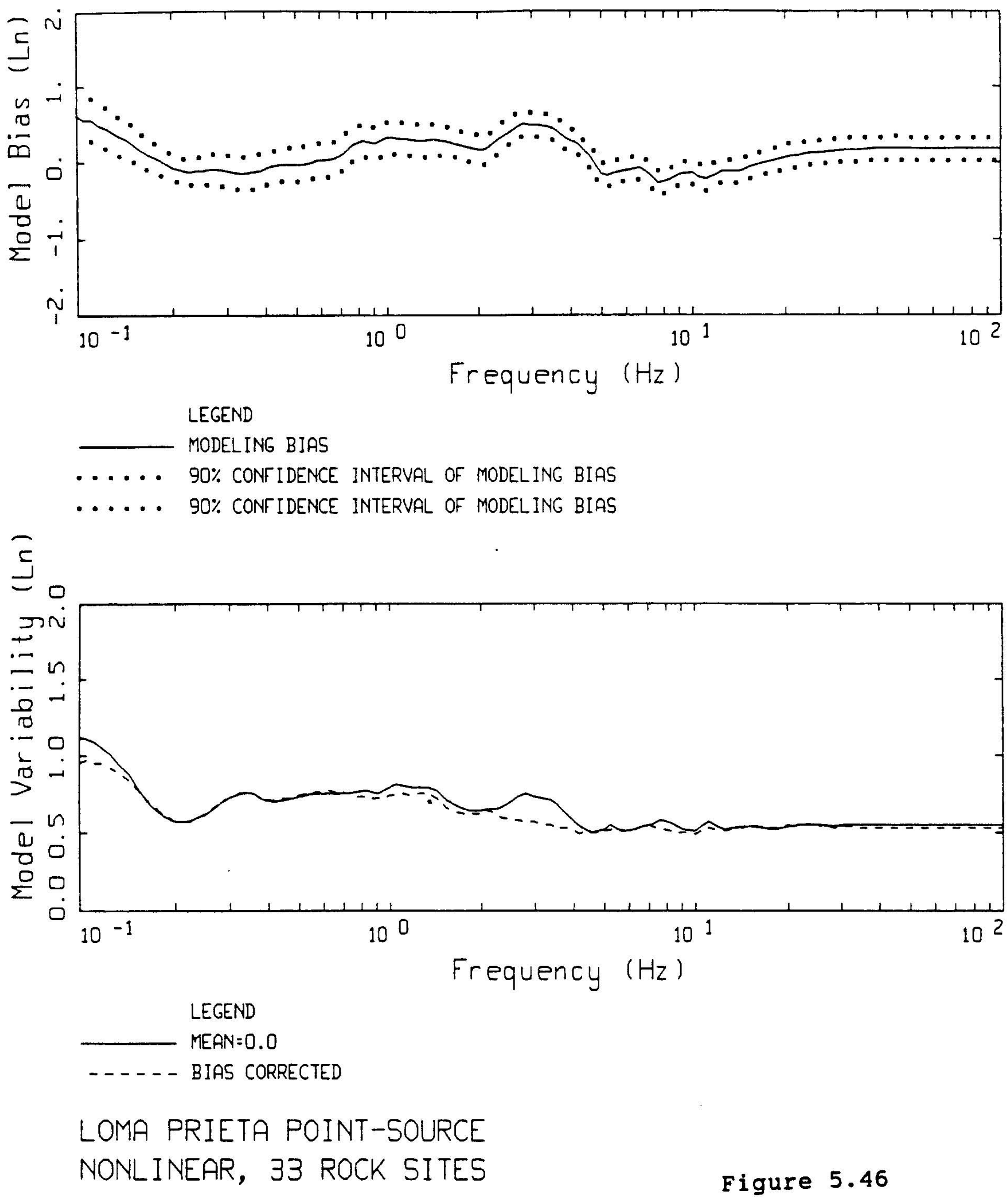

Source: Silva et al. 1996 [DIRS 110474] Figure 5.46

Figure 7-19. Model Bias and Variability Estimates for the Loma Prieta Earthquake Computed Over All 33 Rock Sites for the Point-Source Model

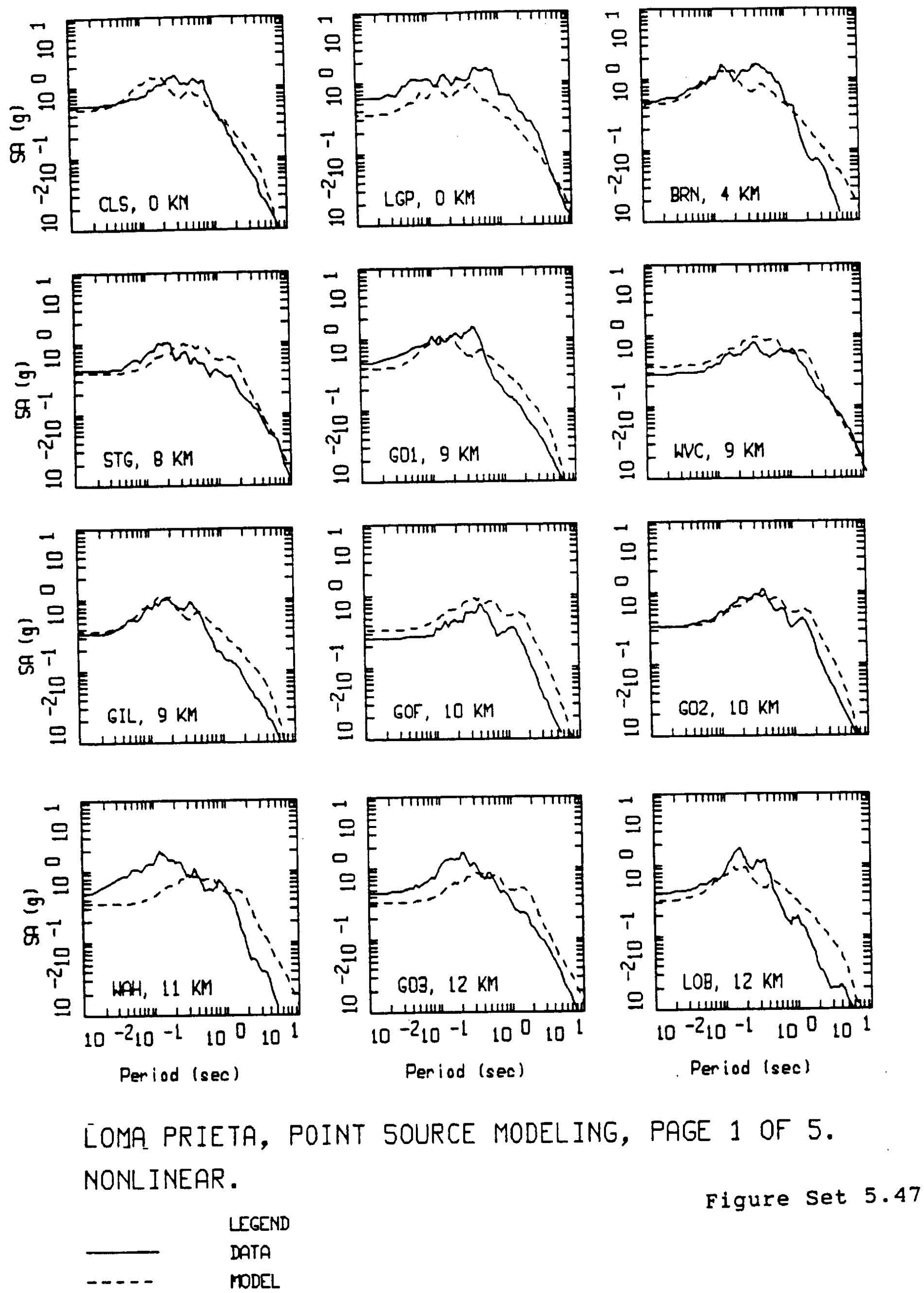

Source: Silva et al. 1996 [DIRS 110474] Figure 5.47

NOTE: Recorded Motions (solid lines), Point-Source Simulations (dashed lines)

Figure 7-20a. Comparison of Average Horizontal Component 5%-Damped Pseudo Relative Absolute Response Spectra: Loma Prieta Earthquake

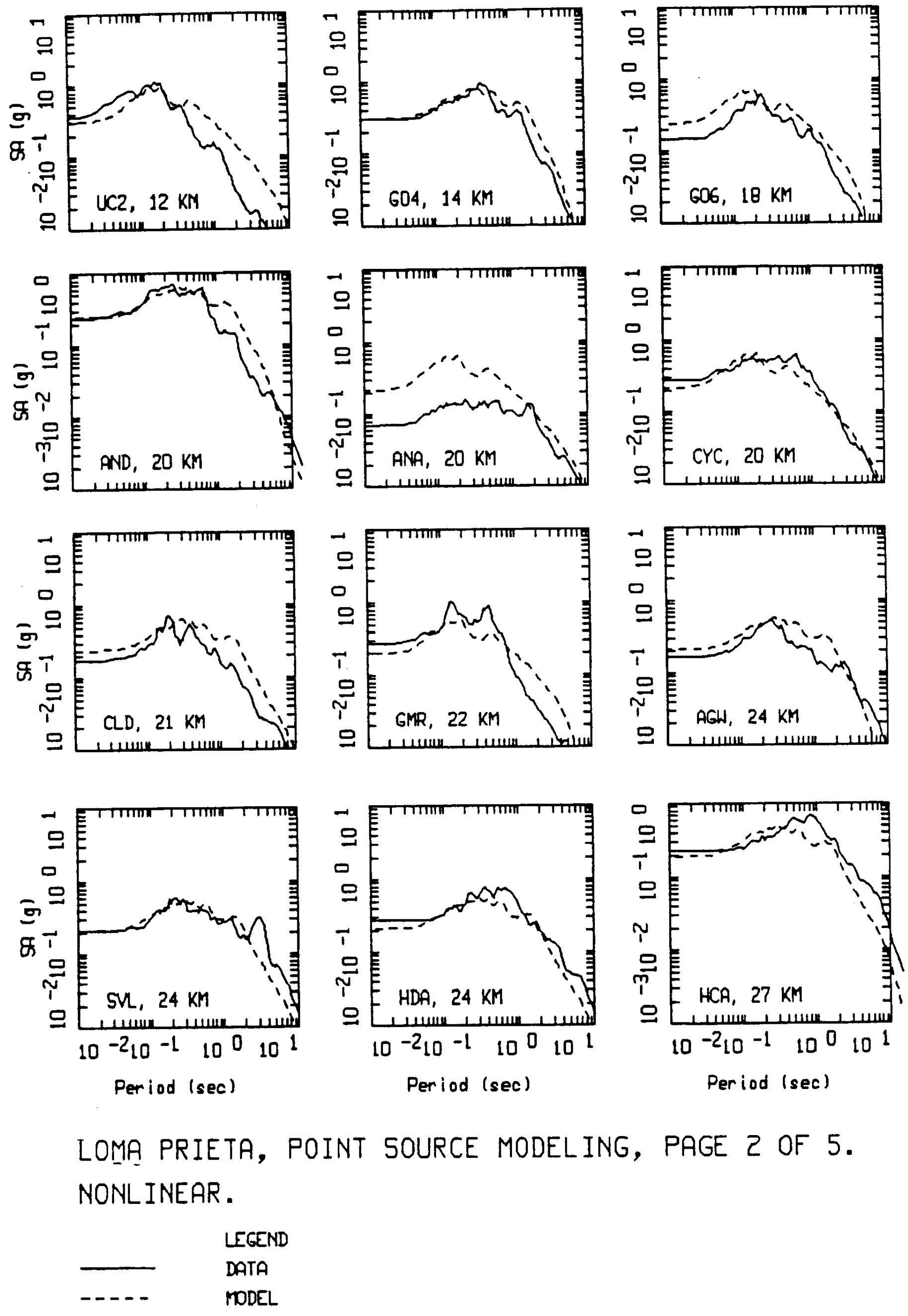

Source: Silva et al. 1996 [DIRS 110474] Figure 5.47

NOTE: Recorded Motions (solid lines), Point-Source Simulations (dashed lines)

Figure 7-20b. Comparison of Average Horizontal Component 5%-Damped Pseudo Relative Absolute Response Spectra: Loma Prieta Earthquake

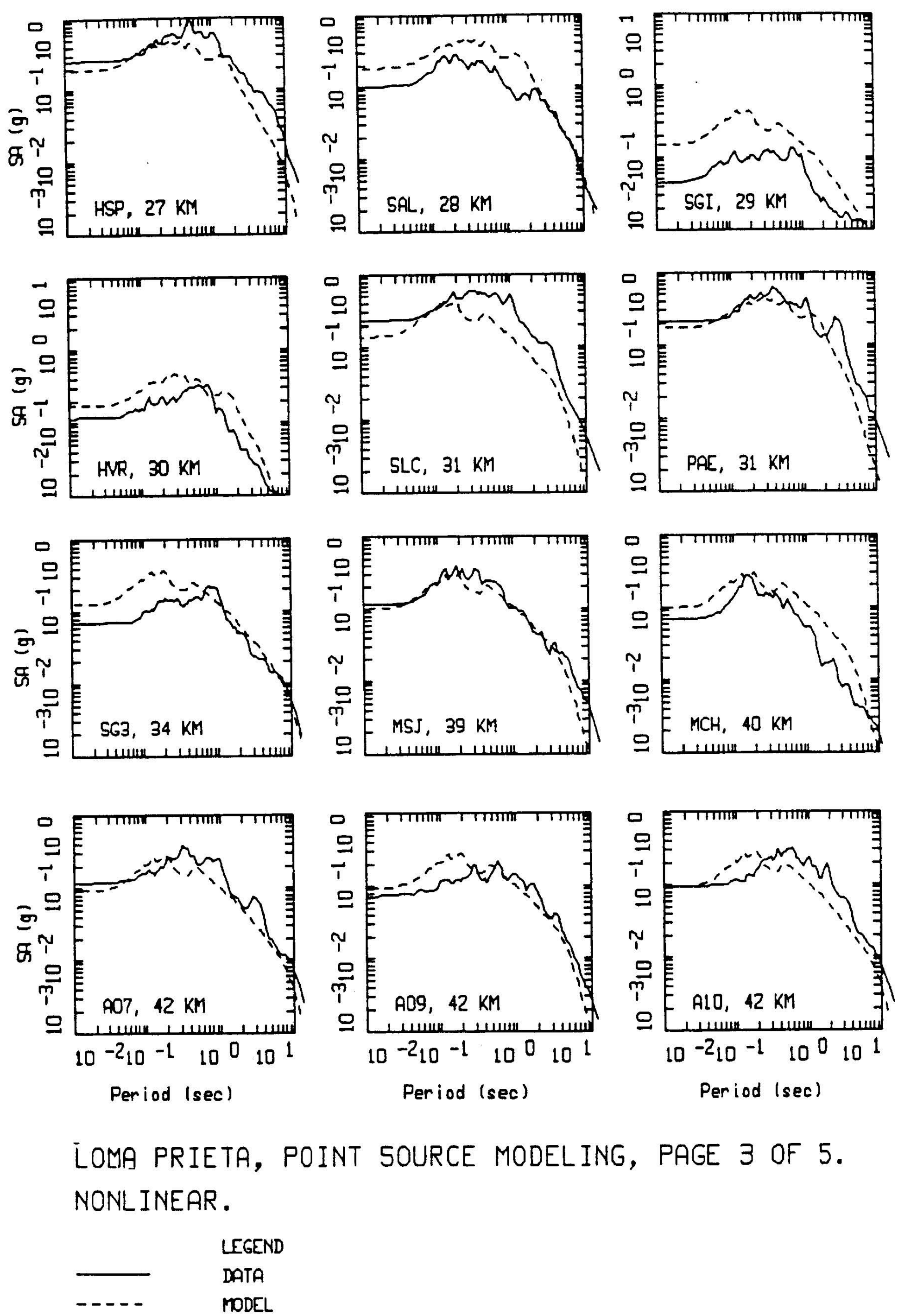

Source: Silva et al. 1996 [DIRS 110474] Figure 5.47

NOTE: Recorded Motions (solid lines), Point-Source Simulations (dashed lines)

Figure 7-20c Comparison of Average Horizontal Component 5%-Damped Pseudo Relative Absolute Response Spectra: Loma Prieta Earthquake

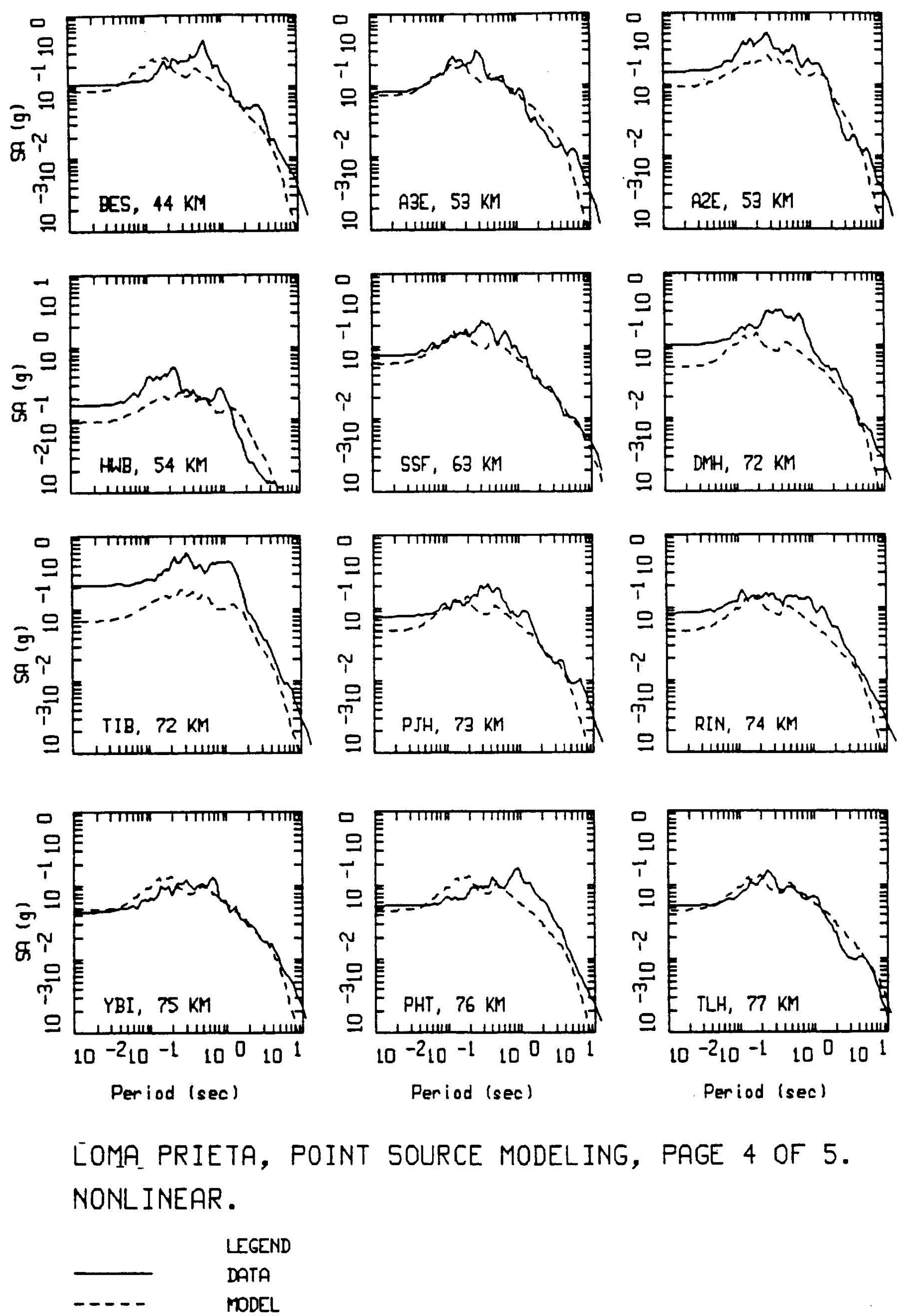

Source: Silva et al. 1996 [DIRS 110474] Figure 5.47

NOTE: Recorded Motions (solid lines), Point-Source Simulations (dashed lines)

Figure 7-20d. Comparison of Average Horizontal Component 5%-Damped Pseudo Relative Absolute Response Spectra: Loma Prieta Earthquake

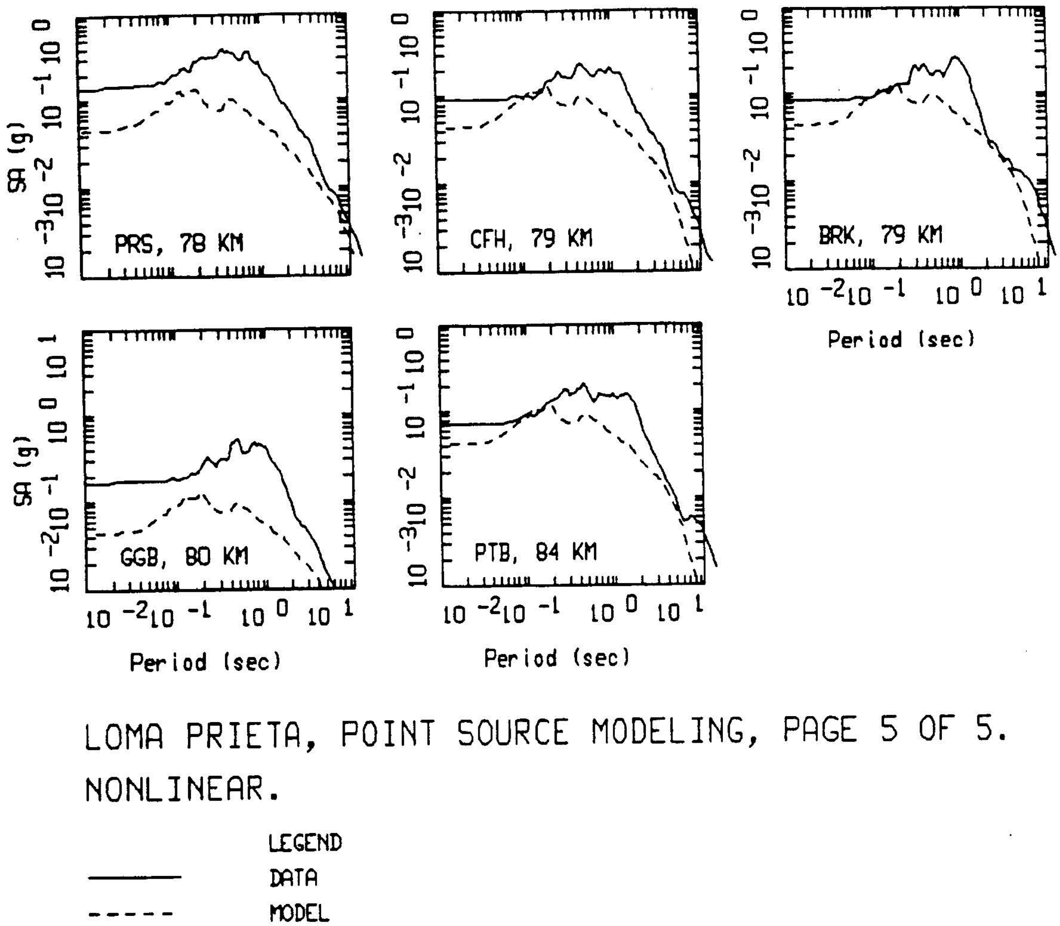

Source: Silva et al. 1996 [DIRS 110474] Figure 5.47

NOTE: Recorded Motions (solid lines), Point-Source Simulations (dashed lines)

Figure 7-20e. Comparison of Average Horizontal Component 5%-Damped Pseudo Relative Absolute Response Spectra: Loma Prieta Earthquake

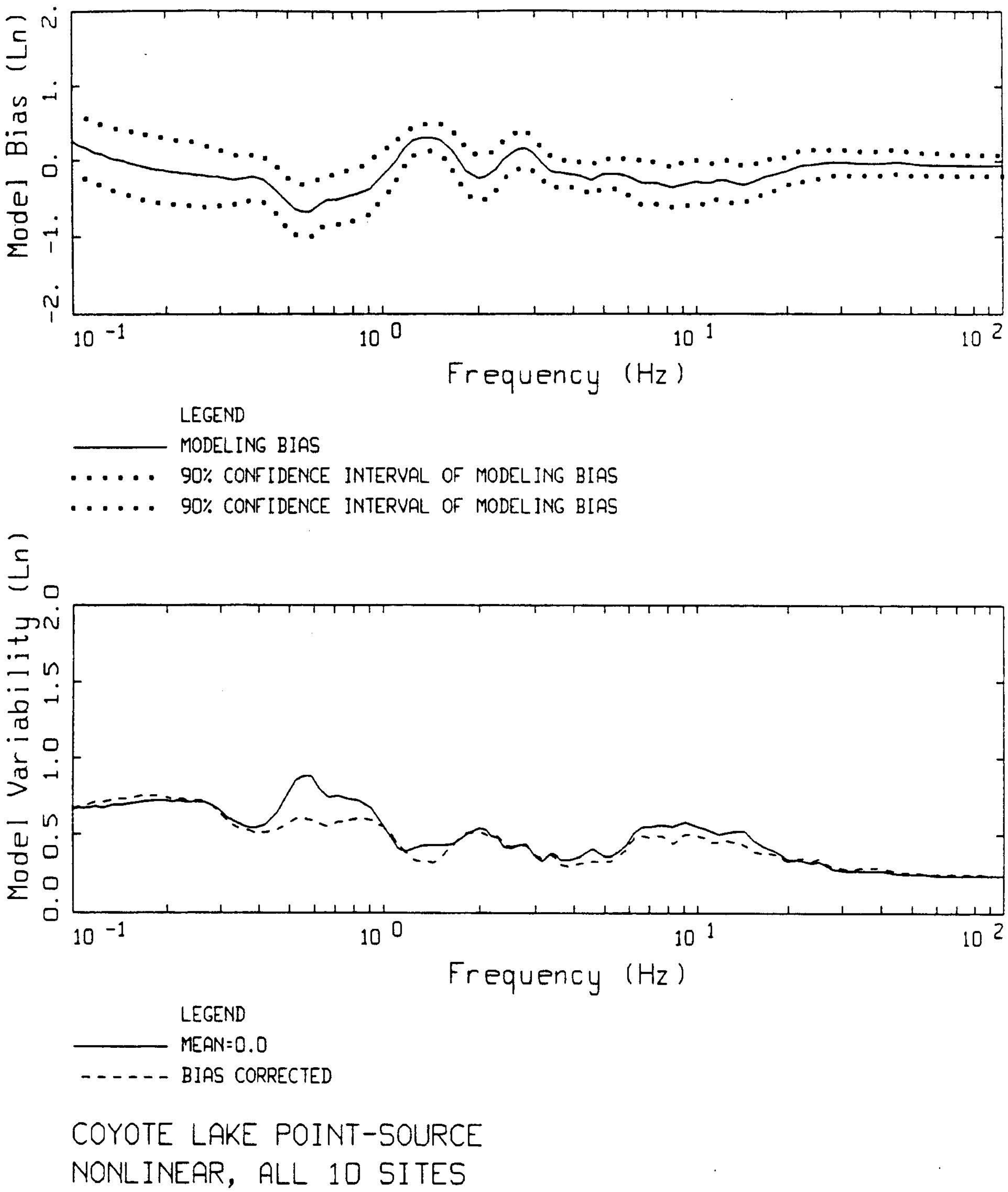

Source: Silva et al. 1996 [DIRS 110474] Figure 5.60

Figure 7-21. Model Bias and Variability Estimates for the Coyote Lake Earthquake Computed Over All 10 Sites for the Point-Source Model

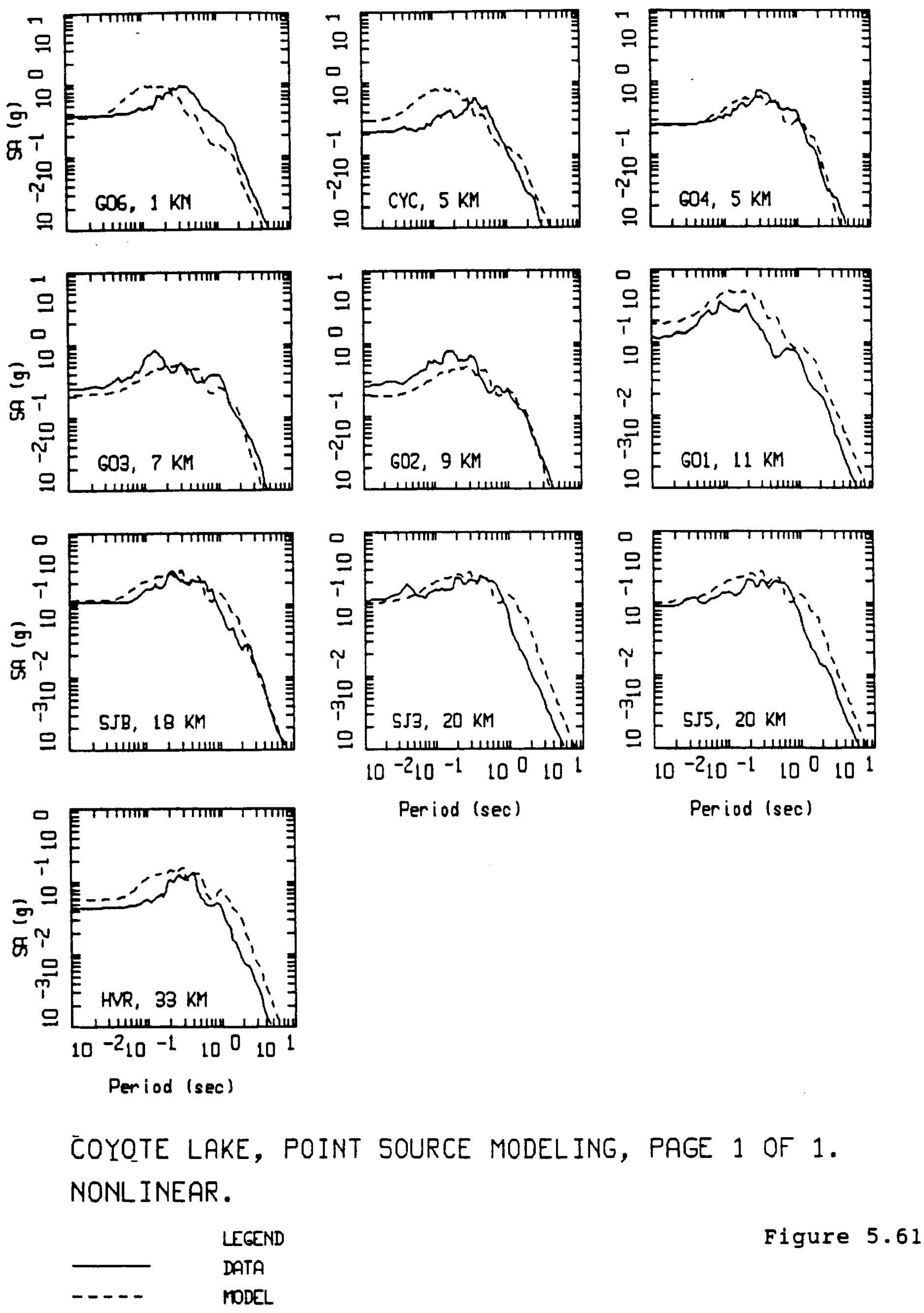

Source: Silva et al. 1996 [DIRS 110474] Figure 5.61

NOTE: Recorded Motions (solid lines), Point-Source Simulations (dashed lines)

Figure 7-22 Comparison of Average Horizontal Component 5%-Damped Pseudo Relative Absolute Response Spectra: Coyote Lake Earthquake

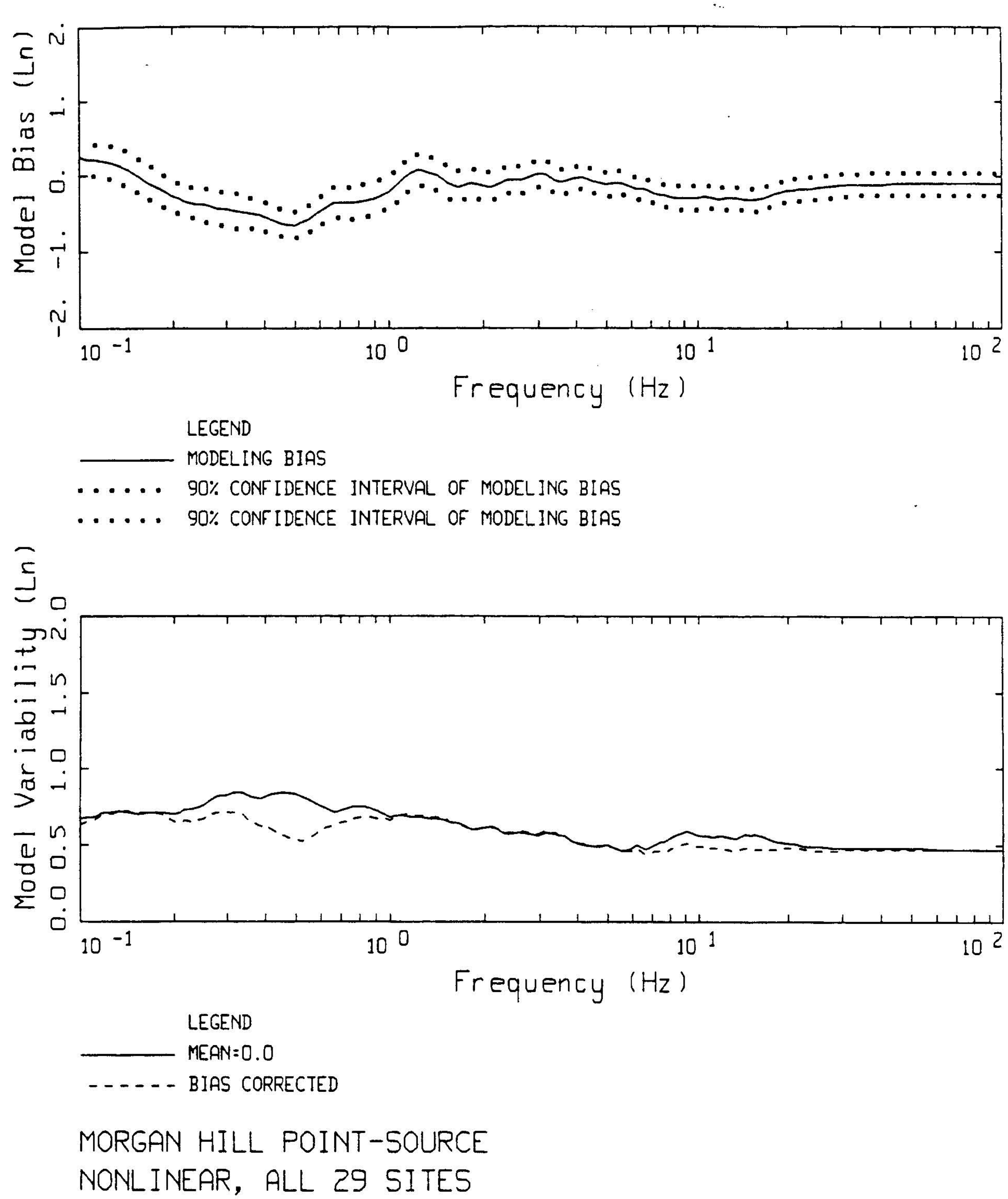

Source: Silva et al. 1996 [DIRS 110474] Figure 5.66

Figure 7-23. Model Bias and Variability Estimates for the Morgan Hill Earthquake Computed Over All 29 Sites for the Point-Source Model

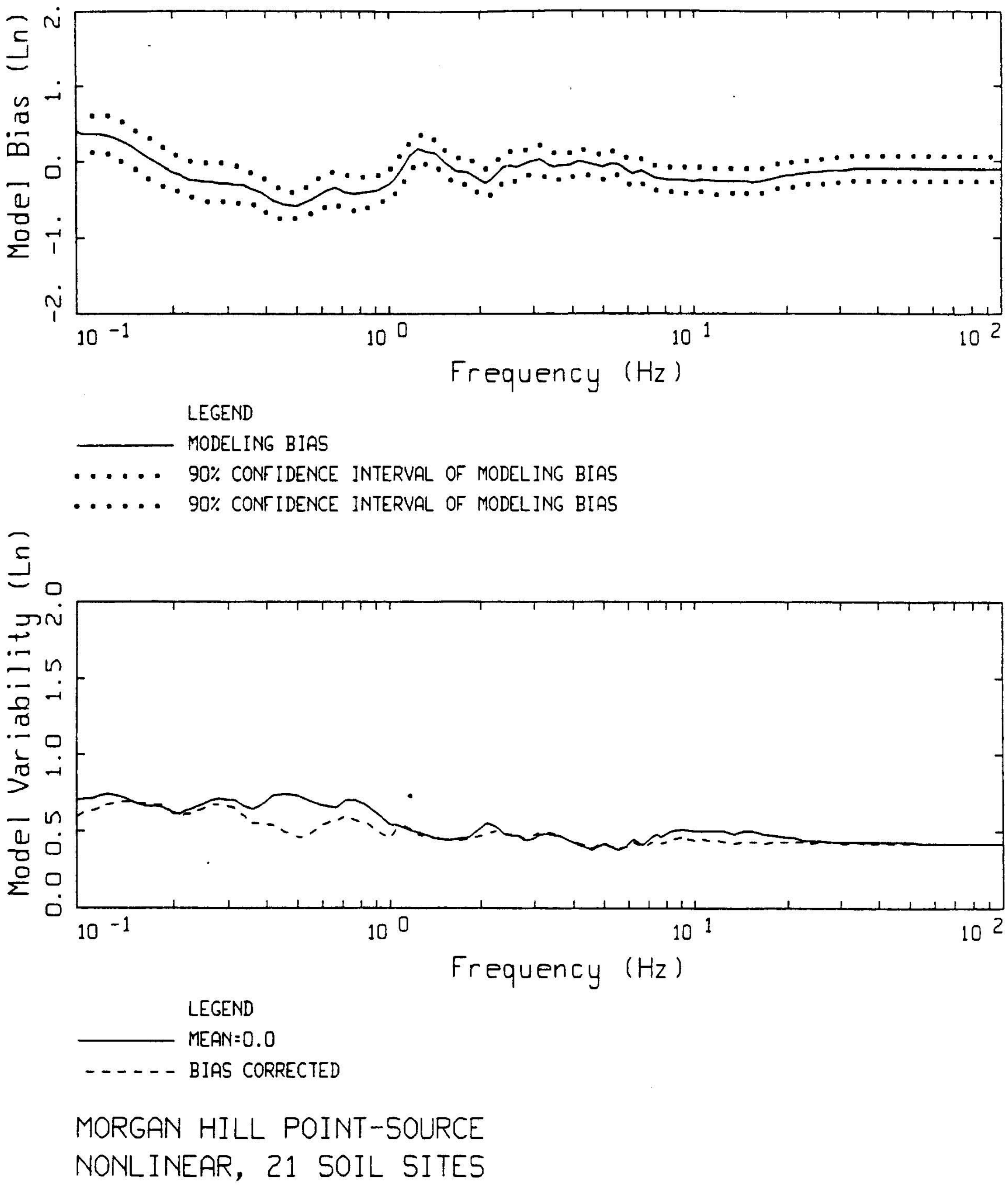

Source: Silva et al. 1996 [DIRS 110474] Figure 5.67

Figure 7-24. Model Bias and Variability Estimates for the Morgan Hill Earthquake Computed Over All 21 Soil Sites for the Point-Source Model

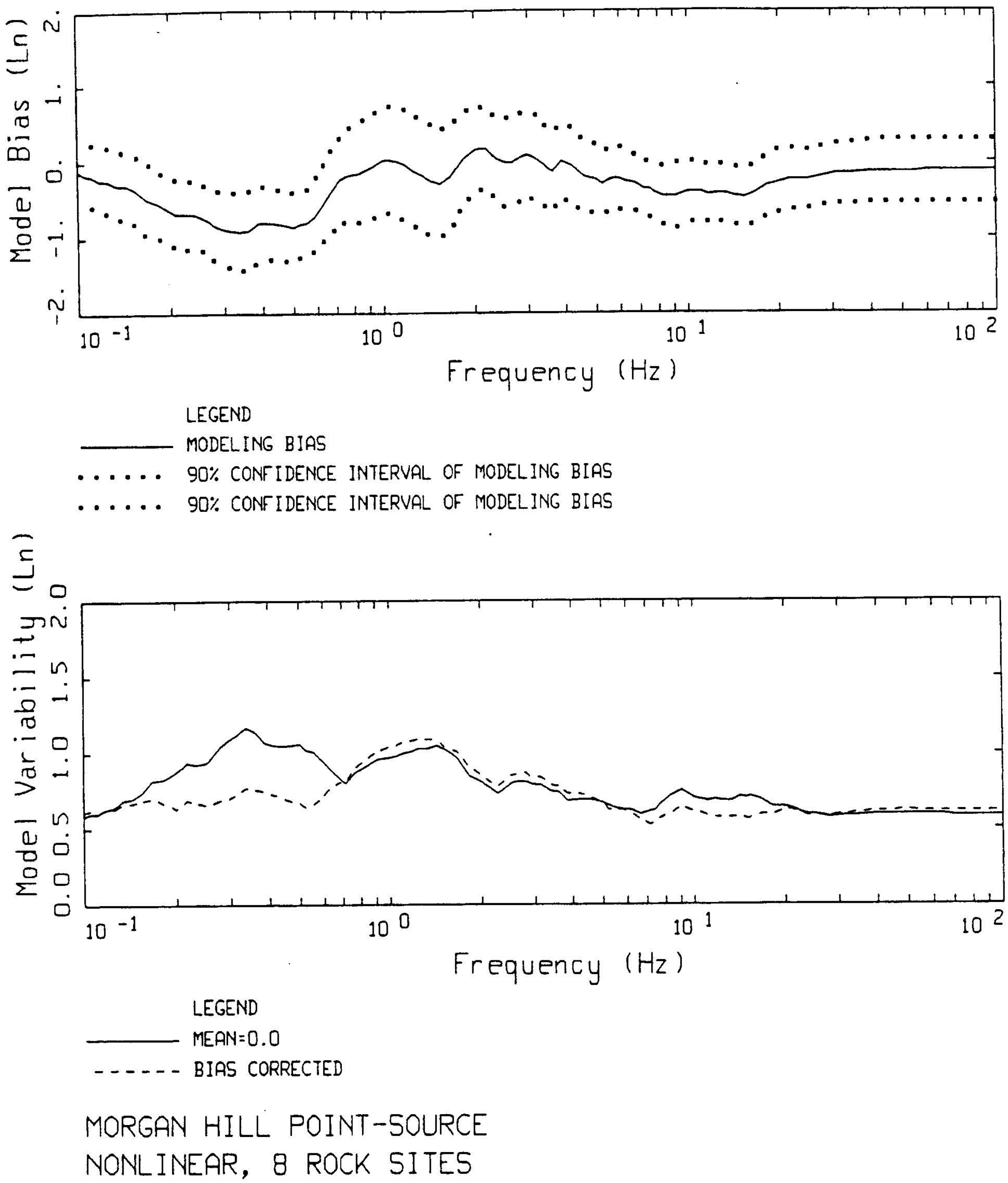

Source: Silva et al. 1996 [DIRS 110474] Figure 5.68

Figure 7-25. Model Bias and Variability Estimates for the Morgan Hill Earthquake Computed Over All 8 Rock Sites for the Point-Source Model

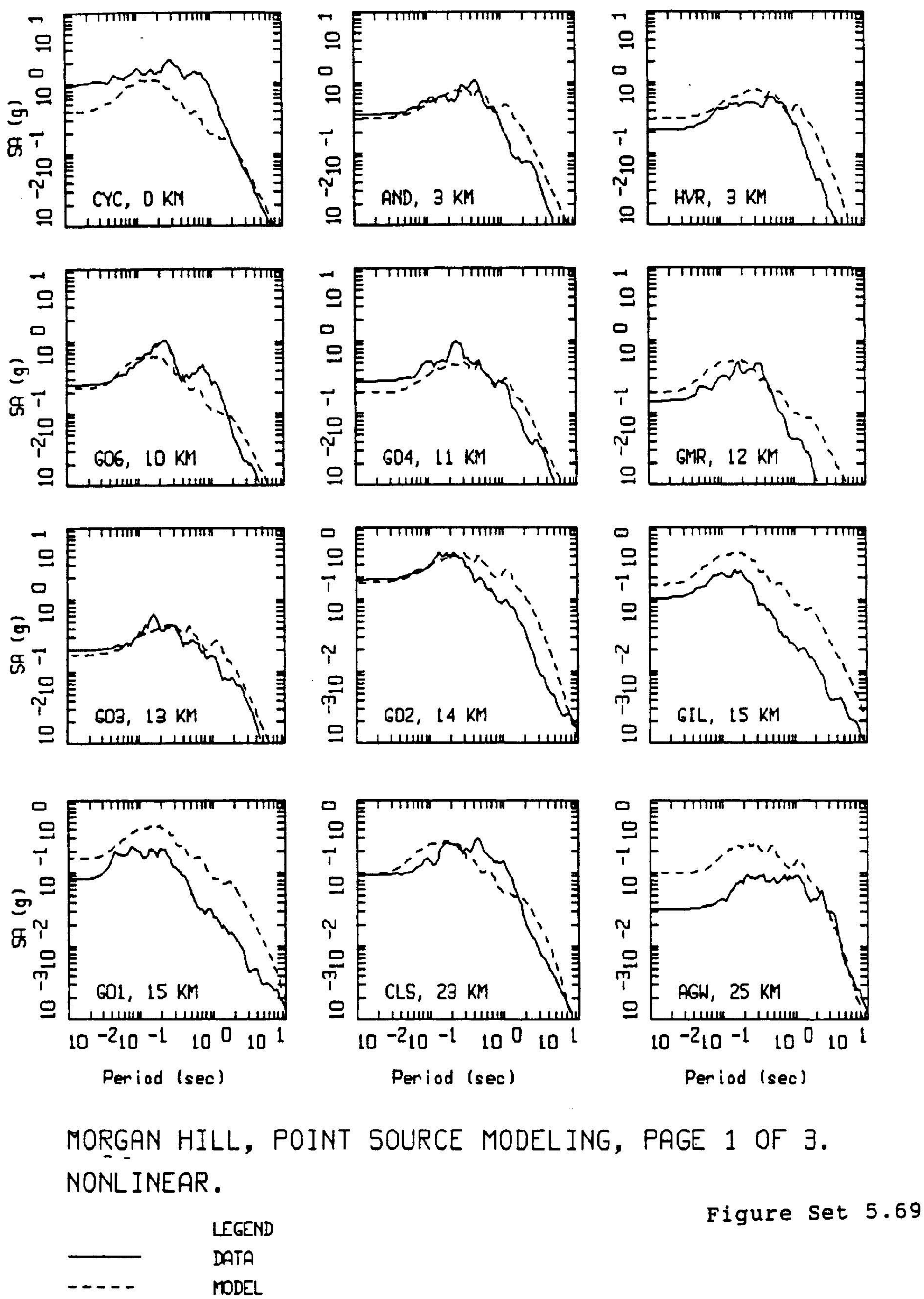

Source: Silva et al. 1996 [DIRS 110474] Figure 5.69

NOTE: Recorded Motions (solid lines), Point-Source Simulations (dashed lines)

Figure 7-26a Comparison of Average Horizontal Component 5%-Damped Pseudo Relative Absolute Response Spectra: Morgan Hill Earthquake

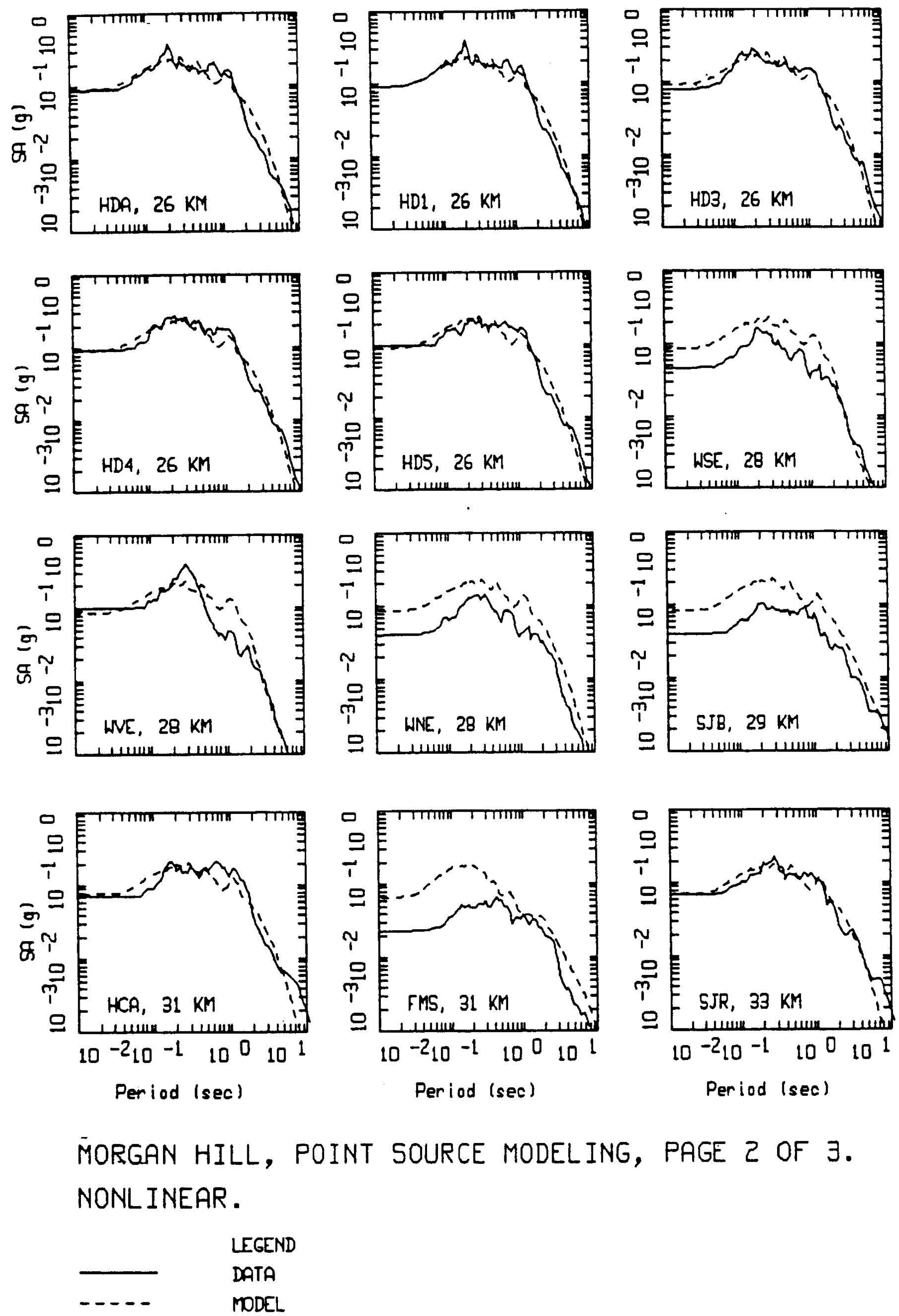

Source: Silva et al. 1996 [DIRS 110474] Figure 5.69

NOTE: Recorded Motions (solid lines), Point-Source Simulations (dashed lines)

Figure 7-26b Comparison of Average Horizontal Component 5%-Damped Pseudo Relative Absolute Response Spectra: Morgan Hill Earthquake

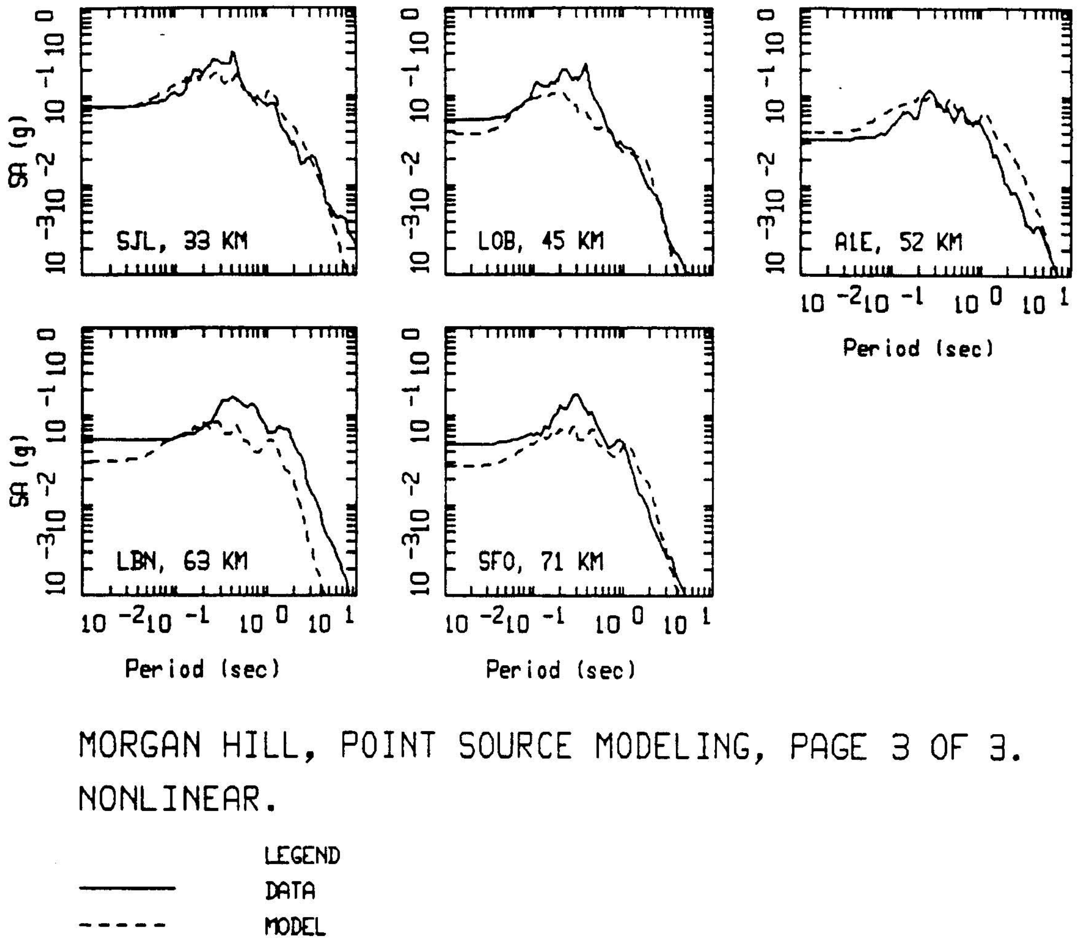

Source: Silva et al. 1996 [DIRS 110474] Figure 5.69

NOTE: Recorded Motions (solid lines), Point-Source Simulations (dashed lines)

Figure 7-26c Comparison of Average Horizontal Component 5%-Damped Pseudo Relative Absolute Response Spectra: Morgan Hill Earthquake

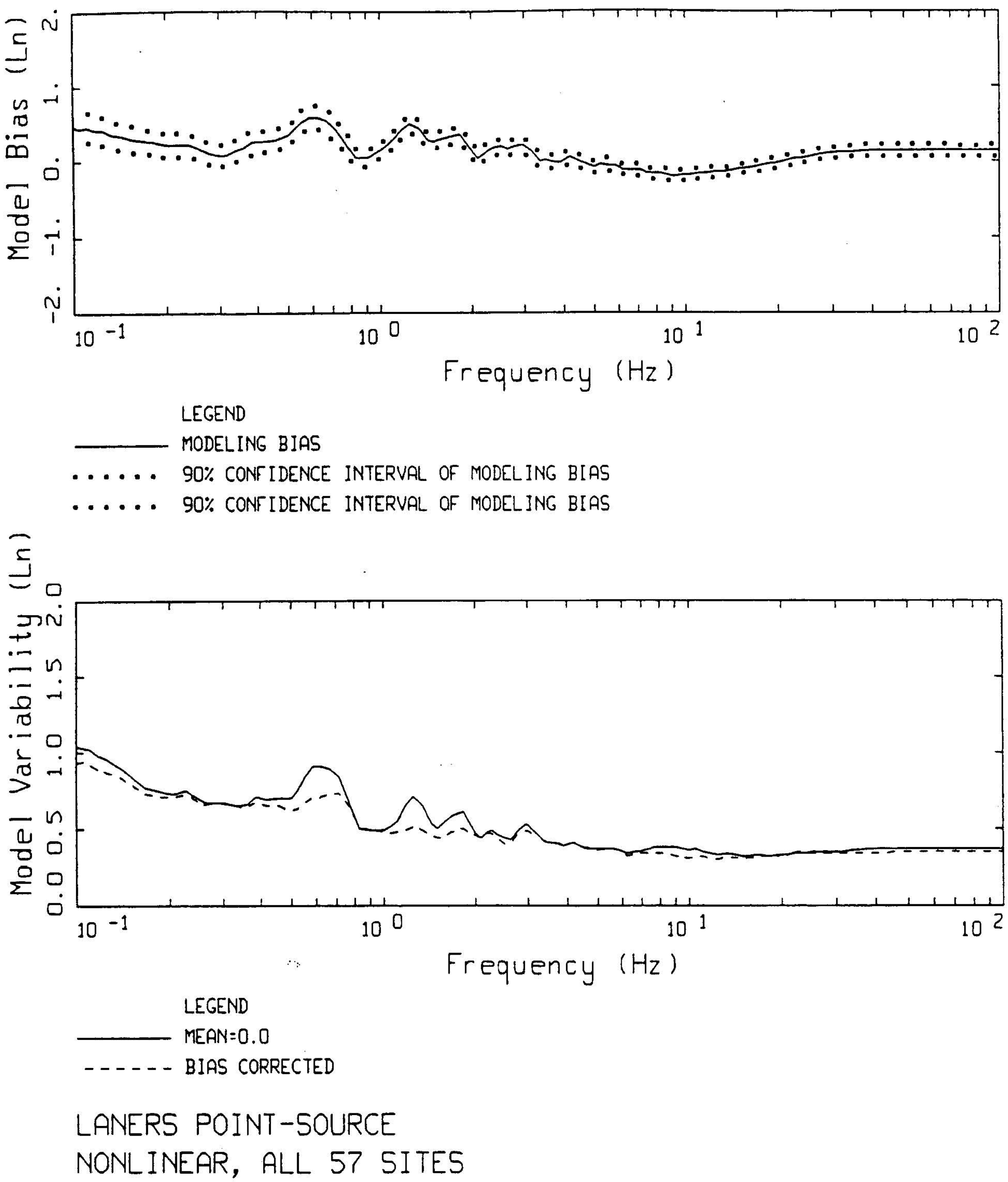

Source: Silva et al. 1996 [DIRS 110474] Figure 5.76

Figure 7-27. Model Bias and Variability Estimates for the Landers Earthquake Computed Over All 57 Sites for the Point-Source Model

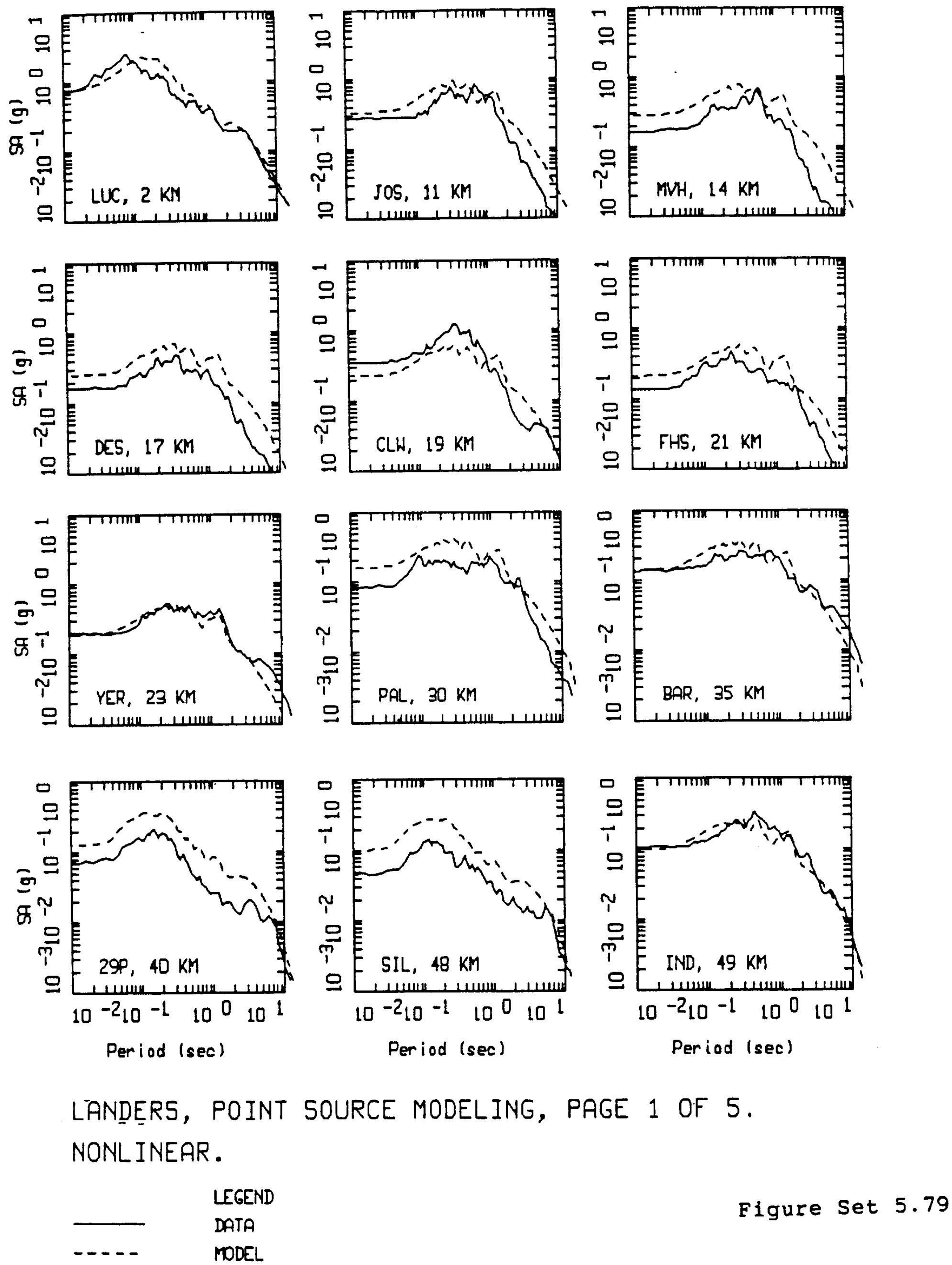

Source: Silva et al. 1996 [DIRS 110474] Figure 5.79

NOTE: Recorded Motions (solid lines), Point-Source Simulations (dashed lines)

Figure 7-28a Comparison of Average Horizontal Component 5%-Damped Pseudo Relative Absolute Response Spectra: Landers Earthquake

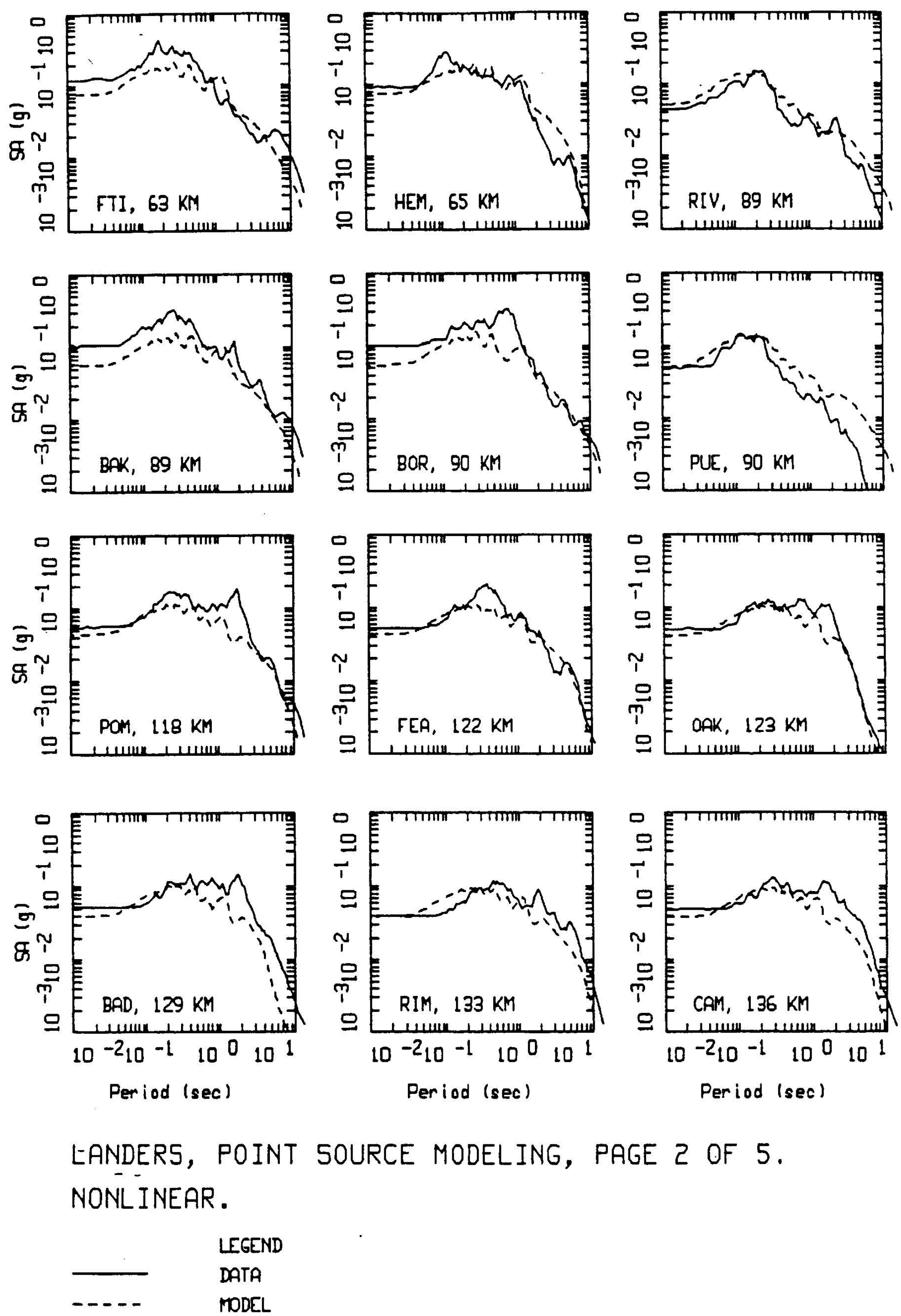

Source: Silva et al. 1996 [DIRS 110474] Figure 5.79

NOTE: Recorded Motions (solid lines), Point-Source Simulations (dashed lines)

Figure 7-28b Comparison of Average Horizontal Component 5%-Damped Pseudo Relative Absolute Response Spectra: Landers Earthquake

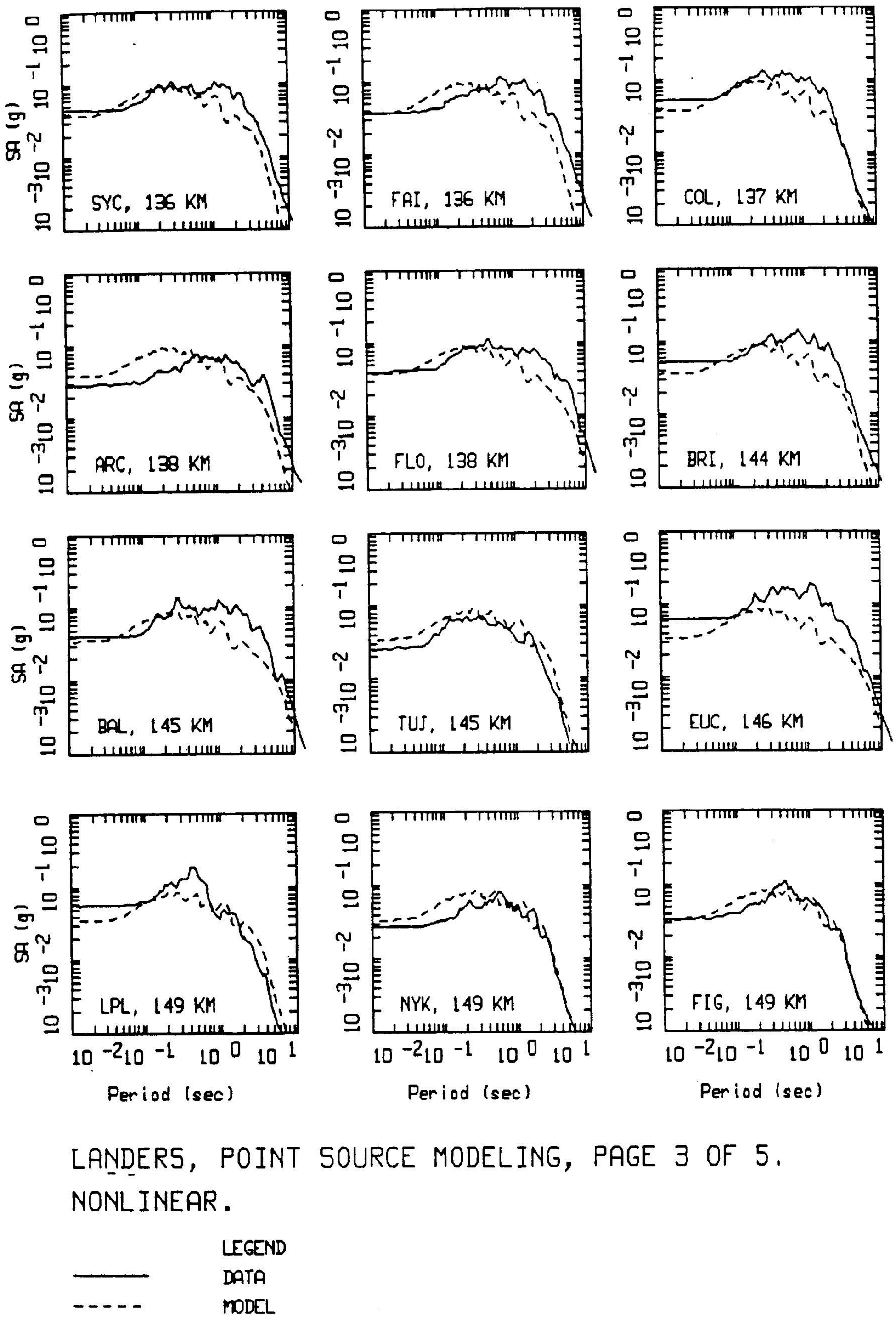

Source: Silva et al. 1996 [DIRS 110474] Figure 5.79

NOTE: Recorded Motions (solid lines), Point-Source Simulations (dashed lines)

Figure 7-28c Comparison of Average Horizontal Component 5%-Damped Pseudo Relative Absolute Response Spectra: Landers Earthquake

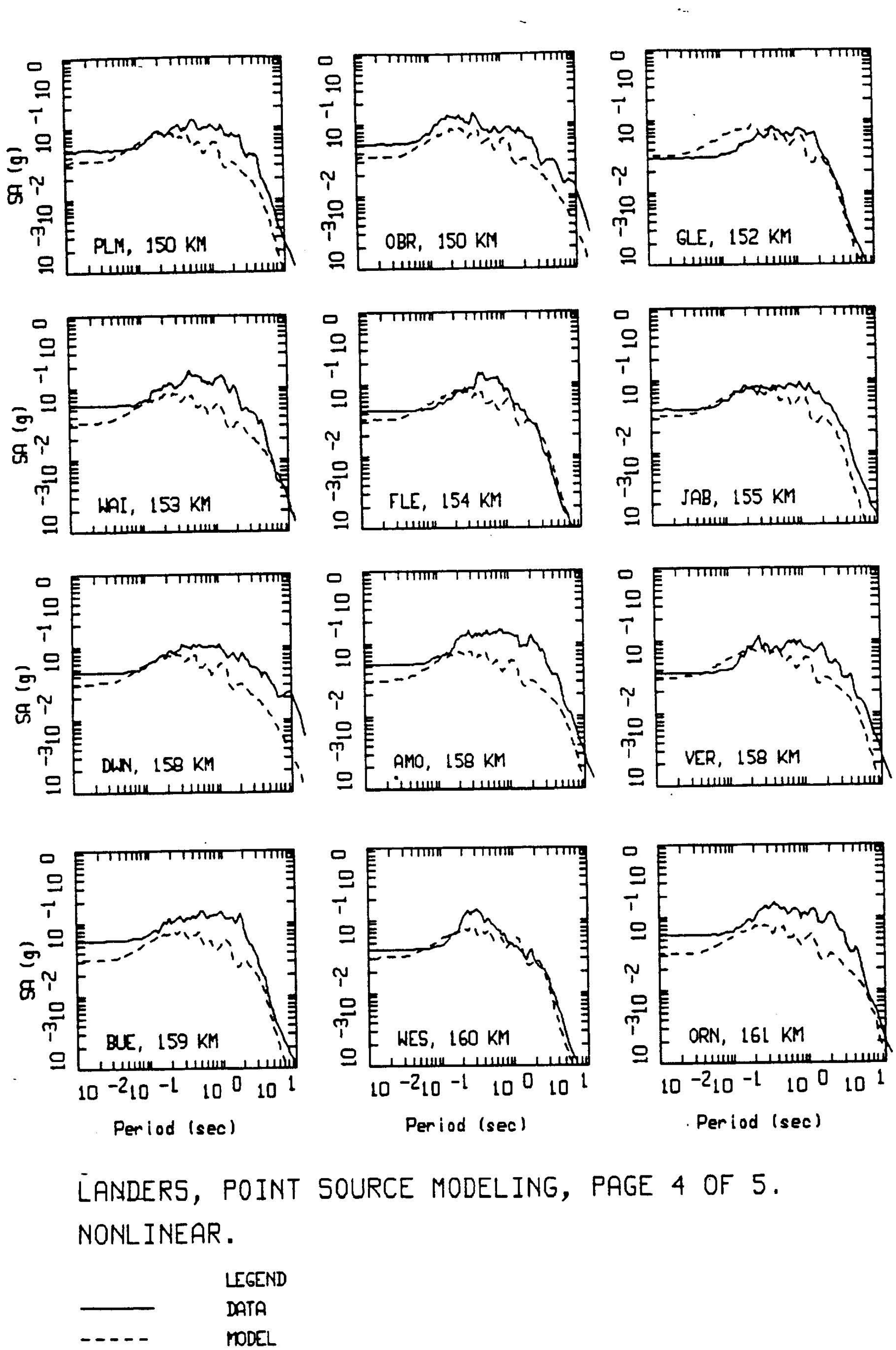

Source: Silva et al. 1996 [DIRS 110474] Figure 5.79

NOTE: Recorded Motions (solid lines), Point-Source Simulations (dashed lines)

Figure 7-28d Comparison of Average Horizontal Component 5%-Damped Pseudo Relative Absolute Response Spectra: Landers Earthquake

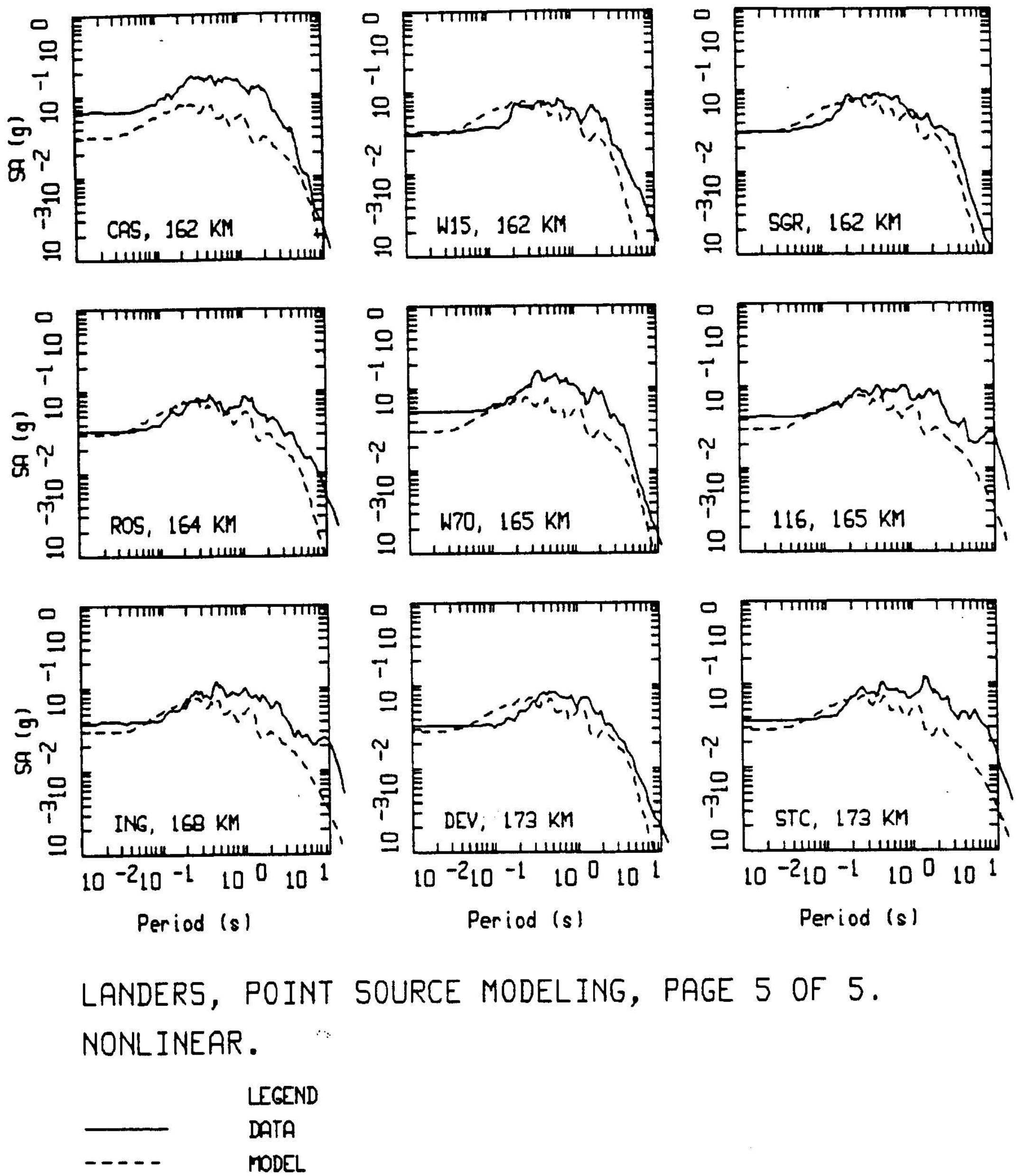

Source: Silva et al. 1996 [DIRS 110474] Figure 5.79

NOTE: Recorded Motions (solid lines), Point-Source Simulations (dashed lines)

Figure 7-28e Comparison of Average Horizontal Component 5%-Damped Pseudo Relative Absolute Response Spectra: Landers Earthquake

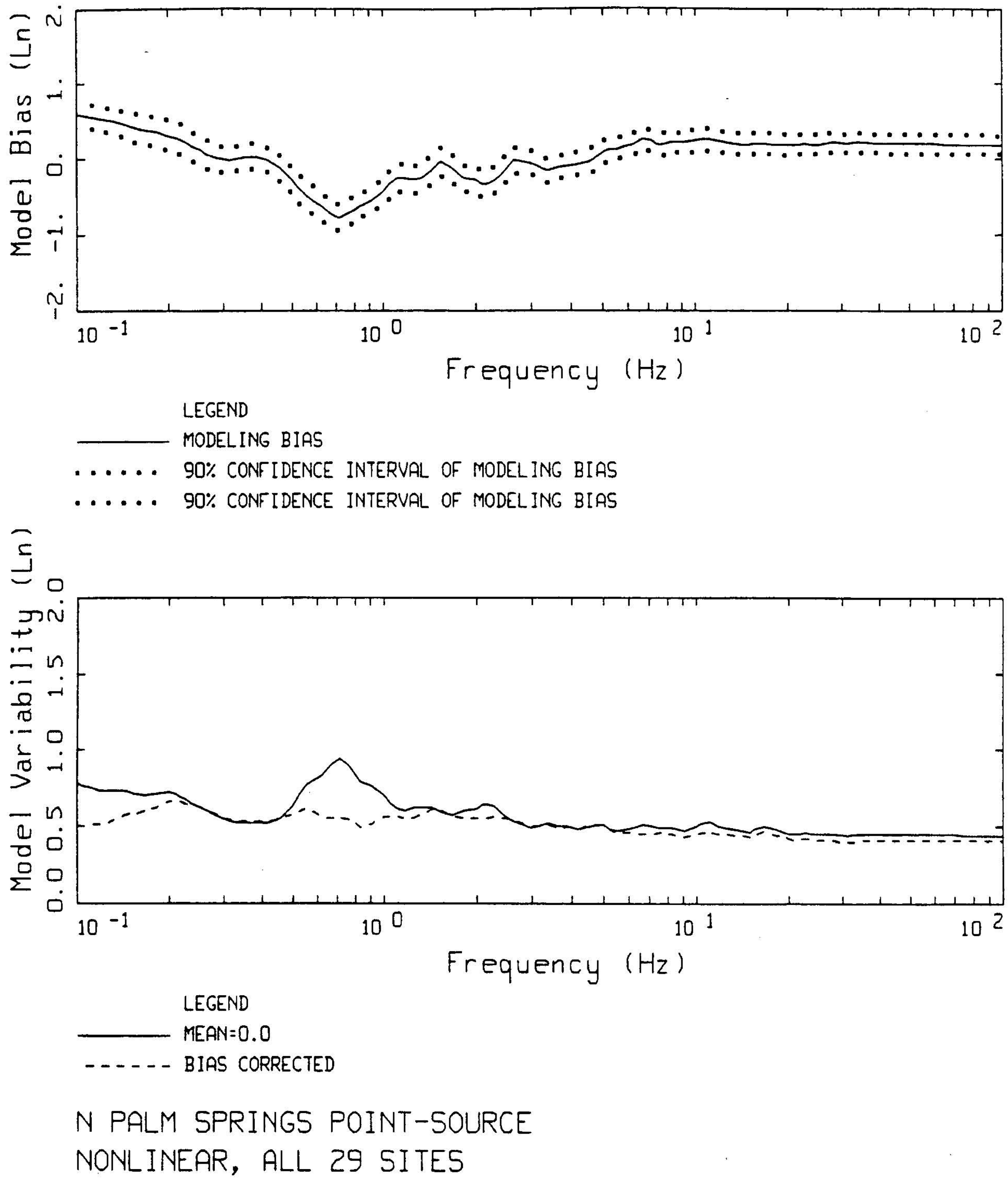

Source: Silva et al. 1996 [DIRS 110474] Figure 5.86

Figure 7-29. Model Bias and Variability Estimates for the North Palm Springs Earthquake Computed Over All 29 Sites for the Point-Source Model

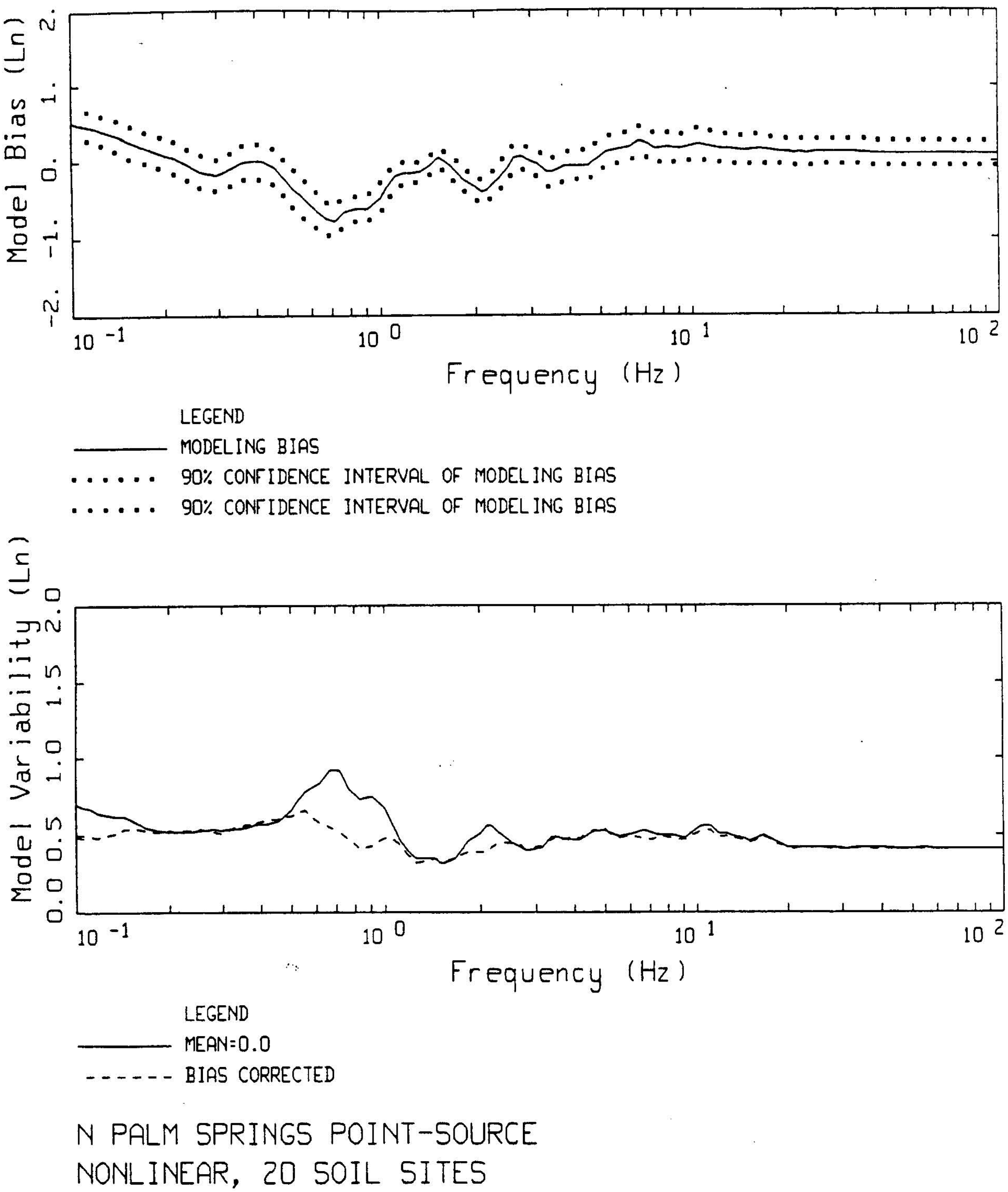

Source: Silva et al. 1996 [DIRS 110474] Figure 5.87

Figure 7-30. Model Bias and Variability Estimates for the North Palm Springs Earthquake Computed Over All 20 Soil Sites for the Point-Source Model

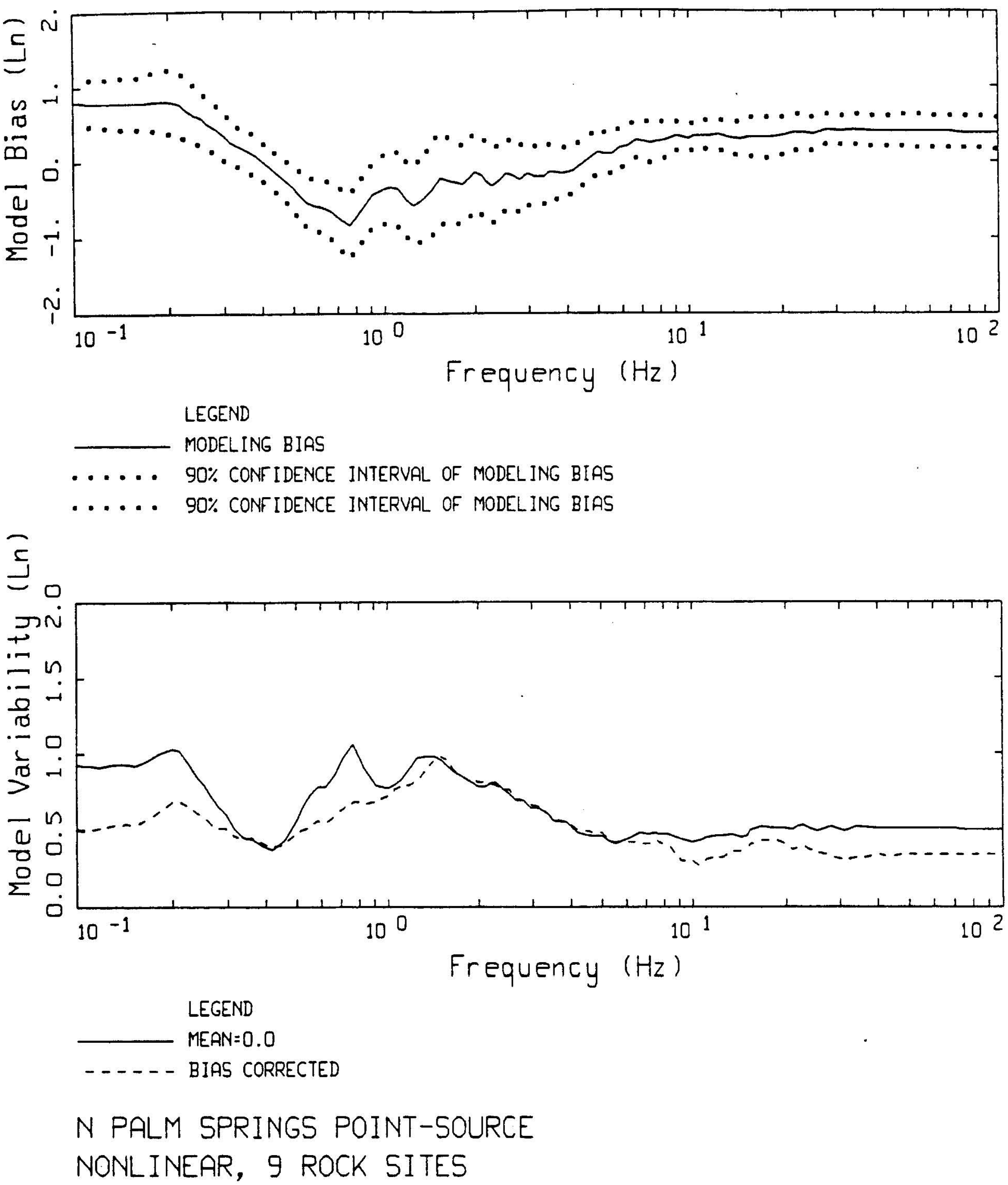

Source: Silva et al. 1996 [DIRS 110474] Figure 5.88

Figure 7-31. Model Bias and Variability Estimates for the North Palm Springs Earthquake Computed Over All 9 Soil Sites for the Point-Source Model

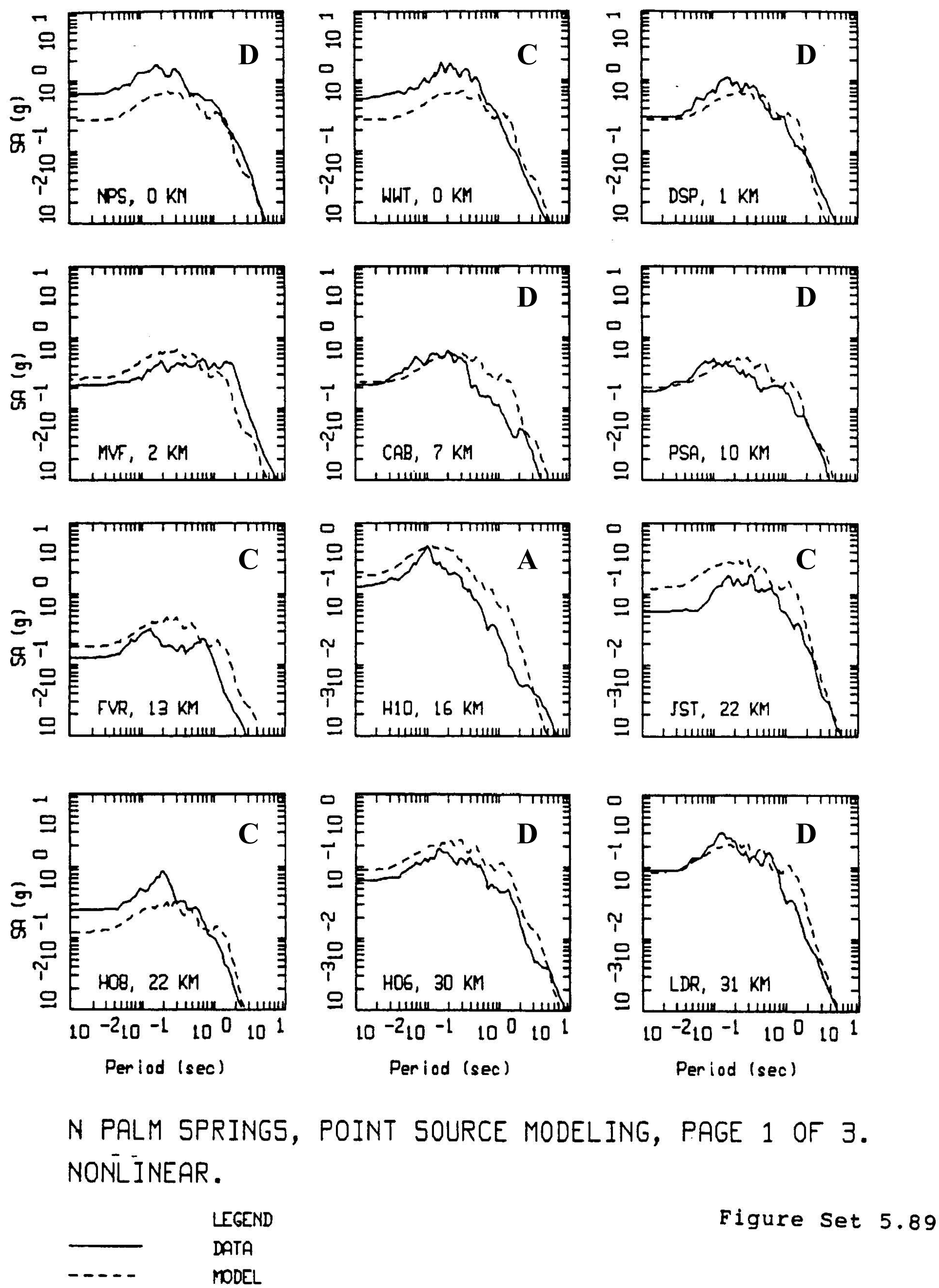

Source: Silva et al. 1996 [DIRS 110474] Figure 5.89

NOTE: Recorded Motions (solid lines), Point-Source Simulations (dashed lines)
Geomatrix site categories (A, B, C, D) are noted for each station.

Figure 7-32a Comparison of Average Horizontal Component 5%-Damped Pseudo Relative Absolute Response Spectra: North Palm Springs Earthquake

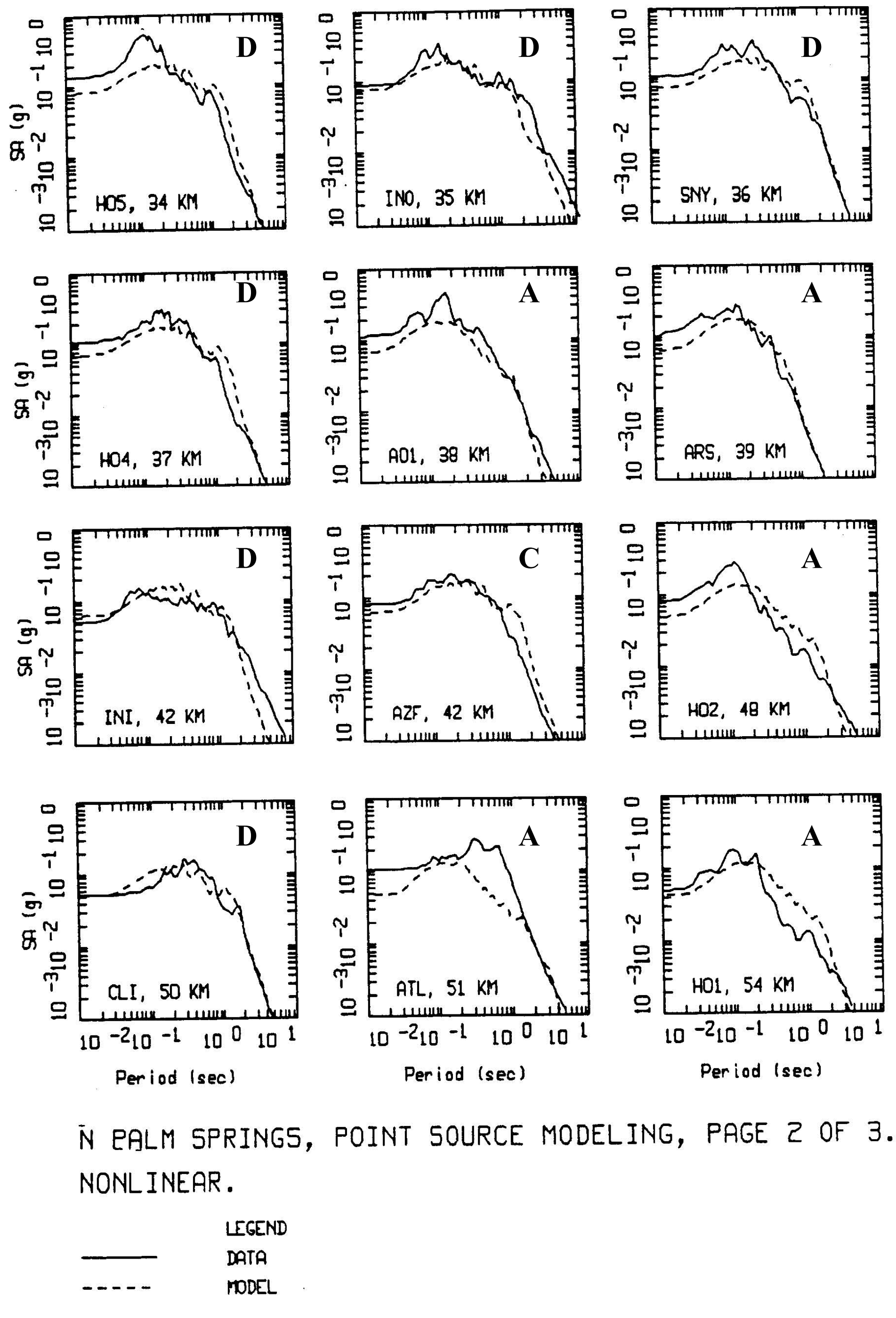

Source: Silva et al. 1996 [DIRS 110474] Figure 5.89

NOTE: Recorded Motions (solid lines), Point-Source Simulations (dashed lines)
Geomatrix site categories (A, B, C, D) are noted for each station.

Figure 7-32b Comparison of Average Horizontal Component 5%-Damped Pseudo Relative Absolute Response Spectra: North Palm Springs Earthquake

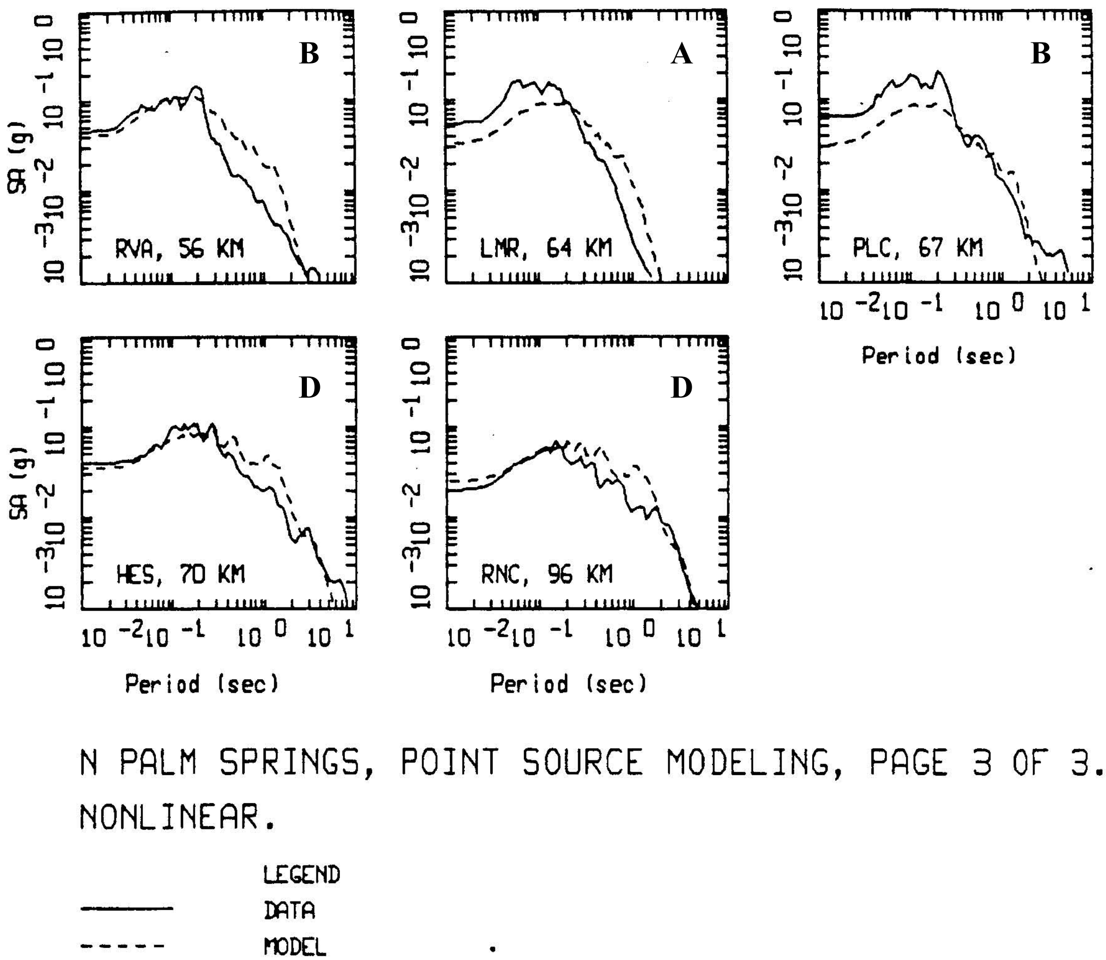

Source: Silva et al. 1996 [DIRS 110474] Figure 5.89

NOTE: Recorded Motions (solid lines), Point-Source Simulations (dashed lines)
Geomatrix site categories (A, B, C, D) are noted for each station.

Figure 7-32c Comparison of Average Horizontal Component 5%-Damped Pseudo Relative Absolute Response Spectra: North Palm Springs Earthquake

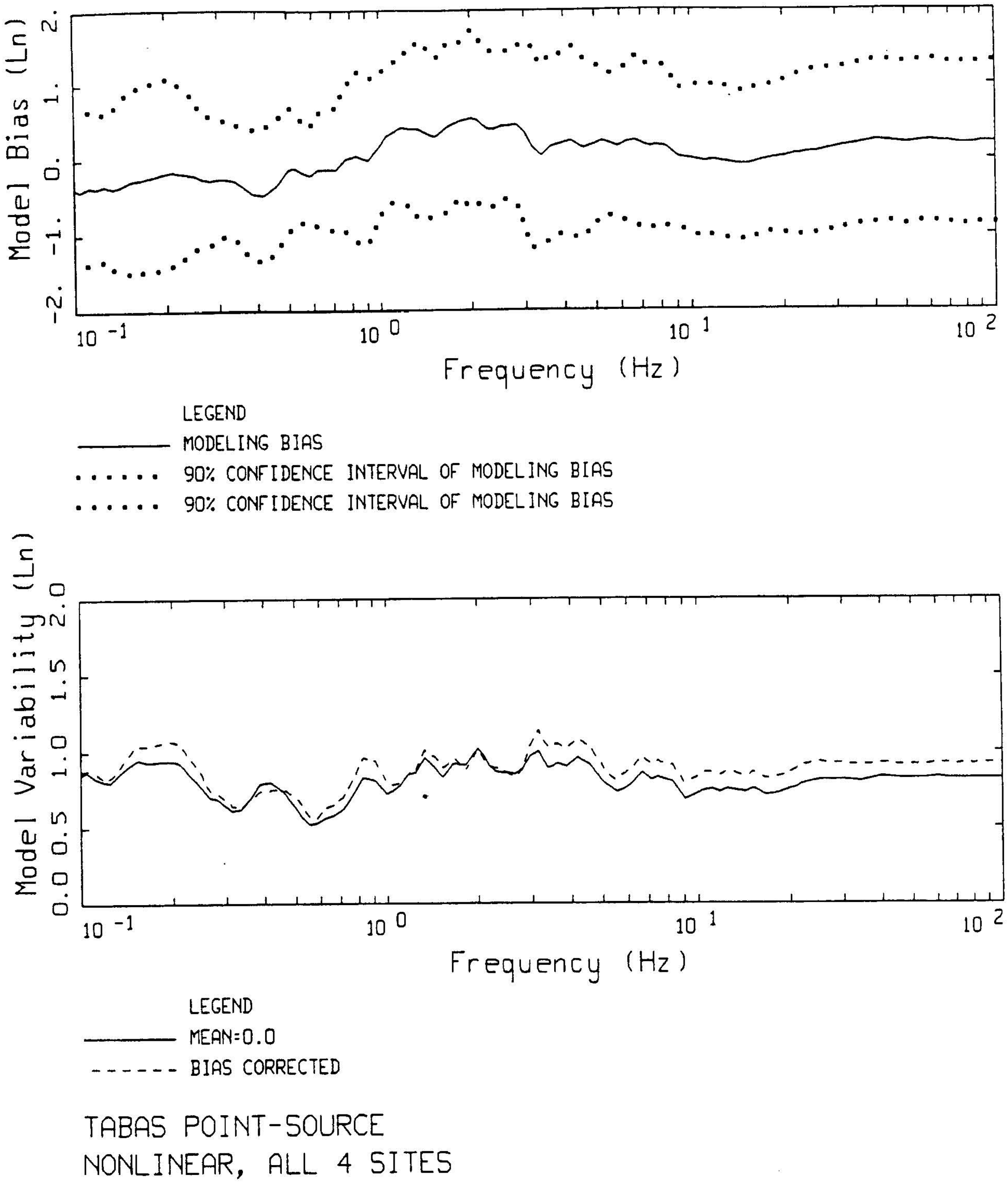

Source: Silva et al. 1996 [DIRS 110474] Figure 5.97

Figure 7-33. Model Bias and Variability Estimates for the Tabas Earthquake Computed Over All 4 Sites for the Point-Source Model

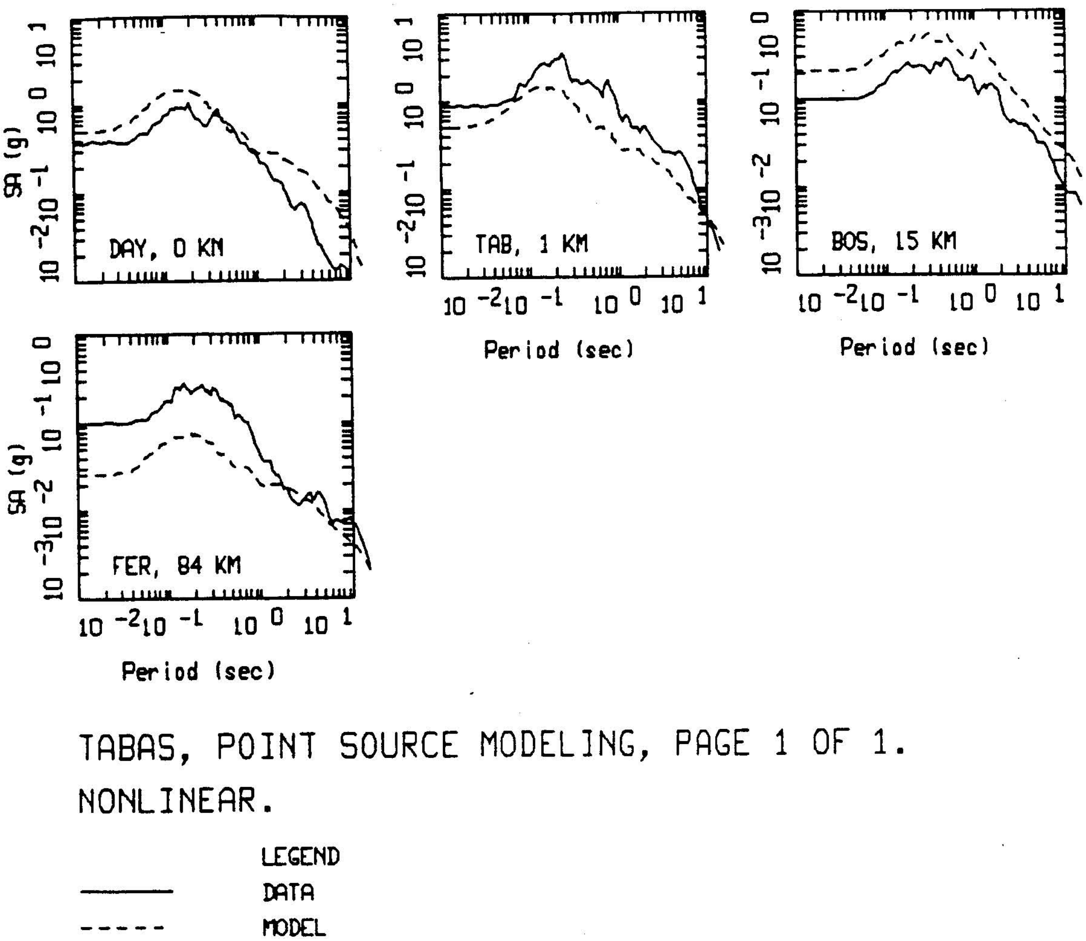

Source: Silva et al. 1996 [DIRS 110474] Figure 5.98

NOTE: Recorded Motions (solid lines), Point-Source Simulations (dashed lines)

Figure 7-34 Comparison of Average Horizontal Component 5%-Damped Pseudo Relative Absolute Response Spectra: Tabas Earthquake

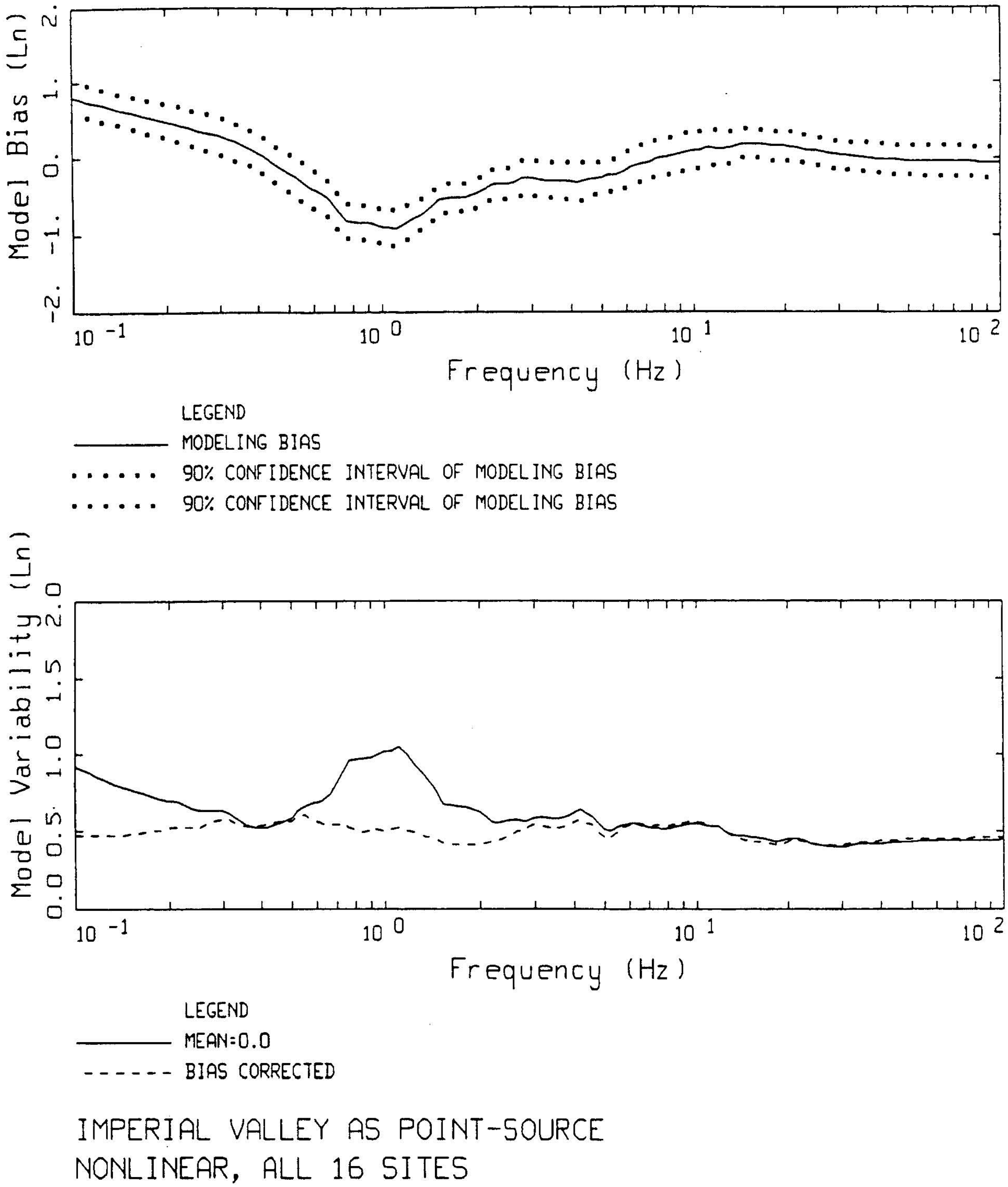

Source: Silva et al. 1996 [DIRS 110474] Figure 5.107

Figure 7-35. Model Bias and Variability Estimates for the Imperial Valley Aftershock Earthquake Computed Over All 16 Sites for the Point-Source Model

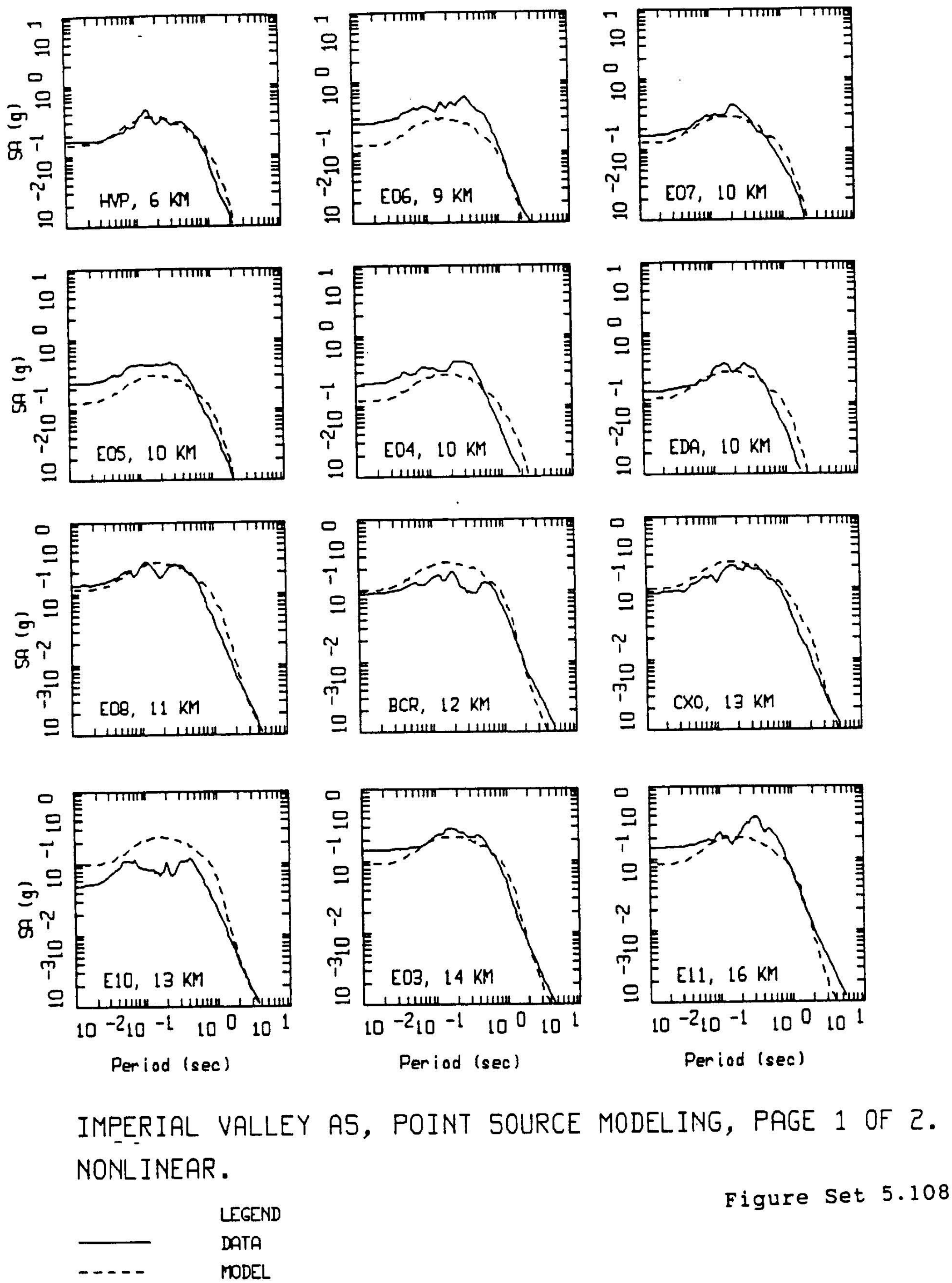

Source: Silva et al. 1996 [DIRS 110474] Figure 5.108

NOTE: Recorded Motions (solid lines), Point-Source Simulations (dashed lines)

Figure 7-36a Comparison of Average Horizontal Component 5%-Damped Pseudo Relative Absolute Response Spectra: Imperial Valley Aftershock Earthquake

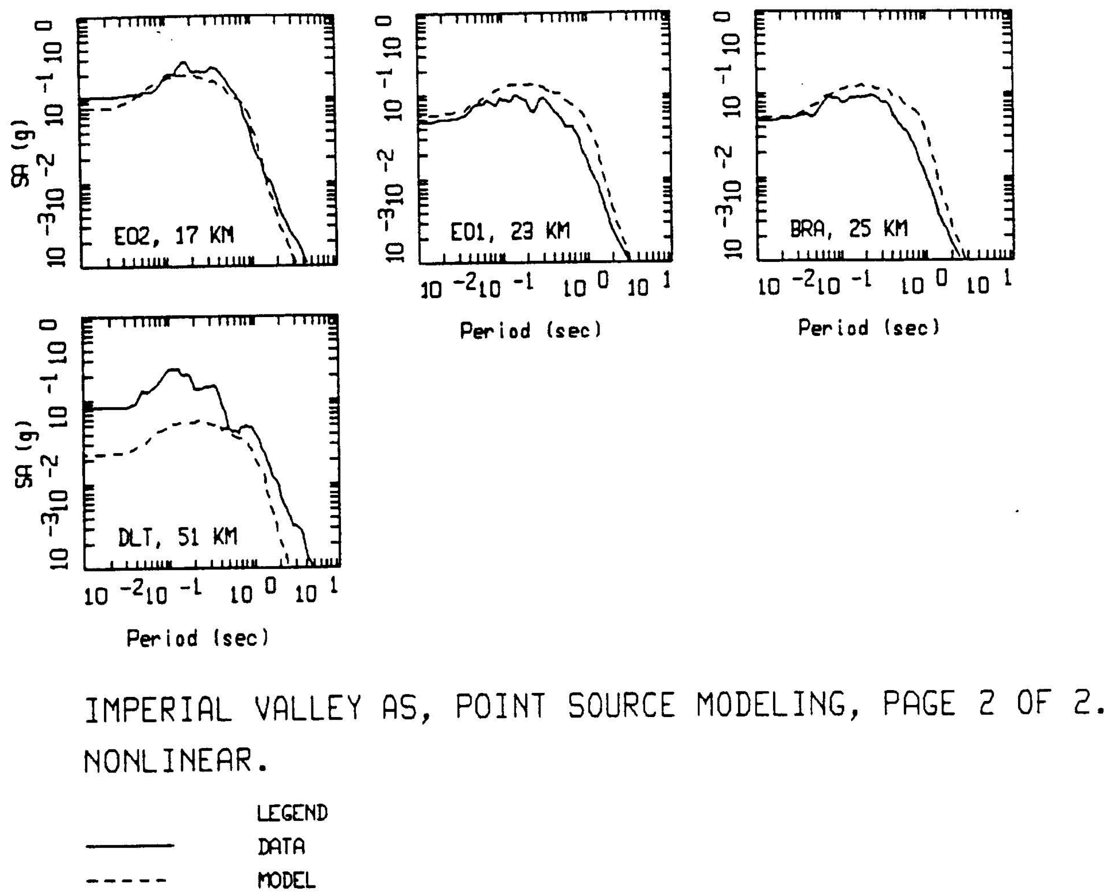

Source: Silva et al. 1996 [DIRS 110474] Figure 5.108

NOTE: Recorded Motions (solid lines), Point-Source Simulations (dashed lines)

Figure 7-36b Comparison of Average Horizontal Component 5%-Damped Pseudo Relative Absolute Response Spectra: Imperial Valley Aftershock Earthquake

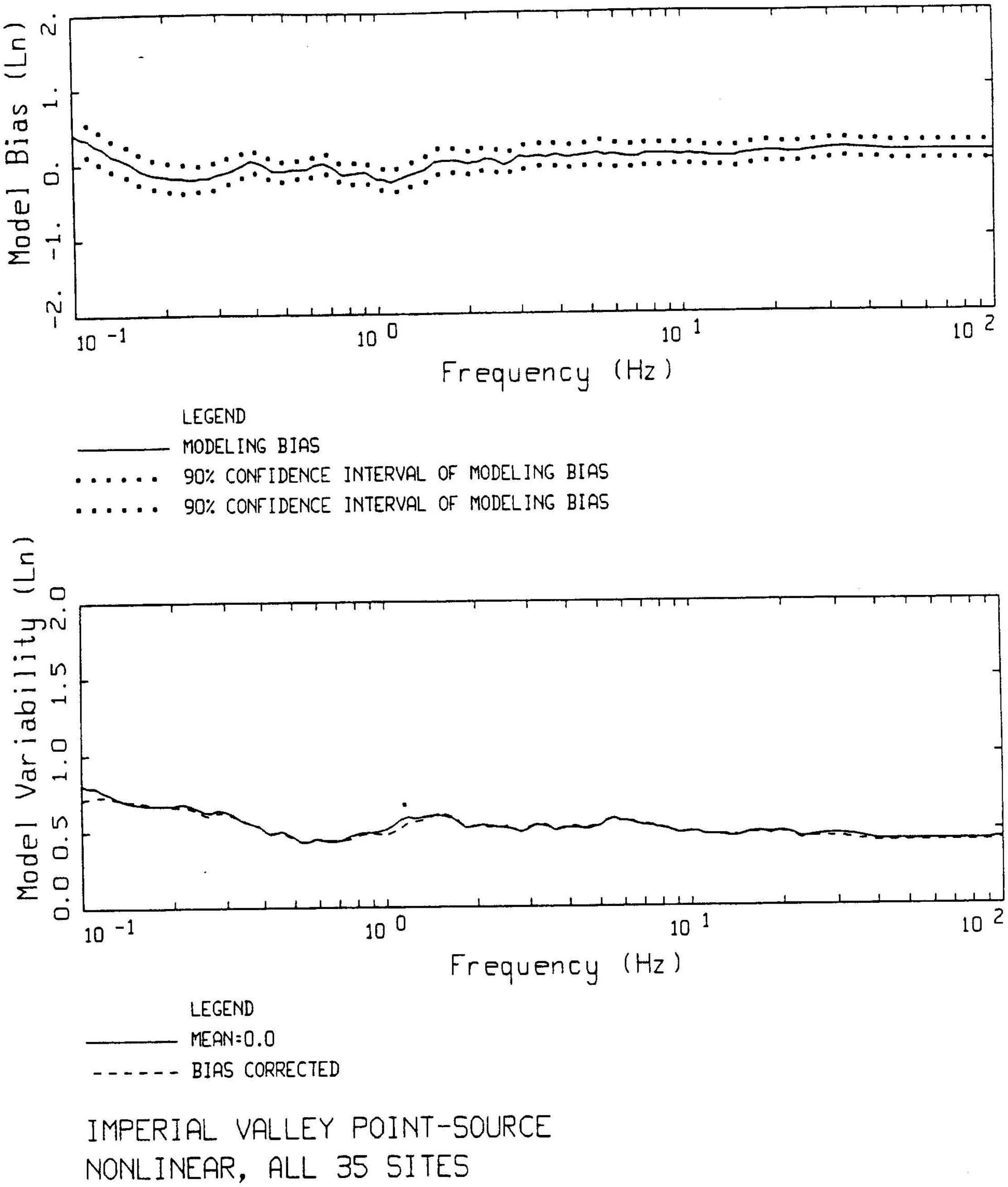

Source: Silva et al. 1996 [DIRS 110474] Figure 5.109

Figure 7-37 Model Bias and Variability Estimates for the Imperial Valley Mainshock Earthquake Computed Over All 35 Sites for the Point-Source Model

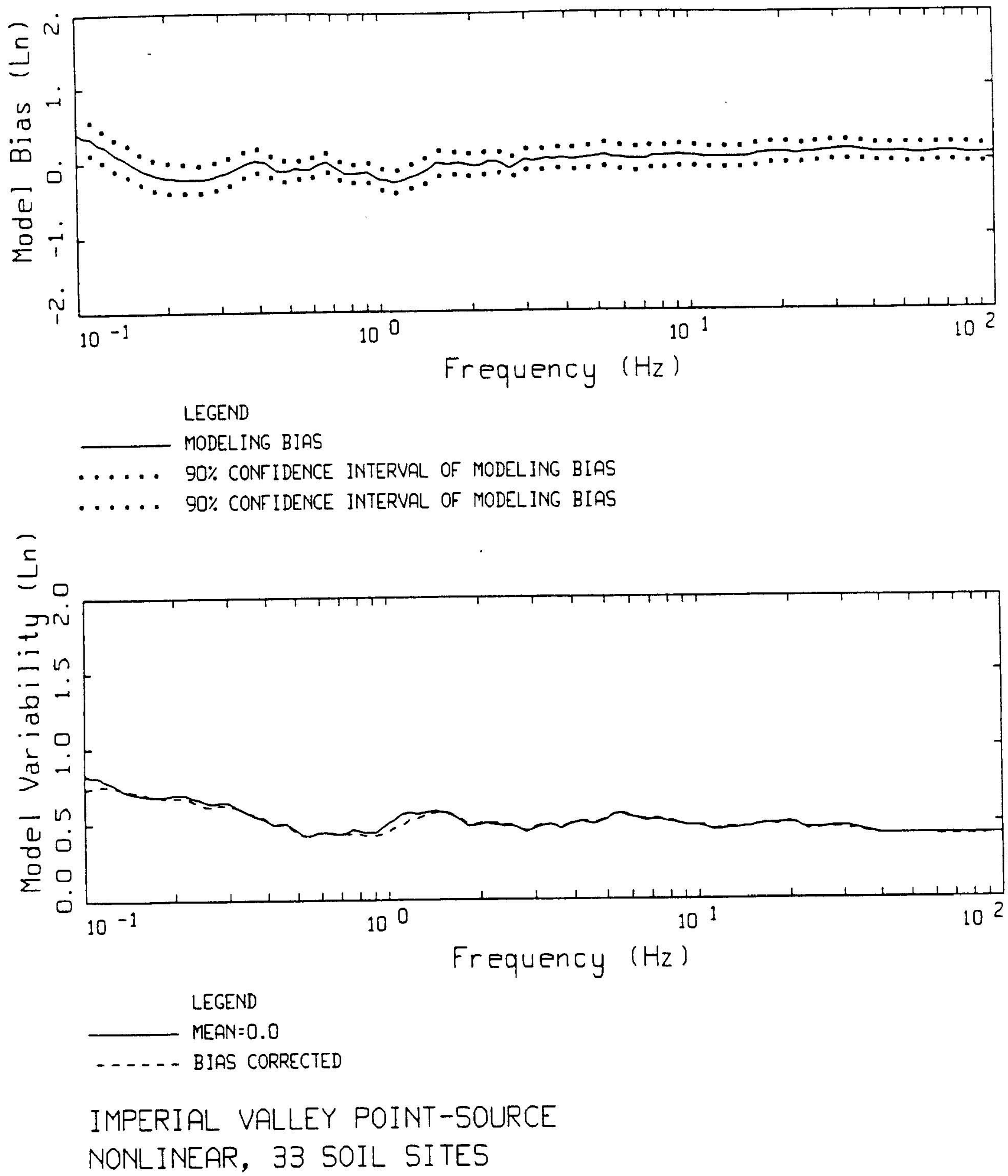

Source: Silva et al. 1996 [DIRS 110474] Figure 5.110

Figure 7-38 Model Bias and Variability Estimates for the Imperial Valley Mainshock Earthquake Computed Over All 33 Soil Sites for the Point-Source Model

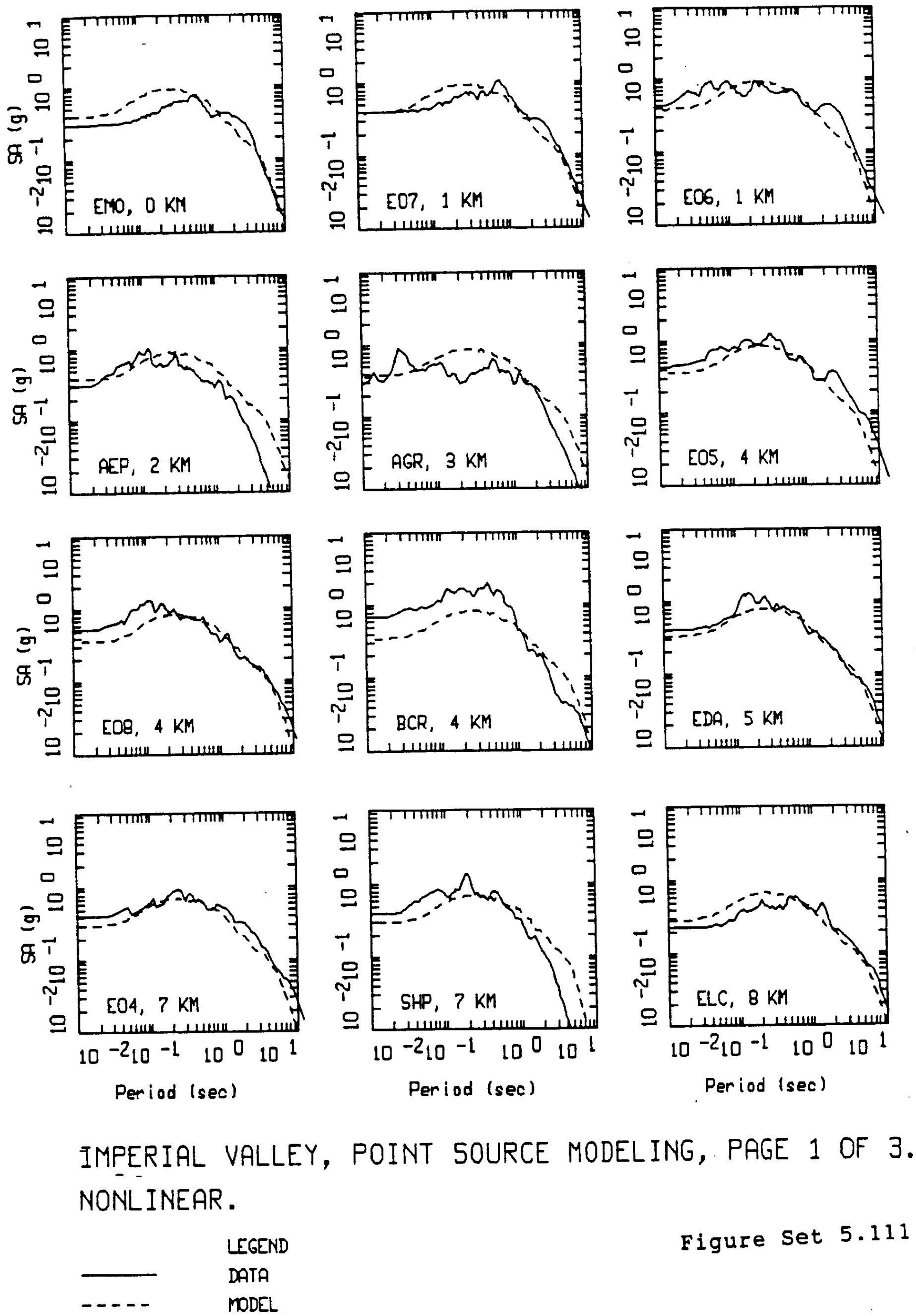

Source: Silva et al. 1996 [DIRS 110474] Figure 5.111

NOTE: Recorded Motions (solid lines), Point-Source Simulations (dashed lines)

Figure 7-39a Comparison of Average Horizontal Component 5%-Damped Pseudo Relative Absolute Response Spectra: Imperial Valley Mainshock Earthquake

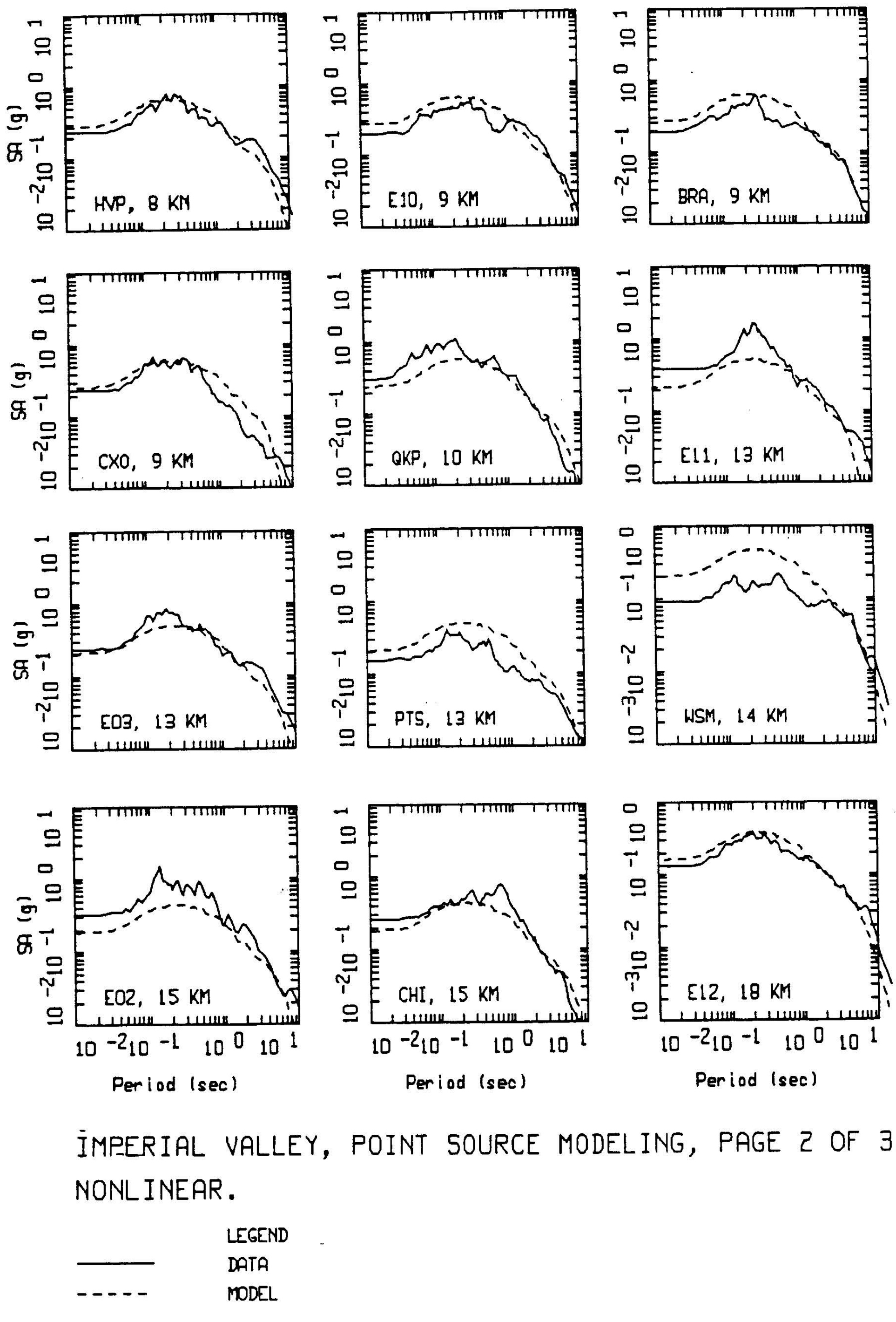

Source: Silva et al. 1996 [DIRS 110474] Figure 5.111

NOTE: Recorded Motions (solid lines), Point-Source Simulations (dashed lines)

Figure 7-39b Comparison of Average Horizontal Component 5%-Damped Pseudo Relative Absolute Response Spectra: Imperial Valley Mainshock Earthquake

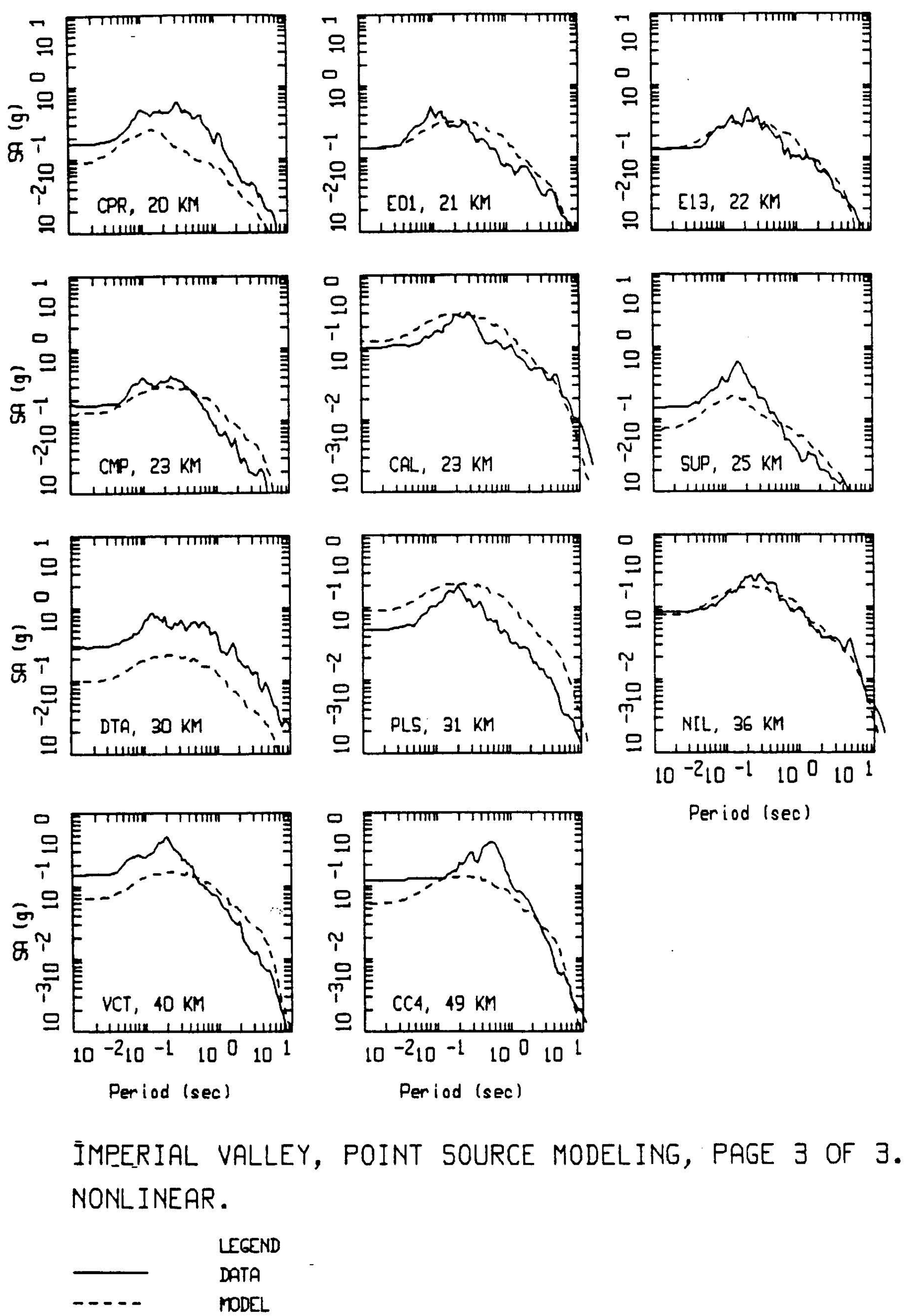

Source: Silva et al. 1996 [DIRS 110474] Figure 5.111

NOTE: Recorded Motions (solid lines), Point-Source Simulations (dashed lines)

Figure 7-39c Comparison of Average Horizontal Component 5%-Damped Pseudo Relative Absolute Response Spectra: Imperial Valley Mainshock Earthquake

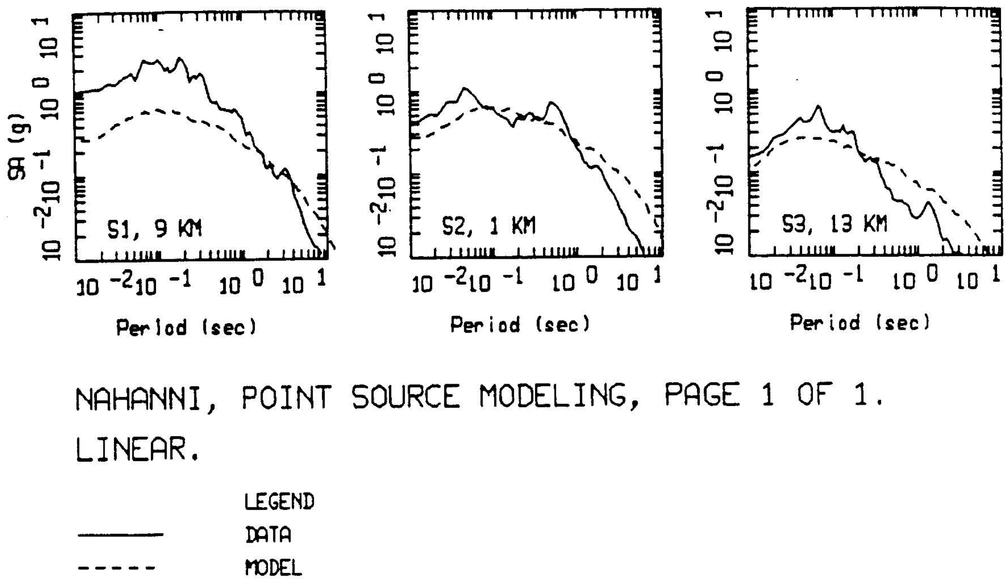

Source: Silva et al. 1996 [DIRS 110474] Figure 5.120

NOTE: Recorded Motions (solid lines), Point-Source Simulations (dashed lines)

Figure 7-40 Comparison of Average Horizontal Component 5%-Damped Pseudo Relative Absolute Response Spectra: Nahanni Earthquake

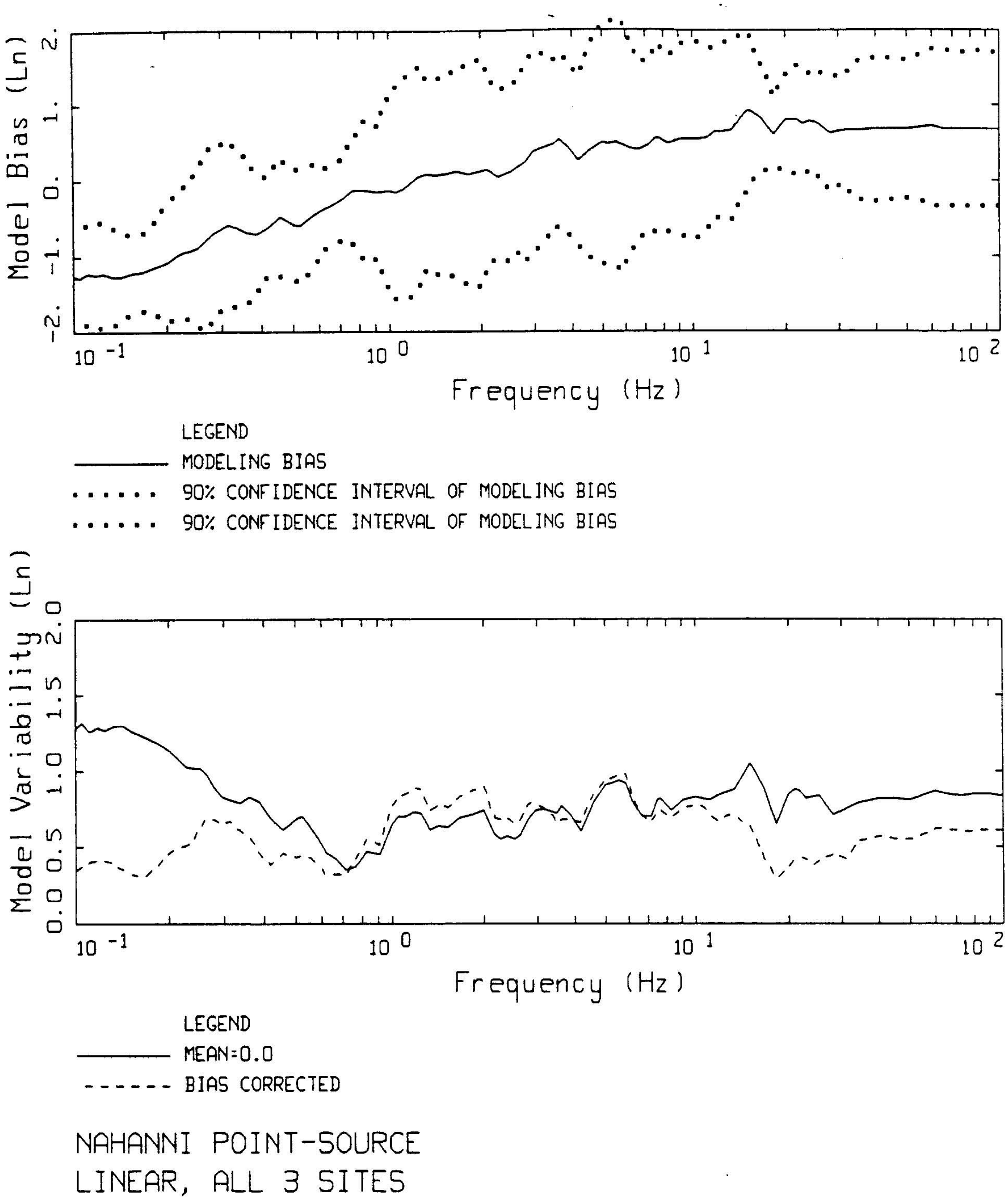

Source: Silva et al. 1996 [DIRS 110474] Figure 5.121

Figure 7-41 Model Bias and Variability Estimates for the Nahanni Earthquake Computed Over All 3 Sites for the Point-Source Model

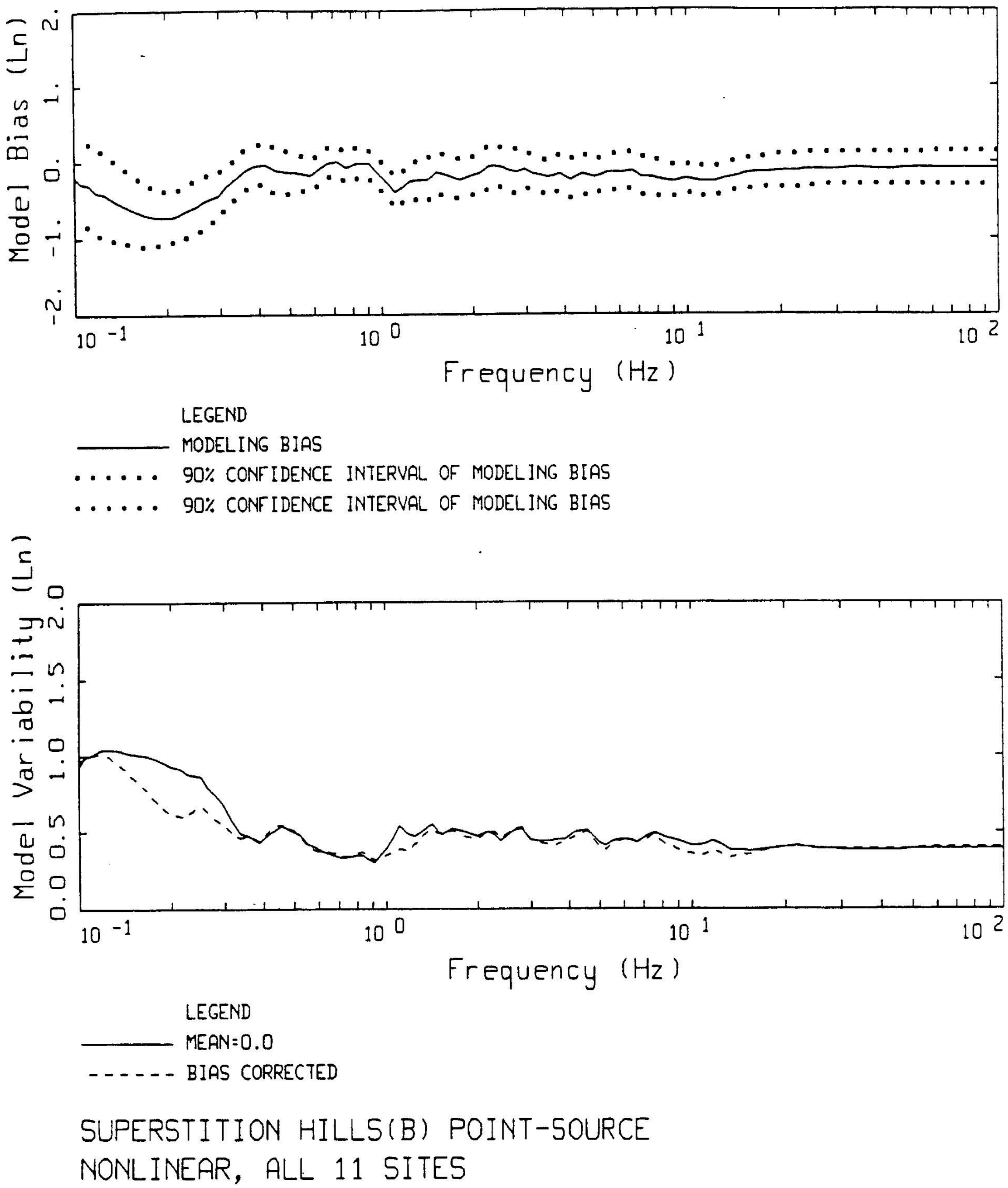

Source: Silva et al. 1996 [DIRS 110474] Figure 5.127

Figure 7-42 Model Bias and Variability Estimates for the Superstition Hills Earthquake Computed Over All 11 Sites for the Point-Source Model

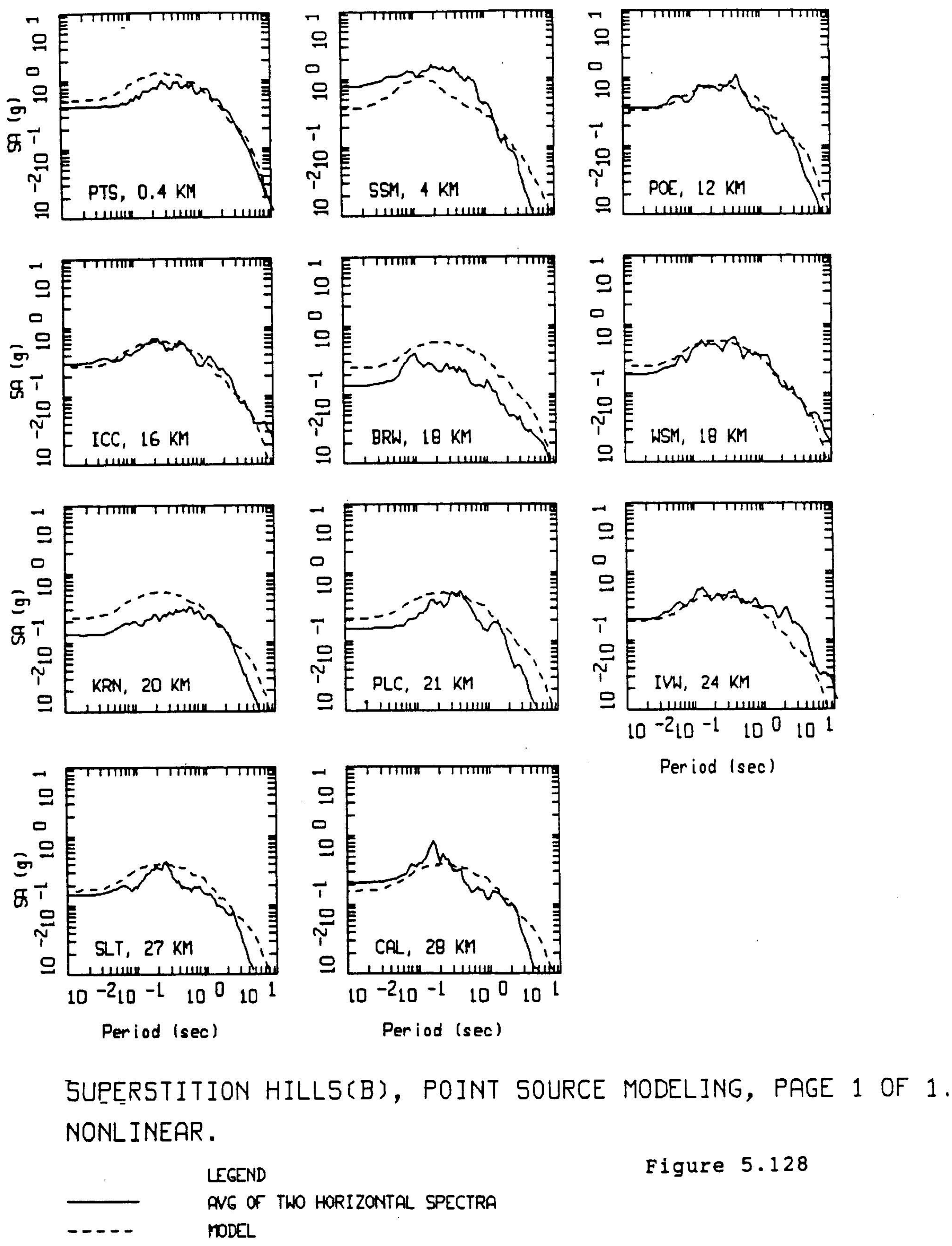

Source: Silva et al. 1996 [DIRS 110474] Figure 5.128

NOTE: Recorded Motions (solid lines), Point-Source Simulations (dashed lines)

Figure 7-43 Comparison of Average Horizontal Component 5%-Damped Pseudo Relative Absolute Response Spectra: Superstition Hills Earthquake

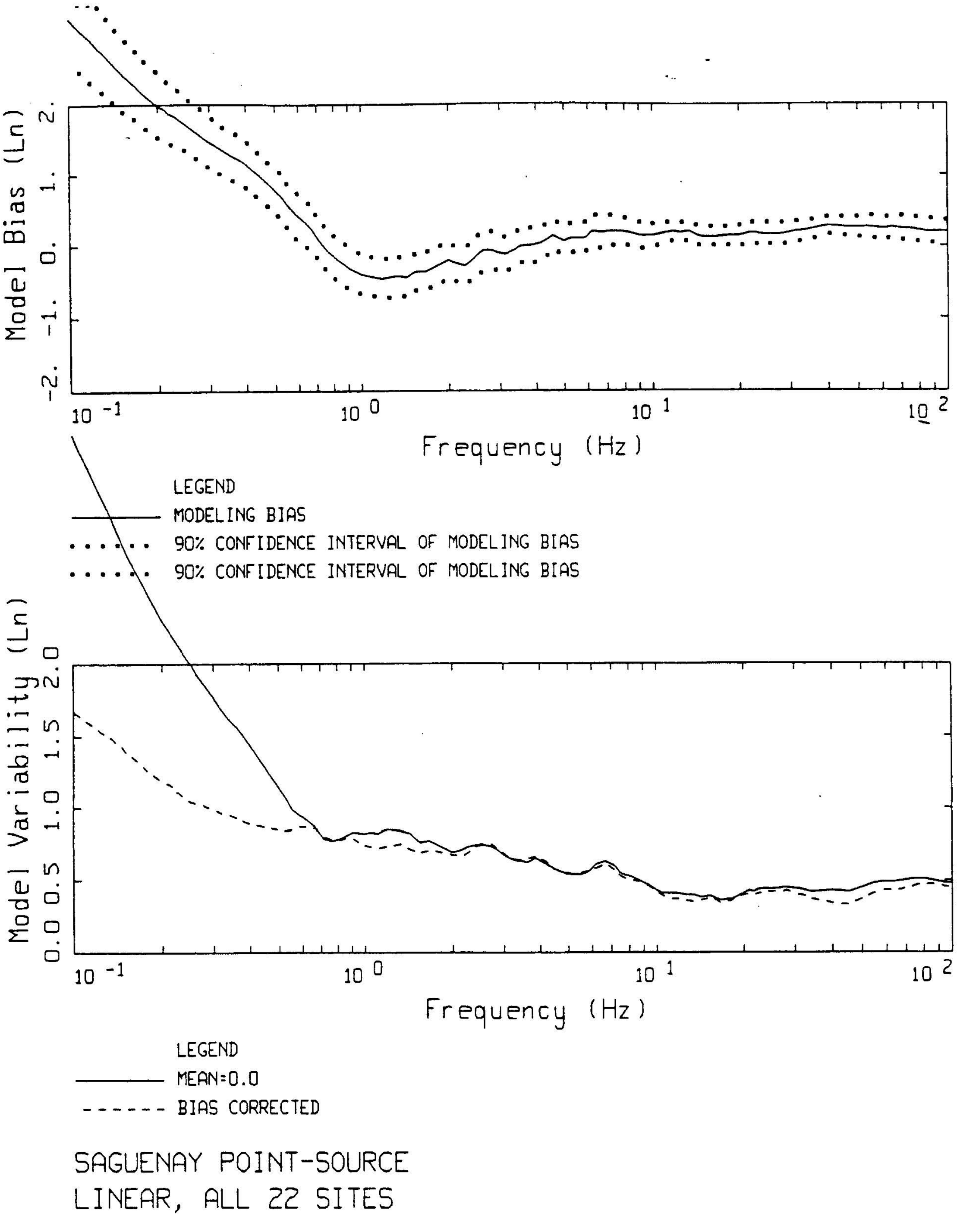

Source: Silva et al. 1996 [DIRS 110474] Figure 5.134

Figure 7-44 Model Bias and Variability Estimates for the Saguenay Earthquake Computed Over All 22 Sites for the Point-Source Model

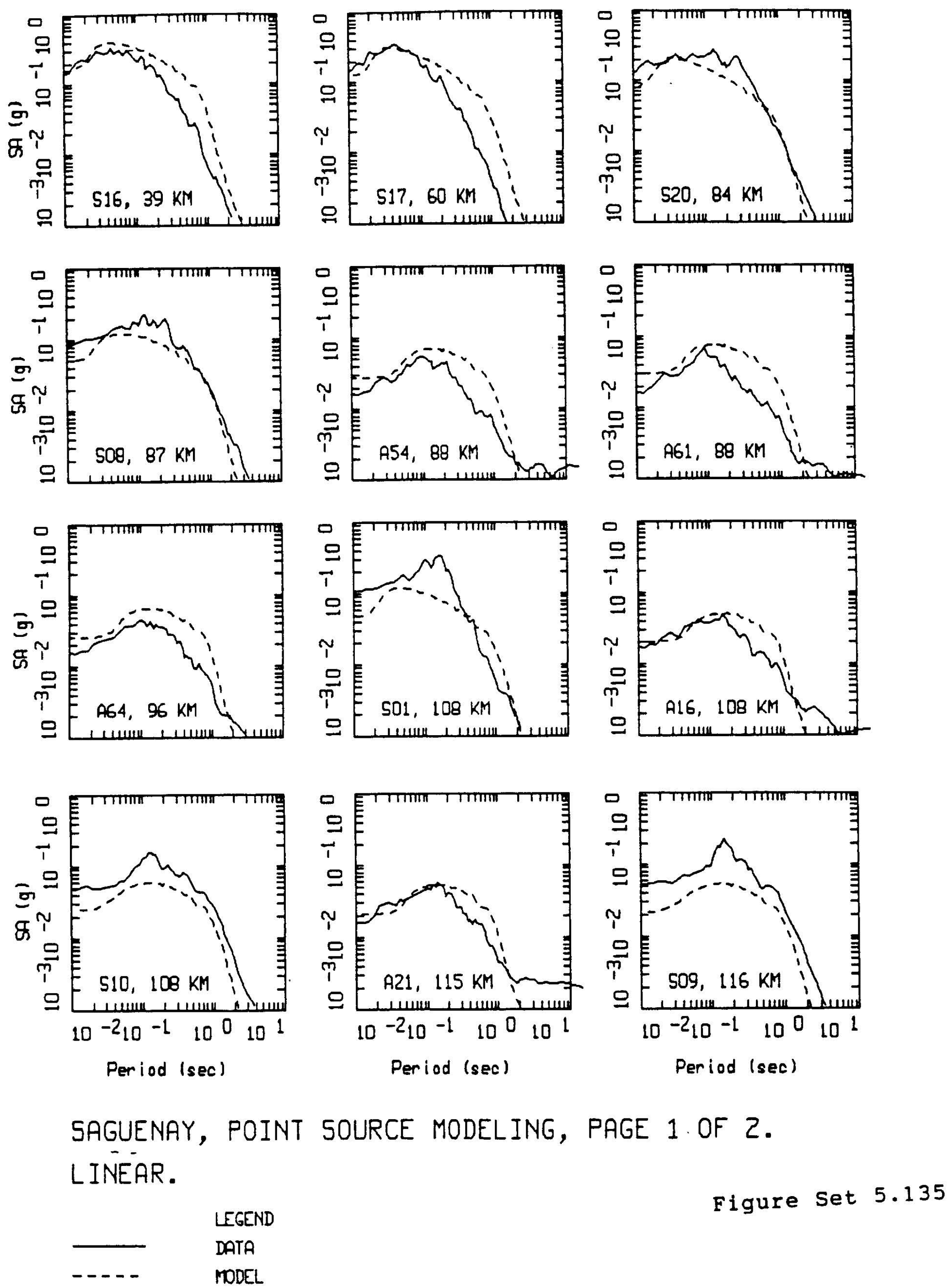

Source: Silva et al. 1996 [DIRS 110474] Figure 5.135

NOTE: Recorded Motions (solid lines), Point-Source Simulations (dashed lines)

Figure 7-45a Comparison of Average Horizontal Component 5%-Damped Pseudo Relative Absolute Response Spectra: Saguenay Earthquake

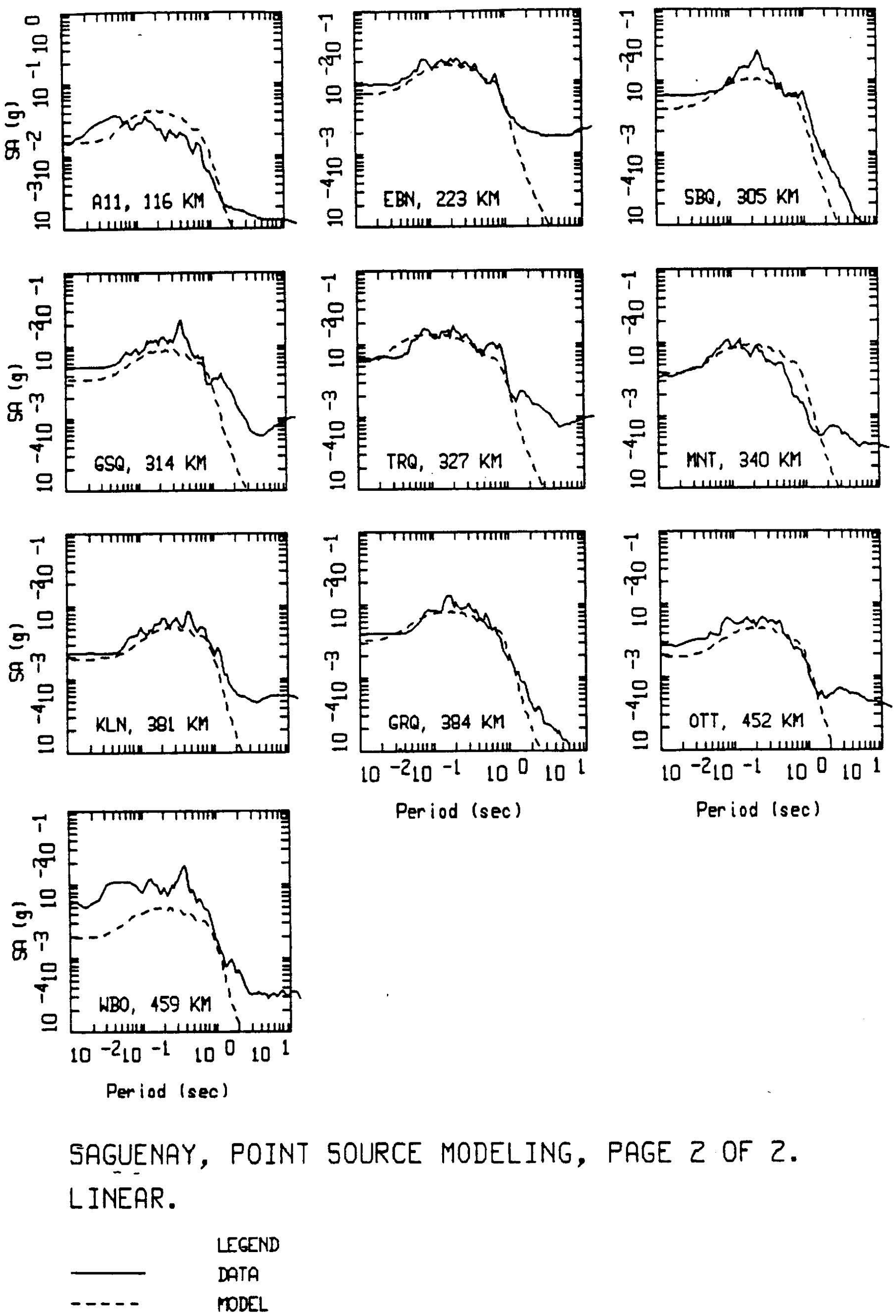

Source: Silva et al. 1996 [DIRS 110474] Figure 5.135

NOTE: Recorded Motions (solid lines), Point-Source Simulations (dashed lines)

Figure 7-45b Comparison of Average Horizontal Component 5%-Damped Pseudo Relative Absolute Response Spectra: Saguenay Earthquake

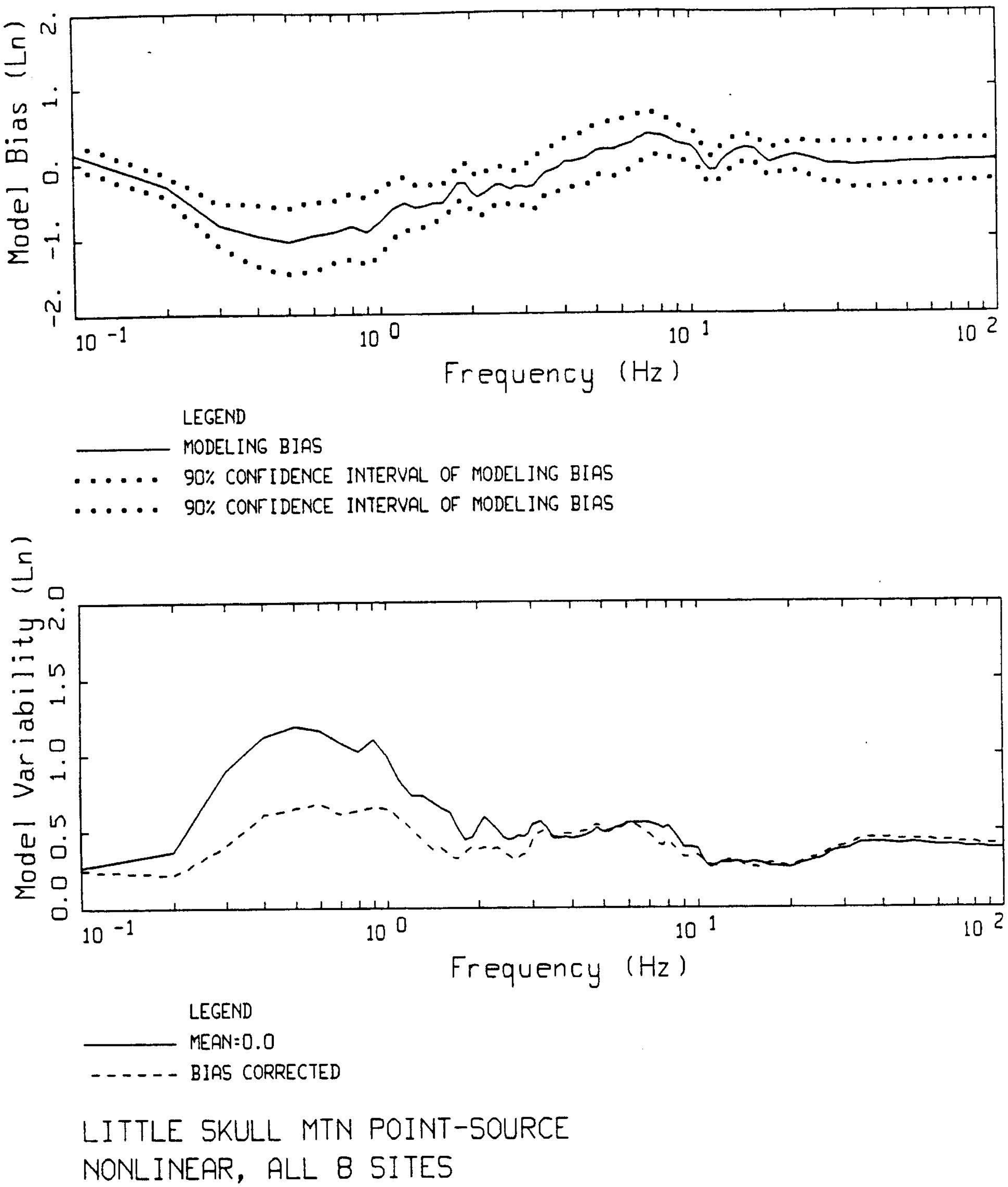

Source: Silva et al. 1996 [DIRS 110474] Figure 5.141

Figure 7-46 Model Bias and Variability Estimates for the Little Skull Mountain Earthquake Computed Over All 8 Sites for the Point-Source Model

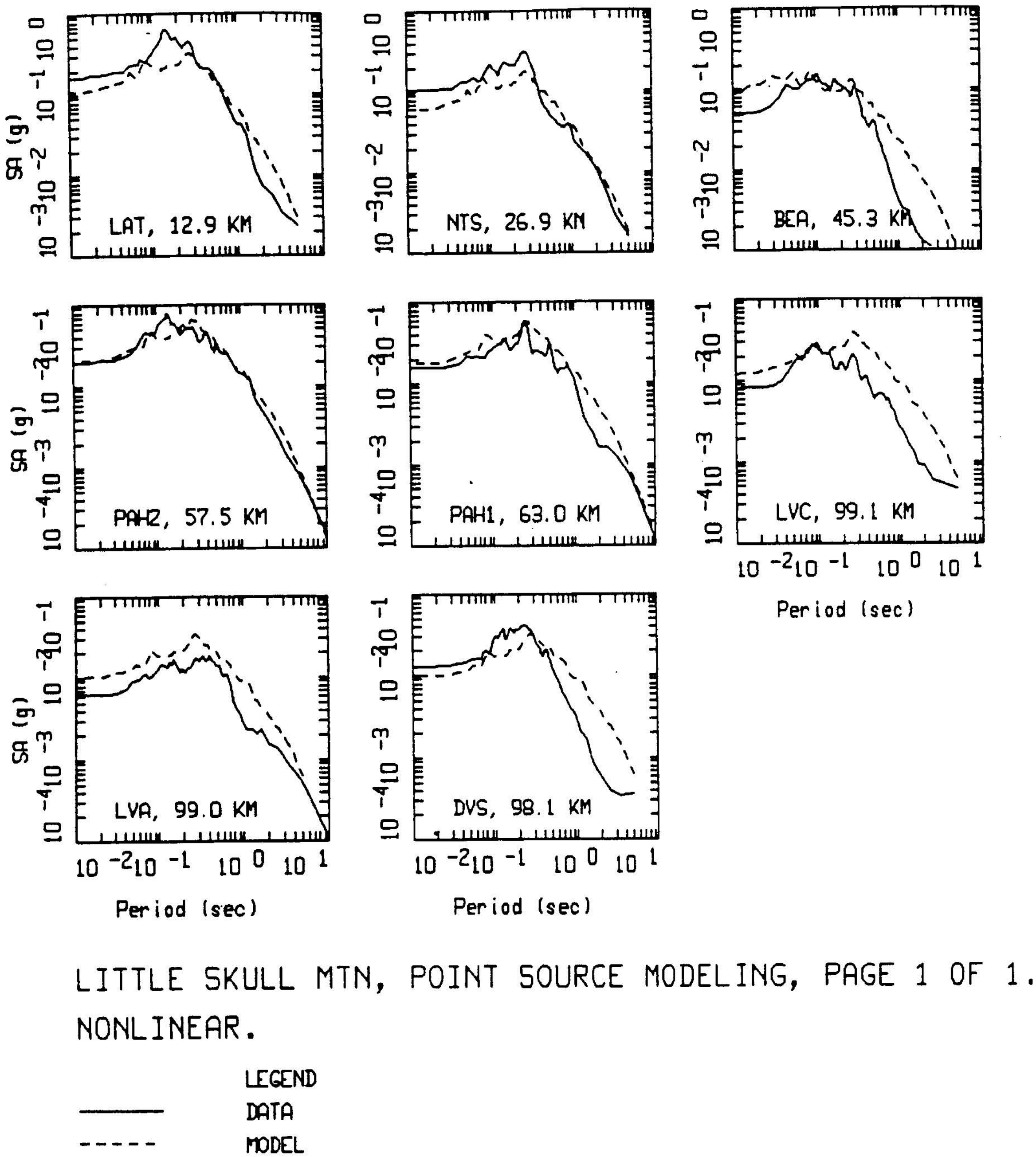

Source: Silva et al. 1996 [DIRS 110474] Figure 5.142

NOTE: Recorded Motions (solid lines), Point-Source Simulations (dashed lines)

Figure 7-47 Comparison of Average Horizontal Component 5%-Damped Pseudo Relative Absolute Response Spectra: Little Skull Mountain Earthquake

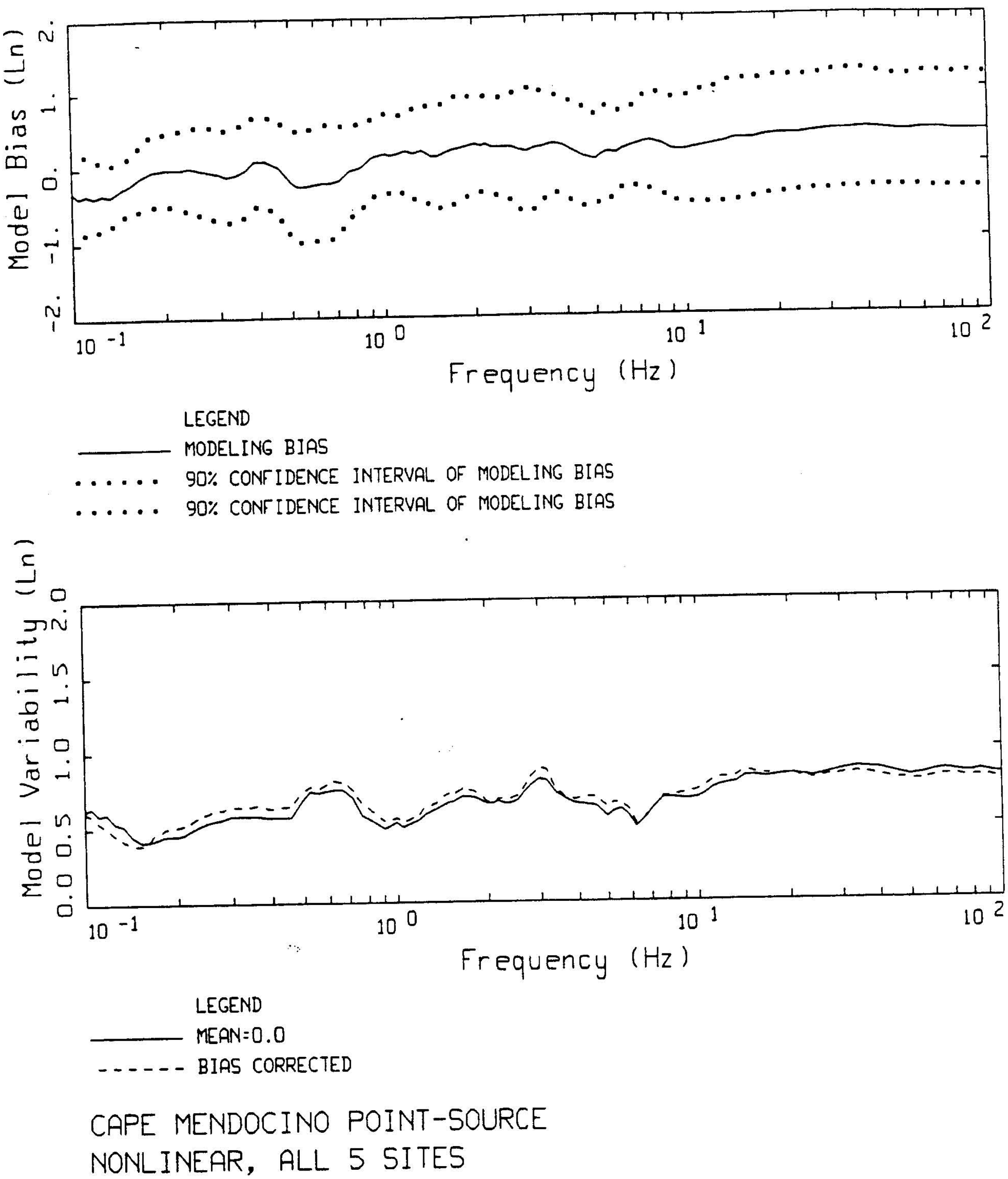

Source: Silva et al. 1996 [DIRS 110474] Figure 5.148

Figure 7-48 Model Bias and Variability Estimates for the Cape Mendo cino Earthquake Computed Over All 8 Sites for the Point-Source Model

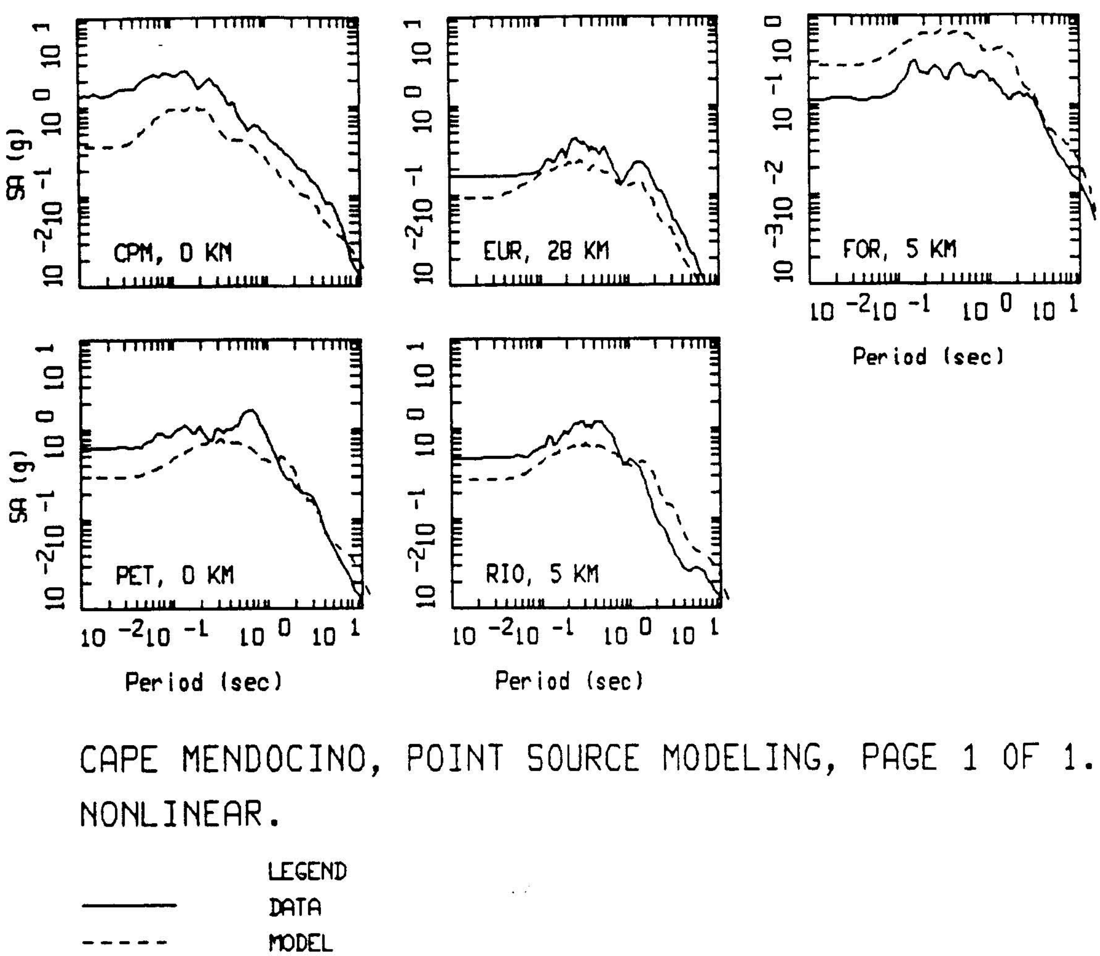

Source: Silva et al. 1996 [DIRS 110474] Figure 5.149

NOTE: Recorded Motions (solid lines), Point-Source Simulations (dashed lines)

Figure 7-49 Comparison of Average Horizontal Component 5%-Damped Pseudo Relative Absolute Response Spectra: Cape Mendocino Earthquake

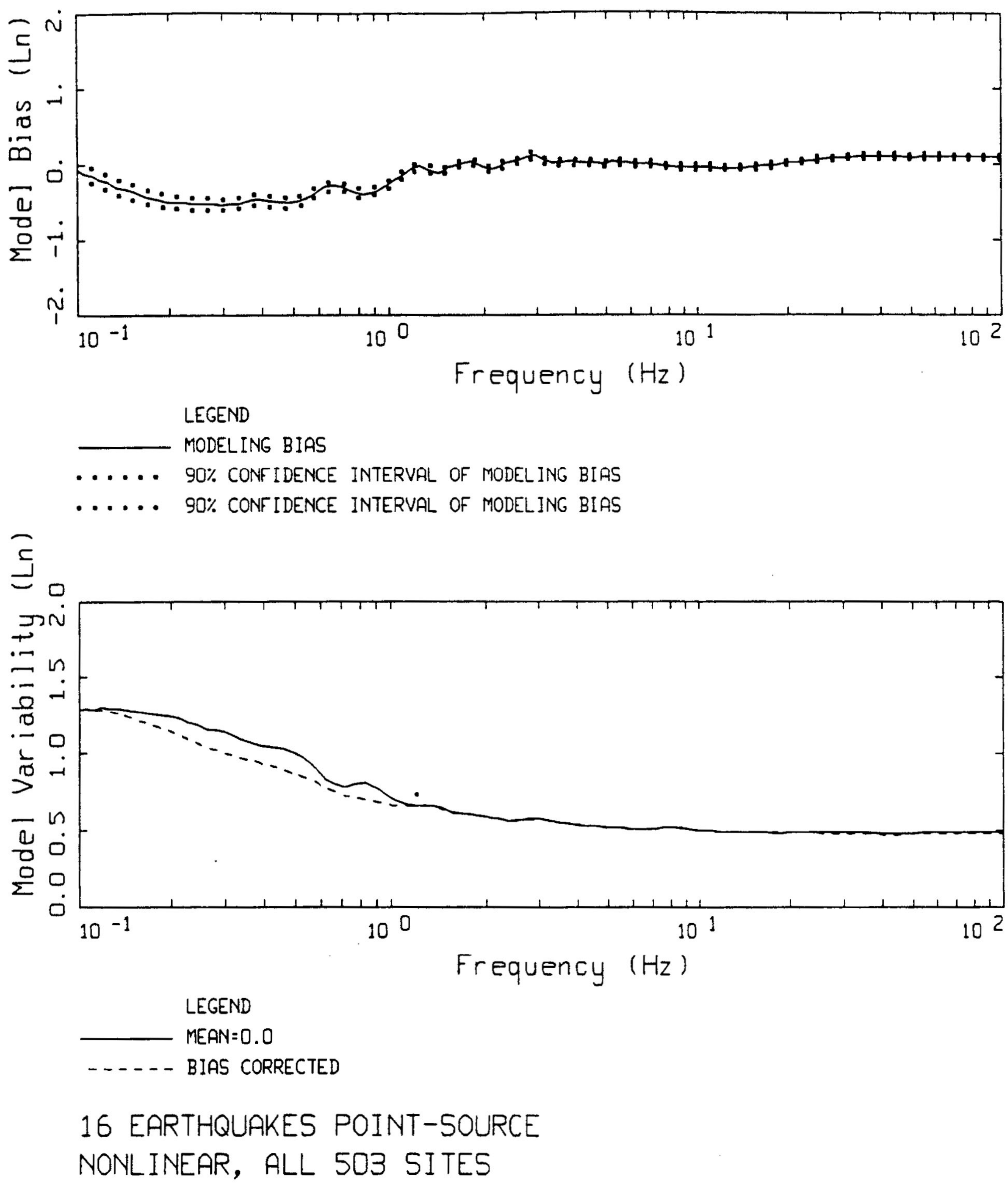

Source: Silva et al. 1996 [DIRS 110474] Figure 5.152

Figure 7-50. Model Bias and Variability Estimates for All Earthquakes Computed Over All 503 Sites for the Point-Source Model

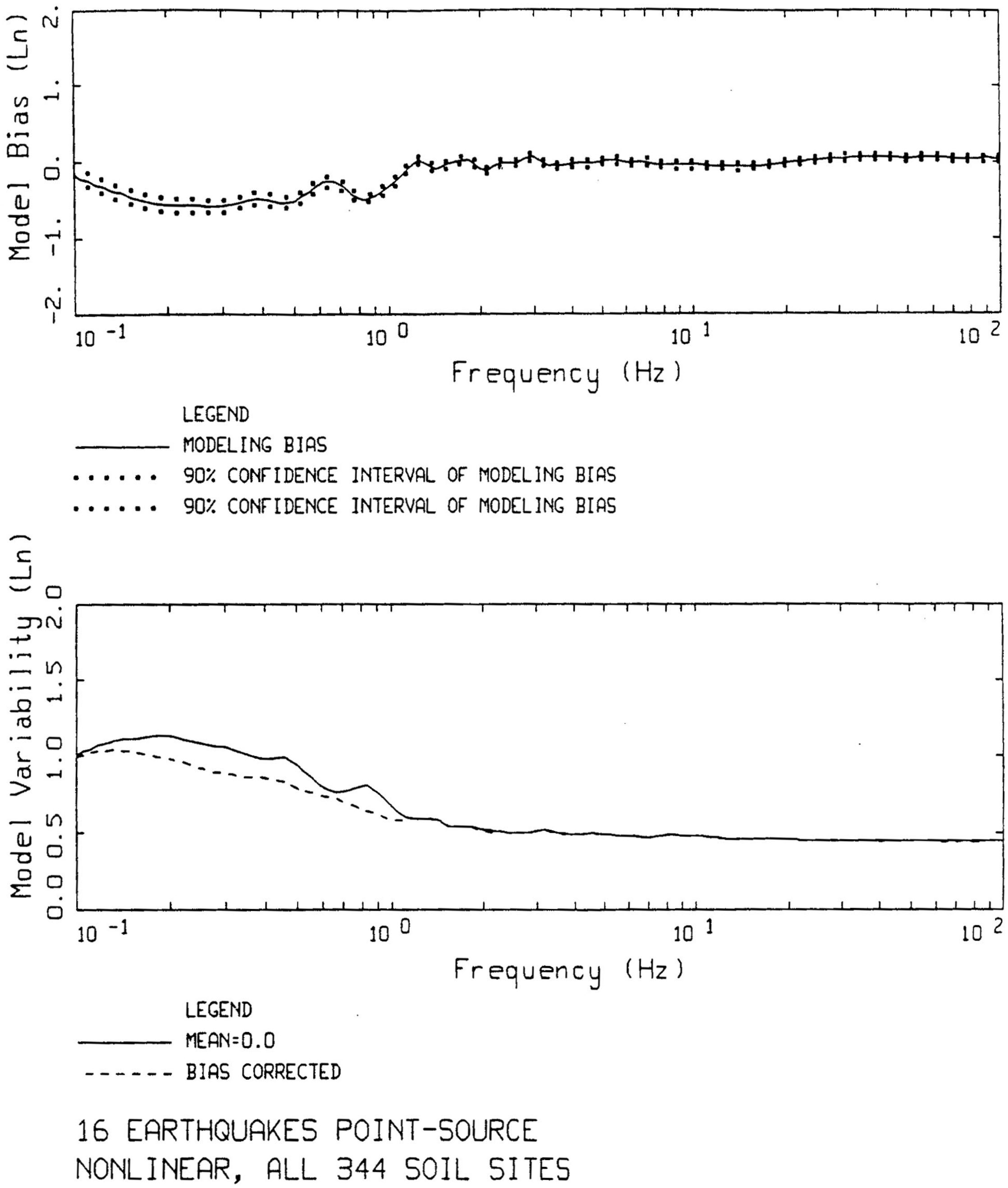

Source: Silva et al. 1996 [DIRS 110474] Figure 5.153

Figure 7-51. Model Bias and Variability Estimates for All Earthquakes Computed Over All 344 Soil Sites for the Point-Source Model

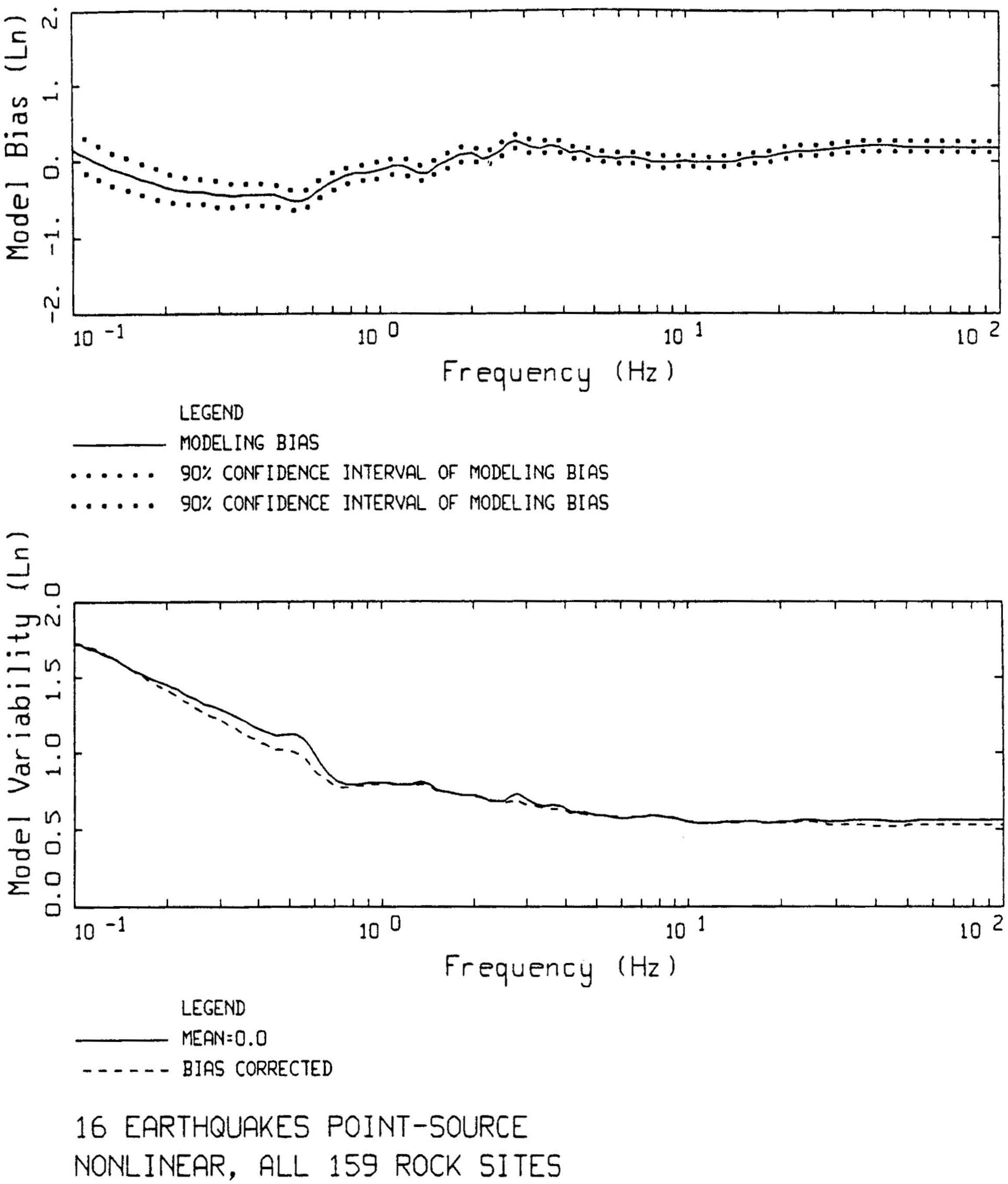

Source: Silva et al. 1996 [DIRS 110474] Figure 5.154

Figure 7-52. Model Bias and Variability Estimates for All Earthquakes Computed Over All 159 Rock Sites for the Point-Source Model

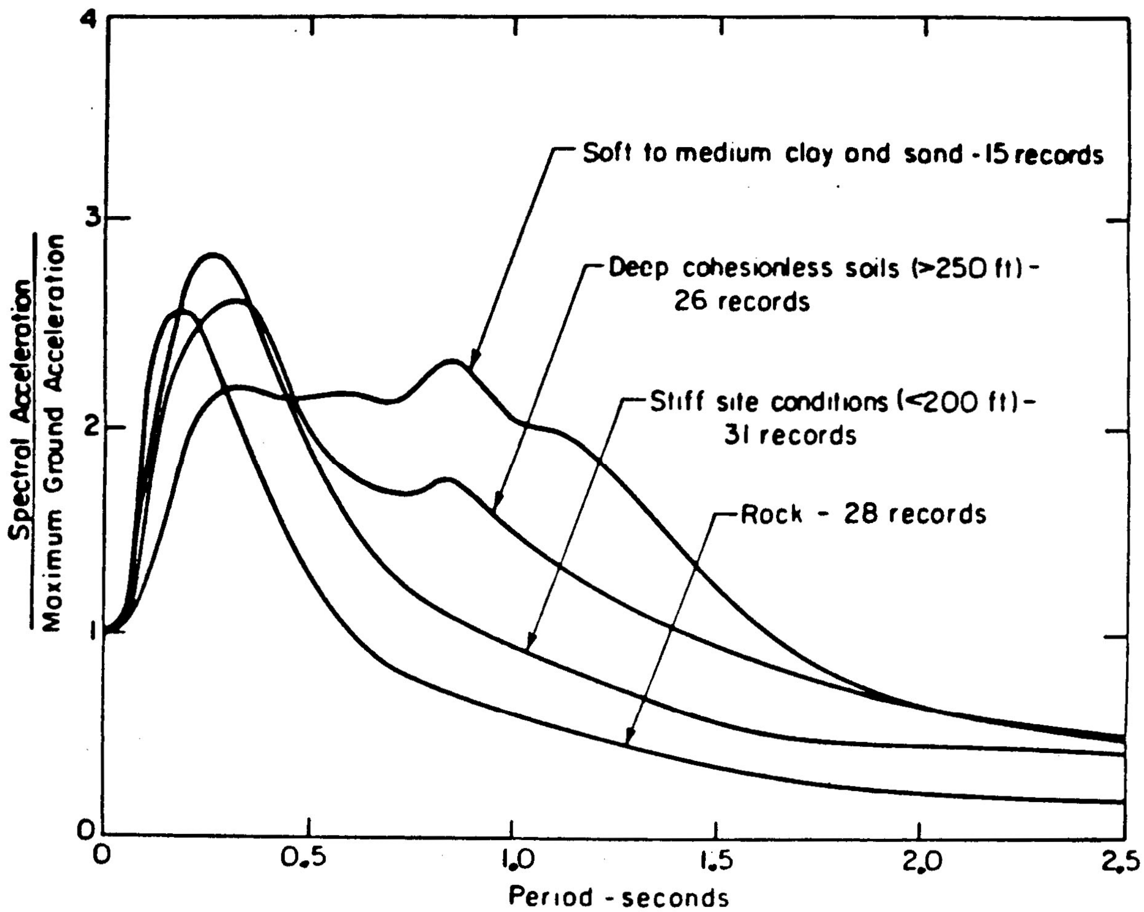

Source: Silva et al. 1996 [DIRS 110474] Figure 7.1

Figure 7-53. Average 5%-Damping Response Spectral Shapes (Sa/a) Computed From Motions Recorded on Different Soil Conditions.

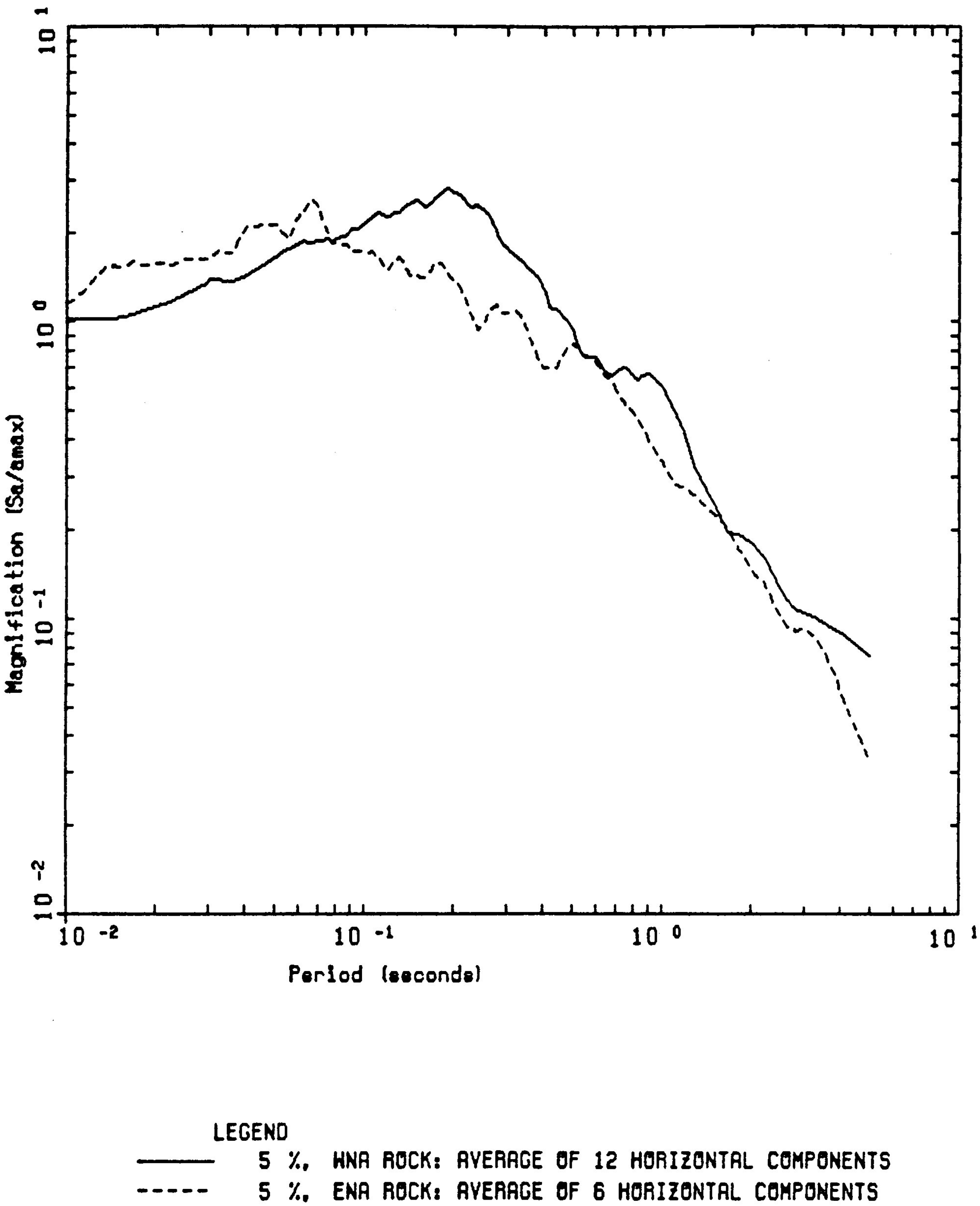

Source: Silva et al. 1996 [DIRS 110474] Figure 7.2

NOTE: ENA average shape is from recordings of the m_b 6.4 Nahanni earthquake. The WNA average shape is from recordings of the San Fernando M_L 6.4 and Imperial Valley M_L 6.6 earthquakes.

Figure 7-54. Comparison of Average 5% Response Spectral Shapes (Sa/amax) Computed From Strong Motion Data Recorded at Rock Sites in ENA (dashed lines) and WNA (solid line)

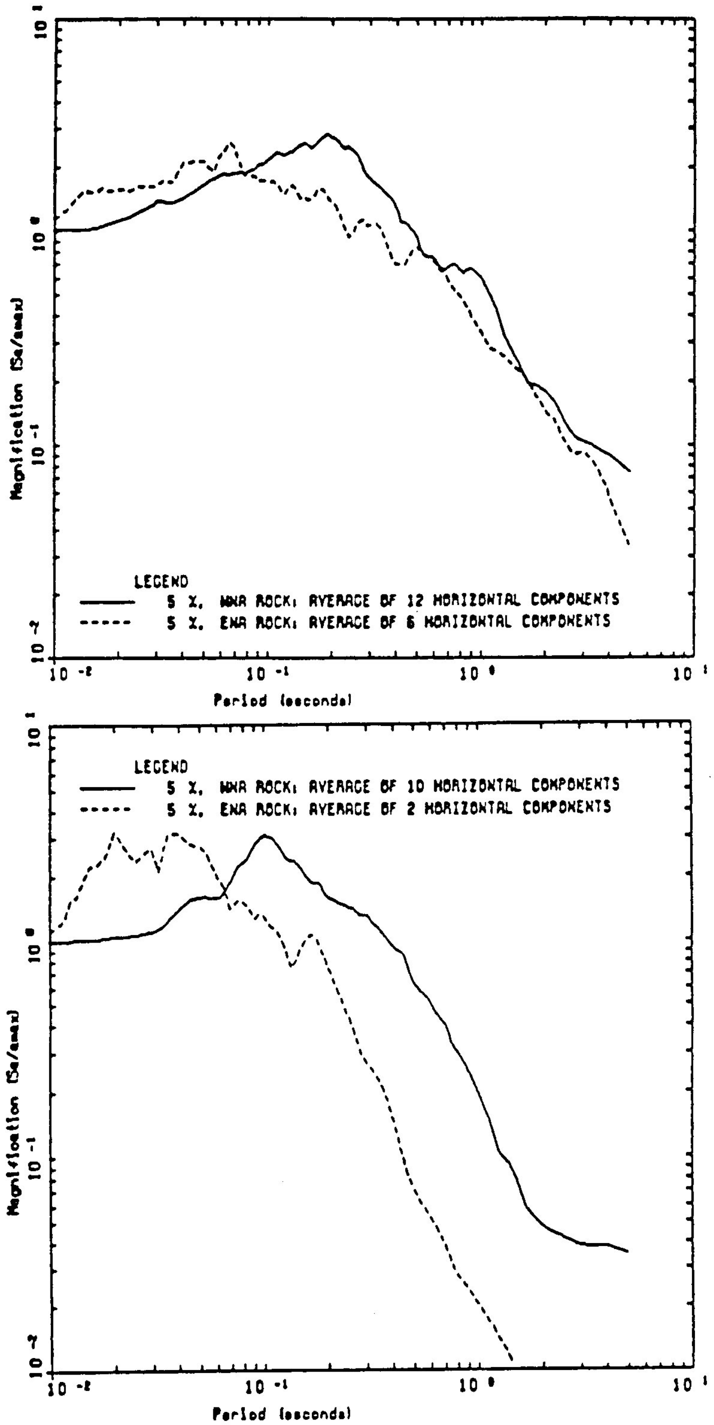

Source: Silva et al. 1996 [DIRS 110474] Figure 7.3

NOTE: In each figure the solid line corresponds to motions recorded in WNA, dashed line to motions recorded in ENA.

Figure 7-55 Comparison of Average 5% Response Spectral Shapes (Sa/amax) Computed From Motions Recorded at Rock Sites at Close Distances to M 6.4 Earthquakes (top figure) and M 4.0 Earthquakes (bottom figure)

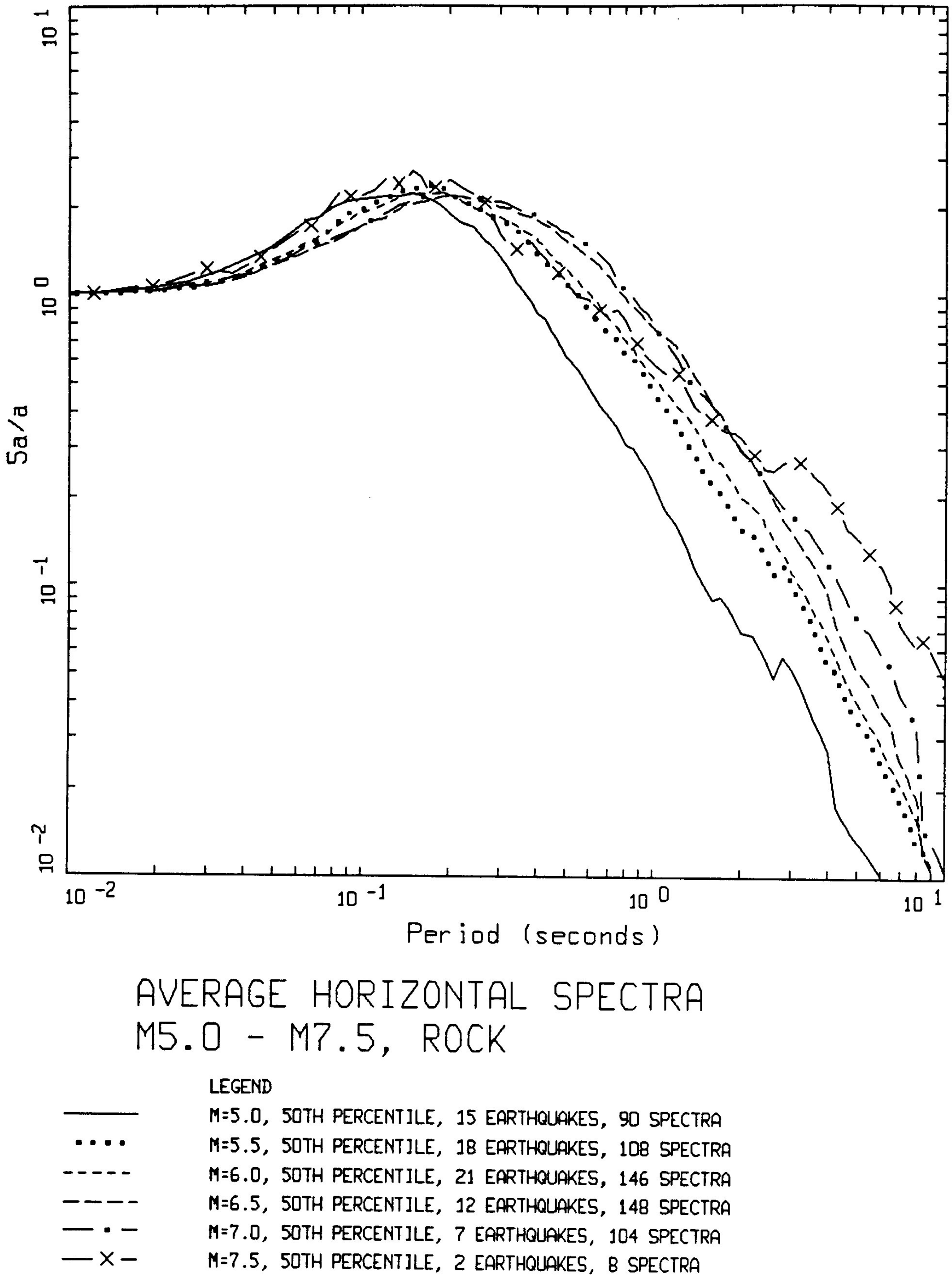

Source: Silva et al. 1996 [DIRS 110474] Figure 7.5

Figure 7-56. Summary Plot of Median Statistical Response Spectral Shapes for Soft Rock Site Conditions

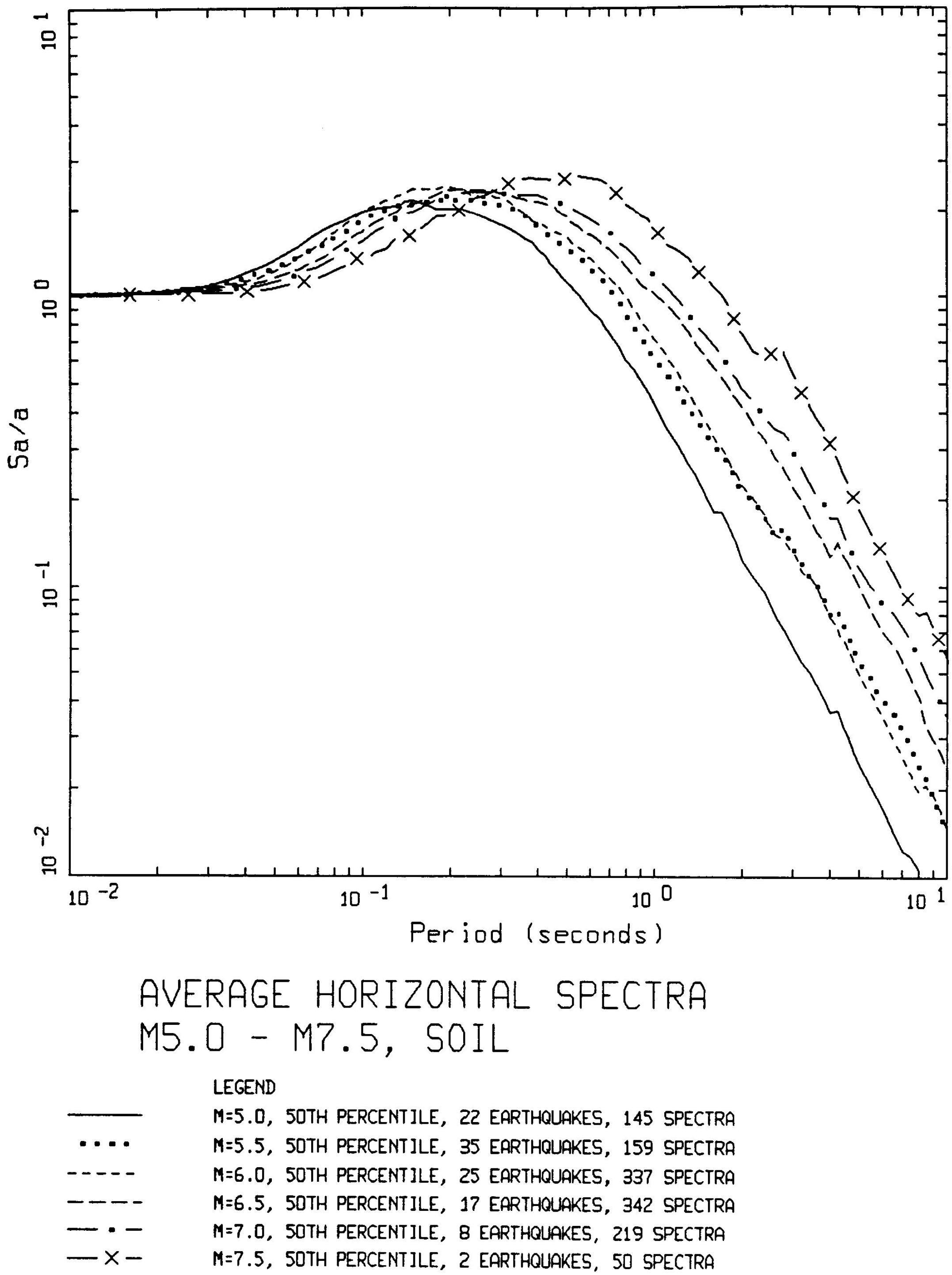

Source: Silva et al. 1996 [DIRS 110474] Figure 7.7

Figure 7-57 Summary Plot of Median Statistical Response Spectral Shapes for Deep Soil Site Conditions

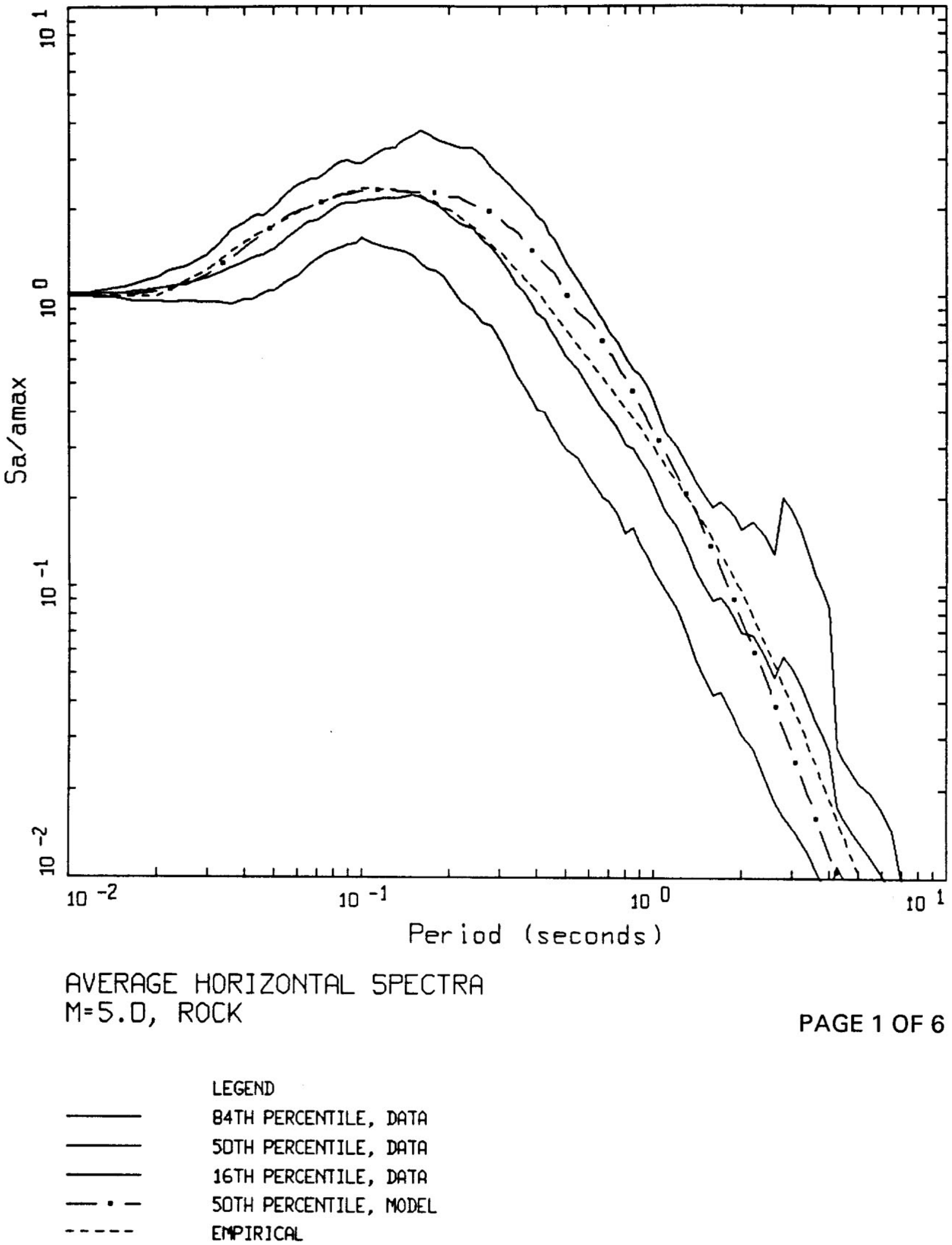

Source: Silva et al. 1996 [DIRS 110474] Figure 7.8

NOTE: The point-source stress drop is 59 bars and M 5.0. Soft rock site conditions.

Figure 7-58a. Comparison of Statistical Response Spectral Shapes with Median Point-Source Model Predictions and Empirical Attenuation Relation for a Vertical Strike-Slip Fault: Soft Rock Sites

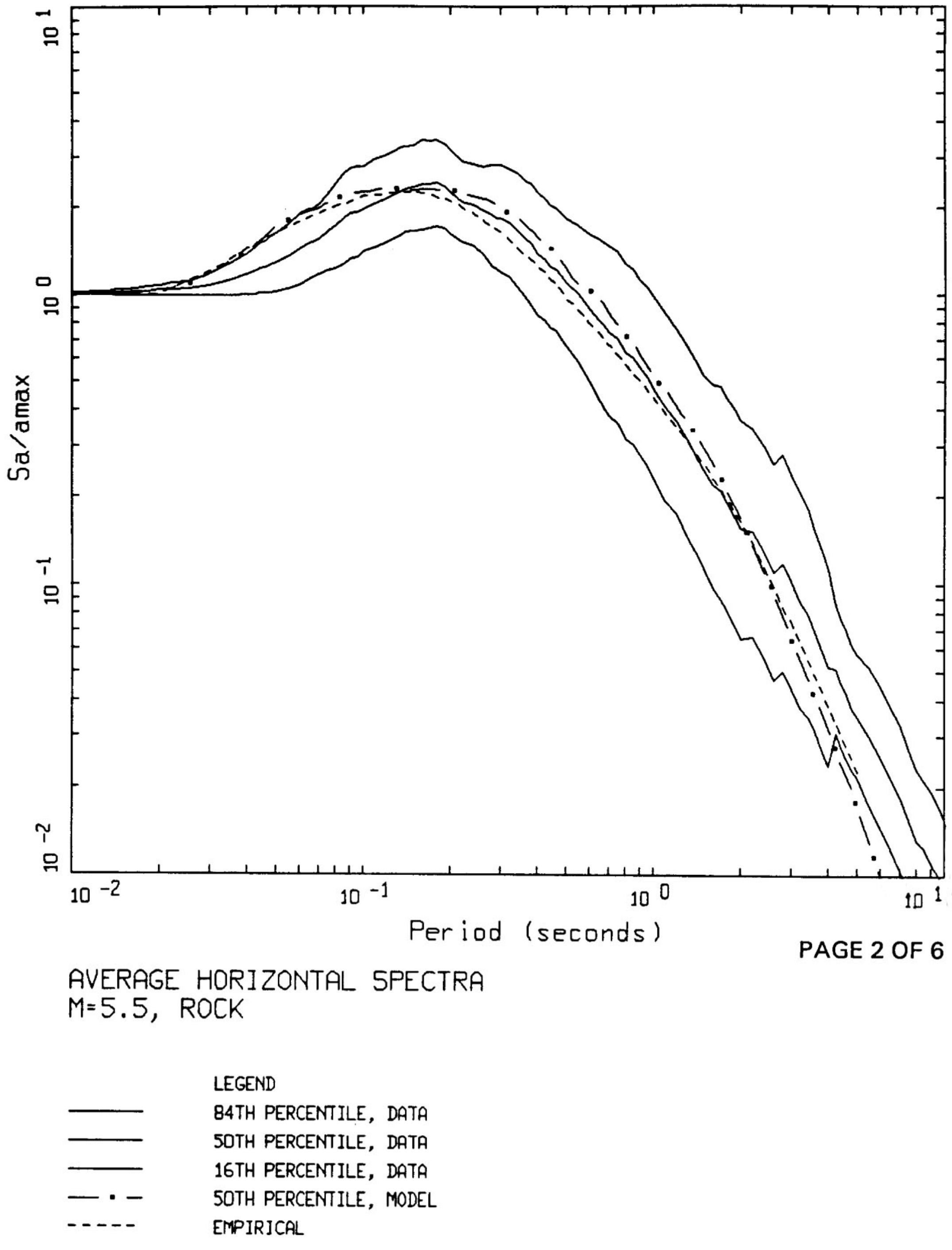

Source: Silva et al. 1996 [DIRS 110474] Figure 7.8

NOTE: The point-source stress drop is 59 bars and M 5.5. Soft rock site conditions.

Figure 7-58b. Comparison of Statistical Response Spectral Shapes with Median Point-Source Model Predictions and Empirical Attenuation Relation for a Vertical Strike-Slip Fault: Soft Rock Sites

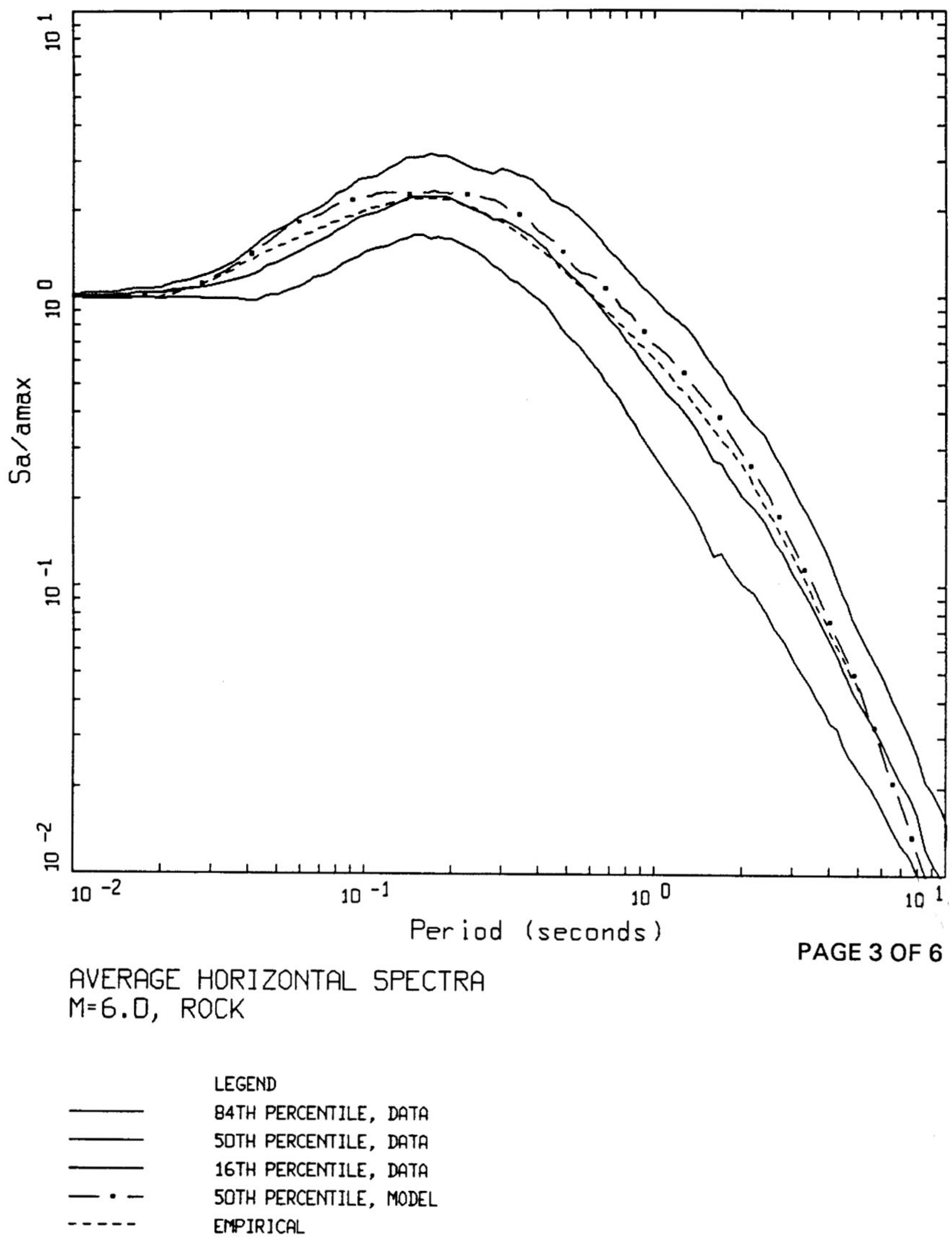

Source: Silva et al. 1996 [DIRS 110474] Figure 7.8

NOTE: The point-source stress drop is 59 bars and M 6.0. Soft rock site conditions.

Figure 7-58c. Comparison of Statistical Response Spectral Shapes with Median Point-Source Model Predictions and Empirical Attenuation Relation for a Vertical Strike-Slip Fault: Soft Rock Sites

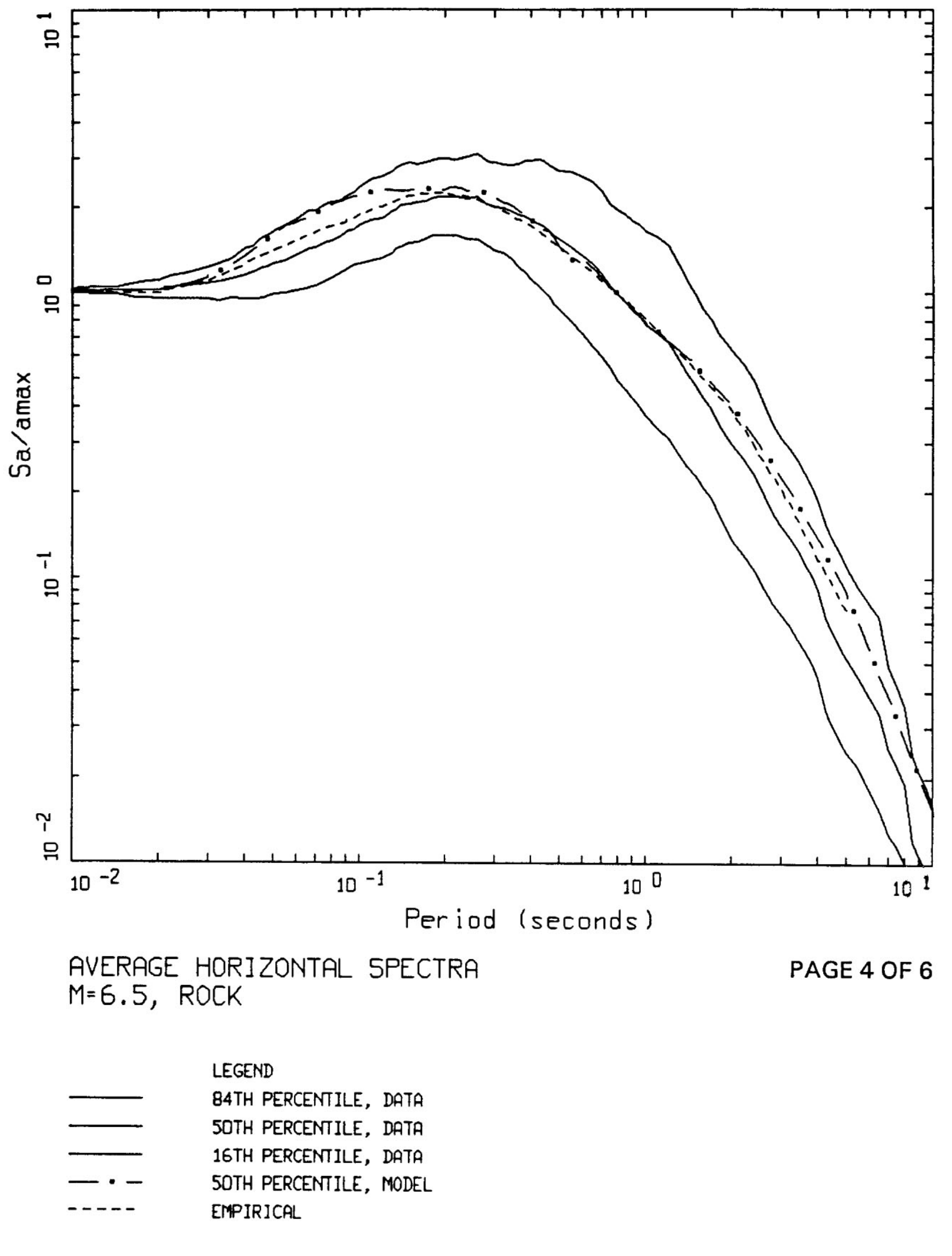

Source: Silva et al. 1996 [DIRS 110474] Figure 7.8

NOTE: The point-source stress drop is 59 bars and M 6.5. Soft rock site conditions.

Figure 7-58d. Comparison of Statistical Response Spectral Shapes with Median Point-Source Model Predictions and Empirical Attenuation Relation for a Vertical Strike-Slip Fault: Soft Rock Sites

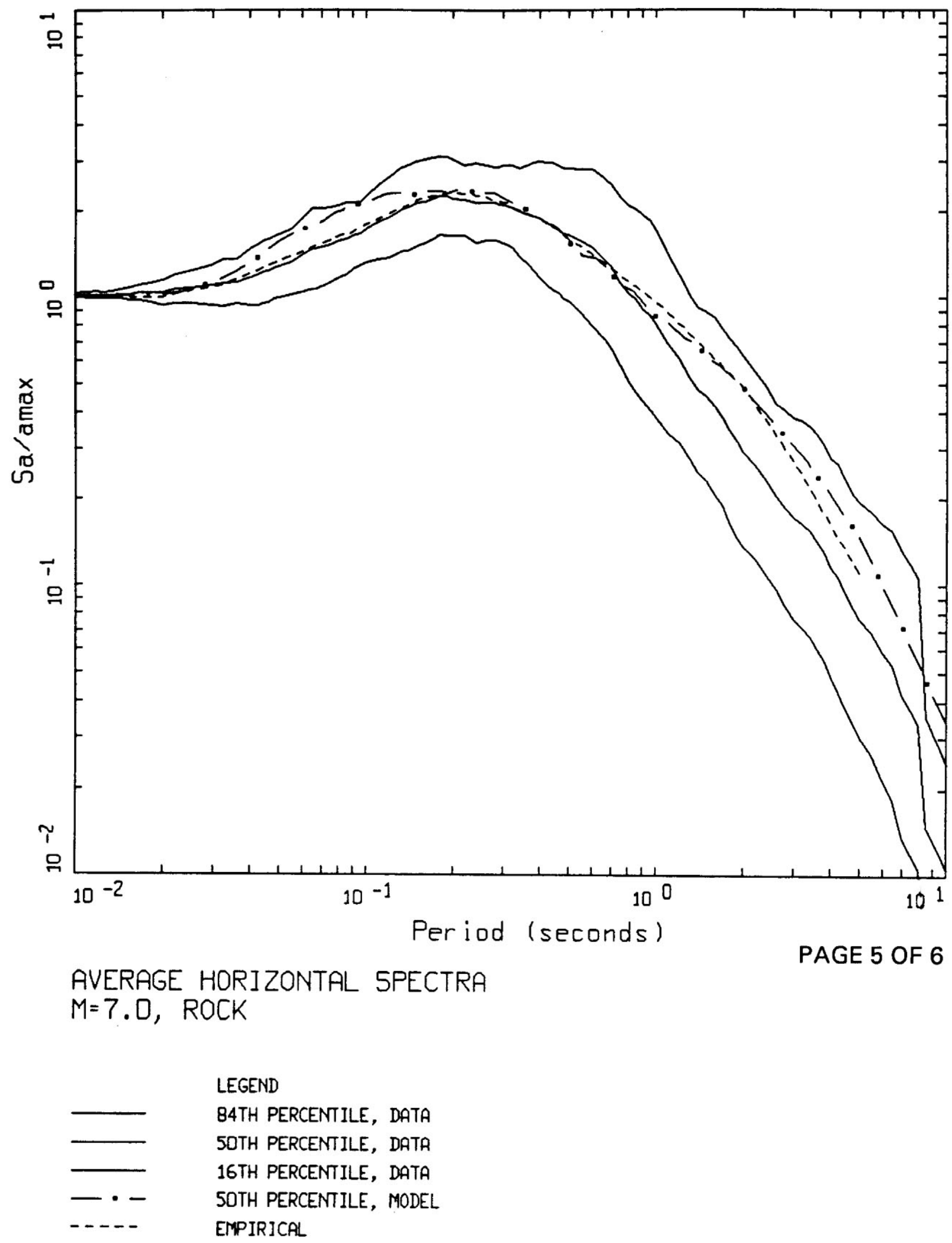

Source: Silva et al. 1996 [DIRS 110474] Figure 7.8

NOTE: The point-source stress drop is 59 bars and M 7.0. Soft rock site conditions.

Figure 7-58e. Comparison of Statistical Response Spectral Shapes with Median Point-Source Model Predictions and Empirical Attenuation Relation for a Vertical Strike-Slip Fault: Soft Rock Sites

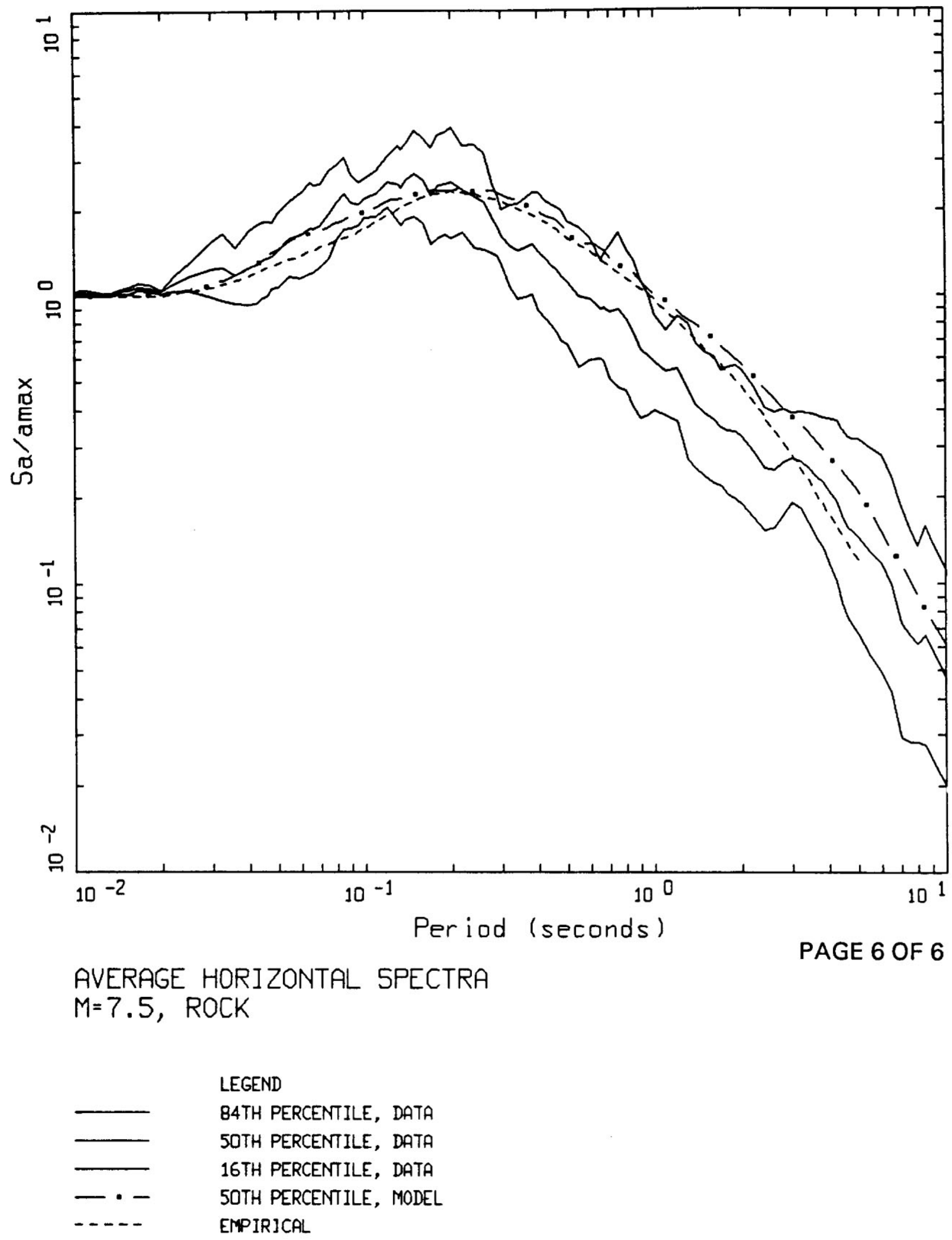

Source: Silva et al. 1996 [DIRS 110474] Figure 7.8

NOTE: The point-source stress drop is 59 bars and M 7.5. Soft rock site conditions.

Figure 7-58f. Comparison of Statistical Response Spectral Shapes with Median Point-Source Model Predictions and Empirical Attenuation Relation for a Vertical Strike-Slip Fault: Soft Rock Sites

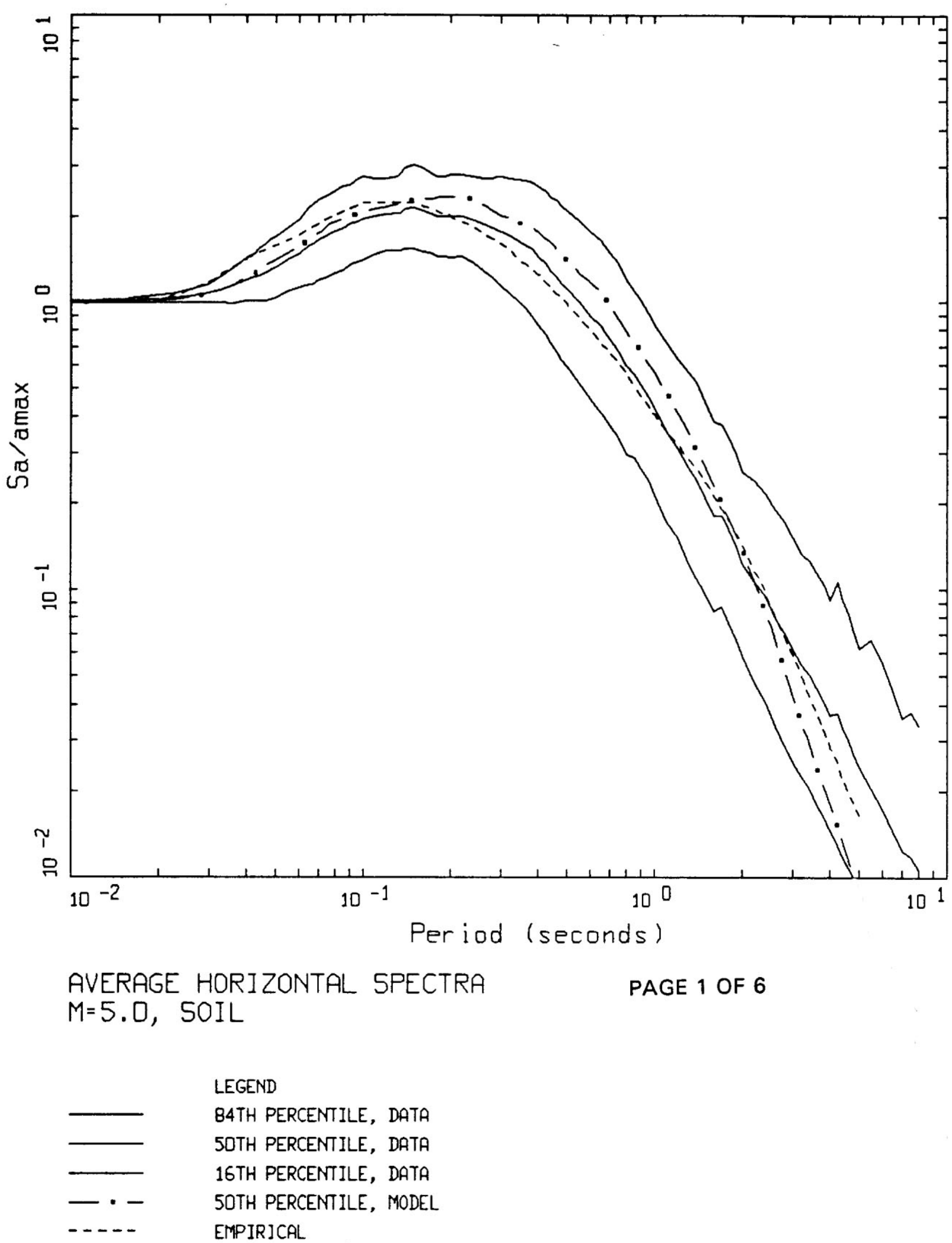

Source: Silva et al. 1996 [DIRS 110474] Figure 7.10

NOTE: The point-source stress drop is 59 bars and M 5.0. Deep soil site conditions.

Figure 7-59a. Comparison of Statistical Response Spectral Shapes With Median Point-Source Model Predictions and Empirical Attenuation Relation for a Vertical Strike-Slip Fault: Deep Soil Sites

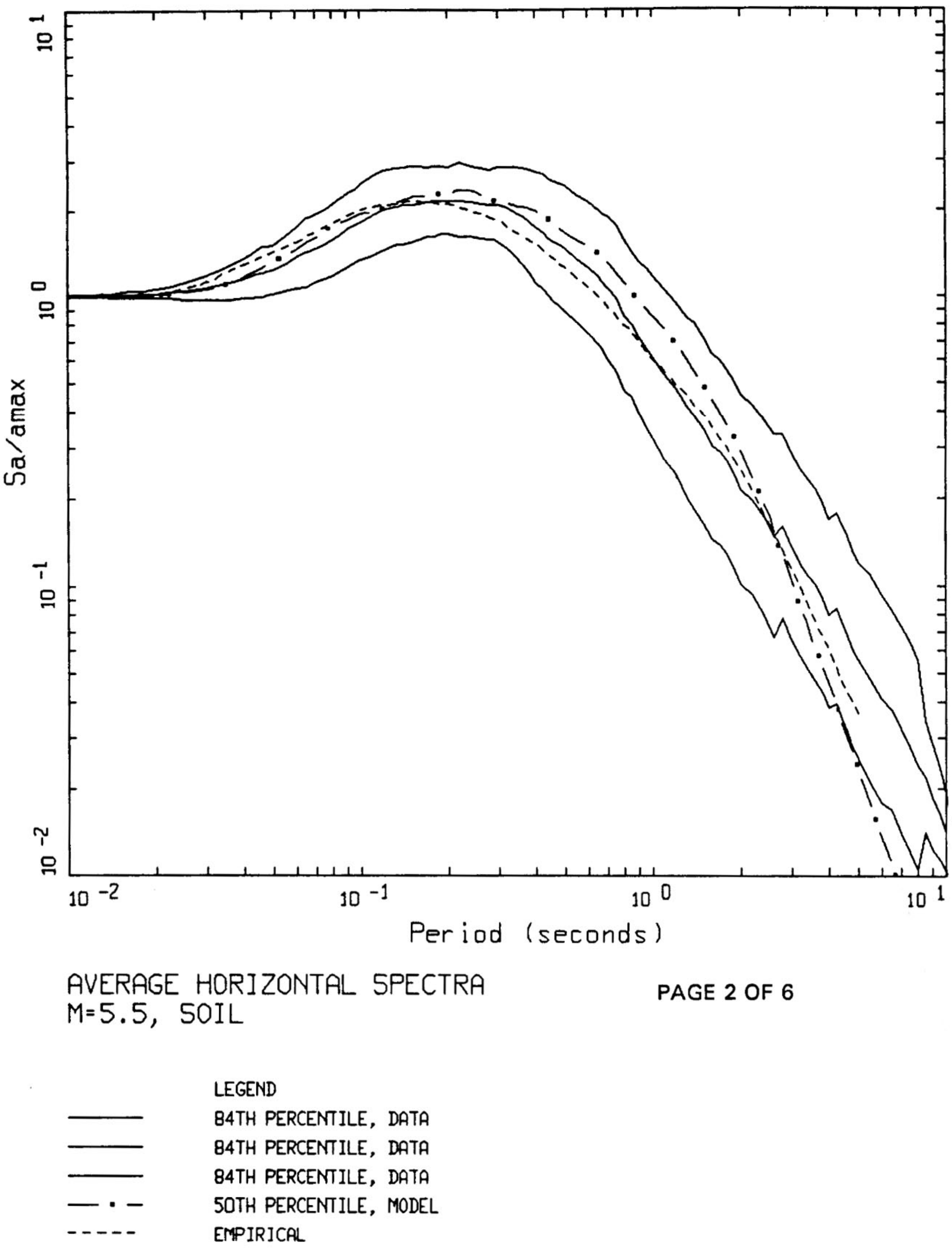

Source: Silva et al. 1996 [DIRS 110474] Figure 7.10

NOTE: The point-source stress drop is 59 bars and M 5.0. Deep soil site conditions.

Figure 7-59b. Comparison of Statistical Response Spectral Shapes With Median Point-Source Model Predictions and Empirical Attenuation Relation for a Vertical Strike-Slip Fault: Deep Soil Sites

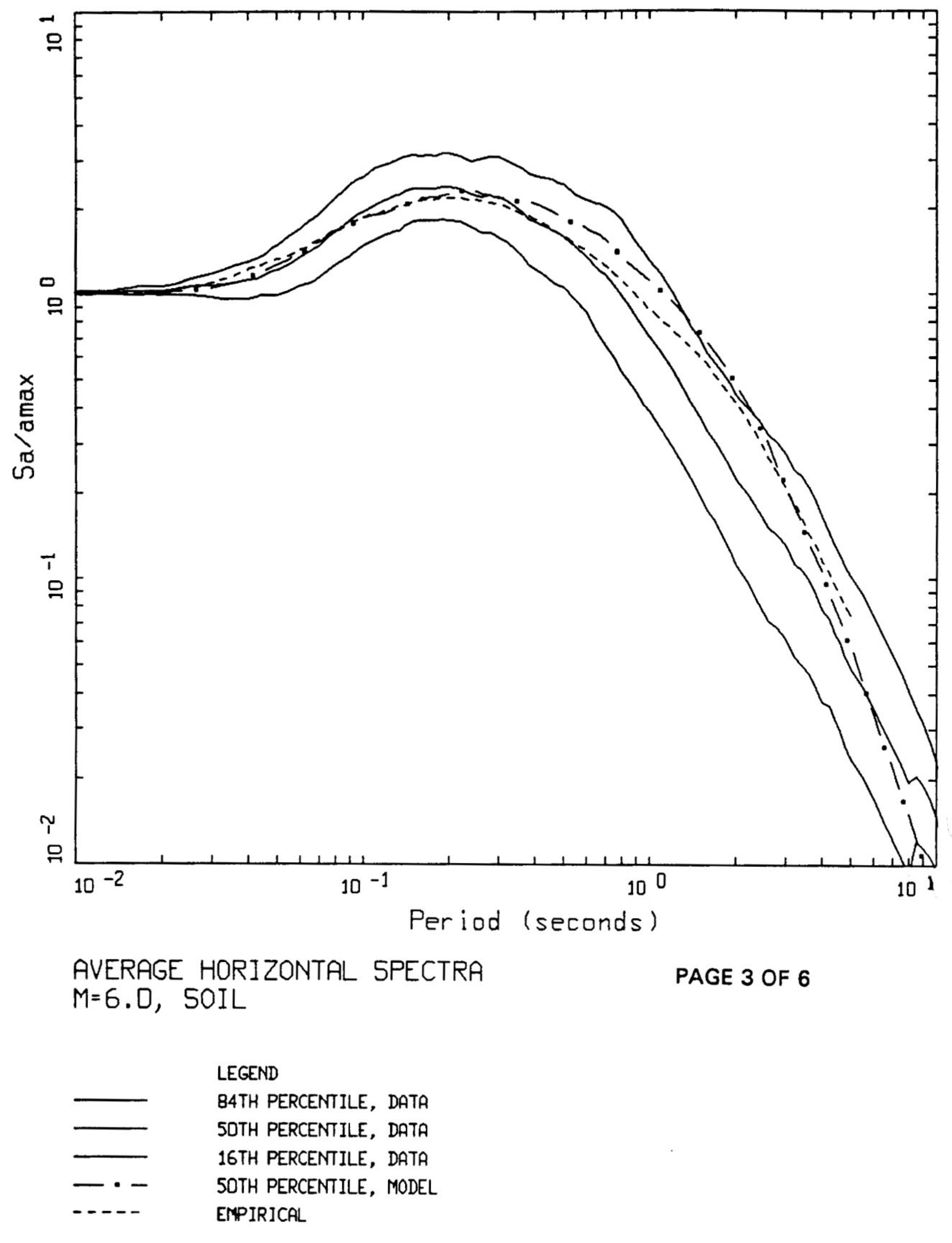

Source: Silva et al. 1996 [DIRS 110474] Figure 7.10

NOTE: The point-source stress drop is 59 bars and M 5.0. Deep soil site conditions.

Figure 7-59c. Comparison of Statistical Response Spectral Shapes With Median Point-Source Model Predictions and Empirical Attenuation Relation for a Vertical Strike-Slip Fault: Deep Soil Sites

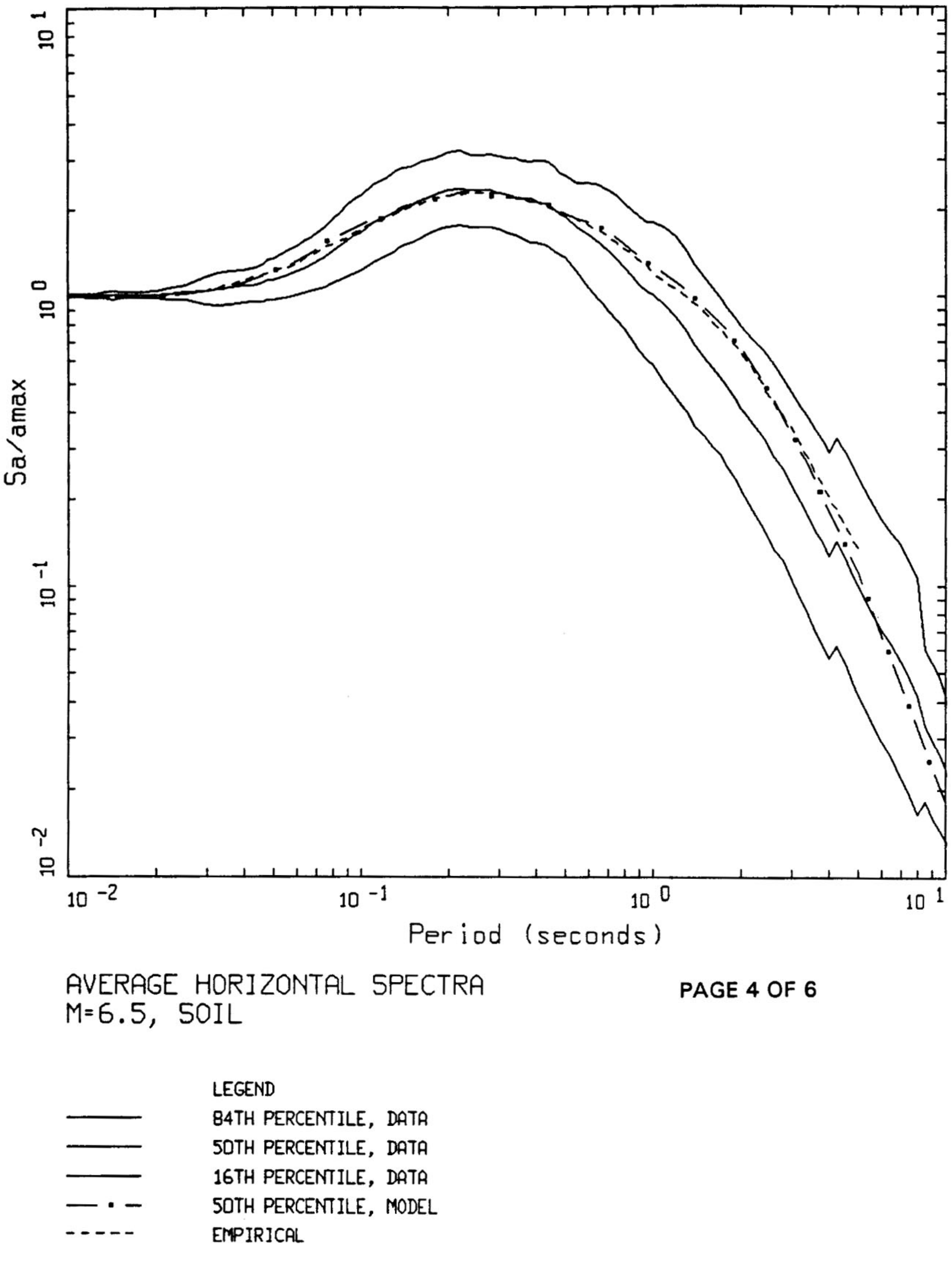

Source: Silva et al. 1996 [DIRS 110474] Figure 7.10

NOTE: The point-source stress drop is 59 bars and M 5.0. Deep soil site conditions.

Figure 7-59d. Comparison of Statistical Response Spectral Shapes With Median Point-Source Model Predictions and Empirical Attenuation Relation for a Vertical Strike-Slip Fault: Deep Soil Sites

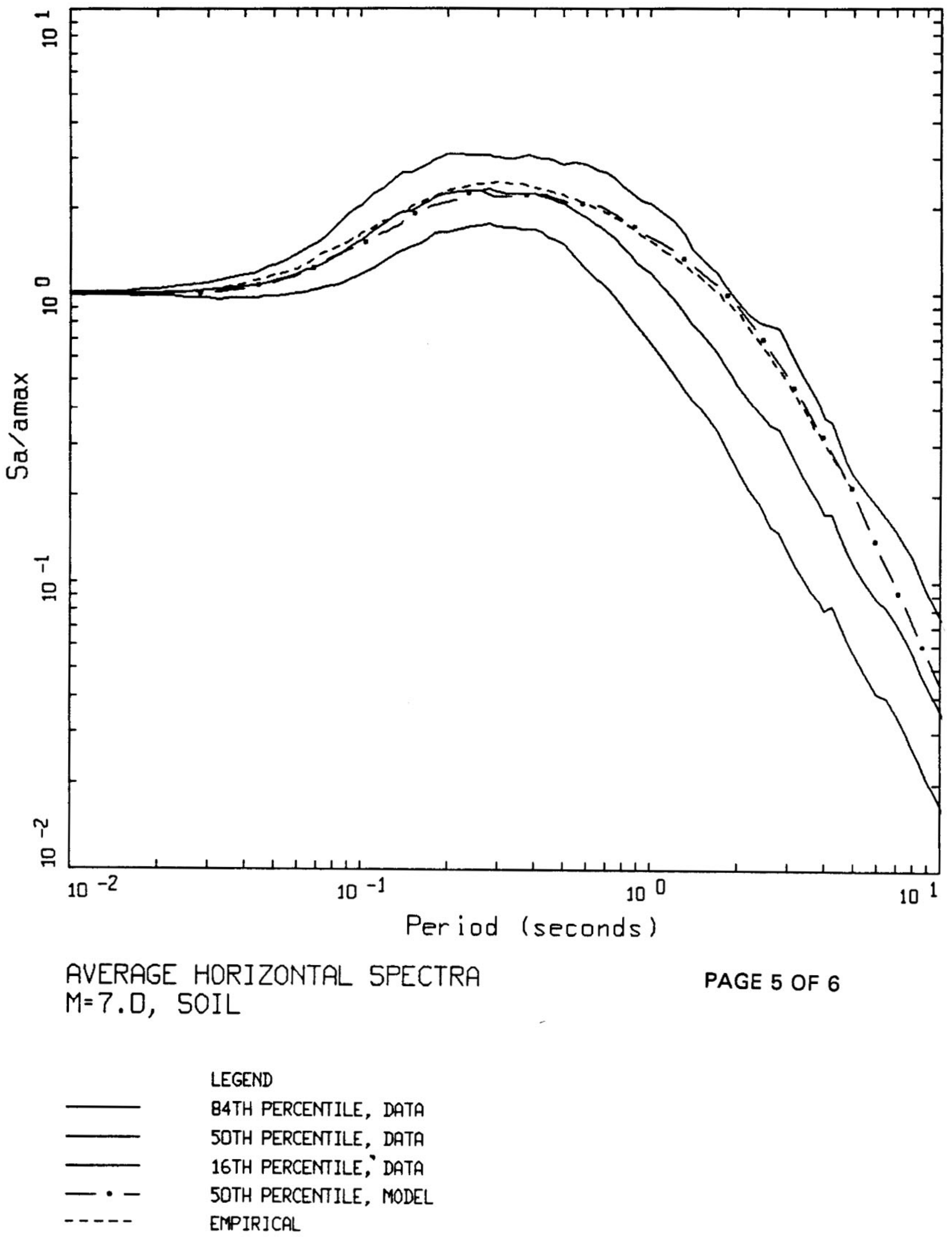

Source: Silva et al. 1996 [DIRS 110474] Figure 7.10

NOTE: The point-source stress drop is 59 bars and M 5.0. Deep soil site conditions.

Figure 7-59e. Comparison of Statistical Response Spectral Shapes With Median Point-Source Model Predictions and Empirical Attenuation Relation for a Vertical Strike-Slip Fault: Deep Soil Sites

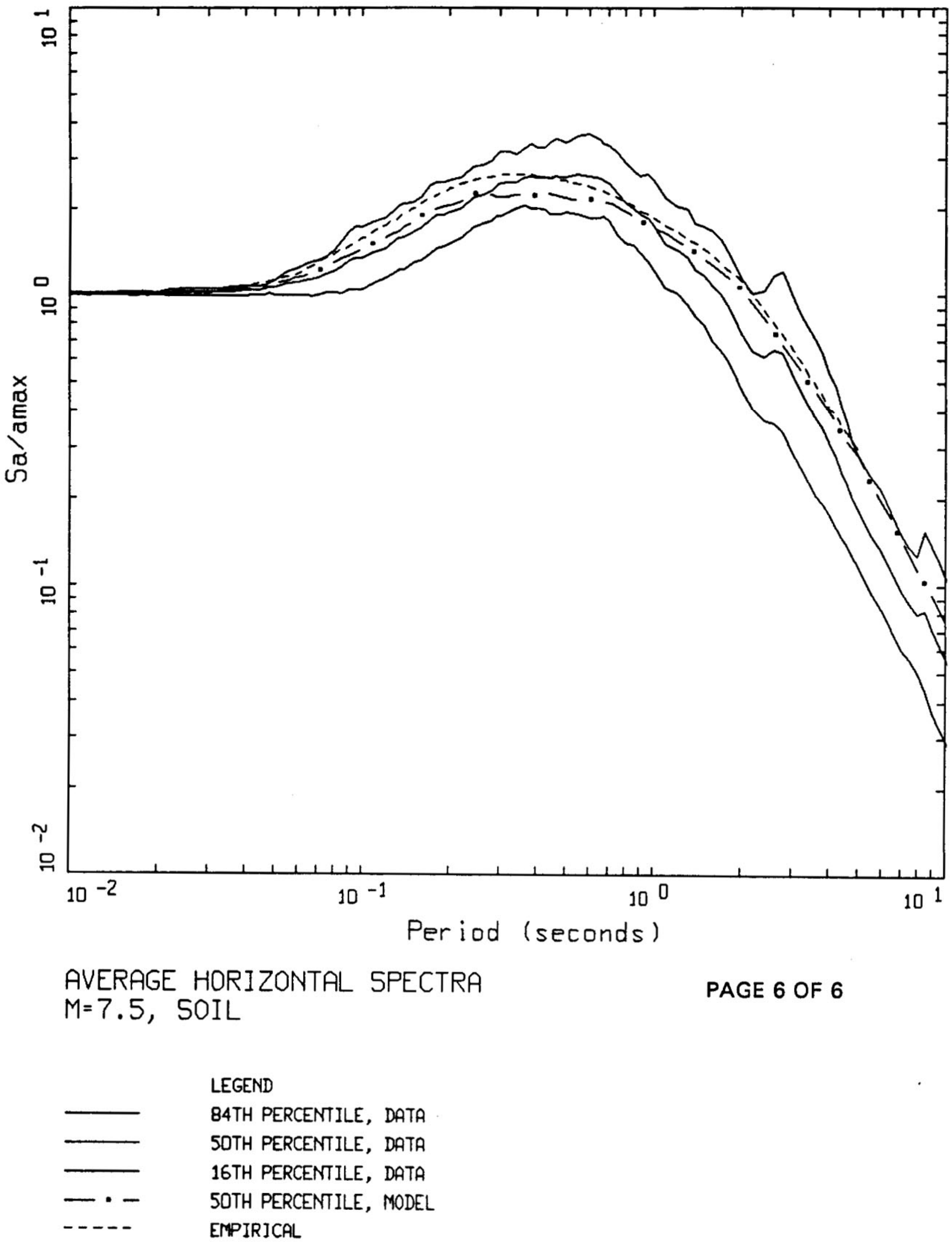

Source: Silva et al. 1996 [DIRS 110474] Figure 7.10

NOTE: The point-source stress drop is 59 bars and M 5.0. Deep soil site conditions.

Figure 7-59f. Comparison of Statistical Response Spectral Shapes With Median Point-Source Model Predictions and Empirical Attenuation Relation for a Vertical Strike-Slip Fault: Deep Soil Sites

8. CONCLUSIONS

A RVT-based equivalent-linear site-response model and stochastic point-source ground motion have been used to develop seismic inputs for use in preclosure design analyses. The overall modeling activity includes analyses to determine model inputs (Section 6.4). The site response model was used to compute the effects of the geology above the reference rock datum and adjust the associated hazard curves. The point-source model was used to characterize the distribution of extreme ground motions and compute V/H ratios. The modeling activity also included implementation of the models to compute preclosure seismic design response spectra for the RB and design response spectra and strain-compatible soil properties for the SFA with AFEs of 10^{-3}, $5x10^{-4}$, and 10^{-4} (Sections 6.5.2 and 6.5.3). On the basis of these model results, additional analyses were carried out to produce time histories for the same (Sections 6.5.2.5 and 6.5.3.6).

Intermediate and final products developed during this modeling activity that have been submitted to the TDMS are summarized in Table 8-1. Other intermediate products used previously in the 2004 study and also herein are reported in BSC (2004 [DIRS 170027).

Table 8-1. Products of Modeling Activity Submitted to the Technical Data Management System

Description	Data Tracking Number	Report Section
Intermediate Products		
Velocity (V_P and V_S) profiles for RB tuff	MO0708BCSSWVGB.001 [DIRS 184464]	6.4.2.6
Velocity (V_P and V_S) profiles for SFA tuff and alluvium	MO0708BCSSWVGB.001 [DIRS 184464]	6.4.2.5
Normalized Shear Modulus Reduction and Material Damping Curves as a Function of Shear Strain for Tuff and Alluvium	MO0708DYNPRP07.000 [DIRS 182579]	6.4.4
Final Products		
Hazard Curves and Mean Uniform Hazard Spectra for the Surface Facilities Area	MO0801HCUHSSFA.001 [DIRS 184802]	6.5.2.2
Hazard Curves and Mean Uniform Hazard Spectra for the Repository Block	MO0801HCUHSREB.001 [DIRS 184803]	6.5.3.1
Design Response Spectra for the RB at 5% Damping	MO0707DSRB5E4A.000 [DIRS 183130] MO0707DSRB1E4A.000 [DIRS 183129] MO0707DSRB1E3A.000 [DIRS 183128]	6.5.2
Design Response Spectra for the SFA at 0.5, 1, 2, 3, 5,7, 10, 15, and 20% Dampings	MO0706DSDR5E4A.001 [DIRS 181422] MO0706DSDR1E4A.001 [DIRS 181421] MO0706DSDR1E3A.000 [DIRS 181423]	6.5.2.3
Strain-Compatible Soil Properties for the SFA	MO0801SCSPS1E3.003 [DIRS 184685] MO0801SCSPS5E4.003 [DIRS 184682] MO0801SCSPS1E4.003 [DIRS 184683]	6.5.2.6.2
Time Histories for the RB 1 three-component sets for AFEs of 10^{-3}, $5x10^{-4}$, and 10^{-4}	MO0707THRB1E4A.000 [DIRS 183200] MO0707THRB5E4A.000 [DIRS 183197] MO0707THRB1E3A.000 [DIRS 183196]	6.5.3.6
Time Histories for the SFA 5 three-component sets for AFEs of 10^{-3}, $5x10^{-4}$, and 10^{-4}	MO0706TH5E4APE.001 [DIRS 181961] MO0706TH1E4APE.001 [DIRS 181960] MO0706TH1E3APE.000 [DIRS 182460]	6.5.2.5

In the computation of the UHS at all AFEs, the spectral values at 3.33 sec derived from the hazard curves and transfer functions using Approach 3 were inadvertently plotted at a period of 3.0 sec. As a result, for periods beyond 2.0 sec the AFE of each UHS is not maintained; ground motion is lower (higher AFE) than the nominal value for periods less than 2.0 sec. Because the design response spectra are based on the UHS, they are also affected by this limitation. The time histories, which are spectrally matched to the design response spectra, have a similar limitation. In using the UHS, design response spectra, and time histories that are an output of this report, the user needs to consider whether this limitation affects the adequacy of the output for a given intended use.

Acceptance Criteria–The work described in this report addresses acceptance criteria from the *Yucca Mountain Review Plan, Final Report* (NRC 2003 [DIRS 163274]). Relevant acceptance criteria are identified in Section 4.2. Table 8-2 lists the acceptance criteria and indicates how they have been addressed.

Table 8-2. Summary of Applicable *Yucca Mountain Review Plan, Final Report* Acceptance Criteria and How They are Addressed in this Report

Yucca Mountain Review Plan, Final Report Acceptance Criteria	Summary of How Acceptance Criteria are Addressed in this Report
Section 1.5.3:	
1. The "General Information" section of the license application contains an adequate description of site characterization activities.	In accordance with part 1 of acceptance criterion 1, this report provides information that contributes to an overview of the site characterization activity to develop seismic inputs for use in preclosure and postclosure analyses.
2. The "General Information" section of the license applications contains an adequate description of site characterization results.	In accordance with part 1 of acceptance criterion 2, Section 6 addresses features and processes that affect seismic ground motions at Yucca Mountain.
	In accordance with part 2 of acceptance criterion 2, Section 6 addresses the seismic ground motions that have the potential to occur in the future at Yucca Mountain.
Section 2.1.1.5.1.3:	
1. Consequence analyses adequately assess normal operations and Category 1 event sequences, as well as factors that allow an event sequence to propagate within the Geologic Repository Operations Area.	In accordance with part 1 of acceptance criterion 1, Section 6.5 provides seismic inputs that represent the seismic hazard for preclosure consequence analyses.
2. Consequence calculations adequately assess the consequences to workers and members of the public from normal operations and Category 1 event sequences.	In accordance with part 1 of acceptance criterion 2, Sections 6.4 and 6.5 provide the technical bases for seismic inputs used in preclosure consequence analyses.
	In accordance with part 3 of acceptance criterion 2, Sections 6.4 and 6.5 describe the development of site-specific seismic inputs and explains how uncertainties are treated.
3. The Dose to Workers and Members of the Public From Normal Operations and Category 1 Event	In accordance with part 1 of acceptance criterion 3, Section 6.5 provides information needed to address seismic

Yucca Mountain Review Plan, Final Report Acceptance Criteria	Summary of How Acceptance Criteria are Addressed in this Report
Sequences is Within the Limits Specified in 10 CFR 63.111(a).	hazards in preclosure consequence analyses.
Section 2.1.1.5.2.3 *1. Consequence analyses include Category 2 event sequences as well as factors that allow an event sequence to propagate within the geologic repository operations area.* *2. Consequence calculations adequately assess the consequences to members of the public from Category 2 event sequences.*	In accordance with part 1 of acceptance criterion 1, Section 6.5 provides seismic inputs that represent the seismic hazard for preclosure consequence analyses. In accordance with part 1 of acceptance criterion 2, Sections 6.4 and 6.5 provide the technical bases for seismic inputs used in preclosure consequence analyses. In accordance with part 3 of acceptance criterion 2, Sections 6.4 and 6.5 describe the development of site-specific seismic inputs and explains how uncertainties are treated.
3. The dose to hypothetical members of the public from category 2 event sequences is within the limits specified in 10 CFR 63.111(b)(2).	In accordance with part 1 of acceptance criterion 3, Sections 6.4 and 6.5 provide information needed to address seismic hazards in preclosure consequence analyses.
Section 2.1.1.1.3 *5. The license application contains descriptions of the site geology and seismology adequate to permit evaluation of the preclosure safety analysis and the Geologic Repository Operations Area design.*	In accordance with part 6 of acceptance criterion 5, Sections 6.4 and 6.5 address the characterization of vibratory ground motions for the repository site. By basing seismic inputs on the results of the PSHA for Yucca Mountain, conditioned to reflect information on extreme ground motions that are consistent with the geologic setting of the site, the results take into account uncertainties and randomness in seismic sources and ground motion.
Section 2.1.1.3.3 *1. Technical basis and assumptions for methods for identification of hazards and initiating events are adequate.*	In accordance with part 1 of acceptance criterion 1, Sections 6.1.6.4 and 6.5 describe how development of seismic inputs is carried out using McGuire et al. (2001 [DIRS 157510]), NRC (2007 [DIRS 180931]), NRC (2007 [DIRS 180932]), and ASCE/SEI 43-05 (2005 [DIRS 173805]). In accordance with part 2 of acceptance criterion 1, Sections 6.1 and 6.5 describe exceptions taken to the guidance mentioned with respect to part 1 above and provides the technical basis for exceptions. In accordance with part 3 of acceptance criterion 1, Sections 6.1, 6.4 and 6.5 describe the development of seismic inputs taking into account site data uncertainty and randomness. In accordance with part 4 of acceptance criterion 1, Section 6.3 describes modeling assumptions and provides their technical basis. Validation of modeling assumptions is described in Section 7.

Yucca Mountain Review Plan, Final Report Acceptance Criteria	Summary of How Acceptance Criteria are Addressed in this Report
2. Site data and system information are appropriately used in identification of hazards and initiating events.	In accordance with part 1 of acceptance criterion 2, Section 6.4 describes the use of site-specific data in determining inputs used for modeling and analyses to develop seismic inputs.
3. Determination of frequency or probability of occurrence of hazards and initiating events is acceptable.	In accordance with part 1 of acceptance criterion 3, Sections 6.1, 6.4, and 6.5 describe how site-response modeling to develop seismic inputs is carried out such that site-specific seismic inputs are consistent with the hazard level of the control motions. The sections also describe how uncertainty and randomness in input data is incorporated in the process.
	In accordance with part 3 of acceptance criterion 3, Section 7 describes validation of the point-source stochastic ground-motion model.
4. Adequate technical bases for the inclusion and exclusion of hazards and initiating events are provided.	In accordance with part 1 of acceptance criterion 4, Sections 6.4 and 6.5 provide the technical basis for seismic inputs that characterize the seismic hazard at Yucca Mountain. Seismic inputs are developed consistent with the available site-specific data and in a manner consistent with the geologic setting. In accordance with part 2 of acceptance criterion 4, Sections 6.4 and 6.5 describe how uncertainties are incorporated into the modeling and analyses carried out to develop seismic inputs.
Section 2.1.1.7.3.1 *1. The relationship between the design criteria and the requirements specified in 10 CFR 63.111(a) and (b), the relationship between the design bases and the design criteria, and the design criteria and design bases for structures, systems, and components important to safety are adequately defined.*	In accordance with part 1 of acceptance criterion 1, Section 6.5 provides design response spectra and associated time histories for DBGM-1, DBGM-2 and BDBGM, both for the surface facilities area and the repository waste emplacement level.
Section 2.1.1.7.3.2 *1. Geologic repository operations area design methodologies are adequate.*	In accordance with part 4 of acceptance criterion 1, development of seismic inputs take into account DOE (2007 [DIRS 181572]).
Section 2.2.1.2.2.3 *1. Events are adequately defined.*	In accordance with part 1 of acceptance criterion 1, Section 6.5 addresses development of seismic inputs for various annual frequencies of exceedance. In accordance with part 2 of acceptance criterion 1, Sections 6.4 and 6.5 indicate that the PSHA provides part of the basis for the control motions used in site response modeling. The PSHA assessments are based on the historical record, paleoseismic studies, and geological analyses. Development of seismic time histories relies on historically recorded strong ground motion data.
2. Probability estimates for future events are supported by appropriate technical bases.	In accordance with part 1 of acceptance criterion 2, Sections 6.4 and 6.5 indicate that the PSHA provides part

Yucca Mountain Review Plan, Final Report Acceptance Criteria	Summary of How Acceptance Criteria are Addressed in this Report
	of the basis for the control motions used in site response modeling. The PSHA assessments are based on past patterns of seismicity and seismic characteristics for the Yucca Mountain vicinity.
3. Probability model support is adequate.	In accordance with part 1 of acceptance criterion 3, Section 6.4 describes how control motions for site response modeling are in part based on the PSHA for Yucca Mountain. The PSHA considered analog data from the Basin and Range province, historical seismicity within 300 km of Yucca Mountain, and tectonic models that were consistent with available data.
4. Probability model parameters have been adequately established.	In accordance with part 1 of acceptance criterion 4, Section 6.4 describes the technical justification for parameter inputs used in ground motion site-response modeling. It describes how those parameter values are determined from available site-specific data.
5. Uncertainty in event probability is adequately evaluated.	In accordance with part 1 of acceptance criterion 5, Sections 6.4 and 6.5 describe how uncertainties and randomness in model input parameters are addressed in the development of seismic inputs for various annual frequencies of exceedance.
Section 2.2.1.3.2.3	
2. Data are sufficient for model justification.	In accordance with part 1 of acceptance criterion 2, Sections 6.4 and 6.5 provide justification for seismic inputs for the repository waste emplacement level.
	In accordance with part 3 of acceptance criterion 2, Section 6.4 describes how data are used to determine inputs for ground motion site-response modeling for the repository waste emplacement level.
3. Data uncertainty is characterized and propagated through the model abstraction.	In accordance with part 1 of acceptance criterion 3, Sections 6.4 provides the technical basis for determining inputs to ground motion site-response modeling for the repository waste emplacement level. The section also, along with Section 6.5, describes how data uncertainties and randomness are addressed.
	In accordance with part 2 of acceptance criterion 3, Sections 6.3 and Section 7 describe the point-source stochastic ground motion model and its validation. Determination of input parameter values on the basis of site-specific data is described in Section 6.4.
	In accordance with part 3 of acceptance criterion 3, Sections 6.4 and 6.5 describe how data uncertainties and randomness are incorporated in the site-response modeling and analyses, including for the repository waste emplacement level.

9. INPUTS AND REFERENCES

9.1 DOCUMENTS CITED

166530 Abrahamson, N.A. and Becker, A.M. 1997. Ground Motion Characterization at Yucca Mountain, Nevada, Volume 1: Reference Material for Proponent Models, February 1997. USGS Level 4 Milestone SPG28EM4. [Denver, Colorado]: U.S. Geological Survey. ACC: MOL.20030205.0119.

164486 Abrahamson, N.A and Shedlock, K.M. 1997. "Overview." *Seismological Research Letters*, 68, (1), 9-23. El Cerrito, California: Seismological Society of America. TIC: 240552.

104205 Abrahamson, N.A. and Silva, W.J. 1997. "Empirical Response Spectral Attenuation Relations for Shallow Crustal Earthquakes." *Seismological Research Letters*, 68, (1), 94-127. El Cerrito, California: Seismological Society of America. TIC: 240553.

183483 Abrahamson, N.A.; Somerville, P.G.; and Cornell, C.A. 1990. "Uncertainty in Numerical Strong Motion Predictions." *Fourth U.S. National Conference on Earthquake Engineering. 1,* 407-416. El Cerrito, California: Earthquake Engineering Research Institute. TIC: 256780.

182349 Aki, K. 1967. "Scaling Law of Seismic Spectrum." *Journal of Geophysical Research, 72,* (4), 1217-1231. Washington, DC: American Geophysical Union. TIC: 259670.

128813 Anderson, J.G. and Hough, S.E. 1984. "A Model for the Shape of the Fourier Amplitude Spectrum of Acceleration at High Frequencies." *Bulletin of the Seismological Society of America,* 74, (5), 1969-1993. El Cerrito, California: Seismological Society of America. TIC: 242440.

184472 Anderson, J.G.; Purvance, M.; Anooshehpoor, A.; and Brune, J.N. 2007. "Simplified Probabilistic Seismic Hazard Analysis for Precarious Rocks on Yucca Mountain, Nevada." *Seismological Research Letters, 78,* (2), 281. El Cerrito, California: Seismological Society of America. TIC: 259966.

184349 Andrews, D.J.; Hanks, T.C.; and Whitney, J.W. 2007. "Physical Limits on Ground Motion at Yucca Mountain." *Seismological Research Letters, 78,* (2), 314. El Cerrito, California: Seismological Society of America. TIC: 259932.

184818 Andrews, D.J.; Hanks, T.C.; and Whitney, J.W. 2007. "Physical Limits on Ground Motion at Yucca Mountain." Bulletin of the Seismologic Society of America, 97, (6), 1771-1792. El Cerrito, California: Seismological Society of America. ACC: 260030.

166350 Atkinson, G.M. 1984. "Attenuation of Strong Ground Motion in Canada from a Random Vibrations Approach." *Bulletin of the Seismological Society of America, 74,* (6), 2629-2653. Berkeley, California: Seismological Society of America. TIC: 259923.

184793 Atkinson, G.M. 1993. "Earthquake Source Spectra in Eastern North America." Bulletin of the Seismological Society of America, 83, (6), 1778-1798. [El Cerrito, California]: Seismological Society of America. TIC: 260021.

184123 Atkinson, G.M. and Boore, D.M. 1995. "Ground-Motion Relations for Eastern North America." *Bulletin of the Seismological Society of America, 85,* (1), 17-30. El Cerrito, California: Seismological Society of America. TIC: 238388.

183437 Atkinson, G.M. and Boore, D.M. 1997. "Some Comparisons Between Recent Ground-Motion Relations." *Seismological Research Letters, 68,* (1), 24-40. El Cerrito, California: Seismological Society of America. TIC: 240552.

184801 Atkinson, G.M. and Boore, D.M. 1997. "Stochastic Point-Source Modeling of Ground Motions in the Cascadia Region." *Seismological Research Letters, 68,* (1), 74-85. El Cerrito, California: Seismological Society of America. TIC: 240552.

163171 Atkinson, G.M. and Silva, W. 1997. "An Empirical Study of Earthquake Source Spectra for California Earthquakes." *Bulletin of the Seismological Society of America, 87,* (1), 97-112. [El Cerrito, California: Seismological Society of America]. TIC: 254822.

177290 Bazzurro, P. and Cornell, C.A. 2004. "Nonlinear Soil-Site Effects in Probabilistic Seismic-Hazard Analysis." *Bulletin of the Seismological Society of America, 94,* (6), 2110-2123. El Cerrito, California: Seismological Society of America. TIC: 257584.

184397 Boatwright, J. and Astrue, M. 1983. "The Effect of Site Response on High Frequency Ground Motions; Analysis of the Aftershocks of the New Brunswick Earthquake." *A Workshop on "Site-Specific Effects of Soil and Rock on Ground Motion and the Implications for Earthquake-Resistant Design".* W.W. Hays. *Proceedings of Conference XXII, U.S. Geological Survey OFR 83-845,* 172-190. Reston, Virginia: U.S. Geological Survey. TIC: 217505.

184601 Bommer, J.J.; Abrahamson, N.A.; Strasser, F.O.; Pecker, A.; Bard, P-Y.; Bungum, H.; Cotton, F.; Fäh, D.; Sabetta, F.; Scherbaum, F.; and Studer, J. 2004. "The Challenge of Defining Upper Bounds on Earthquake Ground Motions." *Seismological Research Letters, 75,* (1), 82-95. El Cerrito, California: Seismological Society of America. TIC: 259995.

103317 Boore, D.M. 1983. "Stochastic Simulation of High-Frequency Ground Motions Based on Seismological Models of the Radiated Spectra." *Bulletin of the Seismological Society of America*, 73, (6), 1865-1894. El Cerrito, California: Seismological Society of America. TIC: 245812.

103318 Boore, D.M. 1986. "Short-Period P- and S-Wave Radiation from Large Earthquakes: Implications for Spectral Scaling Relations Spectra." *Bulletin of the*

Seismological Society of America, 76, (1) 43-64. El Cerrito, California: Seismological Society of America. TIC: 245811.

184354 Boore, D.M. 2000. *SMSIM - Fortran Programs for Simulating Ground Motions From Earthquakes: Version 2.0 - A Revision of OFR-96-80-A.* Open-File Report 00-509. 55. Menlo Park, California: U.S. Geological Survey. TIC: LLR.20080103.0014.

163993 Boore, D.M. 2001. "Comparisons of Ground Motion from the 1999 Chi-Chi Earthquake with Empirical Predictions Largely Based on Data from California." *Bulletin of the Seismological Society of America*, 91, (5), 1212-1217. El Cerrito, California: Seismological Society of America. TIC: 254638.

182044 Boore, D.M. and Atkinson, G.M. 1987. "Stochastic Prediction of Ground Motion and Spectral Response Parameters at Hard-Rock Sites in Eastern North America." *Bulletin of the Seismological Society of America*, 77, (2), 440-467. El Cerrito, California: Seismological Society of America. TIC: 259595.

184133 Boore, D.M. and Atkinson, G.M. 1992. "Source Spectra for the 1988 Saguenay, Quebec, Earthquakes." *Bulletin of the Seismological Society of America, 82,* 683-719. El Cerrito, California: Seismological Society of America. TIC: 259926.

163174 Boore, D.M. and Joyner, W.B. 1984. "A Note on the Use of Random Vibration Theory to Predict Peak Amplitudes of Transient Signals." *Bulletin of the Seismological Society of America*, 74, (5), 2035-2039. El Cerrito, California: Seismological Society of America. TIC: 254639.

124240 Boore, D.M.; Joyner, W.B.; and Fumal, T.E. 1994. *Estimation of Response Spectra and Peak Accelerations from Western North American Earthquakes: An Interim Report, Part 2.* Open-File Report 94-127. Menlo Park, California: U.S. Geological Survey. TIC: 246666.

184351 Brace, W.F. and Kohlstedt, D.L. 1980. "Limits on Lithospheric Stress Imposed by Laboratory Experiments." *Journal of Geophysical Research, 85,* (B11), 6248-6252. Washington, DC: American Geophysical Union. TIC: 259931.

171300 Brandshaug, T.; Cundall, P.; and Damjanac, B. 2004. Generation of Shear-Modulus and Damping-Ratio Degradation Curves from Simulations of Cyclic Shear Tests of Large Rock Mass Samples. ICG04-2133-6-27. Minneapolis, Minnesota: Itasca Consulting Group. ACC: MOL.20040902.0237.

103315 Brune, J.N. 1970. "Tectonic Stress and the Spectra of Seismic Shear Waves from Earthquakes." *Journal of Geophysical Research,* 75, (26), 4997-5009. Washington, D.C.: American Geophysical Union. TIC: 220215.

131516 Brune, J.N. 1971. "Tectonic Stress and the Spectra of Seismic Shear Waves from Earthquakes [Correction]." *Journal of Geophysical Research, 76,* (20), 5002. Washington, D.C.: American Geophysical Union. TIC: 220216.

155187 BSC (Bechtel SAIC Company) 2001. *Ground Control for Emplacement Drifts for SR.* ANL-EBS-GE-000002 REV 00 ICN 01. Las Vegas, Nevada: Bechtel SAIC Company. ACC: MOL.20010627.0028.

157829 BSC (Bechtel SAIC Company) 2002. Geotechnical Data for a Potential Waste Handling Building and for Ground Motion Analyses for the Yucca Mountain Site Characterization Project. ANL-MGR-GE-000003 REV 00. Las Vegas, Nevada: Bechtel SAIC Company. ACC: MOL.20021004.0078.

166274 BSC (Bechtel SAIC Company) 2003. Development of Earthquake Ground Motion Input for Preclosure Seismic Design and Postclosure Performance Assessment of a Geologic Repository at Yucca Mountain, NV. MDL-MGR-GS-000003 REV 00. Las Vegas, Nevada: Bechtel SAIC Company. ACC: DOC.20031201.0001.

162711 BSC (Bechtel SAIC Company) 2003. Drift Degradation Analysis. ANL-EBS-MD-000027 REV 02. Las Vegas, Nevada: Bechtel SAIC Company. ACC: DOC.20030709.0003.

168550 BSC (Bechtel SAIC Company) 2004. Drift Degradation Analysis. ANL-EBS-MD-000027 REV 02, Errata 1. Las Vegas, Nevada: Bechtel SAIC Company. ACC: DOC.20040325.0002; DOC.20030709.0003.

166107 BSC (Bechtel SAIC Company) 2004. Drift Degradation Analysis. ANL-EBS-MD-000027 REV 03. Las Vegas, Nevada: Bechtel SAIC Company. ACC: DOC.20040915.0010; DOC.20050419.0001; DOC.20051130.0002; DOC.20060731.0005.

168030 BSC (Bechtel SAIC Company) 2004. *Characterize Framework for Seismicity and Structural Deformation at Yucca Mountain, Nevada*. ANL-CRW-GS-000003 REV 00 [Errata 001]. Las Vegas, Nevada: Bechtel SAIC Company. ACC: MOL.20000510.0175; DOC.20040223.0007.

170024 BSC (Bechtel SAIC Company) 2004. *Analysis of Mechanisms for Early Waste Package/Drip Shield Failure.* CAL-EBS-MD-000030 REV 00C. Las Vegas, Nevada: Bechtel SAIC Company. ACC: DOC.20040913.0006; DOC.20050606.0005; DOC.20050830.0002.

170029 BSC (Bechtel SAIC Company) 2004. *Geologic Framework Model (GFM2000).* MDL-NBS-GS-000002 REV 02. Las Vegas, Nevada: Bechtel SAIC Company. ACC: DOC.20040827.0008.

170027 BSC (Bechtel SAIC Company) 2004. *Development of Earthquake Ground Motion Input for Preclosure Seismic Design and Postclosure Performance Assessment of a Geologic Repository at Yucca Mountain, NV.* MDL-MGR-GS-000003 REV 01. Las Vegas, Nevada: Bechtel SAIC Company. ACC: DOC.20041111.0006; DOC.20051130.0003.

172801 BSC (Bechtel SAIC Company) 2004. *D&E/RIT IED Subsurface Facilities [Sheet 1 of 4]*. 800-IED-WIS0-00101-000-00B. Las Vegas, Nevada: Bechtel SAIC Company. ACC: ENG.20041130.0002.

169734 BSC (Bechtel SAIC Company) 2004. Yucca Mountain Site Description. TDR-CRW-GS-000001 REV 02 ICN 01. Two volumes. Las Vegas, Nevada: Bechtel SAIC Company. ACC: DOC.20040504.0008.

170137 BSC (Bechtel SAIC Company) 2005. *Peak Ground Velocities for Seismic Events at Yucca Mountain, Nevada.* ANL-MGR-GS-000004 REV 00. Las Vegas, Nevada: Bechtel SAIC Company. ACC: DOC.20050223.0002; DOC.20050725.0002.

175539 BSC (Bechtel SAIC Company) 2005. *Q-List.* 000-30R-MGR0-00500-000-003. Las Vegas, Nevada: Bechtel SAIC Company. ACC: ENG.20050929.0008.

178322 BSC (Bechtel SAIC Company) 2006. *Seismic Studies.* TWP-MGR-GS-000001 REV 05. Las Vegas, Nevada: Bechtel SAIC Company. ACC: MOL.20060925.0057.

180474 BSC (Bechtel SAIC Company) 2007. *Quality Management Directive.* QA-DIR-10, Rev. 1. Las Vegas, Nevada: Bechtel SAIC Company. ACC: DOC.20070330.0001.

182932 BSC (Bechtel SAIC Company) 2007. *Subsurface - Underground Layout Configuration for LA General Arrangement*. 800-KM0-SS00-00301-000 REV 00B. Las Vegas, Nevada: Bechtel SAIC Company. ACC: ENG.20070830.0036.

184595 BSC (Bechtel SAIC Company) 2007. *Supplemental Soils Report*. 100-S0C-CY00-00100-000-00D. Las Vegas, Nevada: Bechtel SAIC Company. ACC: ENG.20080102.0045.

103635 Budnitz, R.J.; Apostolakis, G.; Boore, D.M.; Cluff, L.S.; Coppersmith, K.J.; Cornell, C.A.; and Morris, P.A. 1997. *Recommendations for Probabilistic Seismic Hazard Analysis: Guidance on the Uncertainty and Use of Experts.* NUREG/CR-6372. Two volumes. Washington, D.C.: U.S. Nuclear Regulatory Commission. TIC: 235076; 235074.

100106 Buesch, D.C.; Spengler, R.W.; Moyer, T.C.; and Geslin, J.K. 1996. Proposed Stratigraphic Nomenclature and Macroscopic Identification of Lithostratigraphic Units of the Paintbrush Group Exposed at Yucca Mountain, Nevada. Open-File Report 94-469. Denver, Colorado: U.S. Geological Survey. ACC: MOL.19970205.0061.

163497 Bycroft, G.N. 1980. *El Centro California Differential Ground Motion Array.* Open-File Report 80-919. Menlo Park, California: U.S. Geological Survey. TIC: 254674.

184677 Camacho-Padron, B.I. 2006. *Effect of Particle Cementation on the Stiffness of Uniform Sand as Measured with Stress Wave Velocities.* Ph.D. dissertation. Austin, Texas: University of Texas at Austin. TIC: 260003.

102191 Campbell, K.W. 1981. "Near-Source Attenuation of Peak Horizontal Acceleration." *Bulletin of the Seismological Society of America,* 71, (6), 2039-2070. El Cerrito, California: Seismological Society of America. TIC: 221670.

183814 Campbell, K.W. and Bozorgnia, Y. 2003. "Updated Near-Source Ground Motion (Attenuation) Relations for the Horizontal and Vertical Components of Peak Ground Acceleration and Acceleration Response Spectra." *Bulletin of the Seismological Society of America, 93,* (1), 314-331. El Cerrito, California: Seismological Society of America. TIC: 259845.

164971 Chávez-García, F.J.; Ramos-Martínez, J.; and Romero-Jiménez, E. 1995. "Surface-Wave Dispersion Analysis in Mexico City." *Bulletin of the Seismological Society of America,* 85, (4), 1116-1126. El Cerrito, California: Seismological Society of America. TIC: 254849.

184795 Cocco, M. and Rovelli, A. 1989. "Evidence for the Variation of Stress Drop Between Normal and Thrust Faulting Earthquakes in Italy." *Journal of Geophysical Research, 94,* (B7), 9399-9416. Washington, D.C.: American Geophysical Union. TIC: 260015.

171191 Corradini, M.L. 2003. Responses and Evaluation from the Nuclear Waste Technical Review Board to the U.S. Department of Energy Presentations given at the February 2003 Joint Meeting held by the Natural System and Engineered System Panel Discussing Seismic Issue. Letter from M.L. Corradini (NWTRB) to M.S.Y. Chu (DOE/OCRWM), June 27, 2003. ACC: HQO.20031017.0002.

182407 Cramer, C.H. 2003. "Site-Specific Seismic-Hazard Analysis that is Completely Probabilistic." *Bulletin of the Seismological Society of America, 93,* (4), 1841-1846. El Cerrito, California: Seismological Society of America. TIC: 259664.

183434 Cranswick, E.; Wetmiller, R.; and Boatwright, J. 1985. "High-Frequency Observations and Source Parameters of Microearthquakes Recorded at Hard-Rock Sites." *Bulletin of the Seismological Society of America,* . El Cerrito, California: Seismological Society of America. TIC: 259780.

103731 CRWMS M&O 1998. *Probabilistic Seismic Hazard Analyses for Fault Displacement and Vibratory Ground Motion at Yucca Mountain, Nevada.* Milestone SP32IM3, September 23, 1998. Three volumes. Las Vegas, Nevada: CRWMS M&O. ACC: MOL.19981207.0393.

156499 CRWMS M&O 1998. *Seismic Design Basis Inputs for a High-Level Waste Repository at Yucca Mountain, Nevada.* B00000000-01727-5700-00018 REV 0. Las Vegas, Nevada: CRWMS M&O. ACC: MOL.19990319.0318.

109209 CRWMS M&O 1999. Preliminary Geotechnical Investigation for Waste Handling Building, Yucca Mountain Site Characterization Project. BCB000000-01717-5705-00016 REV 00. Las Vegas, Nevada: CRWMS M&O. ACC: MOL.19990625.0182.

152286 CRWMS M&O 2000. *Fracture Geometry Analysis for the Stratigraphic Units of the Repository Host Horizon*. ANL-EBS-GE-000006 REV 00. Las Vegas, Nevada: CRWMS M&O. ACC: MOL.20000918.0286.

151288 CRWMS M&O 2000. *Preliminary Dynamic Soil-Structure-Interaction Analysis for the Waste Handling Building.* ANL-WHS-ST-000001 REV 00. Las Vegas, Nevada: CRWMS M&O. ACC: MOL.20000504.0313.

183318 Darendeli, M.B. 2001. *Development of a New Family of Normalized Modulus Reduction and Material Damping Curves.* PhD Dissertation. Austin, Texas: University of Texas at Austin. TIC: 259797.

184399 Darragh, R.B.; Green, R.K.; and Turcotte, F.T. 1989. Spectral Characteristics of Small Magnitude Earthquakes With Application to Western and Eastern North American Tectonic Environments: Surface Motions and Depth Effects. Miscellaneous Paper GL-89-16. 89. Washington, DC: U.S. Army Corps of Engineers. TIC: LLR.20080115.0176.

181572 DOE (U.S. Department of Energy) 2007. *Preclosure Seismic Design and Performance Demonstration Methodology for a Geologic Repository at Yucca Mountain Topical Report*. YMP/TR-003-NP, Rev. 5. Las Vegas, Nevada: U.S. Department of Energy, Office of Repository Development. ACC: DOC.20070625.0013.

164249 Eaton, J.P. 1990. "The Earthquake and its Aftershocks from May 2 through September 30, 1983." *The Coalinga, California, Earthquake of May 2, 1983.* Rymer, M.J. and Ellswork, W.L., eds. U.S. Geological Survey Professional Paper 1487. Pages 113-170. Washington, D.C.: U.S. Government Printing Office. TIC: 254830.

107489 EPRI (Electric Power Research Institute) 1988. *Soil Response to Earthquake Ground Motion.* EPRI NP-5747. Palo Alto, California: Electric Power Research Institute. TIC: 254577.

103319 EPRI (Electric Power Research Institute) 1993. *Method and Guidelines for Estimating Earthquake Ground Motion.* Volume 1 of *Guidelines for Determining Design Basis Ground Motion.* EPRI TR-102293. Palo Alto, California: Electric Power Research Institute. TIC: 226495.

103320 EPRI (Electric Power Research Institute) 1993. *Appendices for Ground Motion Estimation.* Volume 2 of *Guidelines for Determining Design Basis Ground Motion.* EPRI TR-102293. Palo Alto, California: Electric Power Research Institute. TIC: 226495.

182324 Foust, L.D. 1995. "Borehole Geophysical Data Technical Assessment (TA)." Letter from L.D. Foust (CRWMS M&O) to S.J. Brocoum (DOE/YMSCO), August 3, 1995, LV:SL:SJB.08/95-068, with enclosures. ACC: MOL.19960320.0013, MOL.19960320.0014, MOL.19960320.0015.

164251 Graves, R.W. [n.d.]. *Simulating the 3D Basin Response in the Portland and Puget Sound Regions from Large Subduction Zone Earthquakes.* Award No. 1434-93-G-02327. [Menlo Park, California]: U.S. Geological Survey. ACC: LLR.20080207.0010.

182045 Hanks, T.C. 1979. "*b* Values and $\omega^{-\gamma}$ Seismic Source Models: Implications for Tectonic Stress Variations Along Active Crustal Fault Zones and the Estimation of High-Frequency Strong Ground Motion." *Journal of Geophysical Research*, 84, (B5), 2235-2242. Washington, D.C.: American Geophysical Union. ACC: LLR.20080122.0002.

182046 Hanks, T.C. 1982. "*f* max." *Bulletin of the Seismological Society of America*, 72, (6), 1867-1879. El Cerrito, California: Seismological Society of America. TIC: 259606.

106061 Hanks, T.C. and Kanamori, H. 1979. "A Moment Magnitude Scale." *Journal of Geophysical Research, 84,* (B5), 2348-2350. Washington, D.C.: American Geophysical Union. TIC: 212607.

163510 Hanks, T.C. and McGuire, R.K. 1981. "The Character of High-Frequency Strong Ground Motion." *Bulletin of the Seismological Society of America*, 71, (6), 2071-2095. El Cerrito, California: Seismological Society of America. TIC: 254646.

105106 Harmsen, S.C. 1993. Seismicity and Focal Mechanisms fo r the Southern Great Basin of Nevada and California in 1991. Open-File Report 92-340. Denver, Colorado: U.S. Geological Survey. ACC: NNA.19920629.0129.

164078 Hartzell, S.H. 1989. "Comparison of Seismic Waveform Inversion Results for the Rupture History of a Finite Fault: Application to the 1986 North Palm Springs, California Earthquake." *Journal of Geophysical Research, 94,* (B6), 7515-7534. Washington, D.C.: American Geophysical Union. ACC: LLR.20080122.0001.

163916 Hartzell, S.H. and Heaton, T.H. 1986. "Rupture History of the 1984 Morgan Hill, California, Earthquake from the Inversion of Strong Motion Records." *Bulletin of the Seismological Society of America, 76,* (3), 649-674. [El Cerrito, California]: Seismological Society of America. TIC: 254648.

184462 Hartzell, S. and Mendoza, C. 1991. "Application of an Iterative Least-Squares Waveform Inversion of Strong-Motion and Teleseismic Records to the 1978 Tabas, Iran, Earthquake." *Bulletin of the Seismological Society of America, 81,* (2), 305-331. El Cerrito, California: Seismological Society of America. TIC: 259994.

184135 Hartzell, S., Langer, C., and Mendoza, C. 1994. "Rupture Histories of Eastern North American Earthquakes." *Bulletin of the Seismological Society of America, 84,* (6), 1703-1724. El Cerrito, California: Seismological Society of America. TIC: 259924.

163513 Haskell, N.A. 1960. "Crustal Reflections of Plane SH Waves." *Journal of Geophysical Research*, 65, (12), 4147-4150. [Washington, D.C.]: American Geophysical Union. TIC: 222421.

164686 Hough, S.E. and Anderson, J.G. 1988. "High-Frequency Spectra Observed at Anza, California: Implications for Q Structure." *Bulletin of the Seismological Society of America*, 78, (2), 692-707. [El Cerrito, California]: Seismological Society of America. TIC: 243238.

184355 Huyse, L.; Gonzalez, S.H.; and Stamatakos, J.A. 2007. "Exploratory Modeling of Extreme Peak Ground Accelerations." *Seismological Research Letters, 78,* (2), 264. El Cerrito, California: Seismological Society of America. TIC: 259929.

183577 Idriss, I.M. 1985. "Evaluating Seismic Risk in Engineering Practice." *Proceedings of the Eleventh International Conference on Soil Mechanics and Foundation Engineering.* Publications Committee of XI ICSMFE. *6,* 255-320. Accord, MA: A.A. Balkema. TIC: 259793.

105524 Idriss, I.M. 1993. *Procedures for Selecting Earthquake Ground Motions at Rock Sites (Revised)*. NIST GCR 93-625. Gaithersburg, Maryland: U.S. Department of Commerce, National Institute of Standards and Technology. TIC: 241629.

163520 Idriss, I.M. and Seed, H.B. 1968. "Seismic Response of Horizontal Soil Layers." *Journal of the Soil Mechanics and Foundations Division,* 94, (SM4), 1003-1031. [Ann Arbor, Michigan]: American Society of Civil Engineers, Soil Mechanics and Foundations Division. TIC: 254670.

110379 Iwan, W.D. 1967. "On a Class of Models for the Yielding Behavior of Continuous and Composite Systems." *Journal of Applied Mechanics,* 612-617. New York, New York: American Society of Mechanical Engineers. TIC: 241280.

110447 Johnson, L.R. and Silva, W. 1981. "The Effects of Unconsolidated Sediments Upon the Ground Motion During Local Earthquakes." *Bulletin of the Seismological Society of America, 71,* (1), 127-142. El Cerrito, California: Seismological Society of America. TIC: 238080.

164134 Joyner, W.B. 2000. "Strong Motion from Surface Waves in Deep Sedimentary Basins." *Bulletin of the Seismological Society of America,* 90, (6B), S95-S112. El Cerrito, California: Seismological Society of America. TIC: 254629.

106268 Joyner, W.B. and Boore, D.M. 1988. "Measurement, Characterization, and Prediction of Strong Ground Motion." *Earthquake Engineering and Soil Dynamics II—Recent Advances in Ground-Motion Evaluation, June 27-30, 1988, Park City, Utah.* Von Thun, J.L., ed. Geotechnical Special Publication No. 20. Pages 43-102. New York, New York: American Society of Civil Engineers. TIC: 241219.

103337 Kramer, S.L. 1996. *Geotechnical Earthquake Engineering.* Prentice-Hall International Series in Civil Engineering and Engineering Mechanics. Hall, W.J., ed. Upper Saddle River, New Jersey: Prentice-Hall. TIC: 243891.

182431 Lee, R.; Silva, W.; and Cornell, A. 1998. "Alternatives in Evaluating Soil- and Rock-Site Seismic Hazard." *Seismological Research Letters, 69,* (1), 81. El Cerrito, California: Seismological Society of America. TIC: 259667.

182432 Lee, R.C.; Maryak, M.E.; and Kimball, J. 1999. "A Methodology to Estimate Site-Specific Seismic Hazard for Critical Facilities on Soil or Soft-Rock Sites." *Seismological Research Letters, 70,* (2), 230. El Cerrito, California: Seismological Society of America. TIC: 259666.

182739 Lin, Y-C. 2007. *Characterizing V_S Profiles by the SASW Method and Comparison with Other Seismic Methods.* Ph.D. dissertation. Austin, Texas: University of Texas at Austin. TIC: 259723.

163922 Liu, H-L. and Helmberger, D.V. 1983. "The Near-Source Ground Motion of the 6 August 1979 Coyote Lake, California, Earthquake." *Bulletin of the Seismological Society of America, 73,* (1), 201-218. [El Cerrito, California]: Seismological Society of America. TIC: 254637.

170902 Lockner, D.A. and Okubo, P.G. 1983. "Measurements of Frictional Heating in Granite." *Journal of Geophysical Research, 88,* (B5), 4313-4320. Washington, D.C.: American Geophysical Union. TIC: 256349.

106330 Majer, E.L.; Feighner, M.; Johnson, L.; Daley, T.; Williams, K.; Karageorgi, E.; and McEvilly, T. 1996. Level 4 Milestone Letter Report on Surface Geophysics Synthesis: Data Processing. Berkeley, California: Lawrence Berkeley National Laboratory. ACC: MOL.19971224.0006.

104685 Majer, E.L.; Feighner, M.; Johnson, L.; Daley, T.; Karageorgi, E.; Lee, K.H.; Williams, K.; and McEvilly, T. 1996. *Surface Geophysics.* Volume I of *Synthesis of Borehole and Surface Geophysical Studies at Yucca Mountain, Nevada and Vicinity.* Milestone OB05M. Berkeley, California: Lawrence Berkeley National Laboratory. ACC: MOL.19970610.0150.

170693 McGarr, A. and Fletcher, J.B. 2003. "Maximum Slip in Earthquake Fault Zones, Apparent Stress, and Stick-Slip Friction." *Bulletin of the Seismological Society of America, 93,* (6), 2355-2362. [El Cerrito, California]: Seismological Society of America. TIC: 256287.

107483 McGuire, R.K. 1995. "Probabilistic Seismic Hazard Analysis and Design Earthquakes: Closing the Loop.≅ *Bulletin of the Seismological Society of America,* 85, (5), 1275-1284. El Cerrito, California: Seismological Society of America. TIC: 232947.

166349 McGuire, R.K.; Becker, A.M.; and Donovan, N.C. 1984. "Spectral Estimates of Seismic Shear Waves." *Bulletin of the Seismological Society of America, 74,* (4), 1427-1440. Berkeley, California: Seismological Society of America. TIC: 259925.

157510 McGuire, R.K.; Silva, W.J.; and Costantino, C.J. 2001. Technical Basis for Revision of Regulatory Guidance on Design Ground Motions: Hazard- and Risk-Consistent

Ground Motion Spectra Guidelines. NUREG/CR-6728. Washington, D.C: U.S. Nuclear Regulatory Commission. TIC: 251294.

163799 McGuire, R.K.; Silva, W.J.; and Costantino, C.J. 2002. Technical Basis for Revision of Regulatory Guidance on Design Ground Motions: Development of Hazard- and Risk-Consistent Seismic Spectra for Two Sites. NUREG/CR-6769. Washington, D.C.: U.S. Nuclear Regulatory Commission. TIC: 254478.

164681 Menq, F-Y. 2003. *Dynamic Properties of Sandy and Gravelly Soils.* PhD dissertation. Austin, Texas: University of Texas at Austin. TIC: 254831.

106384 Mooney, W.D. and Schapper, S.G. 1995. "Seismic Refraction Investigations." Chapter 5 of Major Results of Geophysical Investigations at Yucca Mountain and Vicinity, Southern Nevada. Oliver, H.W.; Ponce, D.A.; and Hunter, W.C., eds. Open-File Report 95-74. Menlo Park, California: U.S. Geological Survey. ACC: MOL.19980305.0122.

101272 Nelson, P.H.; Muller, D.C.; Schimschal, U.; and Kibler, J.E. 1991. *Geophysical Logs and Core Measurements from Forty Boreholes at Yucca Mountain, Nevada.* Geophysical Investigations Map GP-1001. Denver, Colorado: U.S. Geological Survey. ACC: NNA.19920211.0022.

163274 NRC (U.S. Nuclear Regulatory Commission) 2003. *Yucca Mountain Review Plan, Final Report.* NUREG-1804, Rev. 2. Washington, D.C.: U.S. Nuclear Regulatory Commission, Office of Nuclear Material Safety and Safeguards. TIC: 254568.

180931 NRC (U.S. Nuclear Regulatory Commission) 2007. "Seismic Design Parameters." Section 3.7.1 of Standard Review Plan. NUREG-0800, Rev. 3. Washington, D.C.: U.S. Nuclear Regulatory Commission. ACC: MOL.20070521.0104.

180932 NRC (U.S. Nuclear Regulatory Commission) 2007. "Seismic System Analysis." Section 3.7.2 of Standard Review Plan. NUREG-0800, Rev. 3. Washington, D.C.: U.S. Nuclear Regulatory Commission. ACC: MOL.20070521.0105.

101280 Ortiz, T.S.; Williams, R.L.; Nimick, F.B.; Whittet, B.C.; and South, D.L. 1985. *A Three-Dimensional Model of Reference Thermal/Mechanical and Hydrological Stratigraphy at Yucca Mountain, Southern Nevada.* SAND84-1076. Albuquerque, New Mexico: Sandia National Laboratories. ACC: MOL.19980602.0331.

170648 Ou, G. and Herrmann R.B. 1990. "A Statistical Model for Ground Motion Produced by Earthquakes at Local and Regional Distances." *Bulletin of the Seismological Society of America,* 80*,* (6, Part A), p. 1397-1417. El Cerrito, California: Seismological Society of America. TIC: 256274.

182047 Papageorgiou, A.S. and Aki, K. 1983. "A Specific Barrier Model for the Quantitative Description of Inhomogeneous Faulting and the Prediction of Strong Ground Motion. Part II. Applications of the Model." *Bulletin of the Seismological Society of America*, 73, (4), 953-978. El Cerrito, California: Seismological Society of America. TIC: 237411.

119139 Regulatory Guide 1.165. 1997. *Identification and Characterization of Seismic Sources and Determination of Safe Shutdown Earthquake Ground Motion*. Washington, DC: U.S. Nuclear Regulatory Commission. Readily available.

170694 Reiter, L. 2004. "When Are Ground Motion Estimates Too High?" *Seismological Research Letters, 75,* (2), 282. [El Cerrito, California]: Seismological Society of America. TIC: 256283.

106702 Rogers, A.M.; Harmsen, S.C.; Corbett, E.J.; Priestly, K.; and dePolo, D. 1991. "The Seismicity of Nevada and Some Adjacent Parts of the Great Basin." Chapter 10 of The Geology of North America Decade Map. Volume 1. Boulder, Colorado: Geological Society of America. TIC: 243190.

165570 Rollins, K.M.; Evans, M.D.; Diehl, N.B.; and Daily, W.D., III 1998. "Shear Modulus and Damping Relationships for Gravels." *Journal of Geotechnical and Geoenvironmental Engineering, 124,* (5), 396-405. [Reston, Virginia: American Society of Civil Engineers]. TIC: 243461.

182048 Rovelli, A.; Bonamassa, O.; Cocco, M.; Di Bona, M.; and Mazza, S. 1988. "Scaling Laws and Spectral Parameters of the Ground Motion in Active Extensional Areas in Italy." *Bulletin of the Seismological Society of America*, 78, (2), 530-560. El Cerrito, California: Seismological Society of America. TIC: 259594.

100075 Sawyer, D.A.; Fleck, R.J.; Lanphere, M.A.; Warren, R.G.; Broxton, D.E.; and Hudson, M.R. 1994. "Episodic Caldera Volcanism in the Miocene Southwestern Nevada Volcanic Field: Revised Stratigraphic Framework, {superscript 40}Ar/{superscript 39}Ar Geochronology, and Implications for Magmatism and Extension." *Geological Society of America Bulletin, 106,* (10), 1304-1318. Boulder, Colorado: Geological Society of America. TIC: 222523.

103323 Schnabel, P.B.; Lysmer, J.; and Seed; H.B. 1972. *SHAKE: A Computer Program for Earthquake Response.* EERC 72-12. Berkeley, California: Earthquake Engineering Research Center, University of California at Berkeley. TIC: 241102.

103270 Schneider, J.F.; Abrahamson, N.A.; and Hanks, T.C. 1996. Ground Motion Modeling of Scenario Earthquakes at Yucca Mountain, Final Report for Activity 8.3.1.17.3.3. Volume 1. Denver, Colorado: U.S. Geological Survey. ACC: MOL.19980617.0477.

110467 Schneider, J.F.; Silva, W.J.; and Stark, C.L. 1993. "Ground Motion Model for the 1989 M 6.9 Loma Prieta Earthquake Including Effects of Source, Path and Site." *Earthquake Spectra*, 9, (2), 251-287. Oakland, California: Earthquake Engineering Research Institute. TIC: 241769.

163655 Seed, H.B. and Idriss, I.M. 1969. "The Influence of Soil Conditions on Ground Motions During Earthquakes." *Journal of the Soil Mechanics Foundation Engineering Division,* 95, (SM1), 99-137. [New York, New York]: American Society of Civil Engineers. TIC: 254823.

103324 Seed, H.B. and Idriss, I.M. 1970. Soil Moduli and Damping Factors for Dynamic Response Analyses. EERC 70-10. Berkeley, California: University of California, Earthquake Engineering Research Center. TIC: 241070.

163924 Seed, H.B.; Romo, M.P.; Sun, J.I.; Jaime, A.; and Lysmer, J. 1988. "The Mexico Earthquake of September 19, 1985—Relationships Between Soil Conditions and Earthquake Ground Motions." *Earthquake Spectra*, *4*, (4), 687-729. [Oakland, California: Earthquake Engineering Research Institute]. TIC: 254675.

183433 Seed, H.B.; Ugas, C.; and Lysmer, J. 1976. "Site-Dependent Spectra for Earthquake-Resistant Design." *Bulletin of the Seismological Society of America, 66,* (1), 221-243. El Cerrito, California: Seismological Society of America. TIC: 259779.

163656 Silva, W. 1991. "Site Geometry and Global Characteristics." Chapter 6 of Proceedings: NSF/EPRI Workshop on Dynamic Soil Properties and Site Characterization, Palo Alto, California, November 9-10, 1989. EPRI NP-7337, Volume 1. Palo Alto, California: Electric Power Research Institute. TIC: 254752.

170696 Silva, W. 1993. "Factors Controlling Strong Ground Motion and Their Associated Uncertainties." Dynamic Analysis and Design Considerations for High-Level Nuclear Waste Repositories, Proceedings of the Symposium Sponsored by the Nuclear Dynamic Analysis Committee of the Structural Division of the American Society of Civil Engineers and Co-sponsored by the U.S. Department of Energy, Office of Civilian Radioactive Waste Management, San Francisco, California, August 19-20, 1992. Hossain, Q.A., ed. Pages 132-161. New York, New York: American Society of Civil Engineers. TIC: 206451.

163747 Silva, W. 1997. "Characteristics of Vertical Strong Ground Motions for Applications to Engineering Design." Proceedings of the FHWA/NCEER Workshop on the National Representation of Seismic Ground Motion for New and Existing Highway Facilities held at the Park Plaza Hotel, Burlingame, California, May 29-30, 1997. Friedland, I.M.; Power, M.S.; and Mayes, R.L., eds. Technical Report NCEER-97-0010. Pages 205-219. Buffalo, New York: National Center for Earthquake Engineering Research. TIC: 254525.

110474 Silva, W.J.; Abrahamson, N.; Toro, G.; and Costantino, C. 1996. *Description and Validation of the Stochastic Ground Motion Model*. PE&A 94PJ20. El Cerrito, California: Pacific Engineering and Analysis. TIC: 245288.

164081 Silva, W.J.; Costantino, C.; and Iwasaki, Y. 1999. *Assessment of Liquefaction Potential for the 1995 Kobe, Japan Earthquake Including Finite-Source Effects*. Final Report. [Vicksburg, Mississippi]: U.S. Army Corp of Engineers Waterways Experiment Station, Corp of Engineers. ACC: MOL.20030925.0173.

105398 Silva, W.J. and Darragh, R. 1995. *Engineering Characterization of Earthquake Strong Ground Motion Recorded at Rock Sites.* EPRI TR-102262. Palo Alto, California: Electric Power Research Institute. TIC: 245610.

182433 Silva, W.J. and Green, R.K. 1989. "Magnitude and Distance Scaling of Response Spectral Shapes for Rock Sites with Applications to North American Tectonic Environment." *Earthquake Spectra, 5,* (3), 591-624. Oakland, California: Earthquake Engineering Research Institute. TIC: 259668.

103325 Silva, W.J. and Lee, K. 1987. State-of-the-Art for Assessing Earthquake Hazards in the United States. Report 24, WES RASCAL Code for Synthesizing Earthquake Ground Motions. Miscellaneous Paper S-73-1. Washington, D.C.: U.S. Department of the Army. TIC: 241388.

184394 Singh, S.K. and Ordaz, M., 1994, "Seismic Energy Release in Mexican Subduction Zone Earthquakes." *Bulletin of the Seismologic Society of America,* 84, (5), 1006-1018. El Cerrito, California: Seismological Society of America. TIC 259934.

170607 Smith, R.B. and Bruhn, R.L. 1984. "Intraplate Extensional Tectonics of the Eastern Basin-Range: Inferences on Structural Style from Seismic Reflection Data, Regional Tectonics, and Thermal-Mechanical Models of Brittle-Ductile Deformation." *Journal of Geophysical Research, 89*, (B7), 5733-5762. [Washington, D.C.]: American Geophysical Union. TIC: 223264.

183779 SNL (Sandia National Laboratories) 2008. *Technical Report: Geotechnical Data for a Geologic Repository at Yucca Mountain, Nevada.* TDR-MGR-GE-000010 REV 00. Las Vegas, Nevada: Sandia National Laboratories. ACC: DOC.20080206.0001.

178851 SNL (Sandia National Laboratories) 2007. *Mechanical Assessment of Degraded Waste Packages and Drip Shields Subject to Vibratory Ground Motion.* MDL-WIS-AC-000001 REV 00. Las Vegas, Nevada: Sandia National Laboratories. ACC: DOC.20070917.0006.

176828 SNL (Sandia National Laboratories) 2007. *Seismic Consequence Abstraction.* MDL-WIS-PA-000003 REV 03. Las Vegas, Nevada: Sandia National Laboratories. ACC: DOC.20070928.0011.

158656 Stepp, J.C.; Wong, I.; Whitney, J.; Quittmeyer, R.; Abrahamson, N.; Toro, G.; Youngs, R.; Coppersmith, K.; Savy, J.; and Sullivan, T. 2001. "Probabilistic Seismic Hazard Analyses for Ground Motions and Fault Displacement at Yucca Mountain, Nevada." *Earthquake Spectra, 17*, (1), 113-151. [Oakland, California: Earthquake Engineering Research Institute]. TIC: 250931.

183272 Stokoe, K. 2007. Spectral Analysis of Surface Waves (SASW) Measurements at Yucca Mountain [final submittal]. Scientific Notebook SN-M&O-SCI-047-V1. Pages 1-287. ACC: LLR.20070823.0029.

107635 Stokoe, K.; Darendeli, M.B.; and Moulin, B.S. 1998. *Laboratory Evaluation of the Dynamic Properties of Intact Tuff Specimens from the Yucca Mountain Site*. Geotechnical Engineering Report GR98-1. Austin, Texas: University of Texas at Austin. ACC: MOL.19990827.0153.

164689 Stokoe, K.H., II and Valle, C. 2003. *Dynamic Laboratory Tests: Naturally Cemented Sand from Capitol Aggregates Site, Austin, Texas.* Summary Report: GR-03-5. Austin, Texas: University of Texas at Austin, College of Engineering. TIC: 254998.

100087 Su, F.; Anderson, J.G.; Brune, J.N.; and Zeng, Y. 1996. "A Comparison of Direct S-Wave and Coda-Wave Site Amplification Determined from Aftershocks of the Little Skull Mountain Earthquake." *Bulletin of the Seismological Society of America*, 86, (4), 1006-1018. El Cerrito, California: Seismological Society of America. TIC: 236585.

183438 Toro, G.R.; Abrahamson, N.A.; and Schneider, J.F. 1997. "Model of Strong Ground Motions from Earthquakes in Central and Eastern North America: Best Estimates and Uncertainties." *Seismological Research Letters, 68,* (1), 41-57. El Cerrito, California: Seismological Society of America. TIC: 240552.

183435 Toro, G.R. and McGuire R.K. 1987. "An Investigation into Earthquake Ground Motion Characteristics in Eastern North America." *Bulletin of the Seismological Society of America, 77,* (2), 468-489. El Cerrito, California: Seismological Society of America. TIC: 259781.

163890 Van Hoff, D.J. 1993. *Evaluation of the Dynamic Properties of Artificially Cemented Sand at Low Confining Pressures.* Master's thesis. Austin, Texas: University of Texas at Austin. TIC: 254684.

164085 Wald, D.J. and Heaton, T.H. 1994. "Spatial and Temporal Distribution of Slip for the 1992 Landers, California, Earthquake." *Bulletin of the Seismological Society of America,* 84, (3), 668-691. [El Cerrito, California: Seismological Society of America]. TIC: 254815.

184356 Wald, D.J.; Helmberger, D.V.; and Hartzell, S.H. 1990. "Rupture Process of the 1987 Superstition Hills Earthquake From the Inversion of Strong-Motion Data." *Bulletin of the Seismological Society of America, 80,* (5), 1079-1098. El Cerrito, California: Seismological Society of America. TIC: 259930.

164086 Wald, D.J.; Helmberger, D.V.; and Heaton, T.H. 1991. "Rupture Model of the 1989 Loma Prieta Earthquake from the Inversion of Strong-Motion and Broadband Teleseismic Data." *Bulletin of the Seismological Society of America, 81,* (5), 1540-1572. [El Cerrito, California: Seismological Society of America]. TIC: 254817.

170544 Wong, I.; Olig, S.; Dober, M.; Silva, W.; Wright, D.; Thomas, P.; Gregor, N.; Sanford, A.; Lin, K-W.; and Love, D. 2004. "Earthquake Scenario and Probabilistic Ground-Shaking Hazard Maps for the Albuquerque–Belen–Santa Fe, New Mexico, Corridor." *New Mexico Geology, 26*, (1), 3-33. Socorro, New Mexico: New Mexico Bureau of Geology and Mineral Resources. TIC: 256271.

100522 YMP (Yucca Mountain Site Characterization Project). 1997. *Methodology to Assess Fault Displacement and Vibratory Ground Motion Hazards at Yucca Mountain.*

Topical Report YMP/TR-002-NP, Rev. 1. Las Vegas, Nevada: Yucca Mountain Site Characterization Office. ACC: MOL.19971016.0777.

9.2 STATUTES AND REGULATIONS

180319 10 CFR 63. 2007. Energy: Disposal of High-Level Radioactive Wastes in a Geologic Repository at Yucca Mountain, Nevada. Internet Accessible.

173805 ASCE/SEI 43-05. 2005. *Seismic Design Criteria for Structures, Systems, and Components in Nuclear Facilities*. Reston, Virginia: American Society of Civil Engineers. TIC: 257275.

9.3 DATA

158242 GS0204831142 33.004. Geotechnical Field and Laboratory Test Results from Waste Handling Building Foundation Investigation. Submittal date: 04/15/2002.

159542 GS020783114233.005. Gradation Analysis Test Results and Graphical Plots from Tests Performed on Materials Excavated from In-Situ Density Test Locations in Test Pits from the Waste Handling Building Foundation Investigations. Submittal date: 07/23/2002.

164561 GS030783114233.001. Geotechnical Borehole Logs for the Waste Handling Building, Yucca Mountain Project, Nevada Test Site, Nevada, Version 7/16/03. Submittal date: 07/23/2003.

183649 GS070983114233.006. Alluvium Thickness Contour Map of Midway Valley, NV; 07/23/2007 - 08/10/2007. Submittal date: 09/13/2007.

113584 GS960708312132.002. Porosity, Water Content, Mineralogy and Other Data Derived from Geophysical Logs and Cores for 26 Boreholes. Submittal date: 07/09/1996.

150287 GS990908314213.001. Geophysical Logs and Core Measurements from Forty Boreholes, Including Corrected Magnetic Susceptibility for UE-25 A #1. Submittal date: 09/10/1999.

164559 LB0306VSP95DAT .001. Processed VSP and Velocity Survey Data: UZ#16, NRG-6, WT-2, RF-4, RF-7A,SD-12, G-2, G-4. Submittal date: 06/25/2003.

152554 MO0004QGFMPICK.000. Lithostratigraphic Contacts from MO9811MWDGFM03.000 to be Qualified Under the Data Qualification Plan, TDP-NBS-GS-000001. Submittal date: 04/04/2000.

153777 MO0012MWDGFM02.002. Geologic Framework Model (GFM2000). Submittal date: 12/18/2000.

157295 MO0110DVDBOREH.000. Downhole Velocity Data from Boreholes RF-13 and RF-17. Submittal date: 10/17/2001.

158076 MO0110SASWVDYM.000. SASW Velocity Data fr om the Top of Yucca Mountain. Submittal date: 10/02/2001.

157969 MO0110SASWWHBS.000. SASW Velocity Data from the Waste Handling Building Site Characterization Area. Submittal date: 10/02/2001.

157296 MO0111DVDWHBSC.001. Downhole Velocity Data at the Waste Handling Building Site Characterization Area. Submittal date: 11/08/2001.

157298 MO0112GPLOGWHB.001. Developed Geophysical Log Data from Forensic Evaluation of Geophysical Log Data Collected in Support of the Waste Handling Building. Submittal date: 12/03/2001.

158078 MO0202DVDWHBSC.002. Downhole Velocity Data from the Top of Yucca Mountain. Submittal date: 02/11/2002.

158082 MO0203DHRSSWHB.001. Dynamic Laboratory Test Data for Rock and Soil Samples from the Waste Handling Building Site Characterization Area. Submittal date: 03/19/2002.

158084 MO0203SEPSASWD.000. SASW Velocity Data from the Top of Yucca Mountain. Submittal date: 03/28/2002.

158086 MO0204SEISDWHB.001. Suspension Seismic Data for Borehole UE-25 RF#13 at the Waste Handling Building Site Characterization Area. Submittal date: 04/08/2002.

158088 MO0204SEPBSWHB.001. Borehole Suspension Data for Waste Handling Building Site Characterization Area. Submittal date: 04/10/2002.

158125 MO0204SEPGAMDM.000. Statistical Analysis of Gamma-Gamma Density Measurements by Lithostratigraphic Unit. Submittal date: 04/22/2002.

159081 MO0206SASWROCK.000. SASW Velocity Data from Rock Sites on the Crest of Yucca Mountain and in the ESF. Submittal date: 06/19/2002.

163723 MO0206UNHAZ106.001. Uniform Hazard, Reference Event and Deaggregation Event Spectra at 10^{-6} Annual Exceedance Frequency Based on the Probabilistic Seismic Hazard Analyses for Yucca Mountain. Submittal date: 06/03/2002.

163722 MO0208UNHZ5X10.000. Uniform Hazard, Reference Event and Deaggregation Event Spectra at $5x10^{-4}$ Annual Exceedance Frequency Based on the Results of the Probabilistic Seismic Hazard Analyses for Yucca Mountain. Submittal date: 08/06/2002.

163801 MO0208VCPRBWHB.000. Velocity Correlation Parameters for the Yucca Mountain Repository Block and Waste Handling Building Site. Submittal date: 08/20/2002.

163724 MO0209UNHAZ107.000. Uniform Hazard, Reference Event and Deaggregation Event Spectra at 10^{-7} Annual Exceedance Frequency Based on the Results of the Probabilistic Seismic Hazard Analyses for Yucca Mountain. Submittal date: 09/25/2002.

162713 MO0210PGVPB107.000. Design Peak Ground Velocity for the Repository Level (Point B) at 10-7 Annual Exceedance Probability. Submittal date: 10/17/2002.

170423 MO0211DERES 104.000. Reference Event and Deaggregation Event Spectra at 10^{-4} Annual Exceedance Frequency Based on the Results of the Probabilistic Seismic Hazard Analyses for Yucca Mountain. Submittal date: 11/04/2002.

170424 MO0211REDES103.000. Ref erence Event and Deaggregation Event Spectra at 10^{-3} Annual Exceedance Frequency Based on the Results of the Probabilistic Seismic Hazard Analyses for Yucca Mountain. Submittal date: 11/04/2002.

162712 MO0303DPGVB106.002. Design Peak Ground Velocity for the Repository Level (Point B) at 10-6 Annual Exceedance Probability. Submittal date: 03/10/2003.

163721 MO03061E9PSHA1.000. Spectral Acceleration and Velocity Hazard Curves Extended to 1E-9 Based on the Results of the PSHA for Yucca Mountain. Submittal date: 06/09/2003.

165791 MO0306MW DDDMIO.001. Drift Degradation Model Inputs and Outputs. Submittal date: 06/19/2003.

170425 MO0308UNHAZ105.000. Uniform Hazard, Reference Event and Deaggregation Event Spectra at 10^{-5} Annual Exceedance Frequency Based on the Results of the Probabilistic Seismic Hazard Analyses for Yucca Mountain. Submittal date: 08/06/2003.

169099 MO0401SEPPGVRL.022. Peak Ground Velocity for the Repository Level (Point B) at 10-5 Annual Exceedance Frequency. Submittal date: 01/26/2004.

170434 MO0403SDIAWHBC.003. Normalized Shear Modulus and Material Damping Versus Shearing Strain Curves for Rock and Alluvium for Seismic Design Input Analyses. Submittal date: 03/26/2004.

171483 MO0408MW DDDMIO.002. Drift Degradation Model Inputs and Outputs. Submittal date: 08/31/2004.

172216 MO0409MWDGMMIO.000. Ground Motion Model Input and Output Files. Submittal date: 09/30/2004.

172236 MO0410SDSDE103.002. Seismic Design Spectra and Ti me Histories for the Surface Facilities Area (Point D/E) at 10-3 Annual Exceedance Frequency. Submittal date: 10/12/2004.

172237 MO0410SDSTMHIS.005. Seismic Design Spectra and Time Histories for the Surface Facilities Area (Point D/E) at 5E-4 Annual Exceedance Frequency. Submittal date: 10/13/2004.

172238 MO0410WHBDF104.002. Seismic Design Spectra and Time Histories for the Surface Facilities Area (Point D/E) at 10-4 Annual Exceedance Frequency. Submittal date: 10/13/2004.

172682 MO0501BPVELEMP.001. Bounded Horizontal Peak Gr ound Velocity Hazard at the Repository Waste Emplacement Level. Submittal date: 01/11/2005.

182125 MO0609SASWSTDC.003. Surface Spectral Analysis of Surface Waves (SASW) Theoretical Dispersion Curves and Vs Profiles for FY04 and FY05 for YMP. Submittal date: 09/19/2006.

183295 MO0609SASWUTDC.004. Underground Spectral Analysis of Surface Waves (SASW) Theoretical Dispersion Curves and VS Profiles for FY05 for YMP. Submittal date: 09/19/2006.

182483 MO0701ABSRFLL2.000. SASW Investigations for Repository Facilities, As-Built SASW RF Line Locations-2. Submittal date: 01/11/2007.

181423 MO0706DSDR1E3A.000. Seismic Design Spectra for the Surface Facilities Area at 1E-3 APE for Multiple Dampings. Submittal date: 11/01/2006.

181421 MO0706DSDR1E4A.001. Seismic Design Spectra for the Surface Facilities Area at 1E-4 APE for Multiple Dampings. Submittal date: 11/01/2006.

181422 MO0706DSDR5E4A.001. Seismic Design Spectra for the Surface Facilities Area at 5E-4 APE for Multiple Dampings. Submittal date: 11/01/2006.

182460 MO0706TH1E3APE.000. Time Histories for the Surface Facilities Area at 1E-3 APE. Submittal date: 11/01/2006.

181960 MO0706TH1E4APE.001. Time Histories for the Surface Facilities Area at 1E-4 APE. Submittal date: 06/01/2007.

181961 MO0706TH5E4APE.001. Time Histories for the Surface Facilities Area at 5E-4 APE. Submittal date: 05/31/2007.

183128 MO0707DSRB1E3A.000. 5%-Damped Seismic Design Spectra for the Repository Block at 1E-3 APE. Submittal date: 07/23/2007.

183129 MO0707DSRB1E4A.000. 5%-Damped Seismic Design Spectra for the Repository Block at 1E-4 APE. Submittal date: 07/24/2007.

183130 MO0707DSRB5E4A.000. 5%-Damped Seismic Design Spectra for the Repository Block at 5E-4 APE. Submittal date: 07/24/2007.

183196 MO0707THRB1E3A.000. Time Histories for the Repository Block at 1E-3 APE. Submittal date: 07/25/2007.

183200 MO0707THRB1E4A.000. Time Histories for the Repository Block at 1E-4A APE. Submittal date: 07/26/2007.

183197 MO0707THRB5E4A.000. Time Histories for the Repository Block at 5E-4 APE. Submittal date: 07/26/2007.

184464 MO0708BCSSWVGB.001. Base Case Seismic S-Wave and Seismic P-Wave Velocity Profiles at the Surface Facilities Area and Repository Block for use in Ground Motion Modeling. Submittal date: 08/28/2007.

184682 MO0801SCSPS5E4.003. Strain Compatible Soil Properties for the Surface Facilities Area at 5E-4 Annual Probability of Exceedance. Submittal date: 01/14/2008.

184683 MO0801SCSPS1E4.003. Strain Compatible Soil Properties for the Surface Facilities Area at 1E-4 Annual Probability of Exceedance. Submittal date: 01/14/2008.

184685 MO0801SCSPS1E3.003. Strain Compatible Soil Properties for the Surface Facilities Area at 1E-3 Annual Probability of Exceedance. Submittal date: 01/14/2008.

184802 MO0801HCUHSSFA.001. Hazard Curves and Mean Uniform Hazard Spectra for the Surface Facilities Area. Submittal date: 01/11/2008.

184803 MO0801HCUHSREB.001. Hazard Curves and Mean Uniform Hazard Spectra for the Repository Block. Submittal date: 01/14/2008.

184993 MO 0802DYNPRP07.001. Normalized Shear Modulus and Material Damping Versus Shearing Strain for Tuff and Alluvium for Yucca 2007 Seismic Design Input Analyses. Submittal date: 02/05/2008.

182126 MO960408314213.001. Qualified Geophysical Logs from Borehole UE-25A #1. Submittal date: 04/03/1996.

182127 MO960408314213.006. Qualified Geophysical Logs from Borehole UE-25B #1. Submittal date: 04/03/1996.

182128 MO960408314213.007. Qualified Geophysical Logs from Borehole UE-25C #1. Submittal date: 04/03/1996.

182129 MO960408314213.008. Qualified Geophysical Logs from Borehole UE-25C #2. Submittal date: 04/03/1996.

131173 MO960408314213.010. Qualified Geophysical Logs from Borehole UE-25P #1. Submittal date: 04/03/1996.

130536 MO960408314213.023. Qualified Geophysical Logs from Borehole USW G-3. Submittal date: 04/03/1996.

130551 MO960408314213.024. Qualified Geophysical Logs from Borehole USW G-4. Submittal date: 04/03/1996.

103792 MO9905LABDYNRS.000. Laboratory Dynamic Rock/Soil Testing UE-25 RF #13. Submittal date: 05/06/1999.

9.4 SOFTWARE

184876 [Bechtel SAIC Company (BSC)] 2002. *Software Management Report BASE4 Version 4.0*. 10940-SMR-4.0-00. [Las Vegas], [NV]: [Bechtel SAIC Company]. ACC: MOL.20021118.0220.

184877 [Bechtel SAIC Company (BSC)] 2002. *Software Management Report CORBB Version 1.0*. 10941-SMR-1.0-00. [Las Vegas], [NV]: [Bechtel SAIC Company]. ACC: MOL.20030115.0057.

184878 [Bechtel SAIC Company (BSC)] 2002. *Software Management Report DUR Version 1.0*. 10942-SMR-1.0-00. [Las Vegas], [NV]: [Bechtal SAIC Company]. ACC: MOL.20030529.0097.

184882 [Bechtel SAIC Company (BSC)] 2002. *Software Management Report INTEG1 Version 1.0*. 10943-SMR-1.0-00. [Las Vegas], [NV]: [Bechtel SAIC Company]. ACC: MOL.20021118.0277.

184883 [Bechtel SAIC Company (BSC)] 2002. *Software Management Report INTERPOL Version 1.0*. 10944-SMR-1.0-00. [Las Vegas], [NV]: [Bechtel SAIC Company]. ACC: MOL.20030127.0086.

184884 [Bechtel SAIC Company (BSC)] 2002. *Software Management Report MAXMIN Version 1.0*. 10945-SMR-1.0-00. [Las Vegas], [NV]: [Bechtel SAIC Company]. ACC: MOL.20030115.0078.

184889 [Bechtel SAIC Company (BSC)] 2002. *Software Management Report REPLOT Version 1.0*. 10949-SMR-1.0-00. [Las Vegas], [NV]: [Bechtel SAIC Company]. ACC: MOL.20030312.0115.

184891 [Bechtel SAIC Company (BSC)] 2002. *Software Management Report SCALE1 Version 1.0*. 10946-SMR-1.0-00. [Las Vegas], [NV]: [Bechtel SAIC Company]. ACC: MOL.20030203.0334.

184893 [Bechtel SAIC Company (BSC)] 2002. *Software Management Report SPCTLR Version 1.0*. 10947-SMR-1.0-00. [Las Vegas], [NV]: [Bechtel SAIC Company]. ACC: MOL.20030529.0091.

184895 [Bechtel SAIC Company (BSC)] 2002. *Software Management Report XYMULT Version 1.0*. 10919-SMR-1.0-00. [Las Vegas], [NV]: [Bechtel SAIC Company]. ACC: MOL.20021118.0213.

153526 CRWMS M&O 2000. *EARTHVISION V5.1, Validation Test Report Rev 00*. STN: 10174-5.1-00. Las Vegas, Nevada: CRWMS M&O. ACC: MOL.20000927.0145.

184894 DOE (U.S. Department of Energy) 2004. *Software Validation Report for: UDEC Version 3.14 REV. NO.: 00*. 10173-SVR-3.14-00. [Las Vegas], [NV]: U.S. Department of Energy. ACC: MOL.20041105.0013.

184881 DOE (U.S. Department of Energy) 2007. *Software Validation Report for: HAZUHS, Version 1.0 REV. NO.: 00*. 11194-VTR-1.0-00. [Las Vegas], [NV]: U.S. Department of Energy. ACC: MOL.20070731.0247.

184885 DOE (U.S. Department of Energy) 2007. *Software Validation Report for: POST RASCAL, Version 1.0 REV. NO.: 00*. 11231-VTR-1.0-00-DOSEMU. [Las Vegas], [NV]: [Bechtel SAIC Company]. ACC: MOL.20070804.0256.

184886 DOE (U.S. Department of Energy). 2007. *Software Validation Report for: RASCAL SET 1.0 REV. NO.: 00*. 11232-SVR-1.0-00-DOSEMU. [Las Vegas], [NV]: [Bechtel SAIC Company]. ACC: MOL.20070808.0262.

184887 DOE (U.S. Department of Energy) 2007. *Software Validation Report for: RASCAL SET V1.1 REV. NO.: 00*. 11232-SVR-1.1-00-DOS6.22,QEMM9.0. [Las Vegas], [NV]: [Bechtel SAIC Company]. ACC: MOL.20071001.0254.

184888 DOE (U.S. Department of Energy) 2007. *Software Validation Report for: RASCAL SET 1.1 REV. NO.: 00*. 11232-SVR-1.1-01-WIN2003Server. [Las Vegas], [NV]: [Bechtel SAIC Company]. ACC: MOL.20071005.0247.

184892 DOE (U.S. Department of Energy) 2007 . *Software Validation Report for: SIGCOMB, Version 1.1 REV. NO.: 00*. 11233-SVR-1.1-00-DOS 6.22,QEMM9.0. [Las Vegas], [NV]: U.S. Department of Energy. ACC: MOL.10071214.0574.

184890 DOE (U.S. Department of Energy) 2007. *Software Validation Report for: SOILHAZ SET Version 1.0 REV. NO.: 00*. 11234-SVR-1.0-00-DOSEMU. [Las Vegas], [NV]: U.S. Department of Energy. ACC: MOL.20071211.0261.

184880 DOE (U.S. Department of Energy) 2007. *Software Validtion Report for: EXTHC Version 1.0*. 11242-VTR-1.0-00-DOS V6.22. [Las Vegas], {NV]: U.S. Department of Energy. ACC: MOL.20071115.0262.

182936 EXTHC V. 1.0 2007. DOS 6.22. 11242-1.0-00.

182466 HAZUHS V1.0. 2007. PC, DOS 6.22. 11194-1.0-00

182467 POST RASCAL SET V1.0. 2007. PC, DOS 6.22. 11231-1.0-00

182468 RASCAL SET V1.0. 2007. PC, DOS 6.22. 11232-1.0-00

184513 RASCAL SET V1.1. 2007. DOS 6.22, QEMM 9.0. 11232-1.1-00

184053 RASCAL SET V1.1. 2007. PC, Windows 2003. 11232-1.1-01

182835 SIGCOMB v. 1.1 2007. DOS 6.22. 11233-1.1-00.

163293 Software Code: BASE4 V. 4.0. 2002. PC, DOS 6.22. 10940-4.0-00

163295 Software Code: CORBB V. 1.0. 2002. PC, DOS 6.22. 10941-1.0-00

163303 Software Code: DUR V. 1.0. 2003. PC, DOS 6.22. 10942-1.0-00

167994 Software Code: EARTHVISION V. 5.1. 2000. IRIX 6.5. STN: 10174-5.1-00

163304 Software Code: INTEG1 V. 1.0. 2002. PC, DOS 6.22. 10943-1.0-00

163305 Software Code: INTERPOL V. 1.0. 2002. PC, DOS 6.22. 10944-1.0-00

163309 Software Code: MAXMIN V. 1.0. 2002. PC, DOS 6.22. 10945-1.0-00

163318 Software Code: REPLOT V. 1.0. 2003. PC, DOS 6.22. 10949-1.0-00

163319 Software Code: SCALE1 V. 1.0. 2002. PC, DOS 6.22. 10946-1.0-00

163321 Software Code: SPCTLR V. 1.0. 2003. PC, DOS 6.22. 10947-1.0-00

163326 Software Code: XYMULT V. 1.0. 2002. PC, DOS 6.22. 10919-1.0-00

182834 SOILHAZ SET V. 1.0 2007. DOS 6.22. 11234-1.0-00.

172322 UDEC V. 3.14. 2004. WINDOWS 2000. STN: 10173-3.14-00.